



UNIVERSITÀ
DEGLI STUDI
DI PADOVA

Università degli Studi di Padova

**Department of Agronomy Food Natural resources Animals and
Environment (DAFNAE)**

CORSO DI DOTTORATO DI RICERCA IN
SCIENZE DELLE PRODUZIONI VEGETALI

XXXII CICLO

Development of consolidated-bioprocessing yeasts for the second- generation bioethanol production from agricultural residues

Thesis written with the financial contribution of Fondazione Cassa di Risparmio di Padova e Rovigo

Coordinatore: Prof. Sergio Casella
Supervisore: Prof. Sergio Casella
Prof. Marina Basaglia
Co-Supervisore: Dott. Lorenzo Favaro

Dottorando: Nicoletta Gronchi

INDEX

LIST OF ABBREVIATIONS	6
ABSTRACT	9
RIASSUNTO.....	11
AIM OF THE STUDY	13
1. INTRODUCTION	14
1.1 Biomass as bioenergy source to replace fossil fuels.....	14
1.2 Bioethanol: first- and second-generation technology	18
1.3 Industrial routes of bioethanol production.....	20
1.3.1 Ethanol from sugars	20
1.3.2 Ethanol form starch	22
1.3.3 Ethanol from lignocellulose.....	25
1.4 Process consolidation for cost-effective conversion	29
1.5 Development of a CBP microorganism for starch conversion	31
1.5.1 Bioconversion of starch	33
1.5.2 Starch hydrolysing enzymes	34
1.6 Heterologous enzyme expression in <i>Saccharomyces cerevisiae</i>	35
1.6.1 Episomal vectors.....	36
1.6.2 Genome editing methods	37
2. MATERIALS AND METHODS.....	44
2.1 Cultivation media	44
2.2 Strains and growth conditions	45
2.3 Evaluation of fermentative vigour of selected wild type and industrial strains	46
2.3.1 Fermentative vigour in minimal broth.....	47

2.3.2	Fermentative vigour in SSF set up on starchy substrates	47
2.3.3	Scale-up in 1-L fermenter	49
2.4	Genomic DNA extraction and library sequencing of <i>S. cerevisiae</i> L20	49
2.4.1	Next generation sequencing data analysis	50
2.5	Yeast genome engineering	50
2.5.1	Yeast dominant marker resistance	51
2.5.2	Delta integration of <i>AmyA</i> and <i>GlaA</i> genes from <i>A. tubingensis</i> T8.4 into retrotransposons Ty	51
2.5.2.1	Electrotransformation of yeast strains with integrative linear donor DNA fragments.	53
2.5.2.2	Selection of positive transformants	54
2.5.2.3	PCR confirmation of positive integration	54
2.5.2.4	Evaluation of mitotic stability of the recombinants	55
2.5.3	CRISPR/Cas9 mediated integration of <i>AmyA</i> and <i>GlaA</i> genes from <i>A. tubingensis</i> T8.4 into pre-determined loci	56
2.5.3.1	Plasmids construction	59
2.5.3.2	Yeast transformation	63
2.5.3.3	PCR confirmation of positive integration	64
2.5.3.4	Confirmation of amylolytic enzyme(s) secretion	65
2.5.3.5	Plasmid curing and strain stability	65
2.6	Enzymatic assays	66
2.7	SDS-PAGE	67
2.8	Starch CBP fermentation studies	68
2.9	HPLC analysis	69
2.10	Calculations	69
3.	RESULTS AND DISCUSSION	70
3.1	Isolation, genetic characterization and fermentative abilities of novel yeast strains in glucose	71

3.1.2	Fermentative vigour in SSF set up on starchy substrates	73
3.1.3	Scale-up in 1-L fermenter	77
3.2	Genome sequencing of <i>S. cerevisiae</i> L20.....	80
3.3	Yeast genome engineering.....	81
3.3.1	Yeast dominant marker resistance	82
3.3.2	Delta integration of <i>AmyA</i> and <i>GlaA</i> genes from <i>A. tubingensis</i> T8.4	84
3.3.3	CRISPR/Cas9 mediated integration of <i>AmyA</i> and <i>GlaA</i> genes from <i>A. tubingensis</i> T8.4.....	86
3.3.3.1	Plasmid construction	87
3.3.3.2	Yeast transformation	90
3.4	Enzymatic assays	93
3.5	SDS-PAGE protein analysis.....	94
3.6	Starch CBP fermentation studies	95
4.	CONCLUSIONS.....	100
5.	REFERENCES	104
6.	PARTICIPATION TO COURSES, SEMINARS AND CONGRESSES; OTHER EDUCATIONAL ACTIVITIES.....	117
7.	PUBLICATIONS.....	120
8.	ACKNOWLEDGMENTS.....	121

LIST OF ABBREVIATIONS

AFEX	Ammonia fiber explosion
ARP	Ammonia recycling percolation
ARS	Autonomously replicating sequence
BLAST	Basic local alignment search tool
CBP	Consolidated bioprocessing
CEN	Yeast centromere
CRISPR	Clustered regularly interspaced palindromic repeat
DDGS	Distillers dried grains with solubles
DM	Dry matter
DMC	Direct microbial conversion
DSB	Double strand break
E10	10 % ethanol blend with gasoline
E85	85 % ethanol blend with gasoline
FAO	Food and Agriculture Organization
GAU	Glucoamylase units
GHG	Greenhouse gasses
GRAS	Generally recognized as safe
Gt	Gigatons
Gtoe	Billion tons of oil equivalent
HDR	Homology-directed repair
HMF	Hydroxymethyl furfural
HPLC	High performance liquid chromatography
HR	Homologous recombination

IEA	International Energy Agency
LB	Luria Bertani
LTR	Long terminal repeat
mb/d	Million barrels per day
MNS	Must nutrient synthetic
MSW	Municipal solid waste
Mtoe	Million tons of oil equivalent
NHEJ	Non-homologous end joining
OD ₆₀₀	Optical density measured as absorbance at 600 nm
OECD	Organization for Economic Co-operation and Development
PAM	Protospacer adjacent motif
PCR	Polymerase chain reaction
ppm	Parts per million
RNA	Ribonucleic acid
rpm	Revolutions per minute
SAA	Soaking aqueous ammonia
SDS-PAGE	Sodium dodecyl sulfate–polyacrylamide gel electrophoresis
SHF	Separate hydrolysis and fermentation
SLSF	Simultaneous liquefaction, saccharification and fermentation
SSB	Single strand break
SSCF	Simultaneous saccharification and co-fermentation
SSF	Simultaneous saccharification and fermentation
TFA	Trifluoroacetic acid
TPED	Total primary energy demand
US	United States

WL	Wallerstein Laboratory
YCp	Yeast centromeric plasmid
YEp	Yeast Episomal plasmid
YIp	Yeast Integrative plasmid
YNB	Yeast nitrogen base
YPD	Yeast peptone dextrose

ABSTRACT

Today, the fossil materials currently represent the major share of the fuel market. In order to reduce the environmental impact resulting from the massive use of these non-renewable sources, particularly associated with the transport sector, bioethanol represents one of the most favorable, sustainable and ecological alternatives. However, the second-generation bioethanol production from waste plant biomass requires an expensive multi-step process and large dosages of commercial hydrolytic enzymes. The consolidated bioprocessing (CBP) performed by a single fermenting microbe could provide significant energy savings as well as being more cost-effective. Nevertheless, to date no naturally occurring CBP microbe has been described yet.

In this study, a collection of newly isolated *Saccharomyces cerevisiae* strains was screened with the aim of selecting a wild type yeast with superior fermentative traits than the industrial *S. cerevisiae* Ethanol Red[®], which is currently used at industrial scale for first-generation bioethanol production.

The collection has been evaluated for the conversion of starchy substrates into ethanol by a simultaneous saccharification and fermentation (SSF) configuration.

The *S. cerevisiae* L20 strain, which demonstrated the highest fermentation rate and ethanol production, was selected for a genetic engineering program in order to obtain an amylolytic yeast, for an efficient conversion of starch into ethanol.

S. cerevisiae L20 and Ethanol Red[®] were engineered for the constitutive expression of two genes, encoding the α -amylase *AmyA* and the glucoamylase *GlaA* from *Aspergillus tubingensis* T8.4, in order to develop a stable recombinant strain.

The well-established δ -integration strategy was used to obtain recombinants at δ -sequences by using homologous cassettes for *AmyA* and *GlaA*. Alongside, the innovative CRISPR / Cas9 knock-in system was used for the site-specific integration of the same genes in two selected genomic loci, namely mk114 and AD7. Both approaches were evaluated in terms of strain stability and enzymatic activity.

The recombinant strains were verified for correct integration and examined for the effective secretion of amylases on agar plates containing starch. The enzymatic activity of the strains presenting the largest hydrolysis halos was quantified, and their recombinant proteins characterized by sodium dodecyl sulfate–polyacrylamide gel electrophoresis (SDS-PAGE).

The performances of the new CBP strains were then demonstrated on starchy substrates. The most promising recombinant yeast was found to be L20 δ T8, co-expressing both *AmyA* and *GlaA*.

This study demonstrated the superior fermenting abilities of *S. cerevisiae* L20 compared to Ethanol Red[®], confirming its promise as a starting point for the development of a CBP yeast. Genetic editing technologies have both proven to be effective, although further efforts are needed.

RIASSUNTO

Attualmente i materiali fossili costituiscono la maggior parte dei combustibili presenti sul mercato. Al fine di ridurre l'impatto ambientale derivante dall'utilizzo massivo di queste fonti non rinnovabili, in particolare associato al settore dei trasporti, il bioetanolo rappresenta una delle alternative sostenibili ed ecologiche più favorevoli.

La produzione di bioetanolo di seconda generazione da biomassa amidacea richiede un costoso processo articolato in più fasi e alte dosi di enzimi idrolitici commerciali. Il 'consolidated bioprocessing' (CBP), eseguito da un singolo microrganismo fermentante, potrebbe offrire un grande risparmio in termini energetici ed economici. Tuttavia, ad oggi nessun isolato naturale possiede le caratteristiche per il CBP.

In questo studio, è stata vagliata una collezione di ceppi wild type con l'obiettivo di selezionare un ceppo di *Saccharomyces cerevisiae* con capacità fermentative superiori rispetto al ceppo industriale di riferimento *S. cerevisiae* Ethanol Red[®], attualmente utilizzato per la produzione di bioetanolo di prima generazione.

Una nuova collezione di ceppi di *S. cerevisiae* è stata valutata per la conversione di substrati amidacei in etanolo applicando un sistema di simultanea saccarificazione e fermentazione (SSF). Il ceppo *S. cerevisiae* L20, il quale ha dimostrato il più alto tasso di fermentazione e la più alta produzione di etanolo, è stato selezionato per un programma di ingegneria genetica al fine di ottenere un lievito amilolitico, per un'efficiente conversione di amido in etanolo su scala industriale. *S. cerevisiae* L20 e Ethanol Red[®] sono stati ingegnerizzati per l'espressione costitutiva di geni codificanti l' α -amilasi *AmyA* e la glucoamilasi *GlaA* di *Aspergillus tubingensis* T8.4, al fine di sviluppare un ceppo ricombinante stabile. Secondo la strategia δ -integration è stato possibile ottenere ricombinanti a livello delle sequenze δ utilizzando frammenti omologhi per *AmyA* e *GlaA*. Contestualmente, l'innovativo sistema knock-in CRISPR/Cas9 è stato utilizzato per l'integrazione sito-specifica degli stessi geni nel genoma di lievito. Due loci genomici, mk114 e AD7, sono stati selezionati per la ricombinazione. Le due strategie sono state confrontate in termini di stabilità e ripercussioni sul metabolismo di fermentazione.

I ceppi ricombinanti così ottenuti sono stati verificati per la corretta integrazione ed esaminati per l'effettiva secrezione di amilasi su piastre di agar contenenti amido. L'attività

enzimatica dei ceppi che presentavano l'alone di idrolisi più ampio è stata quantificata e le loro proteine ricombinanti caratterizzate da SDS-PAGE.

Le performance dei nuovi ceppi CBP sono state valutate su substrati amidacei. Il lievito ricombinante più promettente è risultato essere L20 δ T8, in grado di co-esprimere sia *AmyA* che *GlaA*.

Questo studio ha dimostrato che le abilità fermentative di *S. cerevisiae* L20 sono superiori rispetto a Ethanol Red[®], confermando quindi il suo ruolo promettente come punto di partenza per lo sviluppo di un lievito CBP. Le tecnologie di editing genetico si sono dimostrate entrambe efficaci, ma necessitano di sforzi ulteriori per il miglioramento. In ogni caso, la stabilità genetica e la fine regolazione che CRISPR/Cas9 può fornire a riguardo dell'integrazione genica, fanno di quest'ultima la tecnologia di elezione per lo sviluppo di un lievito CBP.

AIM OF THE STUDY

In contrast to laboratory strains, wild type *S. cerevisiae* isolates from oenological environments can provide a good starting point to look for natural and highly productive fermenting yeast. With the final purpose of developing a CBP yeast for efficient conversion of starchy biomass into ethanol, this work aimed at (1) selecting a novel *S. cerevisiae* strain among a collection of natural isolates belonging to the DAFNAE (University of Padova). The strain demonstrating a superior fermenting performance than the industrial benchmark Ethanol Red[®] has been considered for a (2) genome engineering program for the heterologous expression of efficient fungal amylases.

1. INTRODUCTION

1.1 Biomass as bioenergy source to replace fossil fuels

Over the last decades, the rapid growth of the global population has led to an exponential rise of energy consumption, mostly in urban areas of developing economies. According to the data reported by the International Energy Agency (IEA; *Table 1.1*), the global energy demand has increased by 40 % from 2000, reaching 13.9 billion tons of oil equivalent (Gtoe) in 2017. The greatest share of energy supply was given by fossil fuels, such as coal, oil and gas, with 27 (3.75 Gtoe), 32 (4.4 Gtoe) and 22 % (3.1 Gtoe) respectively. In the last 25 years, they represented the core of global energy system with a share of 81 % of the energy sources consumed. Only in the last biennium 2017-2018 the growth of the total primary energy demand grew by 2.3 %, nearly twice the average rate of growth since 2010, reaching a total of 14.3 Gtoe in 2018. This rate is presumed to more than double in the future. The projections consider that global primary energy demand will grow by 40 % between today and 2040, being oil at the first place with 25 % increased demand.

	2000	Share (%)	2017	Share (%)	2018	Share (%)	2040	Share (%)
TPED*	10 027	100	13 972	100	14 301	100	19 328	100
Coal	2 308	23	3 750	27	3 778	26	4 769	25
Oil	3 665	36	4 435	32	4 488	31	5 570	29
Gas	2 071	21	3 107	22	3 253	23	4 804	25
Nuclear	675	7	688	5	710	5	951	5
Hydro	225	2	353	3	364	3	514	3
Bioenergy	1 022	10	1 384	10	1 418	10	1 771	9
Other renewables	60	1	254	2	289	2	948	5

*TPED: Total Primary Energy Demand; Mtoe: million tons of oil equivalent

World Energy Outlook 2018

© 2018 OECD/IEA

Table 1.1 World primary energy demand by source (Mtoe).

As recently as in 2000, Europe and North America accounted for more than 40 % of global energy demand and developing economies in Asia for 20 %. By 2040, this situation will be completely reversed (World Energy Outlook 2018, IEA).

According to statistics, the worldwide reliance on liquid fuel has been maintained steady since 1990, ranging around 30 % of total energy supply. The daily global oil demand seems to merely follow the increase of energy demand over the years, nonetheless the biofuel consumption is kept steady at negligible levels (*Table 1.2*). In current policies scenario, the oil consumption is expected to reach more than 5.5 Gtoe by 2040 (*Table 1.1*).

	2000	2017	2018	2040
Total	77.5	95.1	96.6	124.1
Oil	77.3	93.4	94.8	120.5
Biofuel	0.2	1.7	1.8	3.5

World Energy Outlook 2018
© 2018 OECD/IEA

Table 1.2 World liquid fuel demand (mb/d).

To date, road transport accounts for the 57 % of global oil consumption (2 567 Mtoe on total 4 488 Mtoe; *Table 1.1* and *1.3*), being the largest segment of global oil demand. Despite the latest attention directed to the sustainable alternatives to fossil fuels, the oil demand has grown by around 11 million barrels per day (mb/d) since 2000, the largest increase in any sector over this period. Around half of this increase came from cars, nearly 40 % from road freight and the remaining from two/three-wheelers and buses. This increase would have been even bigger without the employment of alternative fuels such as biofuels, which avoided a further 2.5 mb/d increase in oil demand (World Energy Outlook 2018, IEA; Global Energy and CO₂ Status Report 2018, IEA).

In 2018, the largest consumer of oil was the United States (US) with 20 mb/d, followed by Europe (15 mb/d) and China (13 mb/d). The oil demand increases by 1.1 mb/d every year, and it is expected to increase up to 7 mb/d by the end of 2025. Current policies will bring China to be the first consumer by 2040, overcoming the US in terms of oil demand, with developing economies following (IEA, 2018).

	2000	2017	2018	2040
Total	1 958	2 745	2 794	3 964
Oil	1 871	2 530	2 567	3 494
Electricity	19	31	33	94
Biofuels	10	82	86	165
Other fuels	58	102	109	211

World Energy Outlook 2018
© 2018 OECD/IEA

Table 1.3 World energy demand by transportation sector (Mtoe).

The progressive depletion of fossil fuels will be a serious threaten for the global energy security. As the number of vehicles will increase to 1.3 billion by 2030 and to 2 billion by 2050, the exhaustion of petroleum, natural gas and coal reserves at current consumption rate is foreseen in 45, 60 and 120 years, respectively (Baeyens et al., 2015; Guo et al., 2015).

In 2017, the global daily oil production amounted at 95.7 mb/d, and only in 2018 it raised up to 98.3 mb/d. In 2018, an unprecedented expansion of total liquids production increased by a record of 2.2 mb/d, where the US accounted for the 70 % in global oil supplies, with additional 15.6 % than 2017. In this way, the US is predicted to dominate the oil supply over Saudi Arabia in the mid-term. On the other hand, the US are by far the largest oil consumer followed by the Republic of China, India, Japan and the Russian federation.

As a result of higher energy consumption, global energy-related CO₂ emissions in 2018 increased to the historic spike of 33.1 gigatons (Gt) CO₂. It was the highest rate of growth since 2013, and 70 % higher than the average increase since 2010. A continue rising, going up by 10 % to 36 Gt, is expected in 2040 reflecting the increasing fuel demand. Looking back further, emissions have more than doubled since the early seventies and increased by around 40 % since 2000 (23 Gt CO₂). The global annual concentration of CO₂ in the atmosphere averaged at 407.4 ppm in 2018, increasing by 2.4 ppm in the biennium 2017-2018 only. This is a major increase from pre-industrial levels, which ranged between 180 and 280 ppm (World Energy Outlook 2018, IEA).

The fuel combustion resulting from the transportation sector is responsible for the major contribution to greenhouse gasses (GHG) pollution, accounting for 19 % of global CO₂ (about 8 kg CO₂/gallon petrol) production and more than 70 % of carbon monoxide (CO) emissions

(Balat and Balat, 2009). Globally, at nearly 8 Gt CO₂, transportation accounted for one quarter of total emissions in 2016, a level 71% higher than that was recorded in 1990 (IEA, 2018). Emissions of nitrous oxide (N₂O) and methane (CH₄) have also been increasing rapidly through agricultural, energy, and industrial sources.

Nevertheless, the accumulation of CO₂ and other GHGs in the atmosphere is causing climate changes leading to a raise of global average temperature of around 0.8 °C over the last century, and 0.6 °C only during the last three decades (Hansen et al., 2006; Panwar et al., 2011).

The increasing awareness of the climate change and the concern over fossil oil depletion are driving the policies of many countries to (i) reduce the energy consumption, (ii) increase the efficiency of energy conversion or utilization, (iii) switch to lower carbon content fuels, (iv) enhance natural sinks for CO₂, and (v) capture and store CO₂ (Balat et al., 2008). The Organization for Economic Co-operation and Development (OECD) members have already proclaimed commitments to reduce the dependence on fossil fuel by promoting the development and utilization of sustainable energy sources.

The importance of renewable energies is widely recognized for a sustainable development and the simultaneous preservation of the environment (Sims, 2004). In 2018, renewables contributed only for 14.5 % to the global energy demand, showing the same share as in 2000. According to the IEA 2018 forecasts, in 2023 the lowest contribution of renewables will be for the transportation sector with respect of electricity and heating sectors, with a share growing only minimally from 3.4 of 2017 to 3.8 % (Renewables 2018, Analysis and forecasts to 2023, IEA 2018). In short, the strong dependency from fossil fuel reserves must be limited in the near future to ensure global energy security and limit the environmental issues. In this perspective, in Europe the target is to reach a share of 10 % of biofuels on energy basis in the transportation sector by 2020.

Among renewable energy sources, biomass is the only material that can provide an alternative liquid fuel in today's transportation system (Lewandowsky, 2016). Therefore, much attention should be given to the production of biofuel, considering not merely the value as transportation fuels but also the economic and environmental benefits.

Biomass is a cleaner and inexhaustible material, representing the most relevant energy source that can be converted into biofuels. Biomass is predicted to contribute for 46 % of the share in meeting global energy demand among renewable energy sources in 2023 (IEA

forecast). At present, it supplies only 10 % of the global annual energy demand. The use of biomass as a source of energy, as well as displacing fossil fuel, can potentially enhance the energy independence of both developing and industrialized countries. The energy security can be improved by biological diversity of energy supply, reducing the impact of fluctuations of petroleum global market, but also reducing import dependency and promoting rural economies (IEA, 2017).

Biomass is commonly defined as a carbon-rich organic matter having intrinsic chemical energy content that can be exploited via direct (burning) or indirect combustion (biofuels), relying on present technologies. The CO₂ released in the atmosphere can be considered as zero, since biomass uses CO₂ during the growth, resulting in no net releases (Balat and Ayar, 2005; Balat and Balat, 2009). In comparison to fossil fuel which takes millions of years to form, biomass is easy to grow, collect and utilize without depleting natural resources. Presently, it is regarded as a non-fossilized and biodegradable material obtained from agriculture, forestry and food processing, both residual and waste, that is utilized for energy production and other non-food purposes. Biomass-derived bioethanol is now dominating the global production of biofuels, representing over the 90 % of the market (Balat and Balat, 2009).

1.2 Bioethanol: first- and second-generation technology

Bioethanol has considerable advantages over fossil fuels: (i) it can be obtained from several organic materials such as corn, sugar and molasses, (ii) it is readily biodegradable, (iii) it has higher octane number (108) over gasoline, thus preventing knocking and early ignition in combustion engines, (iv) it contains 35 % oxygen, which reduces particulate and NO_x emissions from combustion. It is estimated that the higher oxygen content allows a 15 % improvement in oxidation of gasoline hydrocarbons, when used as enhancer, with consequent cleaner combustion. The result is a reduction of hydrocarbons, CO, and particulate emissions. It can be used either as a fuel or as a gasoline enhancer for spark-ignited engines. Nonetheless, it has 68 % lower energy content compared to petrol (Sanchez and Cardona, 2008; Balat and Balat, 2009; Aditiya et al., 2016; Zabed et al., 2017).

In Brazil, bioethanol is used pure or blended with gasoline in a mixture called gasohol (bioethanol 24 % and gasoline 76 %, v/v), while in several states of the US a small amount of bioethanol (10 % v/v) is added to gasoline, known as E10. Gasoline blends with higher

concentrations of bioethanol are used in the so called flexible-fuel vehicles that can operate on blends of up to 85 % bioethanol (E85). Moreover, ethanol can replace diesel fuel in compression-ignition engines using a proper emulsifier.

In 2018, the global fuel ethanol production has reached about 120 billion liters (OECD-FAO, Agricultural Outlook 2018-2027), being the US and Brazil the leading producers. Jointly, the US and Brazil produced almost 90 % of the world fuel bioethanol (*Figure 1.1*).

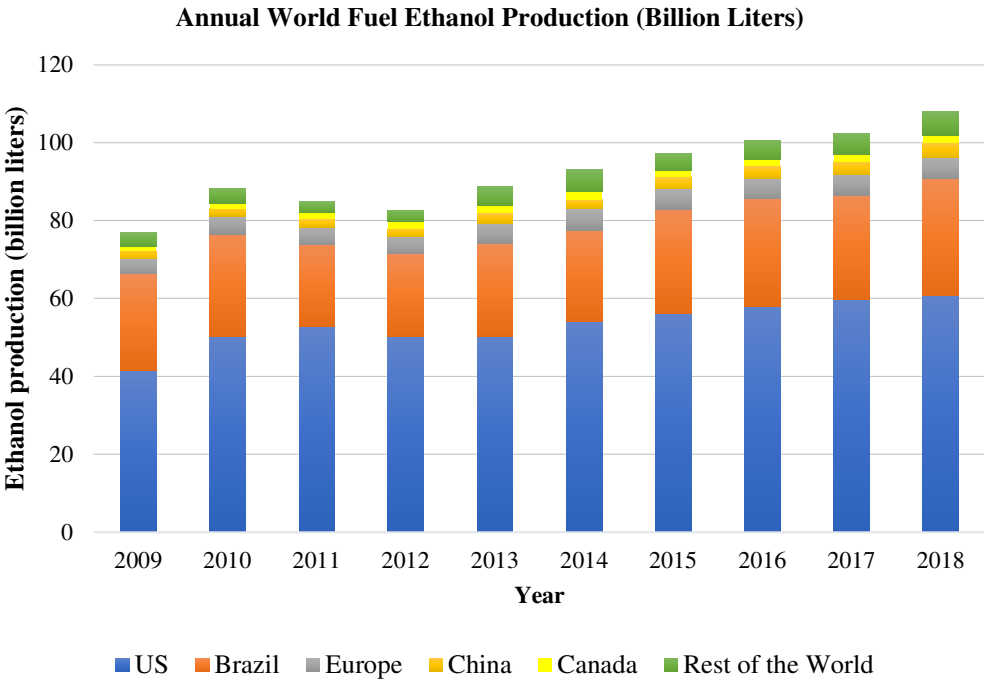


Figure 1.1 Global bioethanol production by country during the last decade (data from Renewable Fuel Association, 2019).

Depending upon the source and production technology, bioethanol can be broadly categorized into first- and second- generation. The first-generation bioethanol is produced from dedicated crops with high starch (such as corn, maize, wheat, barley, cassava and potato) or sugar (such as sugarcane, sugar beet and sorghum) content. Currently, the production of ethanol as liquid fuel belongs to the first-generation. About 60 % of global bioethanol production comes from sugar cane and 40 % from other crops, Brazil and the US exploiting sugar cane and corn as predominant raw material, respectively (Balat et al., 2008). The sustainability of first-

generation bioethanol over the use of arable land and water resources for fuel purposes has led to serious ethical concerns. Water shortage, over-fertilization of soil, loss of biodiversity and the increasing price of food commodities such as cereals, crops and livestock feed are currently a matter of the 'food vs fuel' debate. The socio-economic and environmental consequences of large-scale production must then be taken into consideration (Lennartsson et al., 2014).

The second-generation bioethanol, on the other hand, is more attractive from a sustainability standpoint, as it is based on non-food raw material. The waste biomass available from forestry, agricultural and industrial activities is relatively inexpensive and can be used as feedstock. Although ethanol as fuel from biomass was tested in the early 19th century, the development of a cost-effective and industrially applicable technology was not finalized.

1.3 Industrial routes of bioethanol production

Three are the major steps in ethanol production: (i) obtaining solution that contains fermentable sugars, (ii) converting sugars to ethanol by fermentation and (iii) separating and distilling ethanol (Mohd Azar et al., 2017). Biomass is usually pretreated, with significant implications on the industrial process which makes the hydrolysis easier and produces higher amount of fermentable sugars. Theoretically, all plant materials can be used to obtain bioethanol. However, the final ethanol yield depends on the overall conversion efficiency which differs significantly by the kind of feedstock that is used. The feedstocks for bioethanol production can be classified into three categories: sucrose containing feedstock, starchy materials and lignocellulose. Sugar based raw materials require only an extraction process to get fermentable sugars, while starchy crops need to undergo hydrolysis to convert starch into glucose. Lignocellulosic biomass must be pretreated before hydrolysis in order to alter cellulose structures for enzyme accessibility (Zabed et al., 2017).

1.3.1 Ethanol from sugars

Sugar-based raw materials include some food-crops and sugar refinery wastes, such as molasses. Sugar cane (either in the form of cane juice or cane molasses) and beet molasses are the most popular feedstocks for first-generation ethanol production in Brazil and Europe, respectively. Also, sweet sorghum was proposed as feedstock (Demirbas, 2009).

The chief advantages of sugar-based materials are high yield of sugar per acre and low conversion costs, since the sugar can be readily converted by the fermenting microorganisms. Here, no expensive biomass pretreatments are required, except for mechanical size reduction and pressing. However, their natural seasonal availability is the main issue.

The fermentation of sucrose-containing feedstock is a well-known and mastered process (**Figure 1.2**), however there are still few points to be outlined for an optimal bioethanol production at large-scale. The high ethanol concentration, the osmotic stress due to sugar and salts, the acidity of the medium, sulfite and bacterial contamination are recognized as stress conditions negatively effecting the yeast fermentation (Vohra et al., 2014). Therefore, the optimization of the process requires: (i) the selection of new varieties of plants with higher sucrose content, (ii) the selection of new yeast strains more adapted to stressing conditions of industrial fermentations, (iii) the utilization of residual by-products.

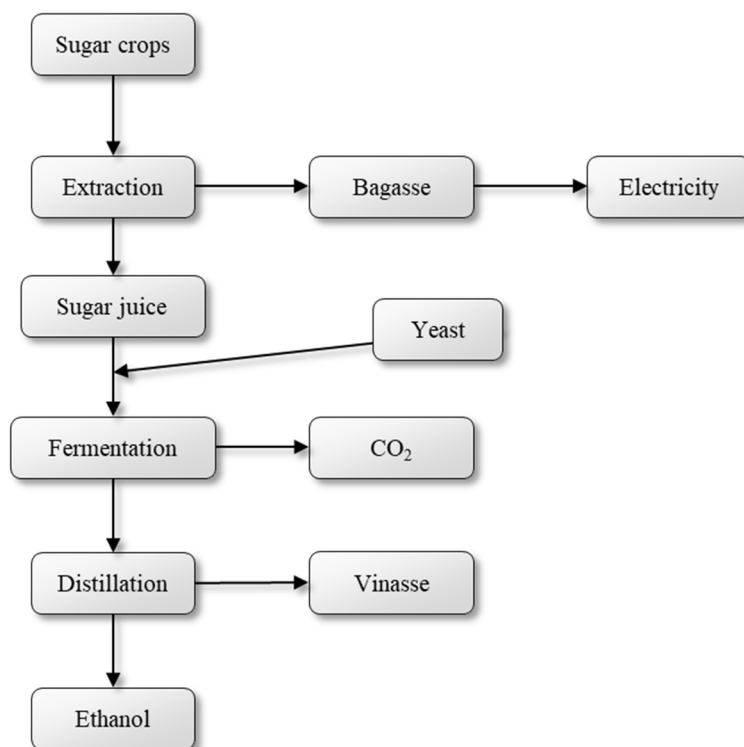


Figure 1.2 Diagram of bioethanol production from sugar biomass (adapted from Zabed et al., 2017).

1.3.2 Ethanol form starch

Starchy crops such as cereals (60-80 % starch), legumes (25-50 % starch), tubers and roots (60-90 % starch) are widely used for bioethanol production due to their availability across the world, ease of conversion, storage capability for a long period and high ethanol yield. Grains such as corn, wheat or barley are the most utilized feedstocks for ethanol production in the US and Europe. In tropical countries, other starchy crops as tubers (e.g. cassava) can be used for commercial production of fuel ethanol.

Starch represents the most relevant form of energy storage in plant, accounting for 20 to 70 % of the dry weight (**Table 1.4**).

Crop	Species	Crop type	Starch content (%)
Babassu	<i>Orbygnia phalerata</i>	Palm	60 <i>a</i>
Banana	<i>Musa paradisiaca</i>	Fruit	27.2 <i>b</i>
Barley	<i>Hordeum vulgare</i>	Cereal	63-69 <i>a</i>
Breadfruit	<i>Artocarpus altilis</i>	Fruit	64.5 <i>a</i>
Buckwheat	<i>Fagopyrum tataricum</i>	Cereal	80.5 <i>a</i>
Cassava	<i>Manihot esculenta</i>	Tuber	35 <i>b</i>
Chestnut	<i>Castanea sativa</i>	Nut	93.2 <i>a</i>
Corn	<i>Zea mays</i>	Cereal	70-72 <i>a</i>
Ginger	<i>Zingiber officinale</i>	Rhizome	85 <i>a</i>
Kudzu	<i>Pueraria lobata</i>	Root	99.5 <i>a</i>
Lentil	<i>Lens culinaris</i>	Legume	51.7 <i>a</i>
Millet	<i>Panicum sumatrense</i>	Cereal	70 <i>a</i>
Oat	<i>Avena sativa</i>	Cereal	65.6 <i>a</i>
Peas	<i>Pisum sativum</i>	Legume	46.2 <i>a</i>
Potato	<i>Solanum tuberosum</i>	Tuber	73 <i>a</i>
Rice	<i>Oryza sativa</i>	Cereal	87.5 <i>a</i>
Sorghum	<i>Sorghum bicolor</i>	Cereal	68-71 <i>a</i>
Sugar beet	<i>Beta vulgaris</i>	Root	8-12 <i>b</i>
Sweet potato	<i>Ipomoea batatas</i>	Root	14-27.5 <i>b</i>
Taro	<i>Colocasia esculenta</i>	Root	15-25 <i>b</i>
Wheat	<i>Triticum aestivum</i>	Cereal	65-76

a, dry weight; *b*, fresh weight

Table 1.4 Starch content in some starchy crops (from Zabed et al., 2017).

The physicochemical properties of starch are often associated with its amylose and amylopectin ratio, which can significantly affect the final ethanol yield (Zabed et al., 2017). As starch is not readily convertible into ethanol by fermenting yeast, this polymer has to be hydrolyzed to sugar monomers.

The industrial production of bioethanol from corn starch is a well-established technology. Two are the main strategies for biomass processing: wet milling and dry milling. In the dry milling process (*Figure 1.3*), biomass is ground into fine particles to facilitate the entry of water and enzymes in the next steps. The powder is mashed with water at 85 °C in the gelatinization step, and the pH is adjusted to 6.0 with lime. In the following liquefaction step, the addition of α -amylase enzymes rapidly reduces the degree of polymerization and mash viscosity. The mash is then heated to 110-150 °C for an hour in a jet cooker. For the subsequent saccharification step, the mash is cooled down to 60-70 °C and the pH adjusted at 4.5 with sulfuric acid. The saccharification occurs when glucoamylases are added to release glucose. After the enzymatic hydrolysis, the syrup is then converted into ethanol through microbial fermentation in the presence of a nitrogen source. Distillation and dehydration are finally performed to yield anhydrous ethanol. In the dry milling process, the average overall yield of ethanol is about 390 L for each ton of corn kernels. The undigested components of corn kernels are centrifuged and dried to a 27 % protein product known as distillers dried grains with solubles (DDGS). It is estimated that each ton of corn kernels generates 285 kg of DDGS. Due to high protein (25-32 %) and fiber (8-35 %) content, it is sold as animal feed (Cardona and Sanchez, 2007; Lennartsson et al., 2014).

The wet milling process (*Figure 1.4*) consists of the fractionation of corn kernels into its components. Corn kernels are soaked in diluted sulfuric acid for 24-48 h at 52 °C to help the softening and breaking down the protein surrounding the starch particles, generating a corn steep liquor which is composed mainly by proteins (about 50 % of the dry mass). The germ is removed from the steeped corn in degerminating mills and further processed for oil extraction. After grinding, the defibering process separates the pericarp of the kernel, which comprises fibers (cellulose, hemicelluloses). As a final fractionation step, the gluten is separated by centrifugation and the starch recovered. Starch granules are enzymatically saccharified and fermented as well as in dry process. Fibrous material, gluten and solids are further sold as animal feed (Cardona and Sanchez, 2007; Zabed et al., 2017).

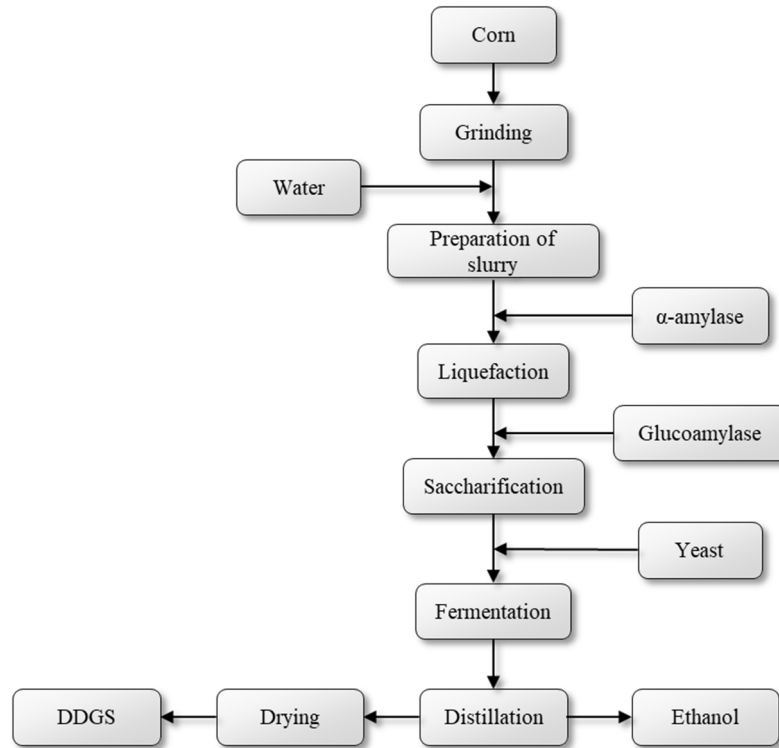


Figure 1.3 Diagram for dry-grind bioethanol production from starch (adapted from Zabed et al., 2017).

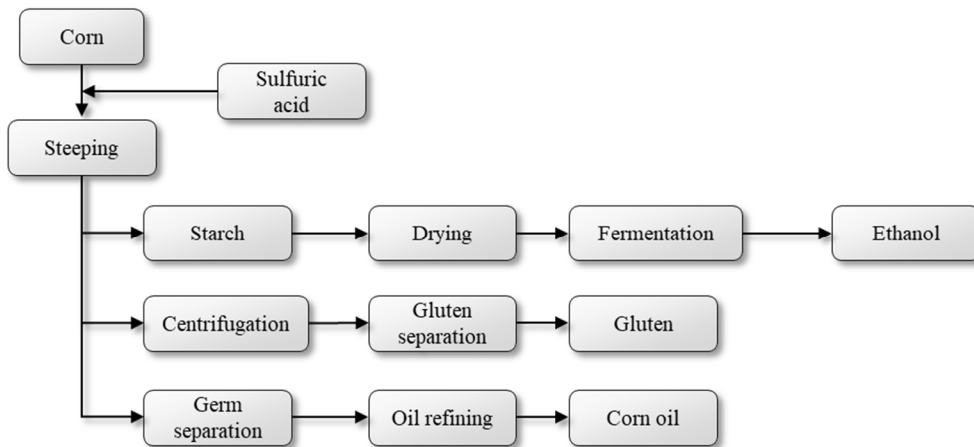


Figure 1.4 Diagram of wet milling bioethanol production from corn (adapted from Zabed et al., 2017).

The wet milling process is complex and a higher capital expenditure is needed than the dry technology, although higher value-added of the resulting co-products can reduce the plant costs.

In last years, the possibility of hydrolyzing starch at low temperatures to ensure energy savings is also being investigated. The production of ethanol by ‘cold hydrolysis’ dispenses energy-demanding steps such as gelatinization and liquefaction. Here, the granular corn is hydrolyzed by amylases and proteases at low temperatures. Therefore, capital and operational costs are approximately 41 and 51% lower, respectively (Cinelli et al., 2015). The suspension is then subjected to simultaneous saccharification and fermentation (SSF). Besides the great energetic advantage over the conventional technologies, the cold hydrolysis also presents lower water and chemicals consumption. The capital expenditure of a plant for conversion of raw starch is potentially lower, since the process is more integrated. The overall yield tends to be higher, due to the absence of Maillard reactions and reduced yeast inhibition. Since the sugars are gradually released, the osmotic stress is reduced and higher alcohol levels are produced. Nevertheless, the susceptibility to microbial contamination is higher since lower temperatures are used, thus affecting the quality of DDGS. Moreover, the higher demand of enzymatic preparation can be less attractive (Castro et al., 2011; Vohra et al., 2014).

1.3.3 Ethanol from lignocellulose

Lignocellulosic biomass can be divided into several groups such as energy-dedicated crops, forest materials, agricultural residues and organic fraction of municipal solid wastes. Energy crops hold potential in bioethanol production since they require a short growth period and, usually, minimal use of water, fertilizer and cultivable lands. Some potential energy crops are miscanthus (*Mischantus* spp.), switchgrass (*Panicum virgatum*), giant reed (*Arundo donax*) and alfalfa (*Medicago sativa*). Forest biomass include mainly woody materials such as hardwoods and softwoods, while forest wastes are sawdust, wood chips and branches. Municipal solid wastes (MSW) is the biomass that originate from residential and non-residential sources such as food wastes and paper mill sludge. The wide MSW diversification in composition and the microbial contamination are making these feedstocks less attractive.

Lignocellulose is composed of cellulose (40-50 %), hemicellulose (25-35 %) and lignin (15-20 %), depending on the types of biomass, which are strongly associated in a complex matrix. The composition and structure of the biomass determine the digestibility of lignocellulose to subsequent chemical or biochemical treatments.

Cellulose is a linear and crystalline structure containing linear chains of glucose units joined by β -1,4 glycosidic bonds, with an average molecular weight of about 100 kDa. Cellulose chains, which are grouped together (20-300) by van der Waals and hydrogen bonds to form microfibrils, are constituted by repeating units of the disaccharide cellobiose. Hydrogen bonds between microfibrils form cellulose fibers, resulting in a robust and tightly packed backbone conferring structural support to the plant. However, this composition causes water insolubility and recalcitrance to depolymerization (den Haan et al., 2013; Meng and Ragauskas, 2014).

Hemicellulose is a complex heteropolymer with an average molecular weight of nearly 30 kDa. It consists of short, linear and highly branched chains of different monomers including hexoses (β -D-glucose, α -D-galactose and β -D-mannose), pentoses (β -D-xylose and α -L-arabinose) and sugar acids. The composition can dramatically vary among plants. The backbone chain of hemicellulose principally consists of pentoses like D-xylose (around 90 %) and L-arabinose (roughly 10 %) that are linked by β -1,4 bonds. The commonly known hemicelluloses are xylans and glucomannans. The role of hemicellulose is to connect lignin and cellulose fibers and giving the whole network more rigidity (Hendriks and Zeeman, 2009).

Lignin is a highly branched aromatic polymer which is present in the plant cell wall. It confers rigidity and impermeability to the structure, offering resistance to microbial attack and oxidative stress. It is a heteropolymer composed of three phenolic compounds such as coumaryl, coniferyl and sinapyl alcohol. Grasses and agricultural residues contain low amounts of lignin, ranging from 10 % to 30 % and 3-15 %, respectively, although softwoods range from 30 % to 60 % and hardwoods vary between 30 and 55 % of lignin (Zabed et al., 2017).

Fermentable sugars for bioethanol production can be obtained from cellulose and hemicellulose. Although the technology has been greatly improved, a cost-effective and competitive production of ethanol is still challenging. The efficient depolymerization of the polymers, by effective pretreatment and hydrolysis, and proficient fermentation of both hexose and pentose sugars must be achieved in the future to increase the overall ethanol yield (Kim et al., 2012; Cinelli et al., 2015).

The major challenge for lignocellulose conversion into ethanol (*Figure 1.5*) is the feedstock pretreatment. The objectives of pretreatments include (i) the reduction in crystallinity and degree of polymerization of cellulose as well as the increase of porosity to enhance

hydrolysis, (ii) prevent the degradation of pentoses, (iii) minimize the formation of inhibitory products for subsequent fermentation processes, (iv) recover lignin for conversion into valuable co-products, and (v) minimize energy inputs to be cost effective and (vi) ease of operation. Several pretreatments strategies have been developed, which can be classified into physical, chemical, physico-chemical and biological pretreatment (Zabed et al., 2017).

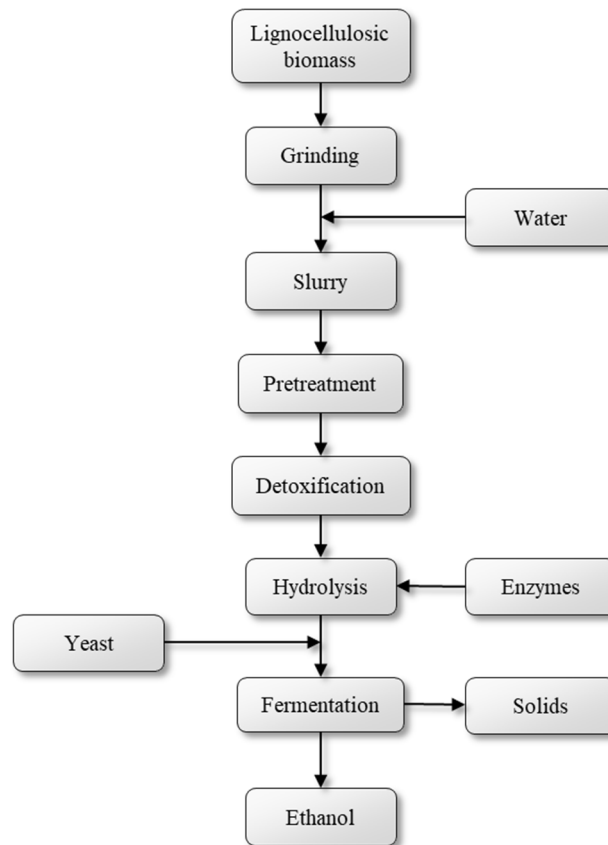


Figure 1.5 Diagram of bioethanol production from lignocellulosic biomass (adapted from Zabed et al., 2017).

Physical methods of pretreatment include mechanical grinding thermolysis and irradiation with gamma rays, electron beam or microwaves. This kind of pretreatment works on the biomass by increasing the surface area and pore volume, decreasing the degree of polymerization of cellulose and its crystallinity, but also on the hydrolysis of hemicelluloses, and partial depolymerization of lignin. During chemical pretreatments, various inorganic acids (H_2SO_4 , HCl , H_3PO_4 and HNO_3), alkali (NaOH , KOH , NH_4OH and $\text{Ca}(\text{OH})_2$), cellulose solvents (H_2O_2 , ozone, glycerol, dioxane, phenol and ethylene glycol) are commonly used to

disrupt cellulose structure and promote the hydrolysis (Alvira et al., 2010). Physico-chemical methods are considerably more effective. The combination of chemical and physical pretreatments led to the development of technologies such as steam explosion, ammonia fiber explosion (AFEX), ammonia recycling percolation (ARP), soaking aqueous ammonia (SAA), wet oxidation and CO₂ explosion. The aims are (i) to increase the accessible surface area, (ii) to decrease the crystallinity of cellulose, and (iii) to remove hemicelluloses and lignin from lignocellulose. Among biological methods white rot, brown rot and soft rot fungi such as *Phanerochaete chrysosporium*, *Trametes versicolor*, *Ceriporiopsis subvermispora*, and *Pleurotus ostreatus* are employed due to the ability to produce lignin degrading enzymes and aromatic radicals. Although this method is cheap, the hydrolysis rate is very low (Saini et al., 2015).

An efficient pretreatment with low inhibitor formation is essential for its application. Indeed, a great number of toxic compounds are formed during pretreatment and hydrolysis processes, which can seriously inhibit the subsequent fermentation. The harsh conditions of pretreatments often lead to partial breakdown of lignocellulose into different products, such as acetic acid, formic acid, levulinic acid, hydroxymethyl furfural (HMF), furfural and other phenolic compounds. These by-products act as inhibitors for both fermenting microorganisms and cellulose degrading enzymes (Alvira et al., 2010; Favaro et al., 2013; Cagnin et al., 2019). The type and amounts of inhibitors generated during pretreatment depend on both the nature of the biomass and the pretreatment conditions. The inhibitors are categorized into three major groups: aliphatic acids, furan derivatives and phenolic compounds. They can be neutralized or removed through a detoxification step, which is carried out by extraction, ion exchange, active coal, overliming, steam stripping or evaporation at low pH, and enzymatic action using laccase and peroxidase (Hamelinck et al., 2005; Jonsson et al., 2013).

The efficient hydrolysis of lignocellulosic biomass into glucose is another challenge to face. Cellulose hydrolysis can be done using both acid and enzymatic mixes. Mostly sulfuric acid (H₂SO₄) is used although other inorganic acids as well as some weak organic acids such as hydrochloric acid (HCl), nitric acid (HNO₃), trifluoroacetic acids (TFA), phosphoric acid (H₃PO₄) have also been reported. The enzymatic hydrolysis requires less energy than acid hydrolysis, however the use of massive quantities of enzymes (glucanases and xylanases) contributes to the major cost of the lignocellulosic bioethanol, accounting for 20-30 % of the

total cost. On the other hand, the addition of other enzymes and the presence of lignin and hemicellulose may increase the cost of enzymatic hydrolysis without improving the efficiency.

Due to the diverse composition of sugars, yeast capable of efficiently fermenting both hexose and pentose are needed. Unfortunately, no natural microorganisms are available (Chen and Fu, 2016; Zabed et al., 2017).

To be competitive, and economically acceptable, the cost for bioconversion of biomass to liquid fuel must be lower than the current gasoline prices (Subramanian et al., 2005).

1.4 Process consolidation for cost-effective conversion

Industrial-scale second-generation bioethanol production requires efficient, low cost processes that will ensure economic viability (Agbor et al., 2014). The reduction of processing steps in order to decrease capital and operational costs, as well as processing time, is the major improvements that is still needed. Research efforts have been recently directed to the integration of pretreatment and hydrolysis steps with fermentation (Zabed et al., 2017).

The bioethanol production at industrial scale from pretreated biomass (starchy or lignocellulosic) requires two biologically mediated events: the production of hydrolytic enzymes and the fermentation of soluble sugars. Typically, enzymatic hydrolysis and fermentation of sugars are done separately, and the process is known as separate hydrolysis and fermentation (SHF; *Figure 1.6*). The enzymatic saccharification of biomass is carried out first at the optimal temperature of the saccharifying enzymes. Subsequently, appropriate microorganisms are added to ferment the saccharified solution. The main advantage of this configuration is the application of optimal temperature conditions of both the enzymatic saccharification and the microbial fermentation, resulting in more efficient conversions at a relatively shorter duration. However, the SHF process is carried out in two separate and independent reactors, resulting in higher capital costs. In SSF process (*Figure 1.6*), enzymatic hydrolysis and alcoholic fermentation are performed simultaneously in the same reactor, thereby reducing the operational costs and increasing hydrolysis rate. Glucose resulting from hydrolysis is readily fermented to ethanol, thus the concentration of the substrate cannot inhibit saccharolytic enzymes (end-product inhibition; Sarris and Papanikolaou, 2016). SSF reduces contamination from external microflora because of high process temperature, anaerobic conditions and the presence of ethanol in the medium, while requiring lower amounts of

enzymes. However, the SSF process has disadvantages when compared with the SHF. The optimum temperature for yeast fermentation is typically lower than that for enzymatic hydrolysis (Ishizaki and Hasumi, 2014). Therefore, the saccharification requires more enzyme than the SHF process. Moreover, thermotolerant strains able to grow well and to produce ethanol at high temperature could be required.

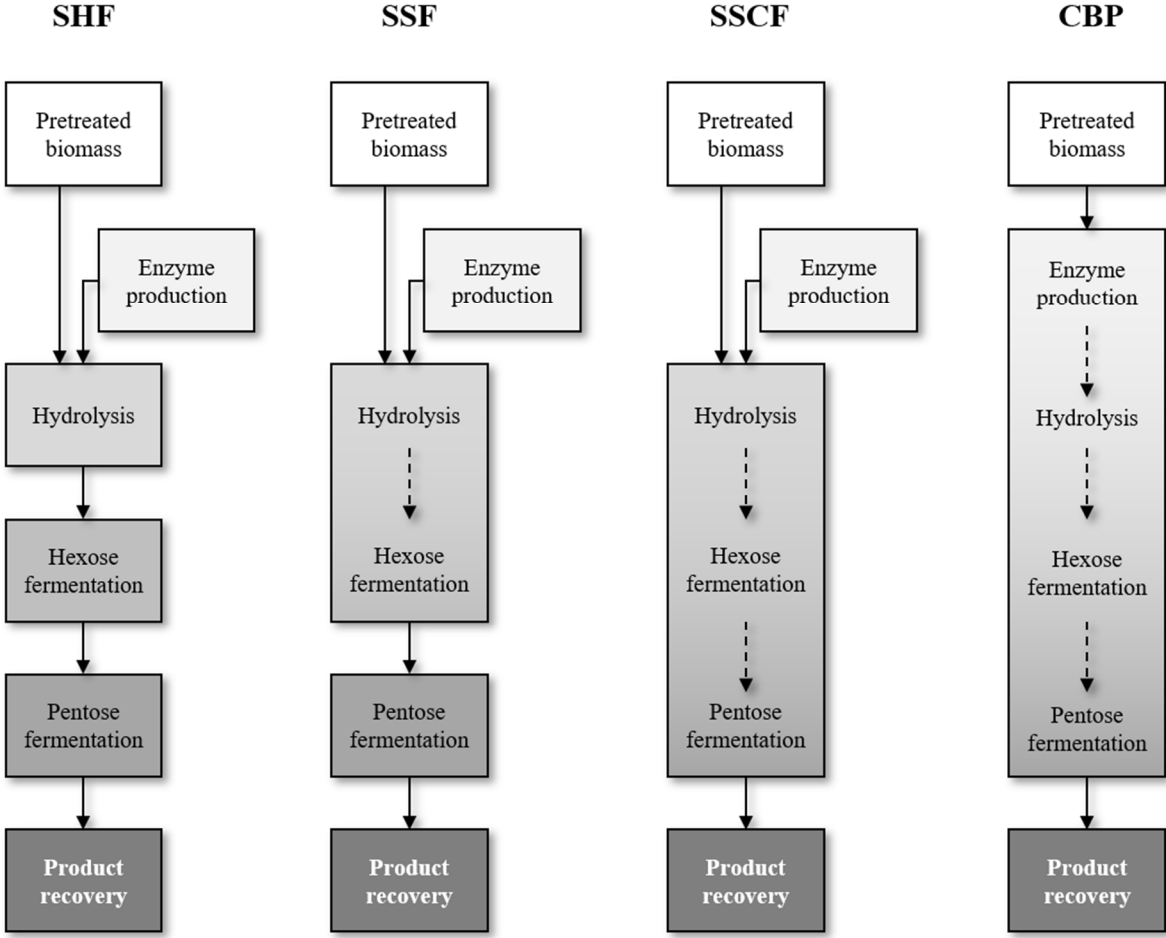


Figure 1.6 Schematic diagram of bioethanol production process configurations (adapted from Aditiya et al., 2016).

Simultaneous saccharification and co-fermentation (SSCF; Figure 1.6) of hexoses and pentoses is similar to the SSF process except that hexose and pentose fermentation occur simultaneously. This configuration requires a separate pentose-utilizing microorganism or an engineered strain capable of efficient co-utilization of hexoses and pentoses (Sarris and Papanikolaou, 2016). The ultimate configuration is the consolidated bioprocessing (CBP;

Figure 1.6), known also as direct microbial conversion (DMC), that combines the substrate hydrolysis and fermentation in one step by the use of a single microorganism. This difference has an important advantage as no capital or operation expenditures are required for enzyme production. Moreover, the enzymatic and fermentation systems are entirely compatible. Of all the reported technological advances to reduce processing costs, CBP offers the greatest potential.

Unfortunately, naturally occurring microorganisms are incapable to perform CBP. Hence, engineered microorganisms need to be developed in order to make this process suitable for industrial applications (Sarris and Papanikolaou, 2015; Ishizaki and Hasumi, 2014; Vohra et al, 2014; Rastogi and Shrivastava, 2017).

1.5 Development of a CBP microorganism for starch conversion

Genetic engineering can help for the development of a CBP strain, a robust strain to handle industrial conditions which is also able to produce bioethanol from biomass at high yield and titer (Olson et al., 2012).

As described by Lynd et al. (1999) for second generation bioethanol production from lignocellulose, two are the main strategies for genetic engineering of microbes for the desirable traits. They can also be considered for starch bioconversion. In the ‘native’ strategy, a natural hydrolytic microorganism having a superior saccharolytic capabilities can be improved by conferring high fermentative traits. On the other side, the ‘recombinant’ strategy involves a natural fermenting microorganism that can be genetically manipulated for hydrolytic enzymes production in the recombinant strategy (Lynd et al., 2005; Olson et al., 2012).

Several microorganisms including fungi, yeast, and bacteria have been reported to produce starch degrading enzymes. *Aspergillus* sp., *Rhizopus* sp. and *Bacillus* sp. are the most common choices (Robertson et al., 2006; Sun et al., 2010). The main challenge is represented by the lack of a consolidated gene-transfer technology to provide natural isolates with fermentative traits. Moreover, native hydrolytic species are isolated from soil or rumen, thus lacking in robustness towards other stressful industrial process conditions.

The primary objective of the recombinant strategy is to provide growth and fermentation capabilities on starchy biomass. Highly fermentative microorganisms can be used as recipient

for the production of heterologous amylases. *Saccharomyces cerevisiae* shows the desired fermentation performances and represents the best candidate for genome engineering. In literature, *S. cerevisiae* has already been reported for the expression of several kinds of saccharolytic enzymes collected in Pretorius (1997), Sun et al. (2010) and van Zyl et al. (2012). Initially, individual α -amylase genes were expressed. However, the very low efficiency of saccharification lead to the co-expression of α -amylase and glucoamylase genes for a synergic approach. Amylases were both secreted or tethered on the cell surface, until Liao et al. (2010) demonstrated that higher ethanol yields were obtained with secretion. The major disadvantage of cell wall-anchored enzymes is that a good mixing is required to facilitate the approach between the cells and the substrate.

To date, no industrial process has used recombinant yeast for direct ethanol production from raw starch (Cinelli et al., 2015). Soluble starch is easier to digest because of the presence of water that facilitates the enzyme to enter the starch molecules. However, the enzymatic hydrolysis of raw starch must take place between the starch granules and water. When raw starch is dispersed in a liquid medium, water molecules are associated and clustered due to hydrogen bonds on the surface of starch granules, which makes it difficult for enzyme to approach the substrate (Sun et al., 2010). It was estimated that the excess of energy demand required for heating the starch slurry during liquefaction and saccharification steps is between 10-20 % of the final ethanol value (Robertson et al., 2006). Nonetheless, the increase in viscosity can make stirring difficult, requiring additional energy inputs (van Zyl et al., 2012).

Few groups have reported bioethanol production using recombinant *S. cerevisiae* yeast capable of utilizing raw starch as carbon source. Studies were conducted on 1-2 % of starch loading obtaining high starch conversion (Favaro et al., 2012, Liao et al., 2010) or 20 % (Kim et al., 2011). They demonstrated that a higher enzyme loading is needed compared to soluble starch, resulting in a very slow rate of substrate conversion and, thus, fermentation. Yamakawa et al. (2010) used a *S. cerevisiae* strain bearing tethered glucoamylase of *Rhizopus oryzae* and α -amylase of *Streptococcus bovis*. They demonstrated a high ethanol production from 20 % of raw starch, however the inoculum was massive. Moreover, cells could be recycled for 23 repetitive fermentations without affecting the fermentative performances. Favaro et al. (2012-2013) engineered an industrial *S. cerevisiae* strain with the *Aspergillus awamori* glucoamylase. Here, the enzymatic activity was lower on raw starch than on soluble starch, because of inefficient starch hydrolysis. The same group constructed two industrial strains co-secreting the

Thermomyces lanuginosus glucoamylase (TLG1) and *Saccharomycopsis fibuligera* α -amylase (SFA1) for the first time (Favaro et al., 2015). The recombinant strains demonstrated a high enzymatic activity on raw corn starch at high loading and produced up to 55 % of the theoretical ethanol yield.

Despite good progress in yeast engineering in terms of stability and ethanol yield, the major challenge remains the production of α -amylases and glucoamylases with high substrate affinities and specific activities at titers that can effectively convert raw starch to glucose within 48-72 h to final ethanol concentrations of 10-12 % (w/v) (Bothast and Schlicher 2005).

1.5.1 Bioconversion of starch

Starch consists of two polymers of α -D-glucopyranosyl units linked by α -glycosidic bonds, namely amylose and amylopectin. Amylose is a relatively long, linear α -glucan containing around 99 % α -1,4 and 1 % α -1,6 linkages. It is composed of around 1 000 glucose units and has a molecular weight of approximately 10^5 – 10^6 Da. Amylopectin is larger than amylose (20-200 000 glucose units), with a molecular weight of 10^7 - 10^9 Da. It has a highly branched configuration with about 95 % α -1,4 and 5 % α -1,6 linkages (every 20 linkages). In common cereals, amylose takes an average of 25 % of the starch, while amylopectin around 75-80 %. The two molecules differ both in size and structure depending on the botanical origin.

In plants, starch is accumulated in many different photosynthetic or non-photosynthetic tissues and is synthesized in amyloplasts starting from a molecule of sucrose. This is derived from photosynthesis and converted in the cytosol to glucose-6-P, then translocated into the amyloplast. Here, starch synthases add glucose units to the non-reducing ends of amylose and amylopectin molecules. The branches in amylopectin are created by starch branching enzymes. The overall starch granule size varies from 1-100 μ m in diameter (Tester et al., 2004) and the polymers are organized into amorphous and crystalline regions. Generally, the crystalline regions are composed of amylopectin, while the amylose is present in the amorphous regions. In cereal starches, the amylose is complexed with lipids that form a weak crystalline structure and reinforce the granule.

While amylopectin is soluble in water, amylose and the starch granule itself are insoluble in cold water. When the water-starch slurry is heated, the granules are subjected to irreversible swelling process, termed gelatinization. At this point, amylose leaches out of the

granule and causes an increase in the viscosity of the slurry. Finally, the granules dissolve resulting in a complete viscous colloidal dispersion (van der Maarel et al., 2002).

1.5.2 Starch hydrolysing enzymes

Efficient starch hydrolysis requires the activities of both α -1,4 and α -1,6- hydrolases. Those can be classified into (i) endoamylases, (ii) exoamylases and (iii) debranching enzymes (van Zyl et al., 2012; Castro et al., 2011; van der Maarel et al., 2002).

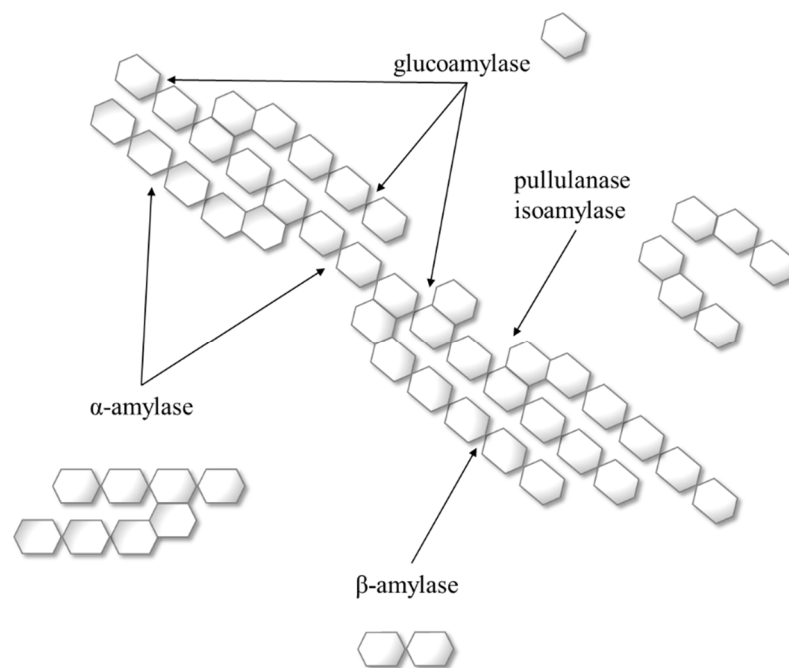


Figure 1.7 Starch molecules and target sites of different amylolytic enzymes (adapted from Aditiya et al., 2016).

Endoamylases primarily catalyze the cleavage of internal α -1,4 bonds in both amylose and amylopectin (**Figure 1.7**). The most-reported endoamylase is α -amylase (EC 3.2.1.1). The end products of α -amylase action are oligosaccharides of different lengths (10 to 20 glucose residues) and α -limit dextrins with an α -configuration. Enzymes from this group play a crucial role in starch liquefaction.

Exoamylases, such as glucoamylase (EC 3.2.1.3) and α -glucosidase (EC 3.2.1.20), act on the external glucose residues producing only glucose by cleaving both α -1,4 and α -1,6

glycosidic bonds (**Figure 1.7**). The rate of hydrolysis between linkages depends on the nature of the linkage in the adjacent molecule. Most forms of the enzyme can rapidly hydrolyze α -1,6 glycosidic bonds when the next bond in the sequence is 1,4-linked (Fierobe et al., 1998), but the specific activity towards the α -1,6 linkage is only 0.2 % of that for the α -1,4 linkage (Fierobe et al., 1996; Frandsen et al., 1995; Sierks and Svensson, 1994). On the other hand, β -amylase (EC 3.2.1.2) exclusively cleaves α -1,4 glycosidic bonds from non-reducing ends releasing maltose which is further hydrolyzed by maltases into two glucose residues. β -amylase and glucoamylase generally belong to the family of inverting enzymes. Their activity converts the anomeric configuration of the released sugar from the α to the β configuration. On the other hand, α -glucosidase is a retaining enzyme, and acts better on short malto-oligosaccharides.

The third group of starch-converting enzymes is represented by the debranching enzymes, that exclusively hydrolyze α -1,6 glycosidic bonds (**Figure 1.7**). Pullanase type I (EC 3.2.1.41) and isoamylase (EC 3.2.1.68) degrade only amylopectin, thus converting into amylose or leaving long linear polysaccharides of 25-30 glucose residues. The former, in addition to amylopectin, can also break down linkages in pullulan and glycogen structures. Pullulanase type II enzymes hydrolyze both α -1,4 and α -1,6 glycosidic bonds and are referred to as α -amylase-pullulanase or amylopullulanase. The main degradation products are maltose and maltotriose.

α -Amylase and glucoamylase play the most important role in starch saccharification in industry, being their synergy fundamental to increase the overall reaction rate. The α -amylases hydrolyze the interior linkages of the starch molecule on the surface of the granules, supplying the glucoamylases with substrate. This hydrolysis results in the formation of small holes in the granular starch molecule, which allows the α -amylase entry into the interior of the starch molecule (Buléon et al., 1998). The combination of α -amylases and glucoamylases supports the complete depolymerization of raw starch into glucose (Sun et al., 2010).

1.6 Heterologous enzyme expression in *Saccharomyces cerevisiae*

Microorganisms play a key role in bioethanol production by converting simple sugars into ethanol and CO₂ through fermentation. Theoretically, each kg of glucose and xylose can produce 0.49 kg of CO₂ and 0.51 kg of ethanol. Nearly 10 % of the total bioethanol production cost is dedicated to the microorganism (van Zyl et al., 2012).

Historically, the most common microbe used for fermentation has been the budding yeast *S. cerevisiae*. This yeast can naturally grow both on simple sugars, such as glucose, and on the disaccharides sucrose and maltose but is not capable of converting pentoses, lactose, or cellobiose. *Saccharomyces* is also generally recognized as safe (GRAS) as a food additive for human consumption and is therefore ideal for producing alcoholic beverages. It is able to ferment sugars at low pH values (4-5), thus minimizing the contamination risk at industrial level. At present, *S. cerevisiae* is widely used for the production of fuels, pharmaceuticals, and other value-added chemicals.

S. cerevisiae is commonly employed in first-generation bioethanol production. Due to general robustness, high ethanol yield and productivity, high ethanol- and osmo-tolerance, it has a long history of industrial use (Walker and Walker, 2018; Favaro et al., 2019). The major limitation, however, is that it cannot utilize complex substrates such as starch.

Since the completion of its genome sequencing (Goffeau et al., 1996), an array of gene manipulation techniques and tools has been developed for the interpretation of gene functionalities. Currently, *S. cerevisiae* is one of the most extensively used eukaryotes, and deep knowledge is now available about metabolic, secretory, transport, signaling and other pathways. Its amenability to genetic modifications makes it the preferred host for development of amylase-producing yeast for second-generation bioethanol production (Da Silva and Srikrishnan, 2012; Carter and Delneri, 2010). However, wild type and industrial strains are poorly characterized and, in contrast to laboratory strains, often recalcitrant to genetic modification because of the complexity of the genome.

Both plasmid vectors and chromosomal integration have been used for metabolic engineering of *S. cerevisiae*, although the choice depends on the overall goal (e.g. overexpression, precise control of gene number, vectors stability, ...).

1.6.1 Episomal vectors

Autonomous replicating plasmids can be categorized by their copy number into two families typically used in metabolic engineering: YCp, a low-copy plasmid, and YEp, a high-copy plasmid. YCp plasmids have a yeast origin of replication (ARS) and a centromere sequence (CEN), have high segregational stability in selective medium, and are maintained at

1-2 copies per cell. YEp plasmids are based on the native 2-micron (2 μ) episomal plasmid found in *S. cerevisiae*. These plasmids can maintain over 10-50 copies per cell, although the number can vary widely with the gene product and level of expression. Auxotrophic markers such as *TRP1*, *HIS3*, *LEU2* and *URA3* allow the positive selection of yeast cells which have correctly incorporated the respective plasmids (Pronk, 2002).

In general, low-copy plasmids are more stable and robust to different fermentation processes than high-copy plasmids and can often handle larger heterologous expression cassettes. However, high-copy plasmids allow for overexpression of the gene of interest (Redden et al., 2015).

Although the number of episomal plasmids available for yeast are much more limited than those for *Escherichia coli*, they have been successfully employed for gene expression. The major limitations are instability due to plasmid loss, the need to maintain selection pressure in culture, as well as variation in gene expression within the population especially during long term and large-scale industrial cultivations in poorly defined media (Shi et al., 2016).

1.6.2 Genome editing methods

Industrial strain development requires the chromosomal integration of expression cassettes (Jansen et al., 2017). The crucial point for genome editing in *S. cerevisiae* is the creation of double-strand breaks (DSBs) at the locus to be modified. The DNA damage can usually be repaired by (i) homologous recombination (HR), which depends on sequence homology, or (ii) non-homologous end joining (NHEJ), which is more error-prone and involves integration between regions of little or no homology. In *S. cerevisiae*, the HR pathway is very efficient (Lorenz et al., 1995) and plays a dominant role in DSB repair, requiring only 38-50 bp of target gene homology of both sides of the marker cassette (Baudin et al., 1993; Sonoda et al., 2006). The NHEJ pathway is mainly observed if the HR mechanism is prevented. Other yeast species favor the NHEJ pathway over HR making precise gene editing difficult and inefficient.

As homologous recombination is so efficient in *S. cerevisiae*, the integration of donor DNA into the genomic target offers an alternative, straightforward mechanism for gene expression (Da Silva and Srikrishnan, 2012).

Chromosomal integration also allows precise control over gene copy number and can ensure segregational stability. For the introduction of multiple genes, long-term stability, and precise control of expression, integration of the genes into the chromosome holds several advantages. A variety of vector- and PCR-based methods have been developed for single- or multicopy integration (Da Silva and Srikrishnan, 2012).

Drug-selectable markers are used for validation and maintenance of the integrated sequences. Auxotrophic markers are supposed to cause fitness changes. This limitation was overcome by using the marker recycling method. If the retention of the selectable marker in the genome is not desirable or it has to be used for another modification, site-specific recombinases can be exploited. Cre-*loxP*-mediated recombinase and *delitto perfetto* are good examples of such a system (Sauer, 1987; McLellan et al., 2017; Storici et al., 2001).

Cre-mediated recombination is a powerful tool to generate genomic rearrangements and overexpression of genes. This method involves the use of a *loxP* site and the expression of the recombinase Cre, isolated from phage P1. The *loxP* site is a 34-bp sequence composed of two 13-bp inverted repeats separated by an asymmetric 8-bp core sequence. When a dominant heterologous antibiotic resistance marker is flanked by the *loxP* sites, it can be easily excised from the genome by Cre-mediated recombination. Therefore, by the action of the Cre recombinase, the selectable marker can be rescued, leaving only one *loxP* ‘scar’ in the genome (Sauer, 1987; McLellan et al., 2017; Fraczek et al., 2018).

Delitto perfetto has been widely used for genome alterations via HR in *S. cerevisiae* (Storici et al., 2001). In the initial step, the CORE cassette (counter selectable markers and reporter genes) is inserted in the region of interest by homologous recombination. The reporter gene allows for the selection of yeast cells that receive the CORE cassette during the first step of the process. Subsequently, the CORE cassette is replaced with DNA containing the mutation of interest.

One of the main features of this technique is the ability to eliminate any marker sequences used for selection, ensuring that no foreign DNA is left in the genome, which may cause unforeseen effects. Compared with the other methods, *delitto perfetto* is simple and can easily be used for any kind of genetic modification, from a single or multiple nucleotide mutation to large deletions or chromosomal translocations (Fraczek et al., 2018).

The chromosomal δ -sequences of the yeast *S. cerevisiae* have been employed as recombination sites. The δ elements are long terminal repeats (LTRs) of the Ty 1 and 2 retrotransposons, which copy number is approximately 35 in the haploid genome. According to the genome sequence of strain S288c (Goffeau et al., 1996), there are several hundred δ elements dispersed in the *S. cerevisiae* chromosomes as solo δ elements or associated with Ty elements (Dujon, 1996). The possibility to integrate at multiple sites in combination with an antibiotic selection has led to high efficiency of multicopy integration in a single transformation. However, despite the large number of possible integration sites, inserts can result in long tandem repeats at one location (Wang et al., 1996; Da Silva and Srikrishnan, 2012). Three are the major drawbacks: (i) the method can generally be used only once or twice due to the inability of marker recycling; (ii) the tandem nature of the integrations can lead to high genome instability; (iii) it is not possible to introduce a precise number of gene copies.

Genetic modification of complex industrial yeast genomes (diploid or polyploid strains) has recently been strongly accelerated by novel genome editing tools (Jansen et al., 2017).

The recently developed Clustered Regularly Interspaced Short Palindromic Repeats (CRISPR)/CRISPR associated (Cas) protein system is widely considered as the technology of choice for metabolic engineering. Compared to other endonuclease-based and recombineering methods, it has proven to be a fast, marker-free, versatile and most importantly targeted genome-editing technique (Jakočiūnas et al., 2016). It is based on the ability to repair the DNA after a DSB. Two are the possible mechanisms: non-homologous end joining (NHEJ) and homology-directed repair (HDR). In NHEJ, the DNA ends are ligated so that a deletion or insertion of one or several nucleotides may arise. In HDR, a template (chromosome, plasmid, exogenous DNA or oligonucleotide) is used to copy the DSB locus. Thus, it is possible to perform a DNA modification by making a DSB in a certain site and a nuclease can repair the damage with high efficiency incorporating the sequence of interest (**Figure 1.8**).

Historically, CRISPR array was first discovered in the *E. coli* genome as palindromic repeats interspaced with short DNA sequences (Ishino et al., 1987). Later, the short DNA sequences (protospacers) were demonstrated to be originally viral or plasmid DNA fragments that were incorporated (spacers) into the host genome.

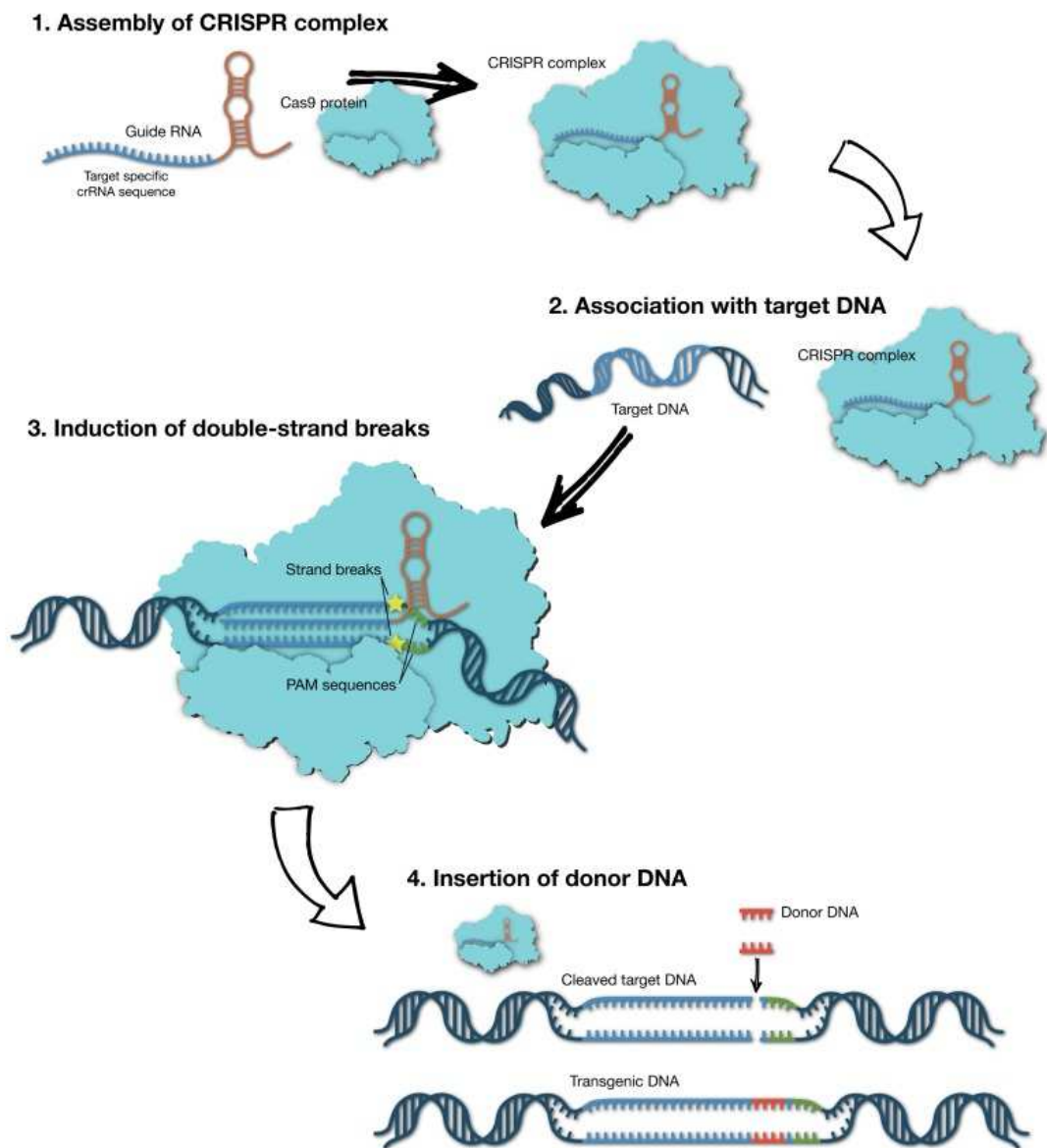


Figure 1.8 Mechanism of CRISPR/Cas9 genome editing. CRISPR/Cas9 genome editing requires a single guide (sg) RNA that directs the Cas9 endonuclease to a specific region of the genomic DNA, resulting in a double strand break. By providing a donor DNA in trans, a transgenic DNA can be created, whereas in the absence of a donor DNA, the double strand break will be repaired by the host cell, resulting in an insertion or deletion, thus potentially disrupting the open reading frame of a gene (Costa et al., 2017).

The spacer-containing CRISPR locus can be transcribed into CRISPR RNAs (crRNAs) molecules that direct nuclease activity. crRNAs undergo maturation and duplex formation with an accessory trans-activating RNA (tracrRNA). The hybrid crRNA-tracrRNA (sgRNA) molecule associates with Cas proteins type II. The ribonucleoprotein complex recognizes the target DNA because of the hybridization to the crRNA spacer, and Cas protein cleaves the sequence creating a blunt-ended DSB. As such, the CRISPR/Cas system is used by bacteria and archaea to degrade exogenous DNA as a defence mechanism against viruses.

The best characterized CRISPR/Cas immune mechanism is the one from *Streptococcus pyogenes* (Jinek et al., 2012; Doudna and Charpentier, 2014). The *S. pyogenes* Cas9 is an endonuclease with two nuclease domains, RuvC and HNH, and a two-lobe structure. The RuvC and HNH nuclease domains, each able to nick a strand of DNA to generate a blunt-ended DSB. With appropriate modifications, such single catalytical domain inactivation, Cas9 can be converted into a DNA nickase that creates a single-stranded break (SSB). The crRNA binds between the two lobes, while the spacer interacts with the α -helix that connects the two lobes. Cas9 recognizes the protospacer when a protospacer adjacent motif (PAM) flanks the sequence. The PAM sequence consists of three nucleotides, whose sequence is 5'-NGG-3', and it is fundamental to activate the Cas9 helicase activity. Cas9 generates a DSB at the position +3 upstream of the PAM, providing the start of the HDR machinery. Theoretically, any genomic loci followed by the 5'-NGG-3' PAM sequence can be targeted by Cas9.

In genome editing, the construction of a crRNA-tracrRNA hybrid, called single guide RNA (sgRNA), was fundamental to direct Cas9 toward a target site. The sgRNA consists of approximately 80 nt, including a 20-nt spacer. Thus, a substitution of only 20 nt makes it possible to target Cas9 to a new DNA site (Bannikov and Lavrov, 2016; Jakočiūnas et al., 2016; Stovicek et al., 2015). The sgRNA efficiency depends on the stability of the molecule, the affinity for Cas9 and the nucleotide sequence. The most efficient sgRNAs have a GC content higher than 50 %, and the stability is given by transient expression rather than continuous. Several web-based computer-aided design tools have been developed to allow facile display and selection of gRNAs with highest sequence-specificity towards the genomic loci of interest (CRISPRdirect; E-CRISP; CRISPy). All together such tools help design suitable gRNAs with minimal off-target effects (Jakočiūnas et al., 2016).

Introduction of DSBs at a specific genomic position by Cas9 has allowed for gene replacement, gene deletions, pathway construction, and single base editing. Cas9 and associated gRNAs have been used in many organisms for gene knock-outs (Gaj et al., 2013) and gene fusions (Wei et al., 2013), as well as genome alteration in bacteria (Jiang et al., 2013; Tsarmopoulos et al., 2016), various fungi (DiCarlo et al., 2013; Wagner and Alper, 2015), zebrafish (Hwang et al., 2013), *Caenorhabditis elegans* (Friedland et al., 2013), *Drosophila melanogaster* (Gratz et al., 2013), plants (Mao et al., 2013), and human cells (Cho et al., 2013; Jinek et al., 2013; Mali et al., 2013; Ran et al., 2013).

Gene insertion is achieved by exogenously supplying repair DNA (donor DNA), either plasmid or PCR amplicon, with proper flanking homologous regions. The HDR efficiency depends on the nature of the donor DNA, although Finnigan and Thorner (2016) demonstrated that even very limited homology of flanking regions can result in efficient repair.

Several efforts were made to adapt the CRISPR/Cas9 system for *S. cerevisiae* genome engineering. Few studies have used the native sequence of *S. pyogenes* Cas9 or a yeast codon-optimized Cas9, but the prevalent strategy is the use of a human codon optimized *S. pyogenes* Cas9 under the control of moderate yeast promoter on a centromeric plasmid (CEN/ARS; Ryan et al., 2014; Stovicek et al., 2015; Jakočiūnas et al., 2015). The gRNA is commonly expressed by the RNA polymerase III promoter (*SNR52*) and the 3' flanking sequence of the yeast tRNA gene *SUP4* as terminator.

Moreover, improvements in targeting multiple genomic loci, termed 'multiplexing', in a single transformation event by cloning and delivery of unique sgRNAs (Jessop-Fabre et al., 2016) have greatly expanded the possibilities for yeast strain creation.

The ability to manipulate the genome through Cas9 editing method has several advantages over conventional cloning methods: (i) the survival after DSBs can be considered as a selection tool in yeast since such damage is poorly tolerated; (ii) a broader range of selectable marker can be used for plasmid vectors; (iii) the choice over the site of integration is fundamental for gene insertion, single-point mutations or editing of essential genes; (iv) the multiplexing allows large-scale gene replacement (Giersch et al., 2017; Fraczek et al., 2018).

Despite all the mentioned points, the major limitation is that Cas9 requires the PAM motif to be recognized and perform the cut. Therefore, the CRISPR/Cas9 system can only be applied to sequences that are proximal to the specific PAM motifs 5'-NGG-3'. The PAM is specific to each Cas9 ortholog, even within the same species, such as 5'-NNA GAAW for *Streptococcus thermophilus* CRISPR1 (Deveau et al., 2008) and 5'-NGGNG for *Streptococcus thermophilus* CRISPR3 (Horvath et al., 2008). Further analysis of microorganisms containing CRISPR loci could lead to the discovery of Cas endonucleases with alternative PAM sequences to expand the chances of targeting sequences of interest.

The short 20-nt target sequences in gRNA could raise an important concern about possible off-target effects. Few studies have demonstrated that the CRISPR/Cas9 system can induce substantial off-target mutations. These off-target effects might play a role in recognizing and destroying hypervariable viral nucleic acids or plasmid DNA, which is beneficial to bacteria and archaea. Although the Cas9-mediated cleavage can be inhibited by a single mismatch between the complementary gRNA and the target sequence of the genome, a mismatch at the 5'-terminal of the target site is better tolerated. Thus, it is important to evaluate the potential effects of off-target mutation by computational methods and predictions. Because of the high efficiency of HDR in yeast, off-targets are unlikely to occur (Peng et al., 2016).

Overall, the combination of HDR and CRISPR/Cas9 system represents a powerful mechanism to enable the marker-free, one-step integration of heterologous genes for the production of proteins in *S. cerevisiae* (Jensen et al., 2015; Stovicek et al., 2017; Giersch et al., 2017; Jakočiūnas et al., 2017; Lian et al., 2018).

2. MATERIALS AND METHODS

2.1 Cultivation media

The media used in this study are reported in *Table 2.1*. All powders were resuspended in deionized water. Chemicals, media components and supplements were of analytical grade standard.

Medium	Composition
Luria Bertani (LB)	g/L: yeast extract, 5; tryptone, 10; NaCl, 10
Wallerstein Laboratory (WL)	g/L: yeast extract, 4; casein hydrolysate, 5; D-glucose, 50; KH ₂ PO ₄ , 0.55; KCl, 0.425; CaCl ₂ , 0.125; MgSO ₄ , 0.125; FeCl ₃ , 0.0025; MnSO ₄ , 0.0025; bromocresol green, 0.022
Yeast Peptone Dextrose (YPD)	g/L: yeast extract, 10; peptone, 20; glucose, 20
Must Nutrient Synthetic (MNS)	g/L: (NH ₄) ₂ SO ₄ , 0.3; (NH ₄) ₂ HPO ₄ , 0.3; KH ₂ PO ₄ , 1; MgSO ₄ ·7H ₂ O, 0.5; NaCl, 0.1; malic acid, 2; tartaric acid, 0.003; biotin, 0.02; D-pantothenic acid, 0.4; myo-inositol, 2; nicotinic acid, 0.4; thiamine, 0.4; pyridoxine, 0.4; p-aminobenzoic acid, 0.2; H ₃ BO ₃ , 0.5; CuSO ₄ ·5H ₂ O, 0.04; KI, 0.1; NaMoO ₄ ·2H ₂ O, 0.2; ZnSO ₄ ·7H ₂ O, 0.4; FeCl ₃ ·6H ₂ O, 0.4; CaCl ₂ ·2H ₂ O, 100
Yeast Nitrogen Base with aminoacids (YNB, Sigma-Aldrich)	g/L: (NH ₄) ₂ SO ₄ , 5; KH ₂ PO ₄ , 1; MgSO ₄ , 0.5; NaCl, 0.1; CaCl ₂ , 0.1 mg/L: L-histidine, 10; DL-methionine, 20; DL-tryptophan, 20 μg/L: biotin, 2; calcium pantothenate, 400; folic acid, 2; inositol, 2000; nicotinic acid, 400; p-aminobenzoic acid, 200; pyridoxine HCl, 400; riboflavin, 200; thiamine HCl, 400 trace elements: H ₃ BO ₃ , CuSO ₄ , KI, FeCl ₃ , MgSO ₄ , Na ₂ MoO ₄ , ZnSO ₄

Table 2.1 Summary and composition of media used in this study.

The solutions were sterilized at 121 °C for 20 minutes, except for YNB and concentrated 20 % w/v glucose solution that were sterilized by filtration through 0.22-μm

sterile filters (Corning). Solid media were obtained supplementing 1.5 % w/v agar (Liofilchem). For selective media, antibiotics such as chloramphenicol (200 mg/L; Sigma-Aldrich), ampicillin (100 mg/L; Sigma-Aldrich), streptomycin (75 mg/L; Sigma-Aldrich), geneticin (200 mg/L; Sigma-Aldrich), hygromycin B (300 mg/L; Invivogen) or nourseothricin (100 mg/L; Jena Bioscience) were used after sterilization by filtration through 0.22- μ m filters.

2.2 Strains and growth conditions

E. coli and *S. cerevisiae* strains used in this study are summarized in **Table 2.2**. A stock culture for each strain was stored at $-80\text{ }^{\circ}\text{C}$ in 20 % v/v glycerol.

Strain	Relevant phenotype / origin	Source
<i>E. coli</i> DH5 α	F- <i>endA1 glnV44 thi-1 recA1 relA1 gyrA96 deoR nupG purB20</i> ϕ 80dlacZ Δ M15 Δ (<i>lacZYA-argF</i>)U169, <i>hsdR17(rK-mK+)</i> , λ -	ThermoFisher
<i>S. cerevisiae</i> Ethanol Red [®]	Industrial yeast strain for bioethanol production	Lesaffre (Marcq-en-Baroeul, France)
<i>S. cerevisiae</i> L1 – L21	Wild type	This study
<i>S. cerevisiae</i> Fm17	Wild type strain with high fermentative vigour and lignocellulosic inhibitors tolerance	Favaro et al., 2013
<i>S. cerevisiae</i> M2n	Industrial distillery strain	Favaro et al., 2015
<i>S. cerevisiae</i> MEL2	Wild type strain from grape marcs	Favaro et al., 2013
<i>S. cerevisiae</i> HR4	Wild type strain from wine fermentation	Jansen et al., 2018
<i>S. cerevisiae</i> WL3	Wild type strain from wine fermentation	Jansen et al., 2018
<i>S. cerevisiae</i> Y130	Wild type strain from wine fermentation	Jansen et al., 2018

Table 2.2 Microbial strains used in this study.

2.3 Evaluation of fermentative vigour of selected wild type and industrial strains

With the final aim to obtain a CBP yeast, *S. cerevisiae* strains were selected among new isolates and reference industrial strains (**Table 2.2**).

Twenty-one new wild type yeast strains (*S. cerevisiae* L1-L21) were previously isolated in 2013 from grape marcs in a winery in Melara (Rovigo, Italy) and identified as *S. cerevisiae*. Briefly, after a storage of 30 days at the winery, 50 g of marcs were dispersed in 500 mL of sterile physiological solution (NaCl 0.85 %). The suspension was plated on WL plates containing chloramphenicol to limit bacterial growth. Plates were incubated at 30 °C for 72 h. Then, yeast colonies were purified by plating on YPD plates at 30 °C for 48 h to further proceed with genetic identification. Genetic identification was achieved by D1/D2 region sequence analysis. Amplification of D1/D2 domain was performed using primers described in **Table 2.3** according to the protocol developed by Kurtzman and Robnett (1998). Amplification products were visualized by 1 % agarose gel electrophoresis and EuroSafe Nucleic Acid Staining Solution in 1X TAE buffer and then subjected to sequencing (BMR Genomics, University of Padova). Species identification was performed after BlastN alignment (<http://blast.ncbi.nlm.nih.gov/Blast.cgi>) of the obtained sequences with those present in the Gen-Bank public database. A minimum sequence similarity level of 99 % was considered for species identification.

Primer name	Sequence
NL1	5' GCA TAT CAA TAA GCG GAG GAA AAG 3'
NL4	5' GGT CCG TGT TTC AAG ACG G 3'

Table 2.3 Primers used for strain identification according to Kurtzman and Robnett (1998).

Seven *S. cerevisiae* control strains were included as benchmark. Three of them, namely *S. cerevisiae* Fm17, M2n and MEL2, have been already employed for ethanol production from different lignocellulosic and starchy substrates (Duan et al., 2018; Favaro et al., 2015; Favaro et al., 2013), whereas three additional strains, namely *S. cerevisiae* HR4, WL3, and Y130, recently characterized for their inhibitors tolerance and fermenting abilities

(Jansen et al., 2018), were included as additional controls. Finally, *S. cerevisiae* Ethanol Red[®] was considered as industrial reference strain, which is widely applied in both first- and second-generation ethanol applications (Walker and Walker, 2018; Favaro et al., 2019).

2.3.1 Fermentative vigour in minimal broth

The fermentative vigour, as the ability to consume glucose, was assessed in minimal medium supplemented with high sugar concentration. The MNS medium (Delfini, 1995) was adopted since it can be described as a synthetic alternative of poor industrial medium. It was supplemented with 20 % w/v glucose, according to the method described by Favaro and colleagues (2013).

A pre-culture of each yeast strain (**Table 2.2**) was prepared in 1-L Erlenmeyer flask containing 500 mL YPD broth and incubated overnight at 30 °C on a rotatory shaker at 120 rpm. The cells were collected by centrifugation at 4 000 rpm for 5 min and washed twice with sterile physiological solution (NaCl 0.85 %). Fermentations were performed in 120-mL serum bottles in 100 mL of MNS medium at pH 3.5 and inoculated with an average cell number of $7.5 \cdot 10^4$ /mL. Serum bottles, sealed with rubber stoppers and a needle for CO₂ removal, were incubated in static conditions at 25 °C. The fermentation vigour was daily monitored by measuring the weight loss related to CO₂ production during fermentation, and a conversion factor of 2.118 (Delfini, 1995) was used to estimate the grams of utilized glucose per liter of MNS. *S. cerevisiae* Ethanol Red[®] was used as benchmark. Each experiment was carried out in triplicate.

2.3.2 Fermentative vigour in SSF set up on starchy substrates

The fermentative abilities of yeast strains (**Table 2.2**) were assessed on starchy substrates in a simultaneous saccharification and fermentation (SSF) configuration. To this purpose, broken rice and raw corn starch were used as representative feedstocks. Broken rice was obtained from La Pila (Isola della Scala, Verona, Italy), dried in a forced-air oven at 60 °C for 48 h and milled in a hammer mill to pass throughout a 1.25 mm screen. Raw starch from corn (Sigma-Aldrich) was used as benchmark. The raw feedstocks were stored at room temperature and no pre-treatments were performed. The starch and protein content

were preliminarily determined according to international standard methods (Horwitz et al., 1975) and reported in **Table 2.4**.

Feedstock	Dry matter, DM (%)	Protein (% DM)	Starch (% DM)
Broken rice	96.0	8.5	84.0
Raw corn starch	90.3	0.3	95.3

Table 2.4 Composition of the feedstocks used in this study.

The content of fermentable sugars, namely glucose, fructose and sucrose, in broken rice was assessed at 11.5 g/Kg on a total of 13 g/Kg of sugars. The enzymatic mixture STARGEN™ 002, kindly supplied by Genencor (DuPont-Danisco group, Itasca, IL, USA), was used for saccharification of the polysaccharide. STARGEN™ 002 is an optimized blend of *Aspergillus kawachii* α -amylase expressed in *Thricoderma reesei* and glucoamylase from *T. reesei* that work synergistically to hydrolyse granular starch to glucose. The total enzymatic activity is 570 Glucoamylase Unit (GAU)/g and specific gravity is 1.14 g/mL. STARGEN™ 002 was used following the supplier's instructions (<http://www.dupont.com/content/dam/dupont/products-and-services/industrialbiotechnology/documents/DuPont-STARGEN002-web-EN.pdf>).

Overnight pre-cultures were prepared in 500 mL YNB broth with 2 % w/v of glucose in 1-L Erlenmeyer flasks and incubated at 30 °C on a rotatory shaker at 120 rpm to reach the stationary phase. The cells were collected by centrifugation at 4 000 rpm for 5 min, then washed twice with sterile physiological solution (NaCl 0.85 %). Fermentations were performed in 120-mL serum bottles with 100 mL of YNB buffered medium (citrate buffer 0.1 M at pH 4) with 20 % w/v of dry substrate. Ampicillin and streptomycin were added to prevent bacterial contamination. The inoculum was set at an OD₆₀₀ value of 1 (10⁷ cells/mL). STARGEN™ 002 was then supplemented at ten times the recommended dosage (11.4 g/Kg of substrate). Bottles were sealed with rubber stoppers and a needle for CO₂ removal, then incubated at 30 °C on a magnetic stirrer (Cimarec i Poly 15 Multipoint stirrer, Thermo Scientific) with agitation speed at 700 rpm. The fermentation vigour was monitored as described in 2.3.1. Samples were withdrawn after 5 days, filtered through 0.22- μ m and

analyzed for glucose, ethanol and glycerol content by high performance liquid chromatography (HPLC). *S. cerevisiae* Ethanol Red[®] was used as benchmark. Each experiment was carried out in triplicate.

2.3.3 Scale-up in 1-L fermenter

The most promising strain, *S. cerevisiae* L20, exhibiting an outstanding fermentative performance at small-scale SSF over Ethanol Red[®], was up-scaled in a 1-L bioreactor (Applikon Biotechnology, Schiedam, The Netherlands) with a working volume of 900 mL. As previously described for small-scale SSF experiments, the fermentations were carried out on 20 % w/v broken rice or raw corn starch (Sigma-Aldrich) and STARGEN[™] 002 was used for saccharification. The broth formulation was already described for small-scale SSF (reported in paragraph 2.3.2) except for pH, which was controlled at 4 using automatic titration of 1 M NaOH solution. To support the oxygen-limited conditions, aeration was not supplied.

Overnight pre-cultures were prepared in 500 mL of YNB broth with 2 % w/v of glucose in 1-L Erlenmeyer flasks and incubated at 30 °C on a rotatory shaker at 120 rpm to reach the stationary phase. The cells were collected by centrifugation at 4 000 rpm for 5 min, then washed twice with sterile physiological solution (NaCl 0.85 %). Yeast cells were inoculated at OD₆₀₀ value of 1. Cultures were stirred at 300 rpm and kept at 30 °C with a heating blanket. All parameters were controlled by my-Control unit (Applikon Biotechnology). The BioXpert software version 1.13 (Applikon Biotechnology) was used for data acquisition. Samples were aseptically collected at regular intervals, then filtered through 0.22-µm and diluted for HPLC analysis. *S. cerevisiae* Ethanol Red[®] was used as benchmark. The experiment was carried out in duplicate.

2.4 Genomic DNA extraction and library sequencing of *S. cerevisiae* L20

The most promising *S. cerevisiae* strain, L20, exhibiting better fermenting abilities than the industrial benchmark *S. cerevisiae* Ethanol Red[®], was selected as recipient for the development of novel industrial CBP yeast strains.

Genomic DNA was extracted from overnight yeast cultures by zymolyase digestion and standard phenol-chloroform extraction (Treu et al., 2014). A combined sequencing approach was then applied using Illumina and Oxford Nanopore MinION single-molecule sequencers. Illumina library was generated using the TruSeq DNA PCR-Free Library Prep Kit (Illumina Inc., San Diego CA) and Covaris S2 (Woburn, MA) for a 550-bp average fragment size. Library was loaded onto the flow cell provided in the NextSeq 500 Reagent kit v2 (150 cycles) (Illumina Inc., San Diego CA) and sequenced on a NextSeq 500 (Illumina Inc., San Diego CA) platform with a paired-end protocol and read lengths of 151 bp at the CRIBI Biotechnology Center (Padova, Italy). Nanopore library was prepared according to SQK-LSK109 ligation sequencing kit and sequenced on a FLO-MIN106 R9 flowcell.

2.4.1 Next generation sequencing data analysis

The genome assembly of *S. cerevisiae* L20 strain was performed with a *de novo* approach by in house developed pipeline for combined Nanopore-Illumina sequences analysis. Briefly, the long reads were corrected with the Canu (Koren et al., 2017) software and assembled with SMARTdenovo (Ruan and Li, 2019). The obtained contigs were polished with Pilon (Walker et al., 2014) software using the independent high-quality Illumina sequences and ordered according to the *S. cerevisiae* S288c reference genome using Mauve software (Darling et al., 2010). A whole-genome alignment was then obtained with nucmer (Kurtz et al., 2004) to highlight genome completeness. The final genome of *S. cerevisiae* L20 was used to create a local database for BLAST analysis.

2.5 Yeast genome engineering

S. cerevisiae L20 was genetically modified for heterologous expression of *Aspergillus tubingensis* T8.4 α -amylase (*AmyA*) and glucoamylase (*GlaA*) genes, using both δ -integration and CRISPR/Cas9 methods. Plasmids yBBH1 carrying the *A. tubingensis* T8.4 α -amylase (*AmyA*) and glucoamylase (*GlaA*) genes, under the control of *ENO1* promoter and *ENO1* terminator, were previously used in the laboratory strain *S. cerevisiae* Y294 and the semi-industrial strain *S. cerevisiae* Mnu α (Viktor et al., 2013).

Restriction enzyme digestion, electrophoresis, DNA cloning, *E. coli* DNA isolation and transformation were performed using the standard methods according to Sambrook and Russell (2001). *S. cerevisiae* Ethanol Red[®] was included in the engineering project as reference industrial strain.

2.5.1 Yeast dominant marker resistance

The innate susceptibility of *S. cerevisiae* L20 and Ethanol Red[®] was tested for geneticin, hygromycin B and nourseothricin. Overnight pre-cultures in 20 mL YPD grown at 30 °C on a rotatory shaker at 120 rpm were used to inoculate at OD₆₀₀ value of 0.01 YPD media containing increasing concentrations of antibiotics. Aliquots of 200 µL were transferred onto a 96-microtiter cell culture plate (Greiner, CELLSTAR), and the growth was monitored at OD₆₀₀ for 24 h at 15-min intervals by using Spark Multimode Microplate Reader (TECAN). The experiment was carried out in triplicate. Yeast growth in absence of any antibiotic was used as positive control.

2.5.2 Delta integration of *AmyA* and *GlaA* genes from *A. tubingensis* T8.4 into retrotransposons Ty

S. cerevisiae L20 and Ethanol Red[®] were transformed with *AmyA* and *GlaA* cassettes targeting the δ -sequences in retrotransposons Ty. The original plasmids yBBH1-*AmyA* and yBBH1-*GlaA*, kindly provided by Professor W. H. van Zyl (Stellenbosch University, South Africa), were used as templates to amplify *ENO1_P-AmyA-ENO1_T* (2.8 kb) and *ENO1_P-GlaA-ENO1_T* (2.8 kb) cassettes. The *TEF1_P-KanMX-TEF1_T* cassette was amplified from pBKD2 plasmid. All plasmids are reported in **Table 2.5**.

PCR reactions were performed in order to provide the expression cassettes *ENO1_P-AmyA-ENO1_T* and *ENO1_P-GlaA-ENO1_T* with a 70-nt homologous flanking sequence to the integrative δ -sequence at the 5' and to ligate *in vivo* to the *TEF1_P-KanMX-TEF1_T* cassette at the 3'. Primers are reported in **Table 2.6**.

The *TEF1_P-KanMX-TEF1_T* cassette was amplified with primers reported in **Table 2.7**. The primers were designed in order to create a cassette with a homologous sequence to *ENO1_T* at the 5' and a 30-nt homologous sequence to the δ -site at the 3'.

Plasmid	Description	Size (kb)	Source/Reference
yBBH1- <i>AmyA</i>	<i>bla</i> URA3 <i>ENO1_P-AmyA-ENO1_T</i>	8.2	Viktor et al., 2013
yBBH1- <i>GlaA</i>	<i>bla</i> URA3 <i>ENO1_P-GlaA-ENO1_T</i>	8.2	Viktor et al., 2013
pBKD2	<i>amp</i> δ -sites- <i>ENO1_P-ENO1_TTEF1_P-KanMX-TEF1_T</i> - δ -sites	5.9	McBride et al., 2008 Patent PCT/US2007/085390

Table 2.5 Plasmids used for δ -integration in this study.

Primer	Sequence	Size of PCR product (kb)
<i>ENO1_P</i> Delta-L	5'- <i>TAT ACC TAA TAT TAT AGC CTT TAT CAA CAA TGG AAT CCC AAC AAT TAT CTA ATT ACC CAC ATA TAT CTC AAC TAG TCT TCT AGG CGG GTT</i> - 3'	2.8
<i>ENO1_T</i> -R	5'- <i>GTC GAA CAA CGT TCT ATT AGG AAT GGC GGA</i> -3'	

Table 2.6 Primers used for *ENO1_P-AmyA-ENO1_T* and *ENO1_P-GlaA-ENO1_T* cassettes amplification. The plasmids yBBH1-*AmyA* and yBBH1-*GlaA* were used as templates, respectively. Sequences in italics are oligos overlapping the homologous regions of δ -sites.

Primer	Sequence	Size of PCR product (kb)
<i>ENO1_T</i> marker-L	5'- <i>CCT CCT AAT GTG TCA ATG ATC ATA TTC TTA</i> - 3'	1.8
Delta-R	5'- <i>ATA TTA CGA TTA TTC CTC ATT CCG TTT TAT</i> -3'	

Table 2.7 Primers used for *TEF1_P-KanMX-TEF1_T* cassette amplification. pBKD2 plasmid (McBride et al., 2008) was used as template. Sequences in italics are oligos overlapping the homologous regions of δ -sites.

All plasmids contained bacterial *ori* and *amp* genes for replication and the expression of ampicillin resistance in *E. coli* strains. Plasmids were recovered from *E. coli* overnight cultures aerobically grown at 37 °C in LB broth containing ampicillin using Nucleospin

Plasmid Easy Pure kit (Macherey-Nagel) and quantified by NanoDrop ND-1000 spectrophotometer (Isogen).

Briefly, Takara Ex Taq DNA Polymerase and 10X Ex Taq Buffer (Takara Bio Inc.) were used for PCR amplification of expression cassettes. The thermal protocol was designed as follows: initial denaturation at 98 °C for 10 sec, followed by annealing at 54 °C for 30 sec and extension at 72 °C for 3 min. A final elongation step was performed at 72 °C for 5 min. Amplification products were checked by 0.8 % agarose gel electrophoresis in 1X TAE buffer and stained with ethidium bromide. The molecular weight was assessed by using O'GeneRuler 1kb Plus DNA Ladder (Thermo Scientific) as reference.

The final DNA sequences used for *in vivo* ligation and multi-copy chromosomal integration were δ -*ENO1_P-AmyA-ENO1_T-KanMX- δ* (4.6 kb) and δ -*ENO1_P-GlaA-ENO1_T-KanMX- δ* (4.6 kb).

2.5.2.1 Electrotransformation of yeast strains with integrative linear donor DNA fragments

Yeast strains were pre-cultured in 5 mL of YPD medium in glass test tubes and incubated overnight on a rotating wheel at 30 °C. An aliquot of 100 μ L was used to inoculate 100 mL of fresh YPD in 250 mL Erlenmeyer flasks and incubated at 30 °C on a rotatory shaker at 200 rpm to reach a log phase at OD₆₀₀ of 0.7-0.9 (about 3 to 4 h). A volume of 5 mL was used to harvest the cells by centrifugation at 4 000 rpm for 2 min. The cells were washed twice with iced cold water to remove salts. Cells were then transferred into Eppendorf tubes and resuspended in 800 μ L of iced cold water, TE buffer (100 mM Tris Cl, 10 mM EDTA, pH 7.5) and 0.1 M LiAC acetate to increase the transformation efficiency. After 45 min of incubation on a rotating wheel at 30 °C, 20 μ L of dithiothreitol (DTT) 1 M was added and the tubes were incubated at 30 °C for additional 15 min. Cells were harvested by centrifugation at 4 000 rpm for 2 min and washed with 1 mL cold water first, then centrifugated again and resuspended with 1 mL electroporation buffer containing 1 M sorbitol and 20 mM HEPES. 50 μ L of cells were transformed according to Cho et al. (1999) with 1 μ g of *ENO1_P-AmyA-ENO1_T*, *ENO1_P-GlaA-ENO1_T* and *TEF1_P-KanMX-TEF1_T* concurrently. In 0.2 cm electroporation cuvettes, an electric pulse of 1.4 kV, 200 Ω and 25 μ F was applied using a BioRad system (GenePluserXcell, Bio-Rad, Hercules, CA, USA).

Cells were immediately suspended in YPD containing 1 M sorbitol and incubated at 30 °C for 3 h to allow recovery. Electroporated cells were then plated onto YPD supplemented with 1 M sorbitol and geneticin (200 mg/L) and incubated at 30 °C for 48 h.

2.5.2.2 Selection of positive transformants

Colonies grown on selective plates were investigated for gene integration and amylolytic activity. As a preliminary screening, potential recombinants were cultured in 5 mL YPD for 72 h at 30 °C on a rotatory shaker at 120 rpm. 5 µL of the culture were spotted onto YNB 0.2 % soluble starch plates and incubated for 48 h at 30 °C. The starch hydrolysis was then visualized by Lugol (Sigma-Aldrich) staining. Colonies secreting α -amylase/glucoamylase resulted in clear zones, as described by Viktor et al. (2013) and Favaro et al. (2015).

2.5.2.3 PCR confirmation of positive integration

To confirm the chromosomal integration of heterologous genes in δ -sites, a PCR amplification was performed by using a pair of primers binding the *AmyA* or *GlaA* genes (**Table 2.8**).

The DNA was extracted using the PCI (phenol:chloroform:isoamyl alcohol 25:24:1, Sigma-Aldrich) solution with subsequent ethanol precipitation. In a screw cap tube, yeast cells were resuspended in 200 µL of deionized water. 1.5 g of glass beads with 0.5 mm diameter and 200 µL of the lower phase of PCI mix were added. The mixture was vortexed for 30 sec at the maximum speed. Following the centrifugation at 14 000 rpm for 10 min, 80 µL of the supernatant was transferred in 1.5 mL Eppendorf tubes. Cold absolute ethanol was added, and the tube stored at - 80 °C for 30 min. The tubes were centrifuged again at 4 °C and 14 000 rpm for 5 min and the supernatant discarded. The resulting pellet was washed with 100 µL of cold 70 % ethanol and centrifuged again. The pellet was dried at 42 °C and dissolved in 50 µL of MilliQ water. The DNA was then used as template. The DNA of the not-transformed strain was used as negative control.

GoTaq G2 DNA Polymerase and 5x Colorless GoTaq Reaction Buffer (Promega) were used for PCR amplification. The thermal protocol was designed as follows: initial

Primer	Binding site	Sequence	Size of PCR product
DeltaAmyA Fw	AmyA gene	5'-GCA TCA GCA ACC TCT ACA ACA-3'	299 bp
C-8799 Rv		5'-CGC GTT TGT GGT GGC TAT CCA GG-3'	
DeltaGlaA Fw	GlaA gene	5'-CAT CCA CAC CTT TGA TCC TG-3'	483 bp
C-8797 Rv		5'-CGA GCA GAA AGC TCG TCG CCA T-3'	

Table 2.8 Primers used to confirm the integration of heterologous genes *AmyA* and *GlaA* at δ -sites in *S. cerevisiae* L20 and Ethanol Red® strains.

incubation at 95 °C for 2 min followed by 30 cycles of denaturation at 95 °C for 40 sec, annealing at 54 °C for 30 sec and extension at 72 °C for 1 min. A final elongation step was performed at 72 °C for 5 min. Amplification products were separated by 1 % agarose gel electrophoresis in 1X TAE buffer and stained with EuroSafe Nucleic Acid Staining Solution. The molecular weight was assessed by using O'GeneRuler 1kb Plus DNA Ladder (Thermo Scientific) as reference. Digital images were acquired by using GENi Gel Documentation System (Syngene).

2.5.2.4 Evaluation of mitotic stability of the recombinants

The yeast strains were subjected to sequential batch cultures using non-selective YPD broth to assess the mitotic stability of the δ -integrated transformants, as reported by Favaro et al. (2012). The strains were initially inoculated in 5 mL of YPD and incubated at 30 °C at 120 rpm. Every 12 h, 5 μ L of the culture were transferred into 5 mL of fresh medium and incubated as before. After 80 generations (about 72 h) the resistance to geneticin and the production of heterologous enzymes were checked by serial dilution of the culture in sterile physiological solution (NaCl 0.85 %) and plated onto YPD plates supplemented with 0 or 200 mg/L of geneticin and onto YNB plates containing 0.2 % w/v of soluble starch. Stable recombinants showed a comparable number of colonies both in presence or absence of selective pressure, after 48 h of incubation at 30 °C.

Mitotically stable recombinants were considered for further characterization.

2.5.3 CRISPR/Cas9 mediated integration of *AmyA* and *GlaA* genes from *A. tubingenensis* T8.4 into pre-determined loci

The CRISPR/Cas9 strategy was used to insert the *AmyA* and *GlaA* heterologous genes into two chromosomal loci named mk114 and AD7. Locus mk114 (sequence 5' CAA AAG CGA CAC GTC GTC TG 3') is present on chromosome IV and was selected as target site to express *ENO1_P-AmyA-ENO1_T* cassette. On the other hand, locus AD7 (sequence 5' TAG CAT CGT GCA TGG GAT AG 3') was selected to insert *ENO1_P-GlaA-ENO1_T* cassette on chromosome VII. Integration at loci mk114 or AD7, both targeting non-coding regions, was reported as not affecting fermentative behaviour (personal communication by Professor J. Thevelein).

Plasmids for CRISPR/Cas9 method were kindly provided by Professor J. Thevelein at the laboratory of Molecular Cell Biology (MCB) of KU Leuven (Belgium). Briefly, the p51 Cas9 plasmid contains the Cas9 endonuclease with constitutive *TEF1* promoter from *S. cerevisiae* and a *KanMX* selection marker. The p59 guide RNA (gRNA) plasmid contains the guide sequence for Cas9 and a *CloNAT* cassette as selective marker. The genes of interest were cloned into the donor DNA vectors p426*hph*-mk114 and p426*hph*-AD7, consisting of sequences for homologous region 1 (HR1) and 2 (HR2) and an hygromycin B marker.

The plasmids used in this study are reported in **Table 2.9**. All plasmids contained bacterial *ori* and *amp* genes, for plasmid replication and for the expression of ampicillin resistance in *E. coli* strains (**Figure 2.1**).

The mk114 and AD7 loci of the selected strain *S. cerevisiae* L20 were first amplified and sequenced to assess the feasibility of the method. *S. cerevisiae* Ethanol Red[®] was used as reference.

The DNA was extracted using the PCI solution with subsequent ethanol precipitation as previously described in 2.5.2.3. Two couples of primers flanking the genomic loci mk114 and AD7 were designed to amplify fragments of 429 and 454 bp, respectively. The non-coding region of 880 bp, including the two ribosomal internal transcribed spacers ITS1, ITS2 and the 5.8S rRNA gene, was amplified as positive control by using the primers ITS1 and ITS4 (Guillamon et al., 1998). Primer sequences are reported in **Table 2.10**.

Plasmid	Resistance	Size (kb)	Source
p51 <i>TEF1-Cas9-KanMX</i>	<i>KanMX</i>	11.1	MCB lab (KU Leuven)
p59 gRNA mk114- <i>CloNAT</i>	<i>CloNAT</i>	6.95	MCB lab (KU Leuven)
p59 gRNA AD7- <i>CloNAT</i>	<i>CloNAT</i>	6.95	MCB lab (KU Leuven)
p426 <i>hph</i> -mk114	<i>HPH</i>	7.13	MCB lab (KU Leuven)
p426 <i>hph</i> -AD7	<i>HPH</i>	7.25	MCB lab (KU Leuven)
p426 <i>hph</i> mk114- <i>AmyA</i>	<i>HPH</i>	10.0	This work
p426 <i>hph</i> -mk114- <i>AmyA-GlaA</i>	<i>HPH</i>	12.8	This work
p426 <i>hph</i> -AD7- <i>GlaA</i>	<i>HPH</i>	10.1	This work
p426 <i>hph</i> -AD7- <i>GlaA-AmyA</i>	<i>HPH</i>	13.0	This work

Table 2.9 Plasmids used for CRISPR/Cas9 transformation. *KanMX*, *CloNAT*, *HPH* stand for geneticin, nourseothricin and hygromycin B resistance genes marker, respectively.

Locus	Primers name/Sequence	Size of PCR product
mk114	G1-mk114-Fw	429 bp
	5'-GCG CTT CTT ACG ATC ACT GG-3'	
	G1-mk114-Rv	
	5'-CTG TCC CAT TCC CCA TCC AT-3'	
AD7	G1-AD7-Fw	454 bp
	5'-GGT TGA TGC AAG TCG ATC TCA-3'	
	G1-AD7-Rv	
	5'-GCC TGG TTC AAT CTA CGG GT-3'	
ITS	ITS1	880 bp
	5'-TCC GTA GGT GAA CCT GCG G-3'	
	ITS4	
	5'-TCC TCC GCT TAT TGA TAT GC-3'	

Table 2.10 Primers used for PCR amplification of ITS1-ITS2 region and the loci mk114 and AD7 in *S. cerevisiae* L20 and Ethanol Red®.

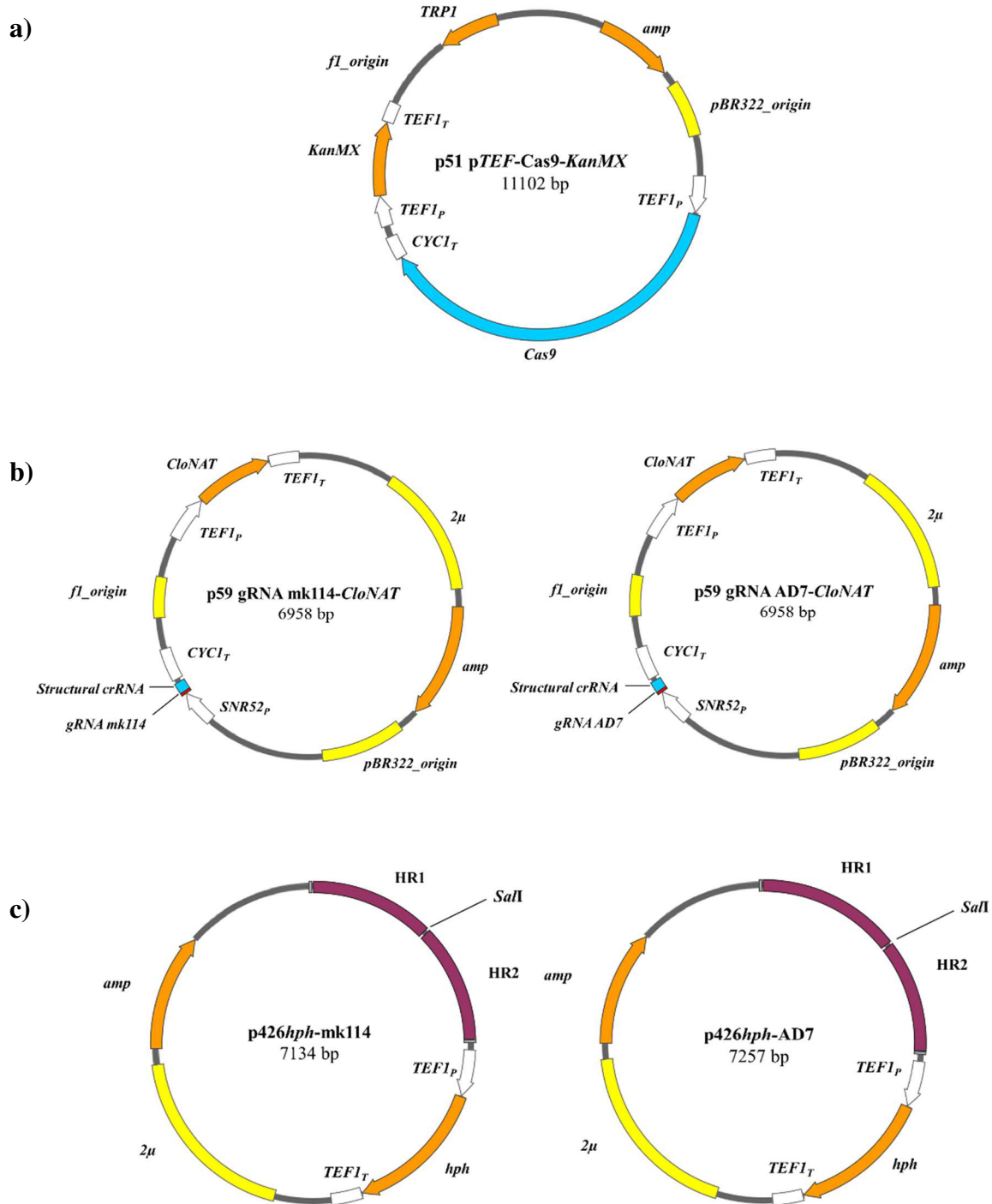


Figure 2.1 Plasmids used for CRISPR/Cas9 integration of *S. cerevisiae* strains: a) p51 *TEF1*-Cas9-*KanMX*; b) p59 gRNA mk114-*CloNAT* and p59 gRNA AD7-*CloNAT*; c) p426*hph*-mk114 and p426 *hph*-AD7 (SnapGene® Viewer 5.0.6).

The GoTaq G2 DNA Polymerase and 5x Colorless GoTaq Reaction Buffer (Promega) were used for PCR amplification. The thermal protocol was designed as follows: initial incubation at 95 °C for 2 min followed by 30 cycles of denaturation at 95 °C for 40 sec, annealing at 55 °C for 30 sec and extension at 72 °C for 1 min. A final extension step was performed at 72 °C for 5 min. The amplicons were separated by 1 % agarose gel electrophoresis in 1X TAE buffer and stained with EuroSafe Nucleic Acid Staining Solution. The molecular weight was assessed by using with O'GeneRuler 1kb Plus DNA Ladder (Thermo Scientific) and then subjected to Sanger sequencing (BMR Genomics, University of Padova). Digital images were acquired by using GENi Gel Documentation System (Syngene).

2.5.3.1 Plasmids construction

The *ENO1_P-AmyA-ENO1_T* (2.8 kb) and *ENO1_P-GlaA-ENO1_T* cassettes (2.8 kb) were directly amplified from yBBH1 plasmids used for δ -integration and cloned into p426*hph*-mk114 and p426*hph*-AD7 vectors, respectively, by Gibson Assembly (New England Biolabs). The virtual sequences of p426*hph*-mk114-*AmyA* and p426*hph*-AD7-*GlaA* were produced *in silico* and primers were designed including a 15-25 nt overlapping sequence in order to assemble adjacent fragments, according to Gibson Assembly protocol. A downstream restriction site (i. e. *KpnI* or *BamHI*) was created to allow linearization and insertion of a second cassette in tandem.

The primer sequences for single gene donor DNA plasmids are reported in **Table 2.11**.

yBBH1-*AmyA*, yBBH1-*GlaA* and donor DNA plasmid vectors were firstly isolated from *E. coli* host using Nucleospin Plasmid Easy Pure kit (Macherey-Nagel) and quantified using NanoDrop ND-1000 spectrophotometer (Isogen).

The cassettes *ENO1_P-AmyA-ENO1_T* and *ENO1_P-GlaA-ENO1_T* were amplified by means of Q5 High Fidelity polymerase and Q5 buffer (New England Biolabs) in a total volume of 50 μ L using 50 ng of template. The thermal protocol was designed as follows: initial incubation 98 °C for 30 sec followed by 30 cycles of denaturation at 98 °C for 10 sec, annealing at 61 °C for 30 sec and extension at 72 °C for 40 sec.

Cassette	Primers name/Sequence	Size of PCR product (kb)
<i>ENO1_p-AmyA-ENO1_T</i>	C-8465 Fw 5'- <i>TCA GAA GCT TAT CGA TAC CGT</i> ACT GAT CCG AGC TTC CAC T-3'	2.8
	C-8466 Rv 5'- <i>AAA GCG ACA CGT CGT GTC GAG GTA CCG</i> TCG AAC AAC GTT CTA TTA GG-3'	
<i>ENO1_p-GlaA-ENO1_T</i>	C-8467 Fw 5'- <i>GCT AAA GCT TAT CGA TAC CGT</i> ACT GAT CCG AGC TTC CAC T-3'	2.8
	C-8468 Rv 5'- <i>GCA TCG TGC ATG GGA GTC GAG GAT CCG</i> TCG AAC AAC GTT CTA TTA GG-3'	

Table 2.11 Primers used for *ENO1_p-AmyA-ENO1_T* and *ENO1_p-GlaA-ENO1_T* cassettes amplification for Gibson Assembly (New England Biolabs). The plasmids yBBH1-*AmyA* and yBBH1-*GlaA* were used as templates. Sequences in italics are oligos overlapping the plasmid vectors.

A final extension step was performed at 72 °C for 5 min. The PCR mix was incubated at 37 °C for 60 min with *DpnI* (New England Biolabs) in order to purify the fragment from the methylated template DNA. The PCR products were loaded onto a 1 % agarose gel to verify the correct amplification using O'GeneRuler 1 kb DNA Ladder (Thermo Scientific) and visualized with SYBR Safe DNA Gel (Invitrogen). Digital images were acquired by using UV light with the EpiChem3 Darkroom (UVP BioImaging Systems) with a Safe Imager from Invitrogen. The corresponding band (2.8 kb) was excised from the gel and purified using the Wizard SV Gel and PCR Clean-Up System (Promega). The fragment was quantified with NanoDrop ND-1000 spectrophotometer (Isogen) and used for subsequent Gibson Assembly (New England Biolabs).

Vectors p426*hph*-mk114 and p426*hph*-AD7 were linearized with the endonuclease *SalI*-HF in CutSmart buffer (New England Biolabs) for 1 h at 37 °C and heat inactivated at 65 °C for 20 min. The linearized vectors were loaded onto a 1 % agarose gel and stained with SYBR Safe DNA Gel (Invitrogen). Digital images were acquired by using UV light with the EpiChem3 Darkroom (UVP BioImaging Systems) with a Safe Imager from Invitrogen.

The band corresponding to the size of the backbone (< 5 kb) was excised from the gel and subsequently purified using the Wizard SV Gel and PCR Clean-Up System (Promega). FastAP alkaline phosphatase (ThermoFisher) was used to catalyze the release of 5'- and 3'-phosphate groups from vector DNA, in order to prevent recircularization during ligation. The incubation was carried out at 37 °C for 10 min and the mix was heat inactivated at 75 °C for 5 min. The vector DNA was quantified with NanoDrop ND-1000 spectrophotometer (Isogen).

The assembly was performed according to the manufacturer's recommendations. In a total volume of 20 µL, an aliquot of the vector was added to an excess of three times of the insert as well as 10 µL of Gibson Assembly Master Mix (New England Biolabs). The reaction was incubated at 50 °C for 60 min.

Competent cells of *E. coli* DH5α were used to propagate the plasmids. 50 µL of competent cells were thawed and gently mixed with 2 µL of Gibson assembled product. The cells were incubated on ice for 30 min, then heat shocked at 42 °C for 2 min. Cells were placed on ice again for 2 min and resuspended in 1 mL of LB without selective antibiotics. After 60 min of incubation at 37 °C, the cells were spread onto LB plates with ampicillin (100 mg/L). The resulting p426*hph*-mk114-*AmyA* and p426*hph*-AD7-*GlaA* plasmids were subsequently recovered by Nucleospin Plasmid Easy Pure kit (Macherey-Nagel) and sent for Sanger sequencing (Mix2Seq; Eurofins Genomics, Germany).

Plasmids p426*hph*-mk114-*AmyA* and p426*hph*-AD7-*GlaA* were subsequently used as vectors to obtain plasmids carrying a double cassette including both the amylase *AmyA* and the glucoamylase *GlaA* genes.

Vectors p426*hph*-mk114-*AmyA* and p426*hph*-AD7-*GlaA* were linearized at 37 °C for 1 h with *KpnI* (New England Biolabs) or *BamHI* (New England Biolabs) endonucleases respectively, with CutSmart buffer and heat inactivated at 65 °C for 20 min. The linearized vectors were loaded onto a 1 % agarose gel, stained with SYBR Safe DNA Gel (Invitrogen) and excised for further purification with Wizard SV Gel and PCR Clean-Up System (Promega). FastAP (ThermoFisher) was used at 37 °C for 10 min and heat inactivated at 75 °C for 5 min as previously described. The vector DNA was quantified with NanoDrop ND-1000 spectrophotometer (Isogen).

A second PCR was performed to amplify *ENO1_P-AmyA-ENO1_T* and *ENO1_P-GlaA-ENO1_T* cassettes from yBBH1-*AmyA* and yBBH1-*GlaA* plasmids, respectively, using a second pair of primers that were designed according to the maps of double gene inserts (**Table 2.12**).

Cassette	Primers name/Sequence	Size of PCR product (kb)
<i>ENO1_P-AmyA-ENO1_T</i>	C-8471 Fw	2.8
	5'- <i>TAA TAG AAC GTT GTT CGA CGT ACT GAT CCG AGC TTC CAC T</i> -3'	
	C-8472 Rv	
	5'- <i>TGC ATG GGA GTC GAG GAT CGT CGA ACA ACG TTC TAT TAG G</i> -3'	
<i>ENO1_P-GlaA-ENO1_T</i>	C-8469 Fw	2.8
	5'- <i>AGA ACG TTG TTC GAC GGT ACT ACT GAT CCG AGC TTC CAC T</i> -3'	
	C-8470 Rv	
	5'- <i>AGC GAC ACG TCG TGT CGA GGT CGA ACA ACG TTC TAT TAG G</i> -3'	

Table 2.12 Primers used for *ENO1_P-AmyA-ENO1_T* and *ENO1_P-GlaA-ENO1_T* cassettes amplification for Gibson Assembly (New England Biolabs) for the double construct. The plasmids yBBH1-*AmyA* and yBBH1-*GlaA* were used as templates. Sequences in italics are oligos overlapping the plasmid vectors.

The amplification was carried out by using the Q5 High Fidelity polymerase and Q5 buffer (New England Biolabs). In a total volume of 50 µL, 50 ng of yBBH1-*AmyA* or yBBH1-*GlaA* were used as template. The thermal protocol was designed as follows: initial incubation 98 °C for 30 sec followed by 30 cycles of denaturation at 98 °C for 10 sec, annealing at 61 °C for 30 sec and extension at 72 °C for 40 sec. A final extension step was performed at 72 °C for 5 min. The PCR mix was directly incubated at 37 °C for 60 min with *DpnI* as previously described. The PCR products were loaded onto a 1 % agarose gel to check for correct amplification by using O'GeneRuler 1 kb DNA Ladder (Thermo Scientific) and visualized with SYBR Safe DNA Gel (Invitrogen). Digital images were acquired by using UV light with the EpiChem3 Darkroom (UVP BioImaging Systems) with

a Safe Imager from Invitrogen. The corresponding band (2.8 kb) was excised from the gel and purified using the Wizard SV Gel and PCR Clean-Up System (Promega). The fragment was quantified with NanoDrop ND-1000 spectrophotometer (Isogen) and quantified used for Gibson Assembly (New England Biolabs).

The Gibson Assembly (New England Biolabs) was performed as previously described and the resulting plasmids p426*hph*-mk114-*AmyA-GlaA* and p426*hph*-AD7-*GlaA-AmyA* were sent for Sanger sequencing (Mix2Seq; Eurofins Genomics, Germany).

2.5.3.2 Yeast transformation

The transformation of yeast cells was carried out using the LiAC/SS carrier DNA/PEG method (Gietz and Schiestl, 2007).

Each strain was subjected to three sequential transformations with:

- 1) p51 *TEF1-Cas9-KanMX* plasmid and selection on YPD supplemented with geneticin (200 mg/L)
- 2) p426*hph* donor DNA and selection on YPD supplemented with geneticin (200 mg/L) and hygromycin B (300 mg/L)
- 3) p59 gRNA plasmid and selection on YPD supplemented with nourseothricin (100 mg/L).

Each transformation was carried out by including a negative control without plasmid.

Briefly, pre-cultures of yeast cells were grown in a test tube in 5 mL of YPD broth and incubated overnight with shaking at 30 °C. The concentration of the cells was evaluated at OD₆₀₀ using an Eppendorf BioPhotometer D30 and the volume was calculated to inoculate 50 mL of selective YPD to an initial OD₆₀₀ value of 0.4. The 50 mL culture was incubated at 30 °C with shaking at 200 rpm until the OD₆₀₀ reached a value of 1. The cells were then collected by centrifugation at 3 000 rpm for 5 min at 4 °C and resuspended in 1 mL of 100 mM LiAC. The cells were transferred to a 1.5 mL Eppendorf tube, pelleted at 3 000 rpm for 2 min and the supernatant removed. Finally, the cells were resuspended to a final volume of 500 µL with 100 mM LiAC. Cells were then incubated for 10 min at room

temperature and a fresh PEG/LiAC mix (1:1:8 1 M LiAC, H₂O, and 3350 PEG 50 %) was prepared. The solution was mixed vigorously by vortexing for approximately 30 sec. For each transformation, 300 µL of PEG/LiAC mix, 50 µL of competent cells, 5 µL boiled SSDNA (10mg/mL; Roche) and 1 µg of plasmid DNA were transferred into a clean Eppendorf tube. The mixture was vortexed for 10 sec and incubated in water bath at 42 °C for 30 min. Cells were recovered by centrifugation at 4 000 rpm for 2 min. A rescue period was included by resuspending the pellet in 1 mL YPD without selective antibiotics and incubating the cells for 4 h in a shaking incubator at 30 °C. After the incubation period, the cells were centrifuged for 2 min at 4 000 rpm and the pellet was resuspended in sterile water for further plating on YPD plates containing the appropriate antibiotic. Plates were finally incubated at 30 °C for 48-72 h.

2.5.3.3 PCR confirmation of positive integration

Chromosomal integration of the heterologous expression cassettes of *AmyA* and/or *GlaA* genes into the yeast genome was confirmed by PCR using appropriate primers for each locus (**Table 2.13**).

Primer	Binding site	Sequence
C-2827 Fw	Chr IV	5'-CTC GTT GGT TGC AGT ATA CT-3'
C-2828 Rv	Chr IV	5'-CGT GGA AGT TGC TGT TAC TG-3'
C-4330 Fw	Chr VII	5'-GGA GCA GAC ATC ACT AAA CG-3'
C-4331 Rv	Chr VII	5'-GCC ACA ACC AAG TGA GAT AC-3'
C-8646 Fw	<i>AmyA</i> gene	5'-CCC CAT CAC CTT CGA AGA ACT CG-3'
C-8797 Rv	<i>GlaA</i> gene	5'-CGA GCA GAA AGC TCG TCG CCA T-3'

Table 2.13 Primers used to confirm the integration of heterologous genes *AmyA* and *GlaA* at mk114 or AD7 loci in *S. cerevisiae* L20 and Ethanol Red® strains.

The primers C-2827 Fw, C-2828 Rv, C-4330 Fw and C-4331 Rv were designed on the HRs of the chromosomes IV and VII resulting in a very long fragment when the genes

are integrated. On the other hand, a very short band was the result of negative integration. Alternatively, a second couple of primers was used to specifically amplify the integrated sequence. In detail, the two primer pairs C-8646 Fw/C-2828 Rv and C-4330 Fw/C-8797 Rv were used as they can amplify within the integrated gene and the other on the chromosome. If a band was observed after gel electrophoresis, the integration was considered successful. The DNA of the parental strains was used as negative control.

The DNA of the transformants was extracted using the PCI (phenol:chloroform:isoamyl alcohol 25:24:1, Sigma-Aldrich) solution as described in 2.5.3 and used as template.

The Ex Taq DNA polymerase (TaKaRa Bio Inc., Japan) was used for PCR amplification of integrated sequences. The thermal protocol was designed as follows: initial denaturation at 94 °C for 4 min, followed by 30 cycles of denaturation at 94 °C for 10 sec, annealing at 54 °C for 30 sec and extension at 72 °C for 2 min. A final elongation step of 10 min at 72 °C was performed. PCR products were separated by 1 % agarose gel electrophoresis in 1X TAE buffer and stained with SYBR Safe DNA Gel (Invitrogen). The molecular weight was assessed by using O'GeneRuler 1 kb DNA Ladder (Thermo Scientific) as reference. Digital images were acquired by using UV light with the EpiChem3 Darkroom (UVP BioImaging Systems) with a Safe Imager from Invitrogen.

2.5.3.4 Confirmation of amyolytic enzyme(s) secretion

Colonies grown on the selective medium were investigated for secretion of amyolytic enzymes. As a preliminary screening, colonies were cultured in 5 mL YPD for 72 h at 30 °C on a rotatory shaker at 120 rpm. 5 µL of the culture were then spotted onto YNB 0.2 % soluble starch plates and incubated for 48 h at 30 °C. The starch hydrolysis was visualized by Lugol (Sigma-Aldrich) staining. As described in Favaro et al. (2013), colonies showing a clear halo were used for further analysis.

2.5.3.5 Plasmid curing and strain stability

The recombinant yeast strains were subjected to sequential batch cultures using non-selective YPD broth in order to let the cells lose the plasmid vectors and, though, the

antibiotic resistance. The strains were initially inoculated in 5 mL YPD without antibiotics and incubated at 30 °C at 120 rpm. Every 12 h, 5 µL of the culture were transferred into 5 mL of fresh medium and incubated as previously. After 80 generations (about 72 h) the resistance to geneticin, hygromycin B and nourseothricin was monitored by serial dilution of the culture in sterile physiological solution (NaCl 0.85 %) and plated onto YPD plates supplemented with antibiotics. The stability of genomic integration was demonstrated by a comparable number of colonies both in presence or absence of selective pressure after 48 h of incubation at 30 °C.

Single cells were selected on YPD plates using the Singer Instruments MSM-400 micromanipulator and incubated for 48 hours at 30 °C. Single cell colonies were used for further characterization.

2.6 Enzymatic assays

The engineered strains, obtained by both δ - and CRISPR/Cas9 integration technologies displaying a promising hydrolytic phenotype and positive genomic integration, were evaluated in terms of extracellular enzymatic activity on starch. The DNS (3,5-dinitro salicylic acid) method described by Miller (1959) was used to colourimetrically quantify the α -amylase activity, in the case of *AmyA*-expressing strains, and the total activity for the strains co-expressing both *AmyA* and *GlaA* by determining the total content of reducing sugars. The glucoamylase activity (released glucose) of the *GlaA*-expressing transformants was assessed by the D-Glucose HK Assay Kit (Megazyme, Ireland), according to the manufacturer's instructions. The assays were performed at optimal pH (pH 5) and temperature (50 °C), as reported by Viktor et al. (2013).

Briefly, yeast transformants were inoculated in 125 mL Erlenmeyer flasks in 20 mL YPD broth at an OD₆₀₀ value of 0.2 for 72 h with agitation at 120 rpm and sampling at 24-h intervals. The supernatant was recovered by centrifugation at 4 000 for 2 min and used to assay the extracellular glucoamylase and/or α -amylase activity. For DNS method, 50 µL of supernatant were incubated at 50 °C for 5 min with 450 µL of citrate buffer 0.05 M at pH 5 containing 0.2 % soluble corn starch (Sigma-Aldrich). The reaction was stopped with 750 µL of DNS solution (g/L: 3,5-dinitrosalicylic acid, 10; potassium sodium tartrate, 200; NaOH, 10; phenol, 2; Na₂SO₃, 0.5) and boiled at 100 °C for 15 min. 200 µL of the solution

were used to measure absorbance at 540 nm in a 96-well microplate (Greiner CELLSTAR) by Spark multimode microplate reader (TECAN).

The same supernatant was used for D-Glucose HK Assay Kit. 50 μ L were incubated at 50 °C for 15 minutes with 450 μ L of citrate buffer 0.05 M at pH 5 containing 0.2 % soluble corn starch (Sigma-Aldrich). The reaction was stopped by boiling at 100 °C for 10 min. 10 μ L of the solution were used as sample for the D-Glucose HK Assay Kit (Megazyme, Ireland). The absorbance was quantified at 340 nm in a 96-well microplate (Greiner CELLSTAR) by Spark multimode microplate reader (TECAN).

Glucose was used to set a standard curve. Enzymatic activities were expressed as nanokatal per mL (nKat/mL), which is defined as the enzyme activity needed to release 1 nmol of glucose per second per mL of culture. The experiments were carried out in triplicate. The parental strains were used as negative controls.

2.7 SDS-PAGE

Recombinant enzymes were characterized by separating the protein fractions by SDS-PAGE (Laemmli, 1970) containing 0.1 % soluble starch. The supernatant was denatured at 100 °C for 3 min in the presence of a loading buffer containing β -mercaptoethanol (Sambrook et al., 1989). Proteins were separated on an 8 % SDS-PAGE gel using a 5 % stacking gel and Tris-glycine buffer. Electrophoresis was performed at 110 V for 90 min. The broad-range PageRuler Prestained Protein Ladder (Fermentas) was used as a molecular mass marker. Proteins were visualised using the silver staining method (O'Connell and Stults, 1997). The solutions used for SDS-PAGE are reported in **Table 2.14**.

Gels were incubated at room temperature with shaking in a fixing solution (ethanol 30 %, 0.5 % acetic acid) for 30 min, then for 10 min in 20 % ethanol. The gels were rapidly washed with water and incubated with sodium thiosulfate solution (0.2 g/L) for 20 min. After a careful wash with water, silver nitrate solution (2 g/L) was used to stain the gel for 20 min. The gels were washed again with water for 10 sec and incubated with developing solution (20 g/L Na_2CO_3 , 900 μ L/L 40 % formaldehyde) for 5 min, till desired colour intensity was reached. Then, a stop solution (EDTA 0.5 M) was used to terminate further developing.

Solution	Composition
Loading buffer 5X	Tris-HCl pH 6.8 60 mM Glycerol 25 % SDS 2 % β -mercaptoethanol Bromophenol blue
Tris-glycine buffer 5X	Tris 25 mM Glycine 250 mM SDS 0.1 %
Separation gel 8 %	Acrylamide 30 % Tris pH 8.8 1.5 M SDS 10 % Ammonium persulfate 10 % TEMED MilliQ water
Stacking gel 5 %	Acrylamide 30 % Tris pH 6.8 1 M SDS 10 % Ammonium persulfate 10 % TEMED MilliQ water

Table 2.14 Solutions used for SDS-PAGE of heterologous enzymes production.

2.8 Starch CBP fermentation studies

The strains showing the highest hydrolysing activities on soluble starch were evaluated for their fermenting abilities on soluble corn starch (Sigma-Aldrich) and raw corn starch (Sigma-Aldrich). Small-scale fermentations were performed in 120-mL serum bottles with 100 mL of YPD broth on 2 % of dry substrate. Pre-cultures were conducted in 1-L Erlenmeyer flasks with 300 mL of YPD and incubated overnight at 30 °C on a rotatory shaker at 120 rpm. Cells were recovered by centrifugation for 5 min at 4 000 rpm and inoculated at an OD₆₀₀ value of 5 to simulate an industrial setting. Ampicillin (100 mg/L) and streptomycin (75 mg/L) were added to prevent bacterial contamination. As previously described paragraph 2.3.2, bottles were sealed with rubber stoppers and a needle for CO₂

removal, then incubated at 30 °C on a magnetic stirrer (Cimarec i Poly 15 Multipoint stirrer, Thermo Scientific) with agitation speed at 700 rpm. Samples were withdrawn every 24 h, filtered through 0.22- μ m and analyzed for glucose, ethanol and glycerol content by high performance liquid chromatography (HPLC). The experiments were carried out in triplicate. Parental strains were used as negative control.

2.9 HPLC analysis

Samples from small-scale fermentations and bioreactor experiments were analysed for their content in glucose, glycerol and ethanol through liquid chromatography using a Shimadzu Nexera HPLC system, equipped with a RID-10A refractive index detector (Shimadzu, Kyoto, Japan). The chromatographic separations were performed using a Rezex ROA-Organic Acid H+ (8 %) column (300 mm 7.8 mm, Phenomenex, Torrance, CA, USA). The column temperature was set at 60 °C and the analysis was performed at a flow rate of 0.6 mL/min using isocratic elution, with 2.5 mM H₂SO₄ as a mobile phase (Cagnin et al., 2019; Gronchi et al., 2019).

2.10 Calculations

The ethanol yield, $Y_{E/S}$, (g of ethanol/g of utilized glucose equivalent) was determined considering the amount of glucose equivalent available and compared to the maximum theoretical yield of 0.51 g of ethanol/g of consumed glucose equivalent.

The volumetric productivity (Q) was intended as grams of ethanol per liter of culture per hour (g/L/h) and the maximum volumetric productivity (Q_{max}) was defined as the highest volumetric productivity displayed by the *S. cerevisiae* strains. The theoretical CO₂ yields were determined based on the ethanol produced by each yeast strain, assuming that equimolar ethanol and CO₂ are produced. The percentage of carbon converted to glucose, ethanol, glycerol, and CO₂ was calculated on a mole carbon basis.

Statistical analyses were assessed using the Graphpad Prism 5 package (Graphpad Software, Inc., San Diego, CA, USA). Descriptive statistics mean values and standard deviations were calculated. Data were analyzed also by two ways factorial Analysis of Variance (ANOVA) with Duncan test.

3. RESULTS AND DISCUSSION

S. cerevisiae is the first choice for bioethanol production at industrial scale, either due to natural high glucose metabolism capacity, or general tolerance to industrial conditions (Walker and Walker, 2018). From an industrial point of view, it is important to select a strain able to produce ethanol at both high titers and rates from cheap substrates.

In this study, a collection of wild type *S. cerevisiae* strains was isolated from the winery environment and evaluated in terms of fermentative abilities in order to select the most suitable yeast platform for genome engineering. The final aim is the development of a CBP microorganism for efficient starch conversion into bioethanol.

The ethanol production was first evaluated on glucose as sole carbon source at high concentration (20 % w/v) to simulate industrial conditions. As a matter of fact, feedstocks with high sugar concentrations are preferred since they would reduce the production costs (Ishmayana et al., 2011). The fermentative vigour was examined in MNS (Delfini, 1995), which is a defined medium with very limited micro- and macronutrients (Dahod, 1999). This broth could be considered quite similar to several poor industrial media (Hahn-Hägerdal et al., 2005; Dahod, 1999). *S. cerevisiae* Ethanol Red[®] was used as reference industrial strain.

The strains with the highest glucose consumption were considered as the most performing, and subsequently screened in an SSF setting on starchy materials. The strain showing superior fermenting abilities, in term of fermentation rate, substrate consumption and ethanol yield, was finally considered to test its abilities at higher scale, in a 1-L bioreactor. Once again, *S. cerevisiae* Ethanol Red[®] was used as industrial benchmark. Among all isolates, the wild-type strain *S. cerevisiae* L20 demonstrated the best fermentation performances and was selected for genome engineering. To this purpose, two different genomic tools were employed to construct a yeast strains with the ability to hydrolyze starch and simultaneously ferment glucose. Namely, the well-consolidated δ -integration and the innovative CRISPR/Cas9 technologies were compared. Beyond PCR confirmation of correct integration, the new amylolytic strains were phenotypically characterised for the secretion of heterologous enzymes. Ultimately, a CBP configuration was set up to evaluate their feasibility as CBP strains on starchy substrates.

3.1 Isolation, genetic characterization and fermentative abilities of novel yeast strains on glucose

With the final aim of selecting superior fermenting strains, the winery background was chosen since it is associated with ethanol production. In this perspective, yeast are expected to produce and tolerate high alcohol concentrations. Yeast strains were isolated from grape marcs and incubated on WL plates at 30 °C. Twenty-one isolates were classified as *S. cerevisiae* species and assessed for their ability to use glucose at 30 °C in MNS minimal medium formulated with 20 % w/v glucose, as such concentration is typical of the first-generation ethanol plants after saccharification of corn (Bothast and Schlicher, 2005). Due to their relatively different phenotypic backgrounds, seven control strains of *S. cerevisiae* were included in this research as reference (**Table 2.2**). Three of these, namely *S. cerevisiae* Fm17, M2n and MEL2, have been already exploited for ethanol production from different lignocellulosic and starchy substrates (Duan et al., 2018; Favaro et al., 2015; Favaro et al., 2013), whereas the additional (*S. cerevisiae* HR4, WL3, YI30) were recently characterized for their inhibitors tolerance and fermenting abilities (Jansen et al., 2018). *S. cerevisiae* Ethanol Red[®] was considered as industrial benchmark strain, which is widely applied in both first- and second-generation ethanol applications (Walker and Walker, 2018; Favaro et al., 2019).

The glucose consumption was evaluated in MNS medium containing 20 % w/v of glucose in oxygen-limited conditions and monitored according to Delfini (1995). In **Figure 3.1** the glucose utilization is reported as grams of consumed glucose per L of MNS medium.

Generally, all strains exhibited a high and comparable level of fermenting vigour (**Figure 3.1**). However, the strains *S. cerevisiae* L1, L2, L5, L7, L8, L9 and L21, were not included as their fermenting abilities were lower than those of the reference strain M2n, which shows the bottom fermenting vigour.

Once incubated in 200 g/L glucose, the isolates quickly consumed all the sugar within 15 days (**Figure 3.1**). Among them, *S. cerevisiae* L6, L14, L15, L16 and L20 demonstrated an outstanding fermentative vigour (with 198.9, 199.2, 198.3, 193.6 and 195.9 g/L of consumed glucose at 360 h, respectively). Interestingly, their ability outperformed those reported for *S. cerevisiae* Ethanol Red[®] (189 g/L or 94.5 % of the available glucose) which exhibited one of the highest fermenting performances in the early stage of

fermentation (24, 48, 72 and 96 h). Among the reference strains, *S. cerevisiae* M2n showed the lowest fermenting vigour with 185 g/L (92.5 %) of consumed glucose. On the other hand, *S. cerevisiae* MEL2 demonstrated an interesting performance, reaching up to 199.4 g/L of consumed glucose (99.7 %). According to these preliminary results, natural isolates were considered having a promising fermentative behaviour over Ethanol Red[®].

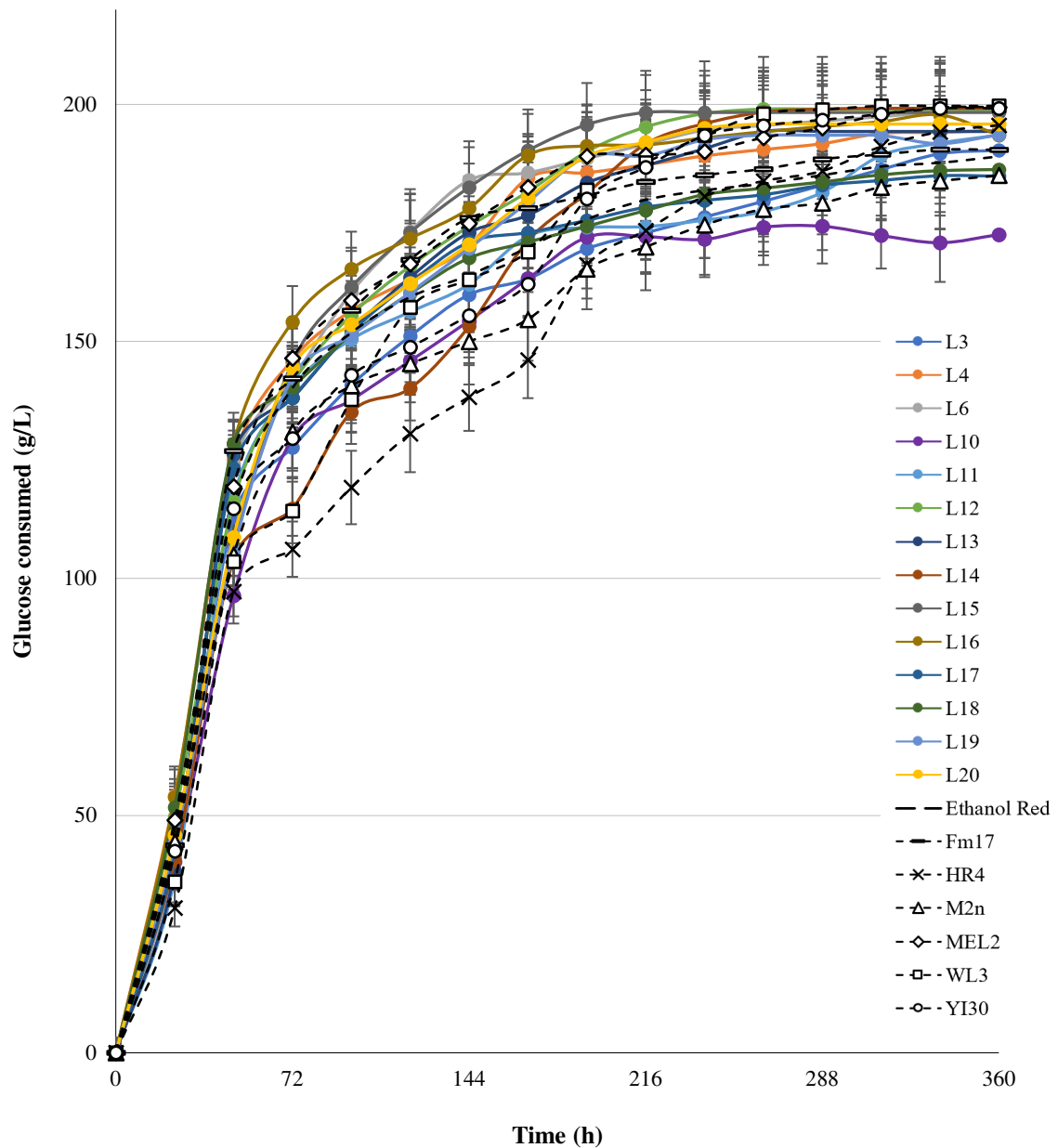


Figure 3.1 Fermentative performance of *S. cerevisiae* strains in MNS medium with glucose (20 % w/v) reported as cumulative sugar utilization (grams of glucose consumed per L of MNS). Error bars represent the standard deviation from the mean of three replicates.

Moreover, the selected newly isolated strains disclosed higher fermentative efficiency from high glucose concentrations than those recently described by several *S. cerevisiae* yeast (Favaro et al., 2013; He et al., 2012; Ortiz-Muniz et al., 2010). As such, the fermenting capabilities of the novel yeast strains are promising, considering also the medium adopted to screen for fermenting vigour. MNS broth, has indeed the lowest levels of macro and micro-nutrients when compared with the formulation of other commonly used defined media (Hahn-Hägerdal et al., 2005; Dahod, 1999). The fermenting abilities of the novel strains can be accounted as very encouraging for bioethanol production, since yeast able to grow rapidly and efficiently ferment in the first 24-48 h under nutrient limitation is of great interest for industrial scale applications. To further assess their aptitude to ferment starchy substrates under SSF configurations that is representative of starch-to-ethanol processes, the novel collection of yeast has been adopted to produce ethanol from broken rice and raw corn starch.

3.1.2 Fermentative vigour in SSF set up on starchy substrates

The strains reported in **Figure 3.1** were tested in an SSF set up to assess the fermentative vigour on raw starchy substrates at high loading (20 % w/v of DM). The commercial enzymatic mixture of amylolytic enzymes STARGEN™ 002 was used to support starch saccharification and the release of glucose. Based on the assumptions that one gram of starch is equivalent to 1.11 g of glucose (Borglum, 1980) and considering the feedstock starch content reported in **Table 2.4**, the final theoretical glucose concentration achievable by complete saccharification was 194 and 235 g/L from 20 % w/v of broken rice and corn starch, respectively.

The glucose consumption was monitored according to Delfini (1995). Due to the great volume of generated data, total cumulative glucose consumption (**Figure 3.2**) and fermentation parameters (**Table 3.1**) are reported only for the best nine fermenting strains (namely L11, L12, L13, L15, L16, L17, L18, L19 and L20) as well as for the top-performing reference yeast *S. cerevisiae* WL3 and Ethanol Red®. The strains demonstrating a glucose consumption significantly lower than Ethanol Red® were not considered as proficient fermenting yeast.

When broken rice was used as feedstock, all strains showed a similar fermenting vigour and only slight differences could be appreciated between the references and the new isolated strains (**Figure 3.2a**). Considering that the theoretical glucose content of broken rice 20 % w/v amounted at 194 g/L, the highest glucose consumption obtained at the end of fermentation was approximately 97 % for *S. cerevisiae* L18 and L20 (188 g/L).

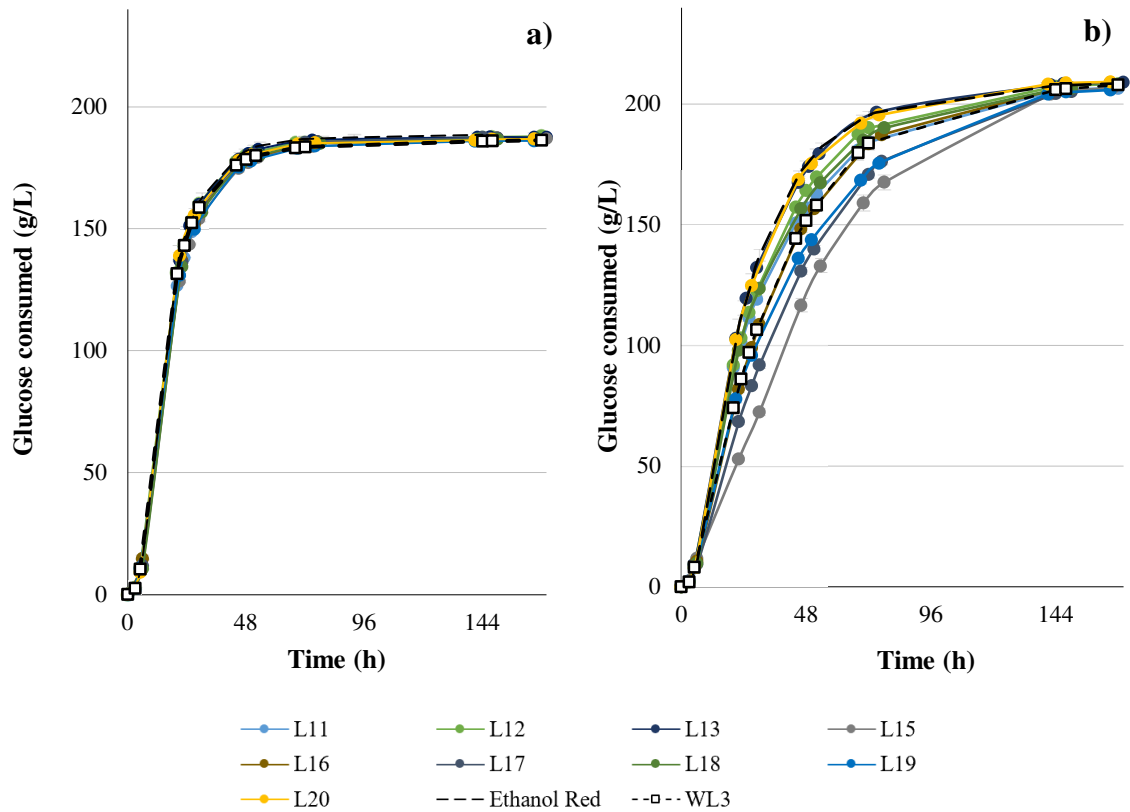


Figure 3.2 Cumulative sugar utilization (g/L) of *S. cerevisiae* strains at 30 °C in YNB medium with 20 % w/v (a) broken rice or (b) raw corn starch, in the presence of STARGEN™ 002. Error bars represent standard deviation from the mean of three replicates.

The very high ethanol levels detected by HPLC confirmed that broken rice is a promising material for ethanol production (Favaro et al., 2017; de Cassia de Souza Schneider et al., 2018; Chu-Ky et al., 2016) with more than 100 g/L of ethanol produced (**Table 3.1**). Nevertheless, this substrate was not suitable for strains selection, since no significant differences, at least in terms of fermenting vigour, were evident among the screened yeast isolates. This could be ascribed to the native high amount of simple sugars

(mainly glucose, fructose and sucrose) and proteins (8.5 % DM) of broken rice (**Table 2.4**), which could have boosted and supported the fermenting activities.

On the other hand, raw corn starch demonstrated to be a useful feedstock for screening the new isolates. The protein content was very limited (0.3 % DM, **Table 2.4**) and no free sugars were available. As reported in **Figure 3.2b**, comparable but different levels of fermenting vigour could be appreciated among the selected strains. However, considering the theoretical glucose content of 235 g/L, only about 85 % of the glucose available was utilized. Noteworthy, a small number of strains, including *S. cerevisiae* L13 (208.9 g/L), L20 (206.5 g/L) and WL3 (207.9 g/L), performed very similarly to Ethanol Red[®] (208.7 g/L) which clearly reaffirmed its great ability to consume glucose.

The HPLC analysis revealed that traces of glucose could be found in only few spent fermentation broths (**Table 3.1**) demonstrating that most of the strains were able to utilize the sugar completely. The cluster of strains reported in **Figure 3.2** produced significantly greater ethanol levels than the industrial *S. cerevisiae* Ethanol Red[®] from both broken rice and raw corn starch. Although presenting the fastest glucose consumption, Ethanol Red[®] was outperformed in terms of ethanol yield by all the selected novel strains as well as by the reference *S. cerevisiae* WL3, recently described for promising fermenting performances (Jansen et al., 2018).

As expected, glycerol was detected as a common secondary fermentation product. According to what is reported in literature for vinification processes, the concentrations of glycerol were found to be nearly 10 times smaller than the produced ethanol (Ribereau-Gayon et al., 2006). To increase ethanol production as biofuel, it is fundamental to minimize glycerol formation to better redirect the carbon flux towards ethanol (Favaro et al., 2019; Gombert and van Maris, 2015). Interestingly, all newly isolated strains together with the reference yeast WL3 produced glycerol at comparable levels from both broken rice and raw corn starch confirming their great ability to rapidly convert glucose into ethanol. On the contrary, *S. cerevisiae* Ethanol Red[®] achieved one of the highest glycerol productions when SSF was conducted on raw starch as well as on broken rice (**Table 3.1**).

Strain	Broken rice (a glucose equivalent of 198.55 g/L)				Raw corn starch (a glucose equivalent of 238.82 g/L)			
	Residual glucose (g/L)	Glycerol (g/L)	Ethanol concentration (g/L)	$Y_{E/S}$	Residual glucose (g/L)	Glycerol (g/L)	Ethanol concentration (g/L)	$Y_{E/S}$
Ethanol Red®	-	8.83 ± 0.12	101.05 ± 0.54	91	0.30 ± 0.06	10.05 ± 0.17	109.36 ± 0.33	86
L11	-	8.75 ± 0.02	107.70 ± 0.44	97	1.68 ± 0.28	9.19 ± 0.20	116.07 ± 0.06	91
L12	0.58 ± 0.14	9.03 ± 0.03	108.39 ± 1.22	98	0.82 ± 0.65	9.21 ± 0.19	116.22 ± 1.97	91
L13	0.62 ± 0.01	9.45 ± 0.18	107.15 ± 0.28	97	1.55 ± 0.76	9.63 ± 0.04	116.12 ± 0.96	91
L15	-	8.90 ± 0.06	107.43 ± 0.16	97	-	8.24 ± 0.08	117.17 ± 0.08	92
L16	-	8.93 ± 0.04	107.77 ± 0.21	97	-	9.25 ± 0.15	117.93 ± 0.14	92
L17	-	8.36 ± 0.02	107.16 ± 0.66	97	-	8.53 ± 0.01	116.78 ± 0.42	92
L18	-	7.79 ± 0.05	106.73 ± 0.34	96	-	8.45 ± 0.09	117.35 ± 1.06	92
L19	-	8.25 ± 0.08	107.32 ± 0.25	97	-	8.60 ± 0.11	116.44 ± 0.21	91
L20	-	8.17 ± 0.14	107.19 ± 0.15	97	-	7.97 ± 0.09	116.98 ± 1.73	92
WL3	0.30 ± 0.01	9.16 ± 0.12	106.17 ± 0.36	96	0.29 ± 0.04	9.60 ± 0.07	115.05 ± 0.24	90

Table 3.1 Ethanol, glucose and glycerol content of SSF experiment at 30 °C using broken rice or raw corn starch as substrate at high loading (20 % w/v). Values represent the mean of three replicates (±SD). $Y_{E/S}$, % of theoretical maximum ethanol yield per gram of glucose equivalent available.

The experiments on fermenting vigour from glucose (*Figure 3.1*) and SSF configurations with broken rice and raw corn starch as substrates (*Figure 3.2* and *Table 3.1*) indicated that the selected strains have great potential as ethanol producers, with performances even higher than those demonstrated by several reference strains. More specifically, *S. cerevisiae* L20 displayed one of the most outperforming phenotypes, particularly in the early stage of fermentation, and was then selected for further fermentation experiments at bioreactor scale.

3.1.3 Scale-up in 1-L fermenter

S. cerevisiae L20 and the industrial benchmark *S. cerevisiae* Ethanol Red[®] have been investigated for SSF in 1-L bench reactor using 20 % w/v of broken rice or raw corn starch (*Figure 3.3* and *Table 3.2*). As previously mentioned for SSF at smaller scale, STARGEN[™] 002 was used to support starch saccharification.

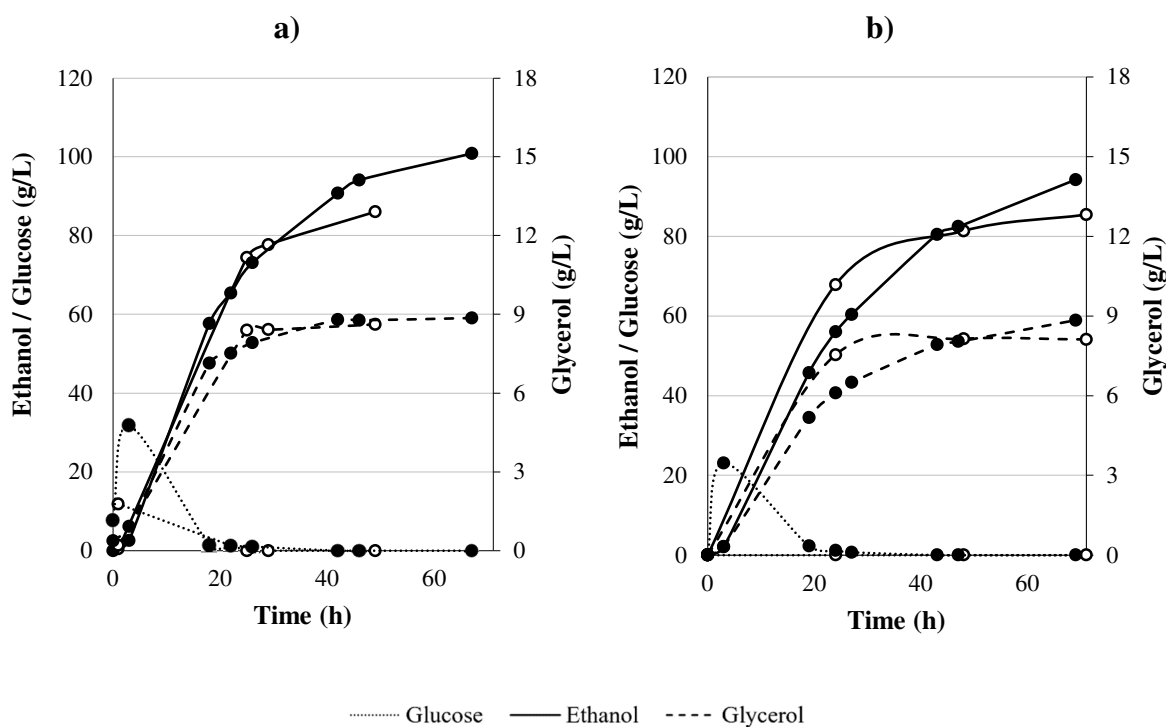


Figure 3.3 Ethanol, glucose and glycerol production by *S. cerevisiae* wild-type strains L20 (a) and Ethanol Red[®] (b) during SSF in 1-L bioreactor with 20 % (w/v) of broken rice (○) and raw corn starch (●). The experiment was conducted in duplicate and average values are presented.

	<i>S. cerevisiae</i> L20		<i>S. cerevisiae</i> Ethanol Red®	
Broken rice*				
Product (g/L)	24 h	72 h	24 h	72 h
Glucose	nd	nd	nd	nd
Glycerol	8.40	8.70	7.54	8.12
Ethanol	74.44	87.01	67.86	85.46
CO ₂	71.20	83.23	64.91	81.74
Total carbon	5.13	5.96	4.67	5.84
Carbon conversion (mol C)	77 %	90 %	71 %	88 %
<i>Y_{ES}</i> (% of theoretical)	73 %	86 %	67 %	83 %
<i>Q</i> (g/L/h)	3.10	1.21	2.83	1.19
<i>Q_{max}</i> (g/L/h)	3.10 after 24 h		2.83 after 24 h	
Raw corn starch **				
Product (g/L)	24 h	72 h	24 h	72 h
Glucose	1.04	nd	1.14	nd
Glycerol	7.92	8.86	6.10	8.84
Ethanol	73.10	100.84	56.02	94.20
CO ₂	69.92	96.46	53.58	90.10
Total carbon	5.06	6.87	3.89	6.43
Carbon conversion (mol C)	64%	86%	49%	81%
<i>Y_{ES}</i> (% of theoretical)	60%	83%	46%	77%
<i>Q</i> (g/L/h)	3.05	1.40	2.33	1.31
<i>Q_{max}</i> (g/L/h)	3.20 after 18 h		2.41 after 18 h	

* a glucose equivalent of 198.55 g/L and a total carbon available (mol C) of 6.62

** a glucose equivalent of 238.82 g/L and a total carbon available (mol C) of 7.93

Table 3.2 Conversion of starchy substrates at 1L-bioreactor level to ethanol and by-products by *S. cerevisiae* L20 and Ethanol Red® strains. *Y_{ES}*, % of theoretical maximum ethanol yield per gram of glucose equivalent available.

Once again, in broken rice the fermentation trend was similar for both strains (**Figure 3.3** and **Table 3.2**) with comparable ethanol levels produced after 72 h of fermentation (87.01 and 85.46 g/L for *S. cerevisiae* L20 and Ethanol Red[®], respectively). However, as reported in **Table 3.2**, the novel strain *S. cerevisiae* L20 displayed higher ethanol production than Ethanol Red[®] after 24 h and with a maximum productivity of 3.10 g/L/h, which was 1.10-fold than that of the industrial benchmark (2.83 g/L/h). Such ethanol productivity values are of great interest and potential industrial application (Görgens et al., 2014; Walker and Walker, 2018). Furthermore, late fermentative efficiencies were also higher, with the novel strain displaying 86 % of the maximum theoretical instead of 83 % detected for *S. cerevisiae* Ethanol Red[®].

On raw corn starch, *S. cerevisiae* L20 confirmed to be a superior strain, with almost 101 g/L ethanol produced within 72 h of incubation. On the contrary, as reported in **Figure 3.3b** and **Table 3.2**, the industrial benchmark produced lower alcohol values (up to 94 g/L). Fermenting parameters were much better for *S. cerevisiae* L20, with a maximum productivity of 3.20 g/L/h, which was 1.33-fold higher than that of the industrial benchmark (2.41 g/L/h). Ethanol yields and carbon conversion values confirmed that the novel strain outperformed the industrial yeast further supporting both the saccharification of starch to glucose and then glucose-to-ethanol fermentation.

As reported in **Table 3.2** and **Figure 3.3**, ethanol levels and efficiencies obtained by both strains from the two tested substrates were found to be lower than those detected at smaller scale (**Figure 3.1**). This finding could be due to an increase of viscosity of the medium which was found to limit the ethanol yield in up-scaling of high gravity SSF experiments on sweet potato (Zhang et al., 2011) or to an intensification of stress exposure linked to limited transportation and elimination of CO₂, toxic metabolites and additional heat generated by agitation (Schmidt, 2005). This calls for further experimental activities in order to optimize the scaling up of the process. Moreover, it is in agreement with lower ethanol yields recently obtained up-scaling the simultaneous liquefaction, saccharification and fermentation (SLSF) of broken rice at high gravity (Chu-Ky et al., 2016).

Because of the superior fermentative abilities from both glucose (**Figure 3.1**) as well as under SSF setting of broken rice (**Figure 3.2a** and **Table 3.2**) and raw corn starch (**Figure 3.2b** and **Table 3.2**), the strain *S. cerevisiae* L20 was selected for a molecular biology programme in

order to develop an efficient CBP yeast. *S. cerevisiae* Ethanol Red[®] was included as reference strain.

3.2 Genome sequencing of *S. cerevisiae* L20

The whole-genome sequence of *S. cerevisiae* L20 was obtained using a novel strategy that combines MiniIon-Illumina approach: the first platform is expected to produce robust scaffolds against which the Illumina reads can be mapped to increase the assembly quality.

The number of paired-end reads (2×150 bp) was 1 221 976, resulting in a 150-fold genome coverage. The number of MiniION sequences were 58 954 with an average length of 6 649 bp. The *de novo* assembly generated a genome of 11.9 Mb, composed by 18 contigs, with a N_{50} of 186 045, with 14 chromosomes assembled in a single contig.

As reported in **Figure 3.4**, genome comparison between *S. cerevisiae* L20 and the reference genome (*S. cerevisiae* S288c R64-1-1) highlights the main structural changes. Most of the Chromosomes assembled entirely in one contig with the exception of Chromosomes VII and XII which assembled in two fragments. Of particular evidence, there is the translocation between Chromosomes VIII and XVI typical of oenological yeast strains found to have increased sulfur dioxide resistance (Perez-Ortin, 2002; García-Ríos et al., 2019; Treu et al., 2014). Such finding is in accordance with the origin of *S. cerevisiae* L20, which was isolated from a winery (Gronchi et al., 2019). This translocation, which involves *SSUI* gene, was indeed previously identified in some wine strains (Perez-Ortin, 2002; García-Ríos et al., 2019). *SSUI* encodes a plasma membrane sulfite pump whose overexpression results in the yeast cell ability to tolerate higher sulfur dioxide concentrations. Moreover, *SSUI* gene was found to have higher gene expression conferring a strain-specific evolutionary advantage to wine environment characterized by high sulfite concentrations (up to 50 mg/L, García-Ríos et al., 2019).

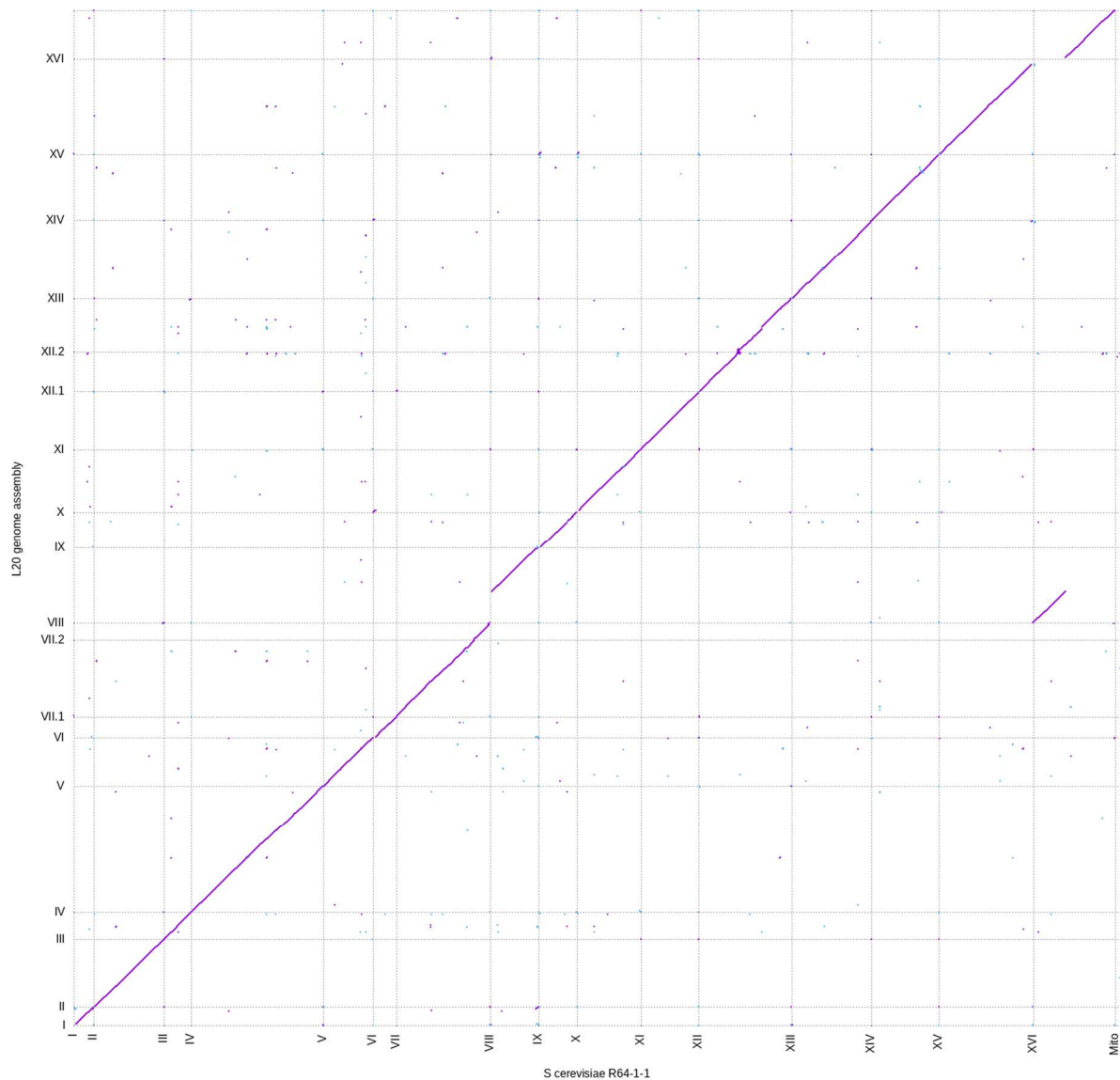


Figure 3.4 Whole genome alignment of *S. cerevisiae* reference genome S288c (R64-1-1) and the genome assembly of *S. cerevisiae* L20 using nucmer (Kurtz et al., 2004). Purple and blue dots indicate similarity between the two forward and reverse strands, respectively.

3.3 Yeast genome engineering

The integration of heterologous sequences in the genome represents an attractive method for a CBP microorganism development (Lian et al., 2018). Unlike episomal plasmids, the chromosomal recombination can provide strain stability without the use of selective pressure.

In the past, Viktor et al. (2013) reported a successful transformation of laboratory and semi-industrial strain with *AmyA* and *GlaA* genes of *A. tubingensis* T8.4, although the expression was mediated by yBBH1 episomal vectors. In this study, the yBBH1 plasmids were used as the template for the construction of linear or plasmid vectors for δ -integration or CRISPR/Cas9 methods, respectively, in order to integrate both genes in the yeast chromosomes. The newly isolated *S. cerevisiae* strain L20 with outstanding fermentative traits was used as platform for the development of the CBP expressing *AmyA* and *GlaA* genes. *S. cerevisiae* Ethanol Red[®] was included as industrial benchmark.

The two technologies, δ -integration and CRISPR/Cas9, were compared. The first provides a large number of recombinants with different phenotypic traits due to the non-site-directed nature of δ -integration (David and Siewers, 2015). The resulting colonies, indeed, demonstrated a great variability in gene expression and deeper analysis was then required. On the other hand, CRISPR/Cas9 could be of benefit for a fine regulation of gene copies as well as for reducing potential phenotype alterations given by multi-copy integration. Two different loci were designated for heterologous gene expression of *AmyA* and *GlaA* in *S. cerevisiae* through CRISPR/Cas9. This strategy demonstrated its good feasibility even in a wild type isolate such as L20. However, due to the nature as diploid strain, the number of gene copies integrated was only two for each locus. As a result, the engineered strains displayed limited starch hydrolyzing activity (**Figure 3.20**) and have to be considered as a starting platform for the further development of a stable, marker-free and amylase-expressing yeast.

To the best of our knowledge, this is the first report about CRISPR/Cas9 genome engineering of a natural isolate for heterologous co-expression of fungal α -amylase and glucoamylase.

3.3.1 Yeast dominant marker resistance

In contrast to *S. cerevisiae* laboratory yeast having multiple auxotrophic mutations, wild type strains are often prototrophic, thus lacking selective genetic markers. Recombinant cells can only be selected by dominant selection markers (Akada, 2002). The innate susceptibility of *S. cerevisiae* L20 and Ethanol Red[®] to three antibiotics, namely geneticin, hygromycin B and nourseothricin used in this study, was determined by monitoring the growth in the presence of increasing concentrations of antibiotics (**Table 3.3**). Briefly, yeast cells were inoculated into

YPD containing increasing levels of each antibiotic and monitored at regular intervals for OD₆₀₀.

	<i>S. cerevisiae</i> L20	<i>S. cerevisiae</i> Ethanol Red [®]
Geneticin (mg/L)		
0	+++	++++
50	n.g.	+++
100	n.g.	++
150	n.g.	+
200	n.g.	n.g.
Hygromycin B (mg/L)		
0	+++	++++
75	n.g.	+++
150	n.g.	+
225	n.g.	n.g.
300	n.g.	n.g.
Nourseothricin (mg/L)		
0	+++	++++
25	n.g.	n.g.
50	n.g.	n.g.
75	n.g.	n.g.
100	n.g.	n.g.

Table 3.3 Dominant selection marker resistance of *S. cerevisiae* L20 and Ethanol Red[®] strains in YPD supplemented with increasing concentrations of antibiotics. (++++: consistent growth; n.g.: no growth)

S. cerevisiae L20 demonstrated a higher sensitivity to antibiotics than Ethanol Red[®]. The concentration of 200, 300 and 100 mg/L of geneticin, hygromycin B and nourseothricin, respectively, were further used for the selection of the recombinants of Ethanol Red[®] whereas a lower concentration of geneticin (150 mg/L) was chosen in the case of *S. cerevisiae* L20.

3.3.2 Delta integration of *AmyA* and *GlaA* genes from *A. tubingensis* T8.4

The yBBH1-*AmyA* and yBBH1-*GlaA* plasmids (**Table 2.5**) were used as template for the amplification of *AmyA* and *GlaA* genes, under the control of *ENO1* promoter and terminator. The primers were designed in order to create overlapping flanking regions for *in vivo* assembly with the *KanMX* cassette, though resulting in linear δ -integrative vectors as represented in **Figure 3.5**.

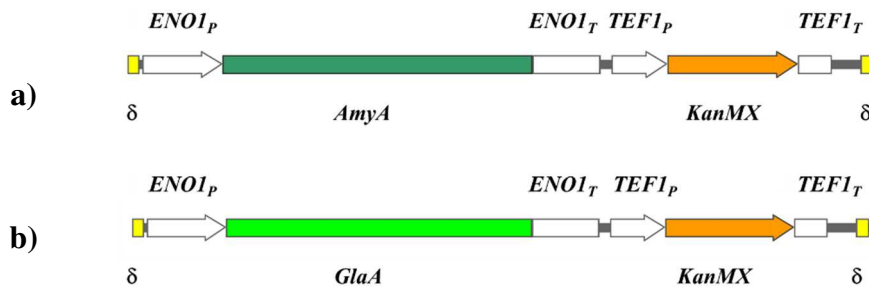


Figure 3.5 Maps of the assembled δ -integrative vectors δ -*AmyA*-*KanMX*- δ (a) and δ -*GlaA*-*KanMX*- δ (b) for constitutive expression in *S. cerevisiae* strains. The gene cassettes were amplified from yBBH1-*AmyA* and yBBH1-*GlaA* plasmids carrying *AmyA* and *GlaA* from *A. tubingensis* T8.4, respectively (Viktor et al., 2013). The *KanMX* marker was amplified from pBKD2 plasmid (McBride et al., 2008; SnapGene® Viewer 5.0.6).

Yeast cells were simultaneously transformed with *AmyA* and *GlaA* linear donor DNA fragments by electroporation as described in 2.5.2.1. The electroporated cells were spread onto YPD plates supplemented with 1 M sorbitol and geneticin (150-200 mg/L) and incubated at 30 °C for 48-72 h to allow cell recovery. The colonies were tested for amylolytic activity on soluble starch agar stained with Lugol solution (**Figure 3.6**). The colonies showing the largest starch hydrolysis halos, namely *S. cerevisiae* L20 δ T8, δ T12, δ T25, δ T53 and *S. cerevisiae* Ethanol Red® δ T16, δ T17 and δ T22, were selected for further analysis.



Figure 3.6 Starch hydrolytic activity of *S. cerevisiae* strains engineered for the expression of *AmyA* and *GlaA* from *A. tubingensis* T8.4 by δ -integration. Pre-cultures were incubated on YNB plates with 0.2 % soluble starch for 48 h at 30 °C and stained with Lugol solution.

A PCR amplification was performed to confirm the chromosomal integration of *AmyA* and *GlaA* into the selected recombinants of both *S. cerevisiae* L20 and Ethanol Red® (**Figure 3.7**). The expected size of the amplicons was 299 and 483 bp for *AmyA* and *GlaA*, respectively. The PCR amplification revealed that all seven engineered strains presented *AmyA* gene sequence(s) into their chromosomes whereas only *S. cerevisiae* Ethanol Red® δ T16 did not show positive *GlaA* PCR product.

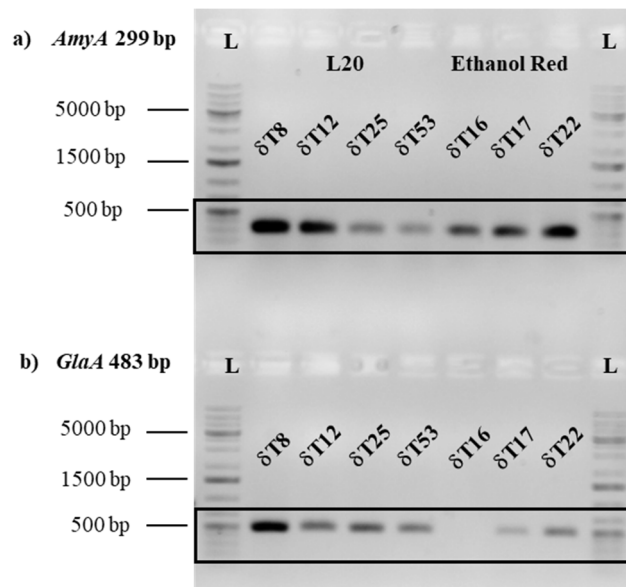


Figure 3.7 Gel electrophoresis of PCR products for *AmyA* (a) and *GlaA* (b) in the selected recombinants of *S. cerevisiae* L20 and Ethanol Red®. L: molecular weight size marker O'GeneRuler 1 kb Plus DNA Ladder (Thermo Scientific).

To study the mitotic stability, the recombinants were grown in sequential batch cultures in non-selective YPD broth. After 80 generations, yeast cells were plated onto selective media supplemented with geneticin or soluble starch, and the number of colonies was monitored.

All the engineered strains displayed both resistance to geneticin and hydrolytic ability on soluble starch. As such, they were considered mitotically stable and further characterized for enzymatic activity and fermenting ability on starch.

3.3.3 CRISPR/Cas9 mediated integration of *AmyA* and *GlaA* genes from *A. tubingensis* T8.4

The loci mk114 and AD7 of *S. cerevisiae* L20 and Ethanol Red[®] were amplified and sequenced to confirm the feasibility of the CRISPR/Cas9 strategy. As described in 2.5.3, a PCR was performed to obtain a 429 bp amplicon for mk114 locus and a 454 bp amplicon for AD7 locus (**Figure 3.8**). The ITS region was considered as positive control (880 bp).

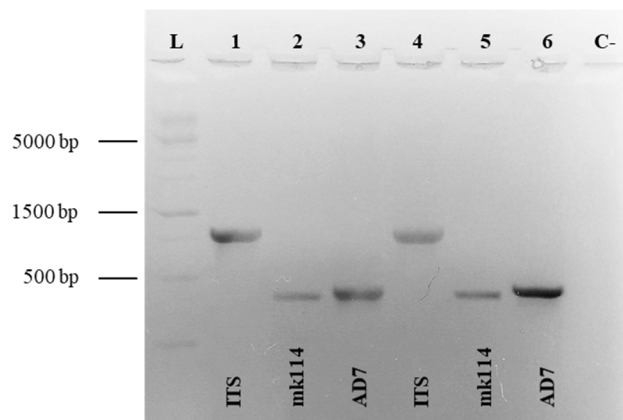


Figure 3.8 Gel electrophoresis of PCR products amplified by primers ITS1/ITS4, G1-mk114-Fw/G1-mk114-Rv, G1-AD7-Fw/G1-AD7-Rv for *S. cerevisiae* L20 (lane: 1-3) and Ethanol Red[®] (lane: 4-6). C-: negative control. L: molecular weight size marker O'GeneRuler 1 kb Plus DNA Ladder (Thermo Scientific).

Amplification products were subjected to sequencing (BMR genomics, University of Padova; data not shown). The BLASTN alignment (<https://blast.ncbi.nlm.nih.gov/Blast.cgi>) against the gRNA sequences showed a 100 % of homology, confirming that loci mk114 and

AD7, as well as the use of p59 gRNA plasmids, were suitable for CRISPR/Cas9 strategy in both *S. cerevisiae* L20 and Ethanol Red®.

3.3.3.1 Plasmid construction

The *ENO1_P-AmyA-ENO1_T* and *ENO1_P-GlaA-ENO1_T* cassettes were amplified from yBBH1-*AmyA* and yBBH1-*GlaA* plasmids (Viktor et al., 2013), respectively, and cloned into donor DNA vectors for CRISPR/Cas9 transformation. The virtual maps of the p426*hph* plasmids with single and double cassettes were produced *in silico* and used as reference to design the primers according to the Gibson Cloning Assembly (New England Biolabs) protocol. The fragments corresponding to the size of the inserts (2.8 kb; **Figure 3.9**) were excised from the gel. Donor DNA vectors p426*hph*-mk114 and p426*hph*-AD7 were confirmed in term of size (**Figure 3.10**).

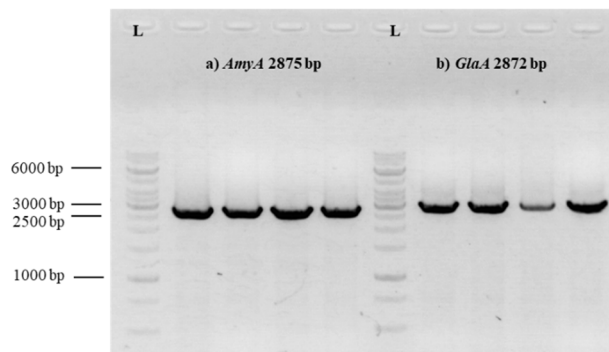


Figure 3.9 Gel electrophoresis of PCR products amplified by primer couple a) C-8465 Fw/C-8466 Rv from yBBH1-*AmyA* and b) C-8467 Fw/C-8468 Rv from yBBH1-*GlaA* plasmids. L: molecular weight size marker O'GeneRuler 1 kb DNA Ladder (Thermo Scientific).

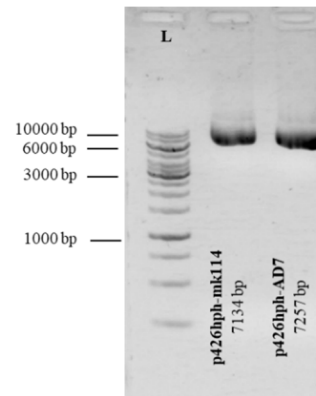


Figure 3.10 Gel electrophoresis of donor DNA empty vectors p426*hph*-mk114 and p426*hph*-AD7 L: O'GeneRuler 1 kb DNA Ladder (Thermo Scientific)..

Both inserts and vectors were prepared for ligation. After Gibson Assembly (New England Biolabs), the plasmids were transformed and propagated in *E. coli*. A gel electrophoresis confirmed the successful ligation (**Figure 3.11**). The final plasmids p426*hph*-

mk114-*AmyA* and p426*hph*-AD7-*GlaA*, whose map is reported in **Figure 3.12**, showed the expected size of 10 and 10.1 kb, respectively, and were confirmed by sequencing (data not shown).

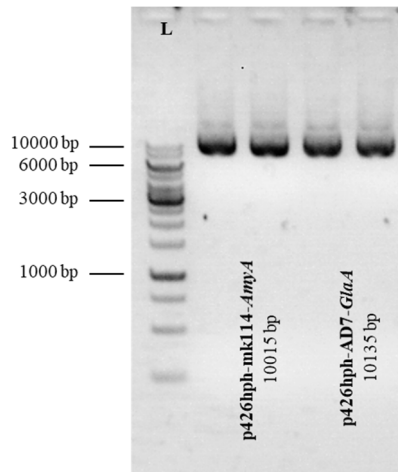


Figure 3.11 Gel electrophoresis of donor DNA plasmids p426*hph*-mk114-*AmyA* and p426*hph*-AD7-*GlaA*. L: O'GeneRuler 1 kb DNA Ladder (Thermo Scientific).

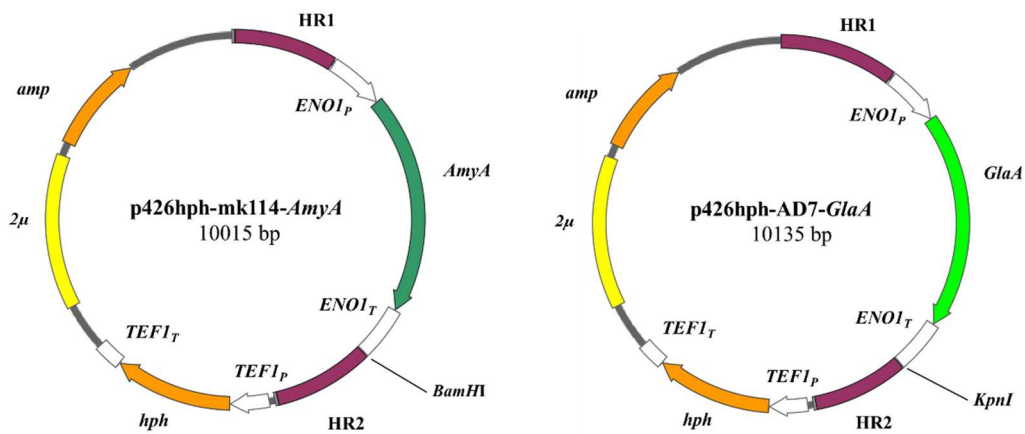


Figure 3.12 Map of the plasmids p426*hph*-mk114-*AmyA* and p426*hph*-AD7-*GlaA* containing the *A. tubingensis* T8.4 *AmyA* and *GlaA* genes, respectively (SnapGene® Viewer 5.0.6).

Subsequently, the *ENO1_P-AmyA-ENO1_T* and *ENO1_P-GlaA-ENO1_T* cassettes were amplified with the second pair of primers (**Table 2.12**) and cloned into the p426*hph*-mk114-

AmyA and p426*hph*-AD7-*GlaA* plasmids (**Figure 3.12**). After Gibson Assembly (New England Biolabs), the plasmids were transformed and propagated in *E. coli*. The successful ligation was confirmed by size after gel electrophoresis (**Figure 3.13**). The plasmids showed the expected size of 12.8 and 13 kb and were confirmed also by sequencing (data not shown). As a result, two additional double-cassette donor plasmids were yielded, namely p426*hph*-mk114-*AmyA*-*GlaA* and p426*hph*-AD7-*GlaA*-*AmyA*. The virtual maps are reported in **Figure 3.14**.

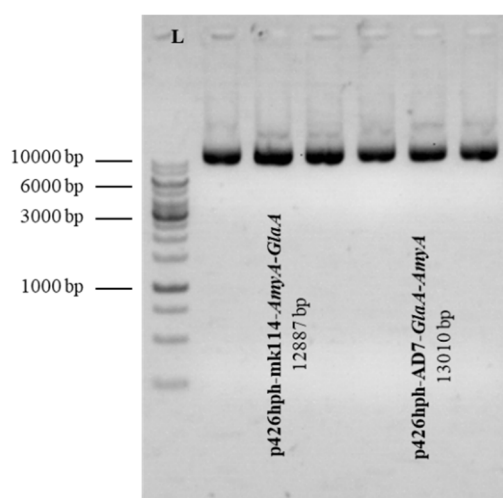


Figure 3.13 Gel electrophoresis of donor DNA plasmids p426*hph*-mk114-*AmyA*-*GlaA* and p426*hph*-AD7-*GlaA*-*AmyA*. L: O'GeneRuler 1 kb DNA Ladder (Thermo Scientific).

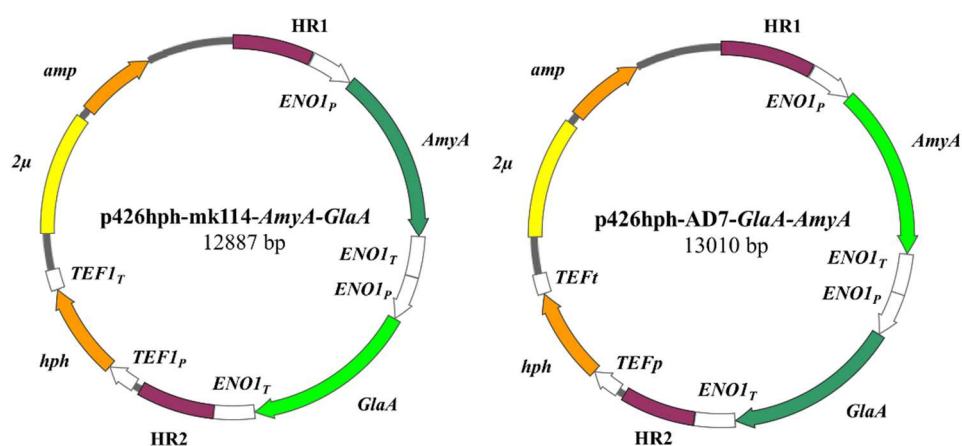


Figure 3.14 Plasmids p426*hph*-mk114-*AmyA*-*GlaA* and p426*hph*-AD7-*GlaA*-*AmyA* containing both the *AmyA* and *GlaA* genes from *A. tubingensis* T8.4 (SnapGene® Viewer 5.0.6).

3.3.3.2 Yeast transformation

The purified plasmids were used to transform yeast cells using LiAC/SS carrier DNA/PEG method (Gietz and Schiestl, 2007). Pre-cultures of *S. cerevisiae* L20 and Ethanol Red[®] were subjected to three consequential transformations, following the order presented in 2.5.3.2. Briefly, in a first instance the strains were transformed with Cas9 plasmid (p51 *TEF1-Cas9-KanMX*) and colonies selected onto YPD and geneticin agar plates. Secondly, cells bearing Cas9 were transformed with donor DNA plasmids (p426*hph*-mk114-*AmyA*, p426*hph*-mk114-*AmyA-GlaA*, p426*hph*-AD7-*GlaA* or p426*hph*-AD7-*GlaA-AmyA*) and selected onto YPD plates supplemented with the combination of selective antibiotics to maintain both Cas9 and donor DNA plasmids (geneticin and hygromycin B). The gRNAs (p59 gRNA mk114-*CloNAT* and p59 gRNA AD7-*CloNAT*) were used in the last step and the transformants were selected onto YPD plates supplemented with nourseothricin. Each time the plates were incubated at 30 °C for 48 or 72 h after plating. Only transformants with expected negative control were considered for further analysis.

The ability of the transformants to produce functional amylases was confirmed as hydrolysis halos on YNB plates supplemented with 0.2 % of soluble starch and stained with Lugol solution (**Figure 3.15**).



Figure 3.15 Starch hydrolytic activity of *S. cerevisiae* strains engineered for the expression of *AmyA* and *GlaA* genes from *A. tubingensis* T8.4 by CRISPR/Cas9. Pre-cultures were incubated on YNB plates 0.2 % soluble starch for 48 h at 30 °C and stained with Lugol solution.

A PCR amplification with primers reported in 2.5.3.3 (**Table 2.13**) was performed to confirm the chromosomal integration of *AmyA* and/or *GlaA* genes. The primers were used to amplify the region between the homologous region and the heterologous expressing cassette.

The expected size of the amplicons was 1.4 and 4.6 kb for *AmyA* and *AmyA-GlaA* transformants, respectively, and 2.9 kb for *GlaA* and *GlaA-AmyA* strains. Results reported in **Figure 3.16-3.19** showed that all the strains were successfully engineered for *AmyA* and/or *GlaA* expression.

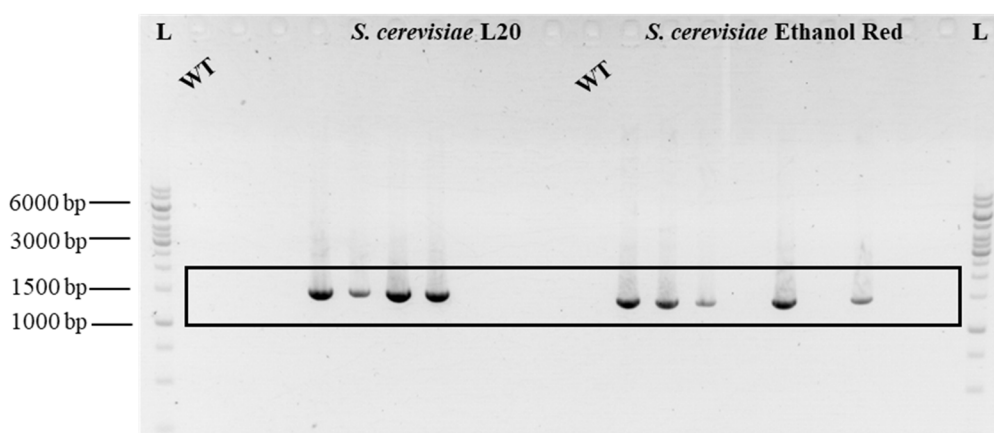


Figure 3.16 Gel electrophoresis of PCR products of *S. cerevisiae* L20 and Ethanol Red[®] transformed with *AmyA* cassette via CRISPR/Cas9. DNA was amplified by primers C-8646 Fw/C-2828 Rv resulting in a 1.4 kb amplicon. WT: wild type. L: molecular weight size marker O'GeneRuler 1 kb DNA Ladder (Thermo Scientific).

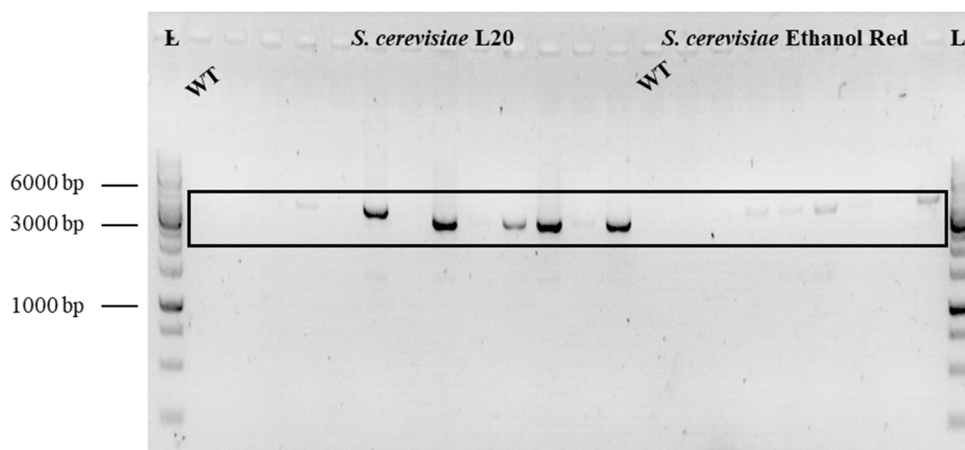


Figure 3.17 Gel electrophoresis of PCR products of *S. cerevisiae* L20 and Ethanol Red[®] transformed with *AmyA-GlaA* cassette via CRISPR/Cas9. DNA was amplified by primers C-8646 Fw/C-2828 Rv resulting in a 4.6 kb amplicon. WT: wild type. L: molecular weight size marker O'GeneRuler 1 kb DNA Ladder (Thermo Scientific).

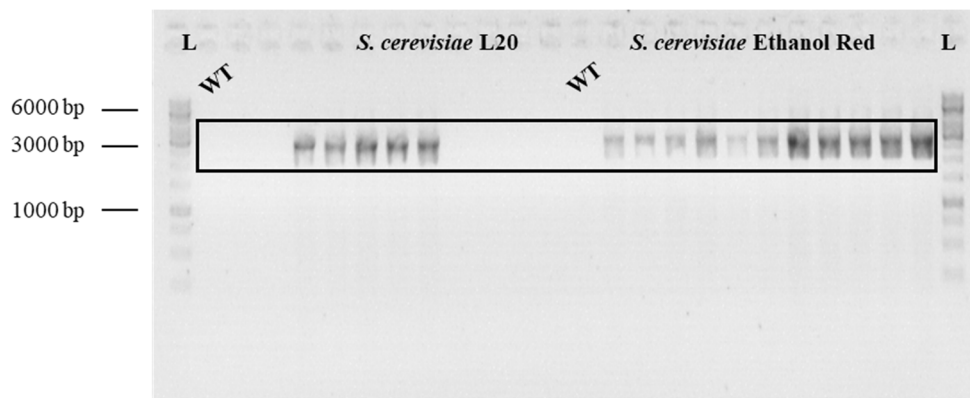


Figure 3.18 Gel electrophoresis of PCR products of *S. cerevisiae* L20 and Ethanol Red[®] transformed with *GlaA* cassette via CRISPR/Cas9. DNA was amplified by primers C-4330 Fw/C-8797 Rv resulting in a 2.9 kb amplicon. WT: wild type. L: molecular weight size marker O'GeneRuler 1 kb DNA Ladder (Thermo Scientific).

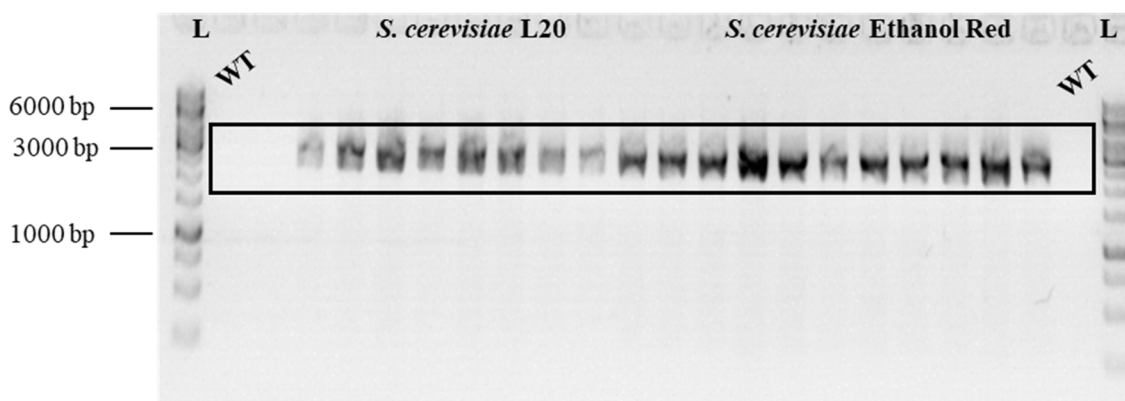


Figure 3.19 Gel electrophoresis of PCR products of *S. cerevisiae* L20 and Ethanol Red[®] transformed with *GlaA-AmyA* cassette via CRISPR/Cas9. DNA was amplified by primers C-4330 Fw/C-8797 Rv resulting in a 2.9 kb amplicon. WT: wild type. L: molecular weight size marker O'GeneRuler 1 kb DNA Ladder (Thermo Scientific).

The transformants were subjected to plasmid curing by repeated batch cultures in non-selective YPD in order to eliminate the plasmid DNAs. After 72 h the cells were diluted in NaCl 0.85 % and spread onto YPD plates with single antibiotic (geneticin, hygromycin B or nourseothricin) and without selective pressure. The mitotic stability was contextually assessed comparing the growth on multiple YPD plates. The recombinants showing comparable number of colonies on YPD and found sensitive to the three antibiotics were considered mitotically stable and assayed in terms of starch-hydrolyzing ability.

3.4 Enzymatic assays

The δ -integrated *AmyA/GlaA* strains and CRISPR/Cas9 engineered strains (carrying single or double constructs) were tested for enzymatic activity on soluble starch as substrate. The supernatant of 24, 48 and 72 h-old cultures was incubated at 50 °C with citrate buffer at pH 5 containing 0.2 % of soluble starch. The enzymatic activity was assessed according to the amount of starch-reducing ends or free glucose released by the enzymes in the system.

The DNS method was used to determine the α -amylase activity of the *AmyA*-expressing strains and the total activity for *AmyA*- and *GlaA*-expressing strains (**Figure 3.20a**). The quantification of reducing sugars enzymatically released from starch was estimated colourimetrically. The glucoamylase activity of the *GlaA*-expressing strains was determined by measuring the released glucose by means of the D-Glucose HK Assay Kit (Megazyme). Enzymatic activities were expressed as nanokatals per mL (nKat/mL), which is defined as the enzyme activity needed to release 1 nmol of glucose per second per mL of culture. The experiments were carried out in triplicate using the parental strains as negative controls.

As reported in **Figure 3.20**, it is evident that the enzymatic activity increases by time, as it was previously reported for other recombinant amylase(s) in industrial yeast strains, more than doubling in most cases (Favaro et al., 2012; Viktor et al., 2013; Favaro et al., 2015; Cripwell et al., 2019). By reducing sugar assay (**Figure 3.20a**), the L20 δ -integrated strains, labelled with δ (*S. cerevisiae* L20 δ T8, δ T12, δ T25 and δ T53) demonstrated a hydrolytic activity higher than that detected for the CRISPR/Cas9 engineered strains (*S. cerevisiae* L20 mk114-*AmyA*, mk114-*AmyA-GlaA*, AD7-*GlaA* and AD7-*GlaA-AmyA*). Moreover, the glucose kit assay revealed the same trend for the enzymatic activity (**Figure 3.20b**). This finding is likely to be attributed to higher gene copy numbers that can be integrated into the chromosomes of the δ -integrated strains. Such hypothesis is under investigation by means of whole-genome sequencing of both δ -integrated and CRISPR/Cas9 engineered yeast.

In the case of Ethanol Red[®] derivatives, all the strains, either obtained by δ -integration, namely *S. cerevisiae* δ T16, δ T17 and δ T22, or CRISPR/Cas9 technology, *S. cerevisiae* mk114-*AmyA*, mk114-*AmyA-GlaA*, AD7-*GlaA* and AD7-*GlaA-AmyA*, displayed comparable lower enzymatic activity in both assays (**Figure 3.20a, b**). Unlike L20, the Ethanol Red[®] transformants showed comparable hydrolytic activities, irrespectively of the technology applied.

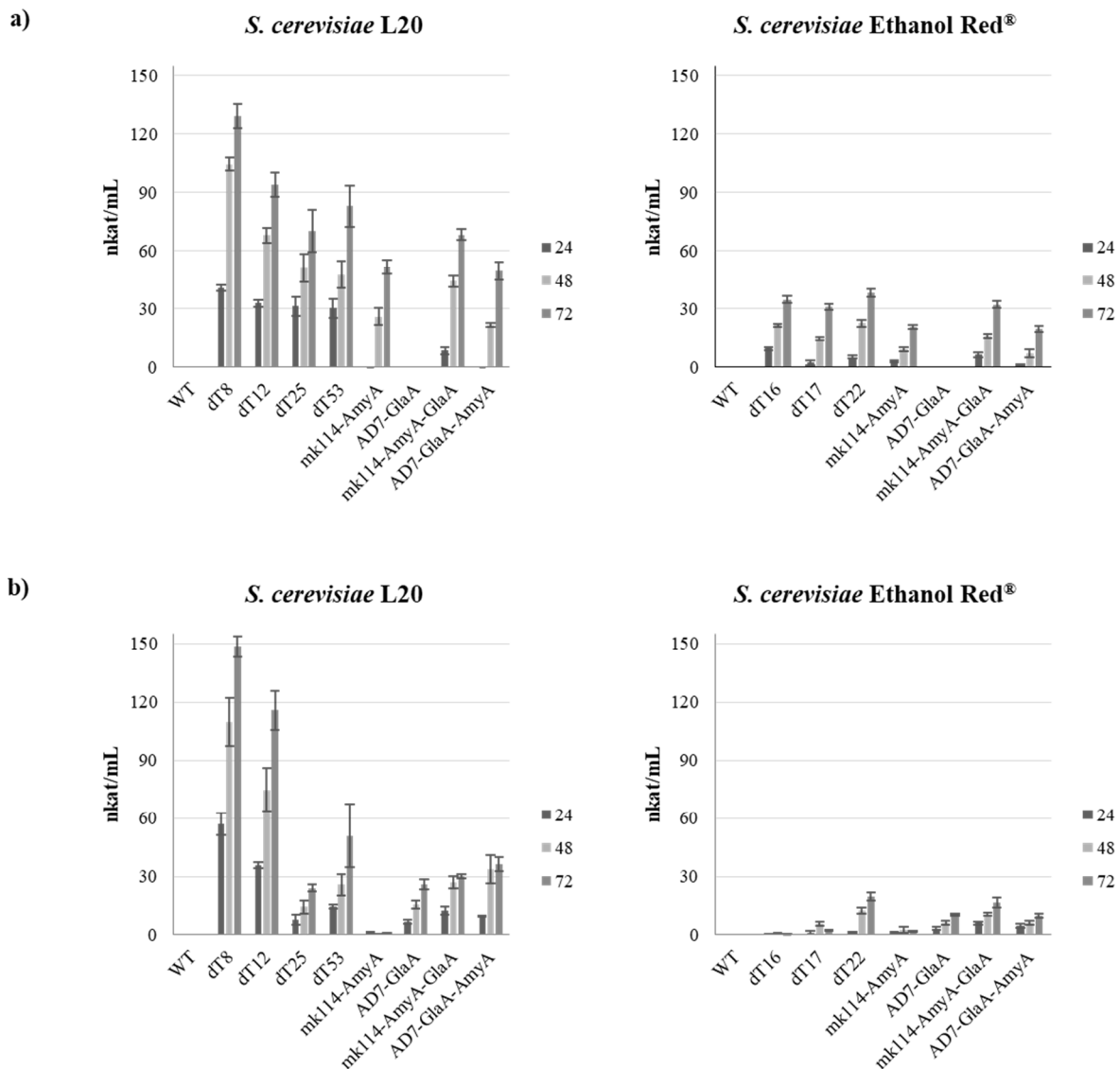


Figure 3.20 Enzymatic activity of the supernatant of *S. cerevisiae* L20 and Ethanol Red® strains expressing *AmyA* and/or *GlaA* genes from *A. tubingensis* T8.4 after 24, 48 and 72 h of incubation in YPD broth resulting from the DNS assay (a) and glucose kit (b). Error bars represent standard deviation from the mean of three replicates.

3.5 SDS-PAGE protein analysis

The supernatant of 72 h-old aerobic cultures of *S. cerevisiae* L20 and Ethanol Red® recombinants was used for protein characterization by SDS-PAGE. Based on the deduced amino acid sequences, the predicted molecular weights of the unglycosylated *AmyA* and *GlaA* were 69.6 kDa and 68 kDa, respectively (Viktor et al., 2013). The SDS-PAGE results indicated

that both proteins were glycosylated: AmyA and GlaA showed a molecular size of 120 and 100 kDa, respectively in the case of L20 engineered strains (**Figure 3.21**) and Ethanol Red[®] recombinants (data not shown). These results are in accordance to Viktor et al. (2013).

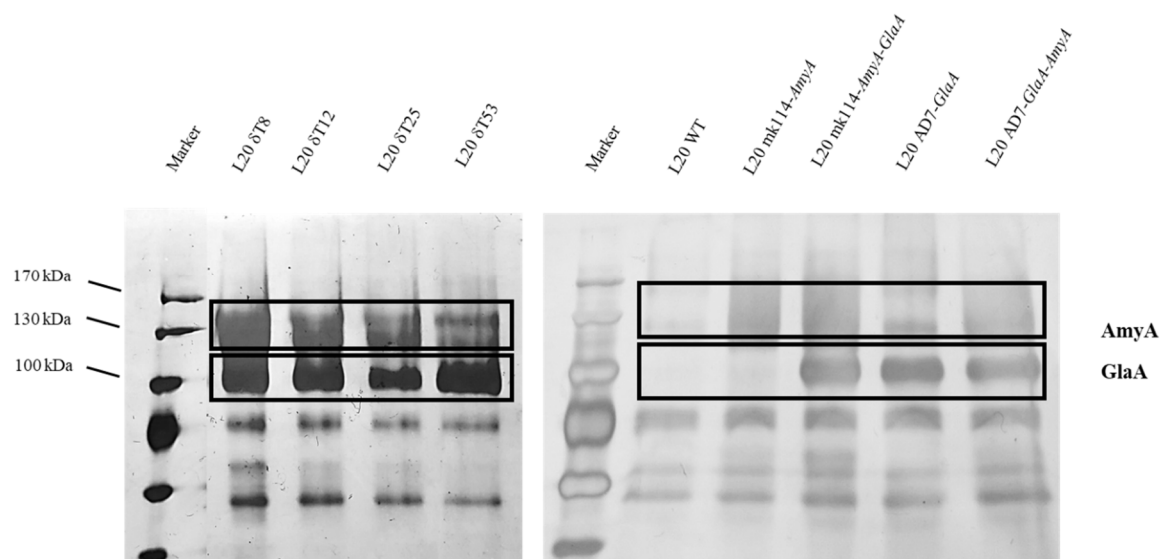


Figure 3.21 SDS-PAGE of the supernatant of 72-h old cultures of *S. cerevisiae* L20 δ -integrated (left) and CRISPR/Cas9 (right) strains followed by silver staining. M: protein size marker PageRuler Prestained Protein ladder.

3.6 Starch CBP fermentation studies

The engineered strains were evaluated for their ability to ferment soluble and raw starch (2 % w/v) under oxygen-limited conditions (**Figures 3.22** and **3.23**), providing a small glucose supplementation (0.05 % w/v). The wild type strains of *S. cerevisiae* L20 and Ethanol Red[®] were used as reference. Within the first 24 h of cultivation on both soluble and raw starch, all strains produced limited amounts of ethanol (about 0.25 g/L), corresponding to the theoretical conversion of 0.05 % w/v of glucose. All the engineered strains, with the exception of L20 δ T8, seemed to reach the highest ethanol production at this time point, showing no further alcohol production and thus displaying limited starch utilization. The ethanol content remained steady for the remaining time of cultivation, with few exceptions that are appreciable only after 72 h. A higher concentration of glucose at the beginning of fermentation may better support the yeast strains, although it has to be considered as an additional economical input that is unattractive from an industrial point of view.

According to the results for *S. cerevisiae* L20 on soluble starch (**Figure 3.22a**), only one of the δ -integrated strains (L20 δ T8) demonstrated to effectively utilize starch and produced ethanol up to 4 g/L after 144 h. This strain demonstrated the highest enzymatic activity in the previous analysis (**Figures 3.20a, b**). However, L20 δ T25 and δ T53 are also demonstrating a modest ethanol concentration after 120 h. Despite the promising results from the enzymatic assays, the hydrolytic activity seems not to be satisfying for a sustainable starch conversion to ethanol. The CRISPR/Cas9 transformants showed an overlapping performance to that of the wild type. On raw corn starch (**Figure 3.22b**), the fermentative trends were the same as on soluble starch. As previously, only L20 δ T8 performed slightly better than the other strains.

S. cerevisiae Ethanol Red[®] obtained by both δ -integration and CRISPR/Cas9 confirmed the poor hydrolytic activity on starch since their ethanol production both from soluble and raw starch were similar to those achieved by their parental *S. cerevisiae* Ethanol Red[®] (**Figure 3.23a, b**).

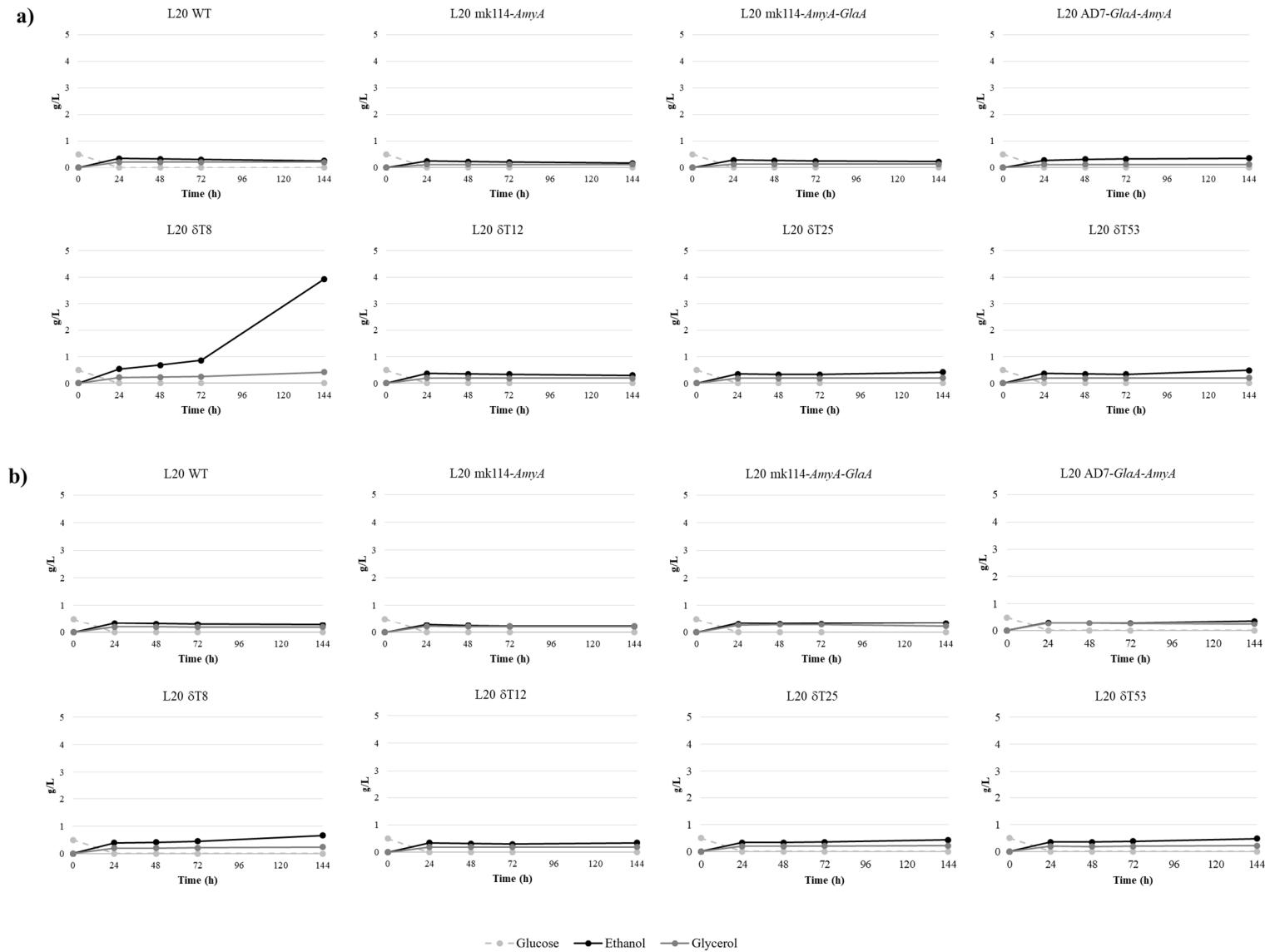


Figure 3.22 Ethanol production of *S. cerevisiae* L20 engineered strains under oxygen-limited conditions in YP medium with soluble starch 2 % (a) or raw starch 2 % (b) and glucose 0.05 %. Values represent the mean of three replicates. *S. cerevisiae* L20 wild type is used as reference.

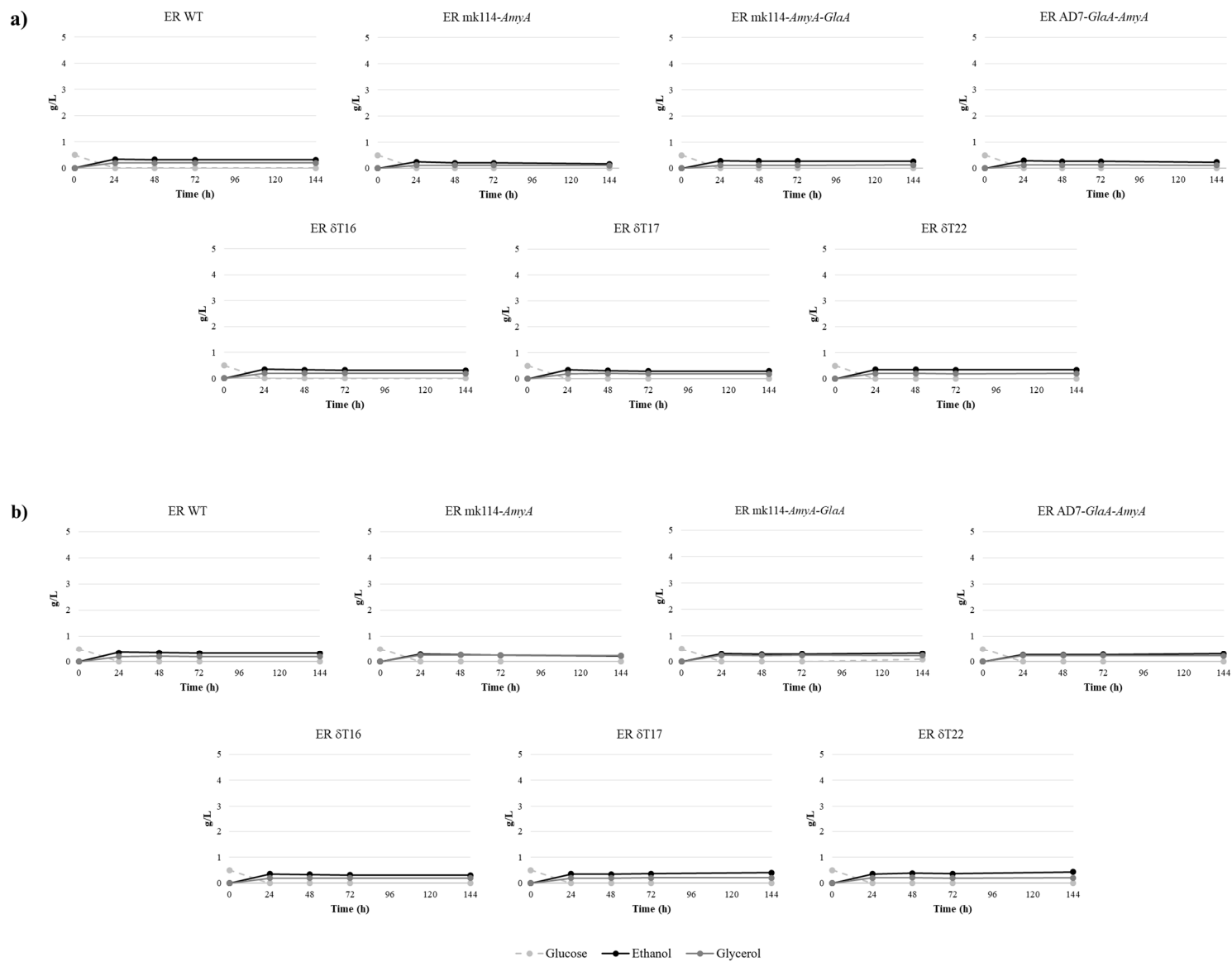


Figure 3.23 Ethanol production of *S. cerevisiae* Ethanol Red[®] engineered strains under oxygen-limited conditions in YP medium with soluble starch 2 % (a) or raw starch 2 % (b) and glucose 0.05 %. Values represent the mean of three replicates. *S. cerevisiae* Ethanol Red[®] wild type is used as reference.

Despite their starch-hydrolyzing activity was confirmed on agar plates, enzymatic assays and SDS-PAGE, most of the engineered strains demonstrated unsatisfying results during the simulation of a CBP process on starchy substrates. The recombinant strains obtained by δ -integration were expected to be good performers since the one-shot multi-site integration is possible. The transformants from CRISPR/Cas9 mediated modification, on the other hand, were predicted to be less performing due to the limited number of gene copies available into the genomes. Focusing on the performance of L20 δ T8 on soluble starch, it is clear that the hydrolysis of starch occurred after 72 h of fermentation, possibly due to the accumulation of an adequate supply of hydrolytic enzymes. This finding has to be considered promising, since, as described in 2.8, the inoculum was applied using only yeast cells and not spent broth containing the secreted recombinant enzymes. Better starch-to-ethanol conversions performances are expected in both δ - and CRISPR/Cas9 mediated recombinants by supplying also the recombinant enzymes produced during the pre-culturing incubation. In this way, larger supplies of enzymes may help the initial starch degradation supporting the cell viability, and thus additional recombinant enzymes production.

4. CONCLUSIONS

A cost-effective technology for direct utilization of biomass for bioethanol production is still lacking (Cinelli et al., 2015). The development of a microbe able to efficiently convert polysaccharides of plant biomass into ethanol is gaining increasing interest in order to reduce the dependence from fossil oil. To date, the functional combination of polysaccharides utilization and alcoholic fermentation at industrial scale has not been described for a single microorganism (Favaro et al., 2019; Walker and Walker, 2018; Jansen et al., 2017).

In this study, a collection of *S. cerevisiae* wild type strains isolated from oenological environment was screened for the ability to produce ethanol under simulated-industrial conditions: at high glucose loading (20 %) and in SSF configuration on starchy substrates. *S. cerevisiae* L20 resulted as a superior fermenting strain, outperforming the *S. cerevisiae* Ethanol Red[®] which is currently used for bioethanol production. It was confirmed as the most promising strain even at higher scale (1-L bioreactor), thus representing an ideal platform for the developing of a starch-hydrolyzing yeast.

A genome engineering program was established in order to develop a *S. cerevisiae* strain secreting efficient fungal amylases. The sequences of α -amylase *AmyA* and glucoamylase *GlaA* genes from *A. tubingensis* T8.4 were integrated into the *S. cerevisiae* L20 genome via both δ -integration and CRISPR/Cas9 methods. *S. cerevisiae* Ethanol Red[®] strain was used as industrial benchmark yeast. The recombinants expressing amylases *AmyA* and *GlaA* were evaluated for genome stability and the secretion of heterologous enzymes. The strains were then tested for the ability to consume starch and produce ethanol. Only one, *S. cerevisiae* L20 δ T8, displayed a slight but promising fermentative trait on soluble starch.

This study represented the first attempt in transforming wild type and industrial yeast with fungal amylases by comparing the outputs of two different engineering techniques. As explained extensively above, δ -integration is a consolidated method for random integration of multiple gene copies. However, the integration of large recombinant DNA molecules could lead to genome instability, thus threatening the final phenotype and the potential application at industrial scale (Cho et al., 1999; Apel et al., 2017). CRISPR/Cas9 is an innovative targeted and marker-less endonuclease-based strategy that was recently applied in yeast species

(DiCarlo et al., 2013). Two genomic loci were chosen for heterologous gene integration, namely mk114 and AD7. The vectors for the expression of *AmyA* and/or *GlaA* genes were constructed to integrate both genes at these specific loci. In *S. cerevisiae* L20 and Ethanol Red[®] diploid strains, the expected number of gene copies was two for both *AmyA* and *GlaA*. On the other hand, by using δ -integration single cassettes of *AmyA* or *GlaA* were integrated randomly at δ -sites, most probably resulting in a copy number possibly larger than two. This could be a reason for the higher enzymatic activity of *S. cerevisiae* L20 δ T8. The gene copies in δ -integrated strains will necessarily be confirmed by sequencing.

In order to improve the starch-to-ethanol abilities of the CRISPR/Cas9-mediated recombinants, multiple rounds of insertion are in progress to develop yeast strains with high copy numbers of multiple integrated genes dispersed over the whole genome. For this purpose, other genomic loci have been identified (Jessop-Fabre et al., 2016).

The number of studies reporting suitable CRISPR/Cas9 integration sites in *S. cerevisiae* is growing day by day. Many computational tools can help to design gRNAs with specificity and efficiency. The specificity of gRNAs is especially important because off-targets can considerably damage the genome and cause unknown changes. If an unintended locus is accidentally cleaved, it can either threaten the cell survival or cause unexpected outcomes. The multiplex transformation has been recently described by Jakočiūnas (2015; 2016) and Ronda et al. (2015). Here, multiple gRNA expression cassettes were cloned into a single gRNA expression vector, resulting in a single efficient transformation. Moreover, Shi et al. (2016) combined the traditional Cas9-based technology with δ -integration to engineer a *S. cerevisiae* strain for xylose utilization and simultaneous butanediol production. By targeting the repeated δ -sites, they were able to perform the integration of a 24-kb DNA fragment. By introducing Cas9-mediated DSBs at the δ -sites, they were able to clone up to 10 copies of a 24-kb construct.

Novel amylases with higher hydrolytic activity than *AmyA* and *GlaA* are under investigation. In this view, different promoters and terminators could be tested for optimal regulation of the expression of heterologous enzymes.

In conclusion, the development of a CBP yeast is of great interest for industrial conversion of starchy biomass into ethanol. In particular, the results of this research mark one step closer to the development of engineered yeast suitable for the direct fermentation of starch into ethanol. In order to further assess the industrial implementation of *S. cerevisiae* L20 δ T8,

future studies will focus on improving the hydrolytic activity through the expression of other groups of enzymes besides amylase. Accessory enzymes, such as pullulanases, proteases and cellulases, will be considered to achieve a more efficient substrate utilization. Moreover, optimizing the CRISPR/Cas9 parameters will be useful for the development of a fermenting yeast with desirable traits for bioethanol production.

5. REFERENCES

- Aditiya H.B., Mahlia T.M.I., Chong W.T., Nur H., and A.H. Sebayang. 2016. Second generation bioethanol production: a critical review. *Renew. Sustain. Energy Rev.* 66: 631–53. <https://doi.org/10.1016/j.rser.2016.07.015>.
- Agbor V., Carere C., Cicek N., Sparling R., and D. Levin. 2014. Biomass pretreatment for Consolidated Bioprocessing (CBP). *Adv. Biorefineries Biomass Waste Supply Chain Exploit.* 234–58. <https://doi.org/10.1533/9780857097385.1.234>.
- Akada R. 2002. Genetically modified industrial yeast ready for application. *J. Biosci. Bioeng.* 94: 536–544. [https://doi.org/10.1016/S1389-1723\(02\)80192-X](https://doi.org/10.1016/S1389-1723(02)80192-X).
- Alvira P., Tomas-Pejo E., Ballesteros M., and M.J. Negro. 2010. Pretreatment technologies for an efficient bioethanol production process based on enzymatic hydrolysis: a review. *Bioresour. Technol.* 101: 4851–61. <https://doi.org/10.1016/j.biortech.2009.11.093>.
- Apel A.R., D’Espaux L., Wehrs M., Sachs D., Li R.A., Tong G.J., Garber M., Nnadi O., Zhuang W., Hillson N.J., Keasling J.D., and A. Mukhopadhyay. 2017. A Cas9-based toolkit to program gene expression in *Saccharomyces cerevisiae*. *Nucleic Acids Res.* 45: 496–508. <https://doi.org/10.1093/nar/gkw1023>.
- Baeyens J., Kang Q., Appels L., Dewil R., Lv Y., and T. Tan. 2015. Challenges and opportunities in improving the production of bioethanol. *Prog. Energy Combust. Sci.* 47: 60–88. <https://doi.org/10.1016/j.pecs.2014.10.003>.
- Balat M., and G. Ayar. 2005. Biomass energy in the World, use of biomass and potential trends. *Energy Sources* 27: 931–40. <https://doi.org/10.1080/00908310490449045>.
- Balat M., Balat H., and C. Oz. 2008. Progress in bioethanol processing. *Prog. Energy Combust. Sci.* 34: 551–73. <https://doi.org/10.1016/j.pecs.2007.11.001>.
- Balat M., and H. Balat. 2009. Recent trends in global production and utilization of bio-ethanol fuel. *Applied Energy* 86: 2273–82. <https://doi.org/10.1016/j.apenergy.2009.03.015>.
- Bannikov A.V., and A.V. Lavrov. 2017. CRISPR/Cas9, the king of genome editing tools. *Mol. Biol.* 51: 514–25. <https://doi.org/10.1134/S0026893317040033>.
- Baudin A., Ozier-kalogeropoulos O., Denouel A., Lacroute F., and C. Cullin. 1993. A simple and efficient method for direct gene deletion in *Saccharomyces cerevisiae*. *Nucleic Acids Res.* 21: 3329–30. <https://doi.org/10.1093/nar/21.14.3329>.
- Borglum G.B. 1980. Starch hydrolysis for ethanol production. *ACS Div. Fuel Chem. Prepr.* 25: 264–269.
- Bothast R.J., and M.A. Schlicher. 2005. Biotechnological processes for conversion of corn into ethanol. *Appl. Microbiol. Biotechnol.* 67: 19–25. <https://doi.org/10.1007/s00253-004-1819-8>.

- Buleon A., Colonna P., Planchot V., and S. Ball. 1998. Starch granules: structure and biosynthesis. *Int. J. Biol. Macromol.* 23: 85–112. [https://doi.org/10.1016/S0141-8130\(98\)00040-3](https://doi.org/10.1016/S0141-8130(98)00040-3).
- Cagnin L., Favaro L., Gronchi N., Rose S.H., Basaglia M., van Zyl W.H., and S. Casella. 2019. Comparing laboratory and industrial yeast platforms for the direct conversion of cellobiose into ethanol under simulated industrial conditions. *FEMS Yeast Res.* 19: 1–13. <https://doi.org/10.1093/femsyr/foz018>.
- Cardona C.A., and O.J. Sanchez. 2007. Fuel ethanol production: process design trends and integration opportunities. *Bioresour. Technol.* 98: 2415–57. <https://doi.org/10.1016/j.biortech.2007.01.002>.
- Carter Z., and D. Delneri. 2010. New generation of *LoxP*-mutated deletion cassettes for the genetic manipulation of yeast natural isolates. *Yeast* 27: 765–75. <https://doi.org/10.1002/yea.1774>.
- Castro A.M., Castilho L.R., and D.M.G. Freire. 2011. An overview on advances of amylases production and their use in the production of bioethanol by conventional and non-conventional processes. *Biomass Convers. Biorefinery* 1: 245–55. <https://doi.org/10.1007/s13399-011-0023-1>.
- Chen H., and X. Fu. 2016. Industrial technologies for bioethanol production from lignocellulosic biomass. *Renew. Sustain. Energy Rev.* 57: 468–78. <https://doi.org/10.1016/j.rser.2015.12.069>.
- Cho K.M., Yoo Y.J., and H.S. Kang. 1999. δ -Integration of endo/exo-glucanase and β -glucosidase genes into the yeast chromosomes for direct conversion of cellulose to ethanol. *Enzyme Microb. Technol.* 25: 23–30. [https://doi.org/10.1016/S0141-0229\(99\)00011-3](https://doi.org/10.1016/S0141-0229(99)00011-3).
- Cho S.W., Kim S., Kim J.M., and J.S. Kim. 2013. Targeted genome engineering in human cells with the Cas9 RNA-guided endonuclease. *Nat. Biotechnol.* 31: 230–32. <https://doi.org/10.1038/nbt.2507>.
- Chu-Ky S., Pham T.H., Bui K.L.T., Nguyen T.T., Pham K.D., Nguyen H.D.T., Luong H.N., Tu V.P., Nguyen T.H., Ho P.H. and T.M. Le. 2016. Simultaneous liquefaction, saccharification and fermentation at very high gravity of rice at pilot scale for potable ethanol production and distillers dried grains composition. *Food Bioprod. Process.* 98: 79–85. <https://doi.org/10.1016/j.fbp.2015.10.003>.
- Cinelli B.A., Castilho L.R., Freire D.M.G., and A.M. Castro. 2015. A brief review on the emerging technology of ethanol production by cold hydrolysis of raw starch. *Fuel* 150: 721–29. <https://doi.org/10.1016/j.fuel.2015.02.063>.
- Costa J.R., Bejcek B.E., McGee J.E., Fogel A.I., Brimacombe K.R., and R. Ketteler. 2017. Genome editing using engineered nucleases and their use in genomic screening. 2017. In: Sittampalam G.S., Grossman A., Brimacombe K., et al., editors. *Assay Guidance Manual*

- [Internet]. Bethesda (MD): Eli Lilly & Company and the National Center for Advancing Translational Sciences; 2004-. Bookshelf URL: <https://www.ncbi.nlm.nih.gov/books/>
- Da Silva N.A., and S. Srikrishnan. 2012. Introduction and expression of genes for metabolic engineering applications in *Saccharomyces cerevisiae*. *FEMS Yeast Res.* 12: 197–214. <https://doi.org/10.1111/j.1567-1364.2011.00769.x>.
- Dahod S.K. Raw material selection and medium development for industrial fermentation processes. In *Manual of Industrial Microbiology and Biotechnology*, 2nd ed. Demain A.L., Davies J.E., Eds. ASM Press: Washington, DC, USA, 1999. pp. 213–220, ISBN 9781555815127.
- Darling A.E., Mau B., and N.T. Perna. 2010. Progressivemaue: multiple genome alignment with gene gain, loss and rearrangement. *PLoS One* 5. <https://doi.org/10.1371/journal.pone.0011147>. Available at <https://journals.plos.org/plosone/article?id=10.1371/journal.pone.0011147>; accessed: 6th May 2019.
- David F., and V. Siewers. 2015. Advances in yeast genome engineering. *FEMS Yeast Res.* 15: 1–14. <https://doi.org/10.1111/1567-1364.12200>.
- de Cassia de Souza Schneider R., Seidel C., Fornasier F., De Souza D., V.A. Corbellini. 2018. Bioethanol production from broken rice grains. *Interciencia* 43: 846–851. ISSN: 22447776.
- Delfini, C. *Scienza e Tecnica di Microbiologia Enologica*. Edizione: Il lievito, Asti, 1995.
- Demirbas, A. 2009. Fuels from biomass. In *Biomass*, 43–59. https://doi.org/10.1007/978-1-84882-511-6_2.
- den Haan R., Kroukamp H., van Zyl J.H.D., and W.H. van Zyl. 2013. Cellobiohydrolase secretion by yeast: current state and prospects for improvement. *Process Biochem.* 48: 1–12. <https://doi.org/10.1016/j.procbio.2012.11.015>.
- Deveau H., Barrangou R., Garneau J.E., Labonte J., Fremaux C., Boyaval P., Romero D.A., Horvath P., and S. Moineau. 2008. Phage response to CRISPR-encoded resistance in *Streptococcus thermophilus*. *J. Bacteriol.* 190: 1390–1400. <https://doi.org/10.1128/JB.01412-07>.
- DiCarlo J.E., Norville J.E., Mali P., Rios X., Aach J., and G.M. Church. 2013. Genome engineering in *Saccharomyces cerevisiae* using CRISPR-Cas systems. *Nucleic Acids Res.* 41: 4336–43. <https://doi.org/10.1093/nar/gkt135>.
- Doudna J.A., and E. Charpentier. 2014. The new frontier of genome engineering with CRISPR-Cas9. *Science* 346: 1258096–1258096. <https://doi.org/10.1126/science.1258096>.
- Duan, N., Ran X., Li R., Kougias P.G., Zhang Y., Lin C., and H. Liu. 2018. Performance evaluation of mesophilic anaerobic digestion of chicken manure with algal digestate. *Energies* 11: 1–11. <https://doi.org/10.3390/en11071829>.

- Dujon B. 1996. The yeast genome project: what did we learn? *Trends Genet.* 12: 263–70. [https://doi.org/10.1016/0168-9525\(96\)10027-5](https://doi.org/10.1016/0168-9525(96)10027-5).
- Favaro L., Basaglia M., and S. Casella. 2012. Processing wheat bran into ethanol using mild treatments and highly fermentative yeasts. *Biomass and Bioenergy* 46: 605–17. <https://doi.org/10.1016/j.biombioe.2012.07.001>.
- Favaro L., Jooste T., Basaglia M., Rose S.H., Saayman M., Görgens J.F., Casella S., and W.H. van Zyl. 2012. Codon-optimized glucoamylase SGAI of *Aspergillus awamori* improves starch utilization in an industrial yeast. *Appl. Microbiol. Biotechnol.* 95: 957–68. <https://doi.org/10.1007/s00253-012-4001-8>.
- Favaro L., Basaglia M., Trento A., van Rensburg E., García-Aparicio M., van Zyl W.H., and S. Casella. 2013. Exploring grape marc as trove for new thermotolerant and inhibitor-tolerant *Saccharomyces cerevisiae* strains for second-generation bioethanol production. *Biotechnol. Biofuels* 6: 168. <https://doi.org/10.1186/1754-6834-6-168>.
- Favaro L., Jooste T., Basaglia M., Rose S.H., Saayman M., Görgens J.F., Casella S., and W.H. van Zyl. 2013. Designing industrial yeasts for the consolidated bioprocessing of starchy biomass to ethanol. *Bioengineered* 4: 97–102. <https://doi.org/10.4161/bioe.22268>.
- Favaro L., Viktor M.J., Rose S.H., Viljoen-Bloom M., van Zyl W.H., Basaglia M., Cagnin L., and S. Casella. 2015. Consolidated bioprocessing of starchy substrates into ethanol by industrial *Saccharomyces cerevisiae* strains secreting fungal amylases. *Biotechnol. Bioeng.* 112: 1751–60. <https://doi.org/10.1002/bit.25591>.
- Favaro L., Cagnin L., Basaglia M., Pizzocchero V., van Zyl W.H., and S. Casella. 2017. Production of bioethanol from multiple waste streams of rice milling. *Bioresour. Technol.* 244: 151–159. <https://doi.org/10.1016/j.biortech.2017.07.108>.
- Favaro L., Jansen T., and W.H. van Zyl. 2019. Exploring industrial and natural *Saccharomyces cerevisiae* strains for the bio-based economy from biomass: the case of bioethanol. *Crit. Rev. Biotechnol.* 39: 800–816. <https://doi.org/10.1080/07388551.2019.1619157>.
- Fierobe H.P., Stoffer B.B., Frandsen T.P., and B. Svensson. 1996. Mutational modulation of substrate bond-type specificity and thermostability of glucoamylase from *Aspergillus awamori* by replacement with short homologue active site sequences and thiol/disulfide engineering. *Biochemistry* 35: 8696–8704. <https://doi.org/10.1021/bi960241c>.
- Fierobe H.P., Clarke A.J., Tull D., and B. Svensson. 1998. Enzymatic properties of the cysteinesulfinic acid derivative of the catalytic-base mutant Glu400→Cys of glucoamylase from *Aspergillus awamori*. *Biochemistry* 37: 3753–59. <https://doi.org/10.1021/bi972232p>.
- Fraczek M.G., Naseeb S., and D. Delneri. 2018. History of genome editing in yeast. *Yeast* 35: 361–68. <https://doi.org/10.1002/yea.3308>.
- Frandsen T.P., Christensen T., Staffer B., Lehmbeck J., Dupont C., Honzatko R.B., and B. Svensson. 1995. Mutational analysis of the roles in catalysis and substrate recognition of arginines 54 and 305, aspartic acid 309, and tryptophan 317 located at subsites 1 and 2 in

- glucoamylase from *Aspergillus niger*. *Biochemistry* 34: 10162–69. <https://doi.org/10.1021/bi00032a009>.
- Friedland A.E., Tzur Y.B., Esvelt K.M., Colaiácovo M.P., Church G.M., and J.A. Calarco. 2013. Heritable genome editing in *C. elegans* via a CRISPR-Cas9 system. *Nat. Methods* 10: 741–43. <https://doi.org/10.1038/nmeth.2532>.
- Gaj T., Gersbach C.A., and C.F. Barbas. 2013. ZFN, TALEN, and CRISPR/Cas-based methods for genome engineering. *Trends Biotechnol.* 31: 397–405. <https://doi.org/10.1016/j.tibtech.2013.04.004>.
- García-Ríos E., Nuévalos M., Barrio E., Puig S., and J.M. Guillamón. 2019. A new chromosomal rearrangement improves the adaptation of wine yeasts to sulfite. *Environ. Microbiol.* 21: 1771–1781. <https://doi.org/10.1111/1462-2920.14586>.
- Giersch R.M., and G.C. Finnigan. 2017. Yeast still a beast: diverse applications of CRISPR/Cas editing technology in *S. cerevisiae*. *Yale J. Biol. Med.* 90: 643–51.
- Gietz R.D., and R.H. Schiestl. 2007. High-efficiency yeast transformation using the LiAc/SS carrier DNA/PEG method. *Nat. Protoc.* 2: 31–34. <https://doi.org/10.1038/nprot.2007.13>.
- Goffeau A., Barrell B.G., Bussey H., Davis R.W., Dujon B., Feldmann H., Galibert F., Hoheisel J.D., Jacq C., Johnston M., Louis E.J., Mewes H.W., Murakami Y., Philippsen P., Tettelin H., and S.G. Oliver. 1996. Life with 6000 genes. *Science* 274: 546–67. <https://doi.org/10.1126/science.274.5287.546>.
- Gombert A.K., and A.J.A. van Maris. 2015. Improving conversion yield of fermentable sugars into fuel ethanol in 1st generation yeast-based production processes. *Curr. Opin. Biotechnol.* 33: 81–86. <https://doi.org/10.1016/j.copbio.2014.12.012>.
- Görgens J.F., Bressler D.C., and E. van Rensburg. 2014. Engineering *Saccharomyces cerevisiae* for direct conversion of raw, uncooked or granular starch to ethanol. *Crit. Rev. Biotechnol.* 8551: 1–23. <https://doi.org/10.3109/07388551.2014.888048>.
- Gratz S.J., Cummings A.M., Nguyen J.N., Hamm D.C., Donohue L.K., Harrison M.M., Wildonger J., and K.M. O’connor-Giles. 2013. Genome engineering of *Drosophila* with the CRISPR RNA-guided Cas9 nuclease. *Genetics* 194: 1029–35. <https://doi.org/10.1534/genetics.113.152710>.
- Gronchi N., Favaro L., Cagnin L., Brojanigo S., Pizzocchero V., Basaglia M., and S. Casella. 2019. Novel yeast strains for the efficient saccharification and fermentation of starchy by-products to bioethanol. *Energies* 12: 714. <https://doi.org/10.3390/en12040714>.
- Guillamon J.M., Sabate J., Barrio E., Cano J., and A. Querol. 1998. Rapid identification of wine yeast species based on RFLP analysis of the ribosomal internal transcribed spacer (ITS) region. *Arch Microbiol.* 169: 387–392.
- Guo M., Song W., and J. Buhain. 2015. Bioenergy and biofuels: history, status, and perspective. *Renew. Sustain. Energy Rev.* 42: 712–25. <https://doi.org/10.1016/j.rser.2014.10.013>.

- Hahn-Hägerdal B., Karhumaa K., Larsson C.U., Gorwa-Grauslund M., Görgens J., and W.H. van Zyl. 2005. Role of cultivation media in the development of yeast strains for large scale industrial use. *Microb. Cell Fact.* 4: 1–16. <https://doi.org/10.1186/1475-2859-4-31>.
- Hamelinck C.N., Van Hooijdonk G., and A.P.C. Faaij. 2005. Ethanol from lignocellulosic biomass: techno-economic performance in short-, middle- and long-term. *Biomass Bioenergy* 28: 384–410. <https://doi.org/10.1016/j.biombioe.2004.09.002>.
- Hansen J., Sato M., Ruedy R., Lo K., Lea D.W., and M. Medina-Elizade. 2006. Global temperature change. *Proc. Natl. Acad. Sci.* 103: 14288–93. <https://doi.org/10.1073/pnas.0606291103>.
- He L.Y., Zhao X.Q., and F.W. Bai. 2012. Engineering industrial *Saccharomyces cerevisiae* strain with the *FLO1*-derivative gene isolated from the flocculating yeast SPSC01 for constitutive flocculation and fuel ethanol production. *Appl. Energy* 100: 33–40. <https://doi.org/10.1016/j.apenergy.2012.03.052>.
- Hendriks A.T.W.M., and G. Zeeman. 2009. Pretreatments to enhance the digestibility of lignocellulosic biomass. *Bioresour. Technol.* 100: 10–18. <https://doi.org/10.1016/j.biortech.2008.05.027>.
- Horvath P., Romero D.A., Coute-Monvoisin A.C., Richards M., Deveau H., Moineau S., Boyaval P., Fremaux C., and R. Barrangou. 2008. Diversity, activity, and evolution of CRISPR loci in *Streptococcus thermophilus*. *J. Bacteriol.* 190: 1401–12. <https://doi.org/10.1128/JB.01415-07>.
- Horwitz W., Senzel A., Reynolds H., Park D.L. *Official Methods of Analysis of the Association of Official Analytical Chemists, 12th ed.* Association of Official Analytical Chemists: Washington, DC, USA, 1975.
- Hung C.W., Martínez-Márquez J.Y., Javed F.T., and M.C. Duncan. 2018. A simple and inexpensive quantitative technique for determining chemical sensitivity in *Saccharomyces cerevisiae*. *Sci. Rep.* 8: 1–16. <https://doi.org/10.1038/s41598-018-30305-z>.
- Hwang W.Y., Fu Y., Reyon D., Maeder M.L., Tsai S.Q., Sander J.D., Peterson R.T., Yeh J.J., and J.K. Joung. 2013. Efficient genome editing in *Zebrafish* using a CRISPR-Cas system. *Nat. Biotechnol.* 31: 227–29. <https://doi.org/10.1038/nbt.2501>.
- IEA (2018), *Global Energy & CO₂ Status Report 2018*. IEA, Paris, <https://www.iea.org/geco/>.
- IEA (2018), *Renewables 2018: Analysis and Forecasts to 2023*. IEA, Paris, https://doi.org/10.1787/re_mar-2018-en.
- IEA (2018), *World Energy Outlook 2018*. IEA, Paris, <https://doi.org/10.1787/weo-2018-en>.
- Ishino Y., Shinagawa H., Makino K., Amemura M., and A. Nakamura. 1987. Nucleotide sequence of the *iap* gene, responsible for alkaline phosphatase isoenzyme conversion in *Escherichia coli*, and identification of the gene product. *J. Bacteriol.* 169: 5429–33.

- Ishizaki H., and K. Hasumi. 2014. Ethanol production from biomass. In *Res. Approaches to Sustain. Biomass Syst.*, 243–58. Elsevier. <https://doi.org/10.1016/B978-0-12-404609-2.00010-6>.
- Ishmayana S., Learmonth R.P., and U.J. Kennedy. 2011. Fermentation performance of the yeast *Saccharomyces cerevisiae* in media with high sugar concentration. In: *2nd International Seminar on Chemistry: Chemistry for a Better Future (ISC 2011)*, 24-25 Nov 2011, Bandung, Indonesia.
- Jönsson L.J., Alriksson B., and N. Nilvebrant. 2013. Bioconversion of lignocellulose: inhibitors and detoxification. *Biotechnol. Biofuels* 6: 16. <https://doi.org/10.1186/1754-6834-6-16>.
- Jakočiūnas T., Rajkumar A.S., Zhang J., Arsovska D., Rodriguez A., Jendresen C.B., Skjødt M.L., Nielsen A.T., Borodina I., Jensen M.K., and J.D. Keasling. 2015. CasEMBLR: Cas9-facilitated multiloci genomic integration of in vivo assembled DNA parts in *Saccharomyces cerevisiae*. *ACS Synth. Biol.* 4: 1126–34. <https://doi.org/10.1021/acssynbio.5b00007>.
- Jakočiūnas T., Jensen M.K., and J.D. Keasling. 2016. CRISPR/Cas9 advances engineering of microbial cell factories. *Metab. Eng.* 34: 44–59. <https://doi.org/10.1016/j.ymben.2015.12.003>.
- Jansen M.L.A., Bracher J.M., Papapetridis I., Verhoeven M.D., de Bruijn H., de Waal P.P., van Maris A.J.A., Klaassen P., and J.T. Pronk. 2017. *Saccharomyces cerevisiae* strains for second-generation ethanol production: from academic exploration to industrial implementation. *FEMS Yeast Res.* 17: 1–20. <https://doi.org/10.1093/femsyr/fox044>.
- Jansen, T., Hoff J.W., Jolly N., and W.H. van Zyl. 2018. Mating of natural *Saccharomyces cerevisiae* strains for improved glucose fermentation and lignocellulosic inhibitor tolerance. *Folia Microbiol. (Praha)*. 63: 155–168. <https://doi.org/10.1007/s12223-017-0546-3>.
- Jensen M.K., and J.D. Keasling. 2015. Recent applications of synthetic biology tools for yeast metabolic engineering. *FEMS Yeast Res.* 15: 1–10. <https://doi.org/10.1111/1567-1364.12185>.
- Jessop-Fabre M.M., Jakočiūnas T., Stovicek V., Dai Z., Jensen M.K., Keasling J.D., and I. Borodina. 2016. EasyClone-MarkerFree: a vector toolkit for marker-less integration of genes into *Saccharomyces cerevisiae* via CRISPR-Cas9. *Biotechnol. J.* 11: 1110–17. <https://doi.org/10.1002/biot.201600147>.
- Jiang W., Bikard D., Cox D., Zhang F., and L.A. Marraffini. 2013. RNA-guided editing of bacterial genomes using CRISPR-Cas systems. *Nat. Biotechnol.* 31: 233–39. <https://doi.org/10.1038/nbt.2508>.
- Jinek M., Chylinski K., Fonfara I., Hauer M., Doudna J.A., and E. Charpentier. 2012. A programmable dual-RNA guided DNA endonuclease in adaptive bacterial immunity. *Science* 337: 816–21. <https://doi.org/10.1126/science.1225829>.

- Jinek M., East A., Cheng A., Lin S., Ma E., and J. Doudna. 2013. RNA-programmed genome editing in human cells. *eLife* 2013: 1–9. <https://doi.org/10.7554/eLife.00471>.
- Kim J.H., Lee J.C., and D. Pak. 2011. Feasibility of producing ethanol from food waste. *Waste Manag.* 31: 2121–25. <https://doi.org/10.1016/j.wasman.2011.04.011>.
- Kim S.R., Ha S.J., Wei N., Oh E.J., and Y. Su Jin. 2012. Simultaneous co-fermentation of mixed sugars: a promising strategy for producing cellulosic ethanol. *Trends Biotechnol.* 30: 274–82. <https://doi.org/10.1016/j.tibtech.2012.01.005>.
- Koren S., Walenz B.P., Berlin K., Miller J.R., Bergman N.H., and A.M. Phillippy. 2017. Canu: scalable and accurate long-read assembly via adaptive k-mer weighting and repeat separation. *Genome Res.* 27: 722–736. <https://doi.org/10.1101/gr.215087.116>.
- Kurtz S., Phillippy A., Delcher A.L., Smoot M., Shumway M., Antonescu C., and S.L. Salzberg. 2004. Versatile and open software for comparing large genomes. *Genome Biol.* 5: 12. Retrieved from <http://www.tigr.org/software/mummer>.
- Kurtzman C.P., and C.J. Robnett. 1998. Identification and phylogeny of ascomycetous yeasts from analysis of nuclear large subunit (26S) ribosomal DNA partial sequences. *Int. J. Gen. Mol. Microb.* 73: 331–371. <https://doi.org/10.1023/A:1001761008817>.
- Laemmli U.K. 1970. Cleavage of structural proteins during the assembly of the head of bacteriophage T4. *Nature* 227: 680–685. <https://doi.org/10.1038/227680a0>.
- Lennartsson P.R., Erlandsson P., and M.J. Taherzadeh. 2014. Integration of the first and second generation bioethanol processes and the importance of by-products. *Bioresour. Technol.* 165: 3–8. <https://doi.org/10.1016/j.biortech.2014.01.127>.
- Lewandowski, I. 2015. Securing a sustainable biomass supply in a growing bioeconomy. *Glob. Food Sec.* 6: 34–42. <https://doi.org/10.1016/j.gfs.2015.10.001>.
- Lian J., Hamedirad M., and H. Zhao. 2018. Advancing metabolic engineering of *Saccharomyces cerevisiae* using the CRISPR/Cas system. *Biotechnol. J.* 13: 1–11. <https://doi.org/10.1002/biot.201700601>.
- Liao B., Hill G.A., and W.J. Roesler. 2010. Amylolytic activity and fermentative ability of *Saccharomyces cerevisiae* strains that express barley α -amylase. *Biochem. Eng. J.* 53: 63–70. <https://doi.org/10.1016/j.bej.2010.09.009>.
- Lorenz M.C., Muir R.S., Lim E., McElver J., Weber S.C., and J. Heitman. 1995. Gene disruption with PCR products in *Saccharomyces cerevisiae*. *Gene* 158: 113–17. [https://doi.org/10.1016/0378-1119\(95\)00144-U](https://doi.org/10.1016/0378-1119(95)00144-U).
- Lynd L.R., Wyman C.E., and T.U. Gerngross. 1999. Biocommodity engineering. *Biotechnol. Prog.* 15: 777–93. <https://doi.org/10.1021/bp990109e>.
- Lynd L.R., van Zyl W.H., McBride J.E., and M. Laser. 2005. Consolidated bioprocessing of cellulosic biomass: an update. *Curr. Opin. Biotechnol.* 16: 577–83. <https://doi.org/10.1016/j.copbio.2005.08.009>.

- Mao Y., Zhang H., Xu N., Zhang B., Gou F., and J.K. Zhu. 2013. Application of the CRISPR-Cas system for efficient genome engineering in plants. *Mol. Plant* 6: 2008–11. <https://doi.org/10.1093/mp/sst121>.
- McBride J.E.E., Deleault K.M., Lynd L.R., and J.T. Pronk. 2008. *Recombinant yeast strains expressing tethered cellulase enzymes*. U.S. Patent Application No. 12/516, 175.
- McLellan M.A., Rosenthal N.A., and A.R. Pinto. 2017. Cre-loxP-mediated recombination: general principles and experimental considerations. *Curr. Protoc. Mouse Biol.* 7: 1–12. <https://doi.org/10.1002/cpmo.22>.
- Meng X., and A.J. Ragauskas. 2014. Recent advances in understanding the role of cellulose accessibility in enzymatic hydrolysis of lignocellulosic substrates. *Curr. Opin. Biotechnol.* 27: 150–58. <https://doi.org/10.1016/j.copbio.2014.01.014>.
- Miller G.L. 1959. Use of Dinitrosalicylic acid reagent for determination of reducing sugar. *Anal. Chem.* 31: 426–428. <https://doi.org/10.1021/ac60147a030>.
- Mohd Azhar S.H., Abdulla R., Jambo S.A., Marbawi H., Gansau J.A., Mohd Faik A.A., and K.F. Rodrigues. 2017. Yeasts in sustainable bioethanol production: a review. *Biochem. Biophys. Reports* 10: 52–61. <https://doi.org/10.1016/j.bbrep.2017.03.003>.
- O’Connell K.L., and J.T. Stults. 1997. Identification of mouse liver proteins on 2D electrophoresis gels by MALDI-MS of in situ enzymatic digests. *Electrophoresis* 18: 349–359.
- OECD/FAO (2018), *OECD-FAO Agricultural Outlook 2018-2027*, OECD Publishing, Paris/FAO, Rome, https://doi.org/10.1787/agr_outlook-2018-en.
- Olson D.G., McBride J.E., Shaw A.J., and L.R. Lynd. 2012. Recent progress in consolidated bioprocessing. *Curr. Opin. Biotechnol.* 23: 396–405. <https://doi.org/10.1016/j.copbio.2011.11.026>.
- Ortiz-Muniz B., Carvajal-Zarrabal O., Torrestiana-Sanchez B., and M.G. Aguilar-Uscanga. 2010. Kinetic study on ethanol production using *Saccharomyces cerevisiae* ITV-01 yeast isolated from sugar cane molasses. *J. Chem. Technol. Biotechnol.* 85: 1361–1367. <https://doi.org/10.1002/jctb.2441>.
- Panwar N.L., Kaushik S.C., and S. Kothari. 2011. Role of renewable energy sources in environmental protection: a review. *Renew. Sustain. Energy Rev.* 15: 1513–24. <https://doi.org/10.1016/j.rser.2010.11.037>.
- Peng R., Lin G., and J. Li. 2016. Potential pitfalls of CRISPR/Cas9-mediated genome editing. *FEBS J.* 283: 1218–31. <https://doi.org/10.1111/febs.13586>.
- Perez-Ortin J.E. 2002. Molecular characterization of a chromosomal rearrangement involved in the adaptive evolution of yeast strains. *Genome Res.* 12: 1533–1539. <https://doi.org/10.1101/gr.436602>.

- Pretorius I.S. 1997. Utilization of polysaccharides by *Saccharomyces cerevisiae*. In: Zimmermann F.K., Entian K.D., (eds). *Yeast sugar metabolism*. Lancaster: Technomic Publishing Company. p 435–458.
- Pronk J.T. 2002. Auxotrophic yeast strains in fundamental and applied research. *Appl. Environ. Microbiol.* 68: 2095–2100. <https://doi.org/10.1128/AEM.68.5.2095-2100.2002>.
- Ran F.A., Hsu P.D., Wright J., Agarwala V., Scott D.A., and F. Zhang. 2013. Genome engineering using the CRISPR-Cas9 system. *Nat. Protoc.* 8: 2281–2308. <https://doi.org/10.1038/nprot.2013.143>.
- Rastogi M., and S. Shrivastava. 2017. Recent advances in second generation bioethanol production: an insight to pretreatment, saccharification and fermentation processes. *Renew. Sustain. Energy Rev.* 80: 330–40. <https://doi.org/10.1016/j.rser.2017.05.225>.
- Redden H., Morse N., and H.S. Alper. 2015. The synthetic biology toolbox for tuning gene expression in yeast. *FEMS Yeast Res.* 15: 1–10. <https://doi.org/10.1111/1567-1364.12188>.
- RFA. *Industry statistics*, Renewable Fuels Association, Washington, DC., USA. (<http://ethanolrfa.org/resources/industry/statistics/#1454099788442-e48b2782-ea53>); 2019.
- Ribereau-Gayon P., Dubourdieu D., Doneche B., Lonvaud A. 2006. Handbook of enology, volume I. *The microbiology of wine and vinifications, 2nd Edition*. John Wiley & Sons, Chichester, UK.
- Robertson G.H., Wong D.W.S., Lee C.C., Wagschal K., Smith M.R., and W.J. Orts. 2006. Native or raw starch digestion: a key step in energy efficient biorefining of grain. *J. Agric. Food Chem.* 54: 353–65. <https://doi.org/10.1021/jf051883m>.
- Ronda C., Maury J., Jakočiūnas T., Baallal Jacobsen S.A., Germann S.M., Harrison S.J., Borodina I., Keasling J.D., Jensen M.K., and A.T. Nielsen. 2015. CrEdit: CRISPR mediated multi-loci gene integration in *Saccharomyces cerevisiae*. *Microb. Cell Fact.* 14: 97. <https://doi.org/10.1186/s12934-015-0288-3>.
- Ruan J., and H. Li. 2019. Fast and accurate long-read assembly with wtdbg2. *bioRxiv* 530972. <https://doi.org/10.1101/530972>.
- Ryan O.W., Skerker J.M., Maurer M.J., Li X., Tsai J.C., Poddar S., Lee M.E., DeLoache W., Dueber J.E., Arkin A.P., and J.H.D. Cate. 2014. Selection of chromosomal DNA libraries using a multiplex CRISPR system. *eLife* 3: 1–15. <https://doi.org/10.7554/eLife.03703>.
- Saini J.K., Saini R., and L. Tewari. 2015. Lignocellulosic agriculture wastes as biomass feedstocks for second-generation bioethanol production: concepts and recent developments. *3 Biotech* 5: 337–53. <https://doi.org/10.1007/s13205-014-0246-5>.
- Sambrook J., Fritsch E.F., and T. Maniatis. 1989. *Molecular cloning: a laboratory manual, 2nd ed.* Cold Spring Harbor Laboratory, Cold Spring Harbor, N.Y.

- Sambrook J., and D.W. Russell. 2001. *Molecular cloning: a laboratory manual, 3rd Edn.* Cold Spring Harb. NY: Cold Spring Harbor Laboratory Press.
- Sanchez O.J., and C.A. Cardona. 2008. Trends in biotechnological production of fuel ethanol from different feedstocks. *Bioresour. Technol.* 99: 5270–95. <https://doi.org/10.1016/j.biortech.2007.11.013>.
- Sarris D., and S. Papanikolaou. 2016. Biotechnological production of ethanol: biochemistry, processes and technologies. *Eng. Life Sci.* 16: 307–29. <https://doi.org/10.1002/elsc.201400199>.
- Sauer B. 1987. Functional expression of the cre-lox site-specific recombination system in the yeast *Saccharomyces cerevisiae*. *Mol. Cell. Biol.* 7: 2087–96. <https://doi.org/10.1128/mcb.7.6.2087>.
- Schmidt F.R. 2005. Optimization and scale up of industrial fermentation processes. *Appl. Microbiol. Biotechnol.* 68: 425–435. <https://doi.org/10.1007/s00253-005-0003-0>.
- Shi S., Liang Y., Zhang M.M., Ang E.L., and H. Zhao. 2016. A highly efficient single-step, markerless strategy for multi-copy chromosomal integration of large biochemical pathways in *Saccharomyces cerevisiae*. *Metab. Eng.* 33: 19–27. <https://doi.org/10.1016/j.ymben.2015.10.011>.
- Sierks M.R., and B. Svensson. 1994. Protein engineering of the relative specificity of glucoamylase from *Aspergillus awamori* based on sequence similarities between starch-degrading enzymes. *Protein Eng* 7: 1479–84. <https://doi.org/10.1093/protein/7.12.1479>.
- Sims R.E.H. 2004. Renewable energy: a response to climate change. *Sol. Energy* 76: 9–17. [https://doi.org/10.1016/S0038-092X\(03\)00101-4](https://doi.org/10.1016/S0038-092X(03)00101-4).
- Sims R., Taylor M., Saddler J., and W. Mabee. 2008. *From 1st to 2nd generation biofuel technologies: an overview of current industry and RD&D activities – extended executive summary.* IEA Bioenergy, no. November 2008. <https://www.ieabioenergy.com/wp-content/uploads/2013/10/Task-IEAHQ-2nd-generation-Biofuels-Executive-Summary.pdf>. Accessed September 23rd, 2019.
- Sonoda E., Hohegger H., Saberi A., Taniguchi Y., and S. Takeda. 2006. Differential usage of non-homologous end-joining and homologous recombination in double strand break repair. *DNA Repair (Amst)*. 5: 1021–29. <https://doi.org/10.1016/j.dnarep.2006.05.022>.
- Storici F., Lewis L.K., and M.A. Resnick. 2001. *In vivo* site-directed mutagenesis using oligonucleotides. *Nat. Biotechnol.* 19: 773–76. <https://doi.org/10.1038/90837>.
- Stovicek V., Borodina I., and J. Forster. 2015. CRISPR-Cas system enables fast and simple genome editing of industrial *Saccharomyces cerevisiae* strains. *Metab. Eng. Commun.* 2: 13–22. <https://doi.org/10.1016/j.meteno.2015.03.001>.
- Stovicek V., Holkenbrink C., and I. Borodina. 2017. CRISPR/Cas system for yeast genome engineering: advances and applications. *FEMS Yeast Res.* 17: 1–16. <https://doi.org/10.1093/femsyr/fox030>.

- Subramanian K.A., Singal S.K., Saxena M., and S. Singhal. 2005. Utilization of liquid biofuels in automotive diesel engines: an Indian perspective. *Biomass Bioenergy* 29: 65–72. <https://doi.org/10.1016/j.biombioe.2005.02.001>.
- Sun H., Zhao P., Ge X., Xia Y., Hao Z., Liu J., and M. Peng. 2010. Recent advances in microbial raw starch degrading enzymes. *Appl. Biochem. Biotechnol.* 160: 988–1003. <https://doi.org/10.1007/s12010-009-8579-y>.
- Tester R.F., Karkalas J., and X. Qi. 2004. Starch - composition, fine structure and architecture. *J. Cereal Sci.* 39: 151–65. <https://doi.org/10.1016/j.jcs.2003.12.001>.
- Treu L., Toniolo C., Nadai C., Sardu A., Giacomini A., Corich V., and S. Campanaro. 2014. The impact of genomic variability on gene expression in environmental *Saccharomyces cerevisiae* strains. *Environ. Microbiol.* 16: 1378–1397. <https://doi.org/10.1111/1462-2920.12327>.
- Tsarmopoulos I., Gourgues G., Blanchard A., Vashee S., Jores J., Lartigue C., and P. Sirand-Pugnet. 2016. In-yeast engineering of a bacterial genome using CRISPR/Cas9. *ACS Synth. Biol.* 5: 104–9. <https://doi.org/10.1021/acssynbio.5b00196>.
- van der Maarel M.J.E.C., van der Veen B., Uitdehaag J.C.M., Leemhuis H., and L. Dijkhuizen. 2002. Properties and applications of starch-converting enzymes of the α -amylase family. *J. Biotechnol.* 94: 137–55. [https://doi.org/10.1016/S0168-1656\(01\)00407-2](https://doi.org/10.1016/S0168-1656(01)00407-2).
- van Zyl W.H., Bloom M., and M.J. Viktor. 2012. Engineering yeasts for raw starch conversion. *Appl. Microbiol. Biotechnol.* 95: 1377–88. <https://doi.org/10.1007/s00253-012-4248-0>.
- Viktor M.J., Rose S.H., van Zyl W.H., and M. Viljoen-Bloom. 2013. Raw starch conversion by *Saccharomyces cerevisiae* expressing *Aspergillus tubingensis* amylases. *Biotechnol. Biofuels* 6: 167. <https://doi.org/10.1186/1754-6834-6-167>.
- Vohra M., Manwar J., Manmode R., Padgilwar S., and S. Patil. 2014. Bioethanol production: feedstock and current technologies. *J. Environ. Chem. Eng.* 2: 573–84. <https://doi.org/10.1016/j.jece.2013.10.013>.
- Wagner J.M., and H.S. Alper. 2016. Synthetic biology and molecular genetics in non-conventional yeasts: current tools and future advances. *Fungal Genet. Biol.* 89: 126–36. <https://doi.org/10.1016/j.fgb.2015.12.001>.
- Walker B.J., Abeel T., Shea T., Priest M., Abouelliel A., Sakthikumar S., Cuomo C.A., Zeng Q., Wortman J., Young S.K., and A.M. Earl. 2014. Pilon: an integrated tool for comprehensive microbial variant detection and genome assembly improvement. *PLoS One* 9(11). <https://doi.org/10.1371/journal.pone.0112963>.
- Walker G.M., and R.S.K. Walker. 2018. Enhancing yeast alcoholic fermentations. *Adv. Appl. Microbiol.* Vol. 105. Elsevier Ltd. <https://doi.org/10.1016/bs.aambs.2018.05.003>.
- Wang X., Wang Z., and N.A. Da Silva. 1996. G418 selection and stability of cloned genes integrated at chromosomal δ sequences of *Saccharomyces cerevisiae*. *Biotechnol.*

Bioeng.49 (1): 45–51. [https://doi.org/10.1002/\(SICI\)1097-0290\(19960105\)49:1<45::AID-BIT6>3.0.CO;2-T](https://doi.org/10.1002/(SICI)1097-0290(19960105)49:1<45::AID-BIT6>3.0.CO;2-T).

Yamakawa S.I., Yamada R., Tanaka T., Ogino C., and A. Kondo. 2010. Repeated batch fermentation from raw starch using a maltose transporter and amylase expressing diploid yeast strain. *Appl. Microbiol. Biotechnol.* 87 (1): 109–15. <https://doi.org/10.1007/s00253-010-2487-5>.

Zabed H., Sahu J.N., Suely A., Boyce A.N., and G. Faruq. 2017. Bioethanol production from renewable sources: current perspectives and technological progress. *Renew. Sustain. Energy Rev.* 71 (October 2015): 475–501. <https://doi.org/10.1016/j.rser.2016.12.076>.

Zhang L., Zhao H., Gan M., Jin Y., Gao X., Chen Q., Guan J., and Z. Wang. 2011. Application of simultaneous saccharification and fermentation (SSF) from viscosity reducing of raw sweet potato for bioethanol production at laboratory, pilot and industrial scales. *Bioresour. Technol.* 102(6): 4573–4579. <https://doi.org/10.1016/j.biortech.2010.12.115>.

6. PARTICIPATION TO COURSES, SEMINARS AND CONGRESSES; OTHER EDUCATIONAL ACTIVITIES

Abstracts at international conferences

Cagnin L., Favaro L., **Gronchi N.**, Rose S. H., Basaglia M., van Zyl W. H., Casella S. (2017). Engineering robust yeast strains for cellobiose fermentation in presence of real lignocellulosic hydrolysates. ISSY33 Exploring and Engineering Yeasts for Industrial Application – Cork, Ireland; June 26 - 29th 2017

Favaro L., Cagnin L., Basaglia M., **Gronchi N.**, Pizzocchero V., van Zyl W. H., Casella S. (2017). Production of bioethanol from multiple waste streams of rice milling. 4th International Conference on Microbial Diversity – Bari, Italy; October 24 – 26th 2017

Favaro, L., Brojanigo, S., **Gronchi, N.**, Rodriguez Gamero, J. E., Pizzocchero, V., Basaglia, M., Casella, S. (2019) Microbial processing of organic waste streams into PHAs and other high value bio-products. Trends and Prospects in Medicinal and Pharma Biotechnologies in Europe – Bratislava, Slovakia; June 2 - 5th 2019

Gronchi N., Favaro L., Cripwell R., Basaglia M., van Zyl E., Casella S. (2019). Developing novel yeast strains for the consolidated bioprocessing of starchy substrates into bioethanol. 5th International Conference on Microbial Diversity – Catania, Italy; September 25 – 27th 2019

Oral communication at international conferences

Gronchi N., Favaro L., Cagnin L., Pizzocchero V., Basaglia M., and Casella S. (2018) “Novel industrial yeast strains for future consolidated bioprocessing of starchy by-products to ethanol” at NAXOS 2018 6th International Conference on Sustainable Solid Waste Management, Naxos Island, Greece; June 13 -16th 2018

Seminars

- Giornate formative SIROE 2017, *Gli oli essenziali: applicazioni nei settori agroalimentare, agronomico, delle produzioni animali e della medicina veterinaria*, September 15th 2017, Legnaro (PD)
- Svetoslav Todorov, *Application of bacteriocins as biopreservative tools*, April 18th 2018, Legnaro (PD)
- Maria Flora Mangano, *Giornata CRS*, June 7th 2018, Legnaro (PD)
- 2nd Yeast colloquium, *Novel industrial yeast for future consolidated bioprocessing of starchy residues into ethanol*, July 18th , 2018, Stellenbosch University (South Africa)
- MCB 22th Annual Lab Meeting, *Novel industrial yeast for future consolidated bioprocessing of starchy residues into ethanol*, October 24 – 26th 2018, Blankenberge (Belgium)
- 1st BERA *Workshop on Bioenergy*, November 11th 2018, Brussel (Belgium)
- Matteo Brillì, *NGS Bioinformatics seminars and training*, March 15-22-29th 2019, Legnaro (PD)
- Maria Flora Mangano, *Giornata CRS*, June 12th 2019, Legnaro (PD)

Attended Courses

- Alessandro Leonardi, *Introduction to Mendeleev*, October 12th 2016, Legnaro (PD)
- Barbara De Mori, *Ethics and Science. Part 1*, October 13 – 25 – 26th 2016, Legnaro (PD)
- Massimo Minervini, *Challenges and opportunities of affordable image-based plant phenotyping*, October 20th 2016, Legnaro (PD)
- Giulio Cozzi, *Research Organization and Communication “How to prepare a scientific paper”*, October 26th 2016, Legnaro (PD)
- Giulio Cozzi, *Research Organization and Communication “How to write a scientific paper”*, November 3rd 2016, Legnaro (PD)

- Simone Belluco, *How to use a systematic review approach*, November 8th 2016, Legnaro (PD)
- Enrico Sturaro, *How to present the outcome of scientific research*, November 9th 2016, Legnaro (PD)
- Marco Borga, Giulia Zuecco, *Basic Statistics; introduction to R*, November 15 – 16 – 17 – 18th 2016, Legnaro (PD)
- *Winter School*, January 23 – 26th 2017, Paluzza (UD)
- Anders Krogh, *Bioinformatics of high-throughput DNA sequencing*, February 2nd 2017, Legnaro (PD)
- Franck A. Ditengou, *Plant adaptation to the environment: the role of auxin*, March 3rd 2017, Legnaro (PD)
- Mark Olson, *Scientific Writing in English*, March 6 – 9th 2017, Legnaro (PD)
- Riccardo Crestani, *Academic English*, January – March 2018, Centro Linguistico di Ateneo, Padova
- *Winter School*, January 22 – 25th 2018, Paluzza (UD)

Teaching support

Organization and management of lab activities as part of the “Microbiologia agraria” course for undergraduate students from School of Agriculture (A.A. 2017-2018, 2018-2019), under the supervision of Prof. Sergio Casella (University of Padua, Legnaro, PD)

7. PUBLICATIONS

Gronchi N., Favaro L., Cagnin L., Brojanigo S., Pizzocchero V., Basaglia M. and Casella S. (2019). Novel Yeast Strains for the Efficient Saccharification and Fermentation of Starchy By-Products to Bioethanol. *Energies* 12 (4): 714. <https://doi.org/10.3390/en12040714>.

Cagnin L., Favaro L., **Gronchi N.**, Rose S. H., Basaglia M., van Zyl W. H., and Casella S. (2019). Comparing Laboratory and Industrial Yeast Platforms for the Direct Conversion of Cellobiose into Ethanol under Simulated Industrial Conditions. *FEMS Yeast Research* 19 (2): 1–13. <https://doi.org/10.1093/femsyr/foz018>.

8. ACKNOWLEDGMENTS

I would like to thank my Supervisors and my Co-Supervisor for their guidance throughout this journey. Their knowledge and support were fundamental for the success of the thesis.

I would like to express my gratefulness to Professor van Zyl and Doctor Rosemary Cripwell, that followed me not just during my research at Stellenbosch University (South Africa), contributing a lot to my personal and professional growth. In this regard, I am very honoured for the opportunity to be part of the bilateral joint research projects between Italy and South Africa (ZA18MO04).


A huge appreciation to Professor Thevelein and Doctor Maria Foulquié Moreno from KU Leuven (Belgium) for their expertise, advices and hospitality to the MCB lab.

Lastly but not least, I want to say thank you to all my lab fellows for their encouragement and technical support.

To my family, for the endless patience and care.

Article

Novel Yeast Strains for the Efficient Saccharification and Fermentation of Starchy By-Products to Bioethanol

Nicoletta Gronchi, Lorenzo Favaro * , Lorenzo Cagnin, Silvia Brojanigo, Valentino Pizzocchero, Marina Basaglia and Sergio Casella

Department of Agronomy, Food, Natural resources, Animals and the Environment (DAFNAE), University of Padova, Agripolis, 35020 Legnaro (PD), Italy; nicoletta.gronchi@studenti.unipd.it (N.G.); lorenzocagnin@gmail.com (L.C.); silvia.brojanigo@gmail.com (S.B.); valentino.pizzocchero@unipd.it (V.P.); marina.basaglia@unipd.it (M.B.); sergio.casella@unipd.it (S.C.)

* Correspondence: lorenzo.favaro@unipd.it; Tel.: +39-049-8272800; Fax: +39-049-8272929

Received: 16 January 2019; Accepted: 19 February 2019; Published: 22 February 2019



Abstract: The use of solid starchy waste streams to produce value-added products, such as fuel ethanol, is a priority for the global bio-based economy. Despite technological advances, bioethanol production from starch is still not economically competitive. Large cost-savings can be achieved through process integration (consolidated bioprocessing, CBP) and new amylolytic microbes that are able to directly convert starchy biomass into fuel in a single bioreactor. Firstly, CBP technology requires efficient fermenting yeast strains to be engineered for amylase(s) production. This study addressed the selection of superior yeast strains with high fermentative performances to be used as recipient for future CBP engineering of fungal amylases. Twenty-one newly isolated wild-type *Saccharomyces cerevisiae* strains were screened at 30 °C in a simultaneous saccharification and fermentation (SSF) set up using starchy substrates at high loading (20% w/v) and the commercial amylases cocktail STARGEN™ 002. The industrial yeast Ethanol Red™ was used as benchmark. A cluster of strains produced ethanol levels (up to 118 g/L) significantly higher than those of Ethanol Red™ (about 109 g/L). In particular, *S. cerevisiae* L20, selected for a scale-up process into a 1-L bioreactor, confirmed the outstanding performance over the industrial benchmark, producing nearly 101 g/L ethanol instead of 94 g/L. As a result, this strain can be a promising CBP host for heterologous expression of fungal amylases towards the design of novel and efficient starch-to-ethanol routes.

Keywords: ethanol; starchy waste; natural yeast strains; consolidated bioprocessing; broken rice

1. Introduction

In the near future, the non-renewable resources such as crude oil, coal and natural gases, that collectively account for about 82% of global energy needs [1], will no longer be viable. Therefore, the global communities are moving toward the search for reducing fossil oil dependence and long-term sustainable forms of energies such as biofuels [2–6].

Among liquid biofuels, bioethanol has emerged as a clean and eco-friendly fuel that could replace gasoline, both as pure ethanol in specially designed engines, or most widely as blends with fossil gasoline ranging from 5 to 20% (also referred to as E5 or E20) [1,7,8]. Although the energy equivalent of ethanol as fuel is 66% than petroleum, its combustion is 15% more efficient because of higher oxygen content and less exhaust emissions, such as sulfur and nitrogen oxides, are produced [9]. It has been estimated that the use of 10% ethanol blends could reduce greenhouse gasses emissions by 12–19% compared to conventional fossil fuel [10].

In Brazil and US, the leading producers, first generation bioethanol is obtained from sugarcane or corn starch, respectively. However, since bioethanol market is expanding further, a good strategy is to look for alternative feedstocks that do not compete with food supplies [11]. In this perspective, biomasses are accounted as the fourth largest source of energy on Earth [1,12] and it is expected that the only foreseeable primary source that could provide adequate fuel supplies for transportation sector is waste biomass [13]. Before being processed to any added-valued compounds, solid waste streams have to be carefully managed through the promotion of safe practices and effective technologies, such as source separation, biological treatment and supply chain development to ensure the overall economic feasibility of the process. A wide variety of waste organic materials, like residues from agricultural, forest and industrial processing as well as the organic fraction of municipal solid waste, actually contains considerable amounts of fermentable glucose, as monomers or polymers (i.e., starch, cellulose), that have been used for biofuels, biopolymers and enzymes production [14–20].

Lignocellulosic biomasses are the most promising raw materials considering their great availability and limited cost [11,21,22]. Along with lignocellulose, starchy waste streams with high starch content could be exploited for bioethanol production [23–27]. Indeed, starch is the most abundant form of energy storage in plants. The structure can vary regarding the botanical species (starch content can range from 50 to 90% in cereals, tubers and roots) and represents a high-yielding ethanol resource [2,9,28].

The current industrial process of starch conversion into bioethanol, involves four steps: (I) liquefaction at high temperatures (80–100 °C), (II) saccharification into glucose by thermostable α -amylases and glucoamylases, (III) microbial fermentation to ethanol and (IV) alcohol distillation and dehydration [29]. However, the global-scale application is hampered by high cost processing. The feedstock (corn) is considered as the main share (60%) followed by processing expenditures (10–20%). To ensure the economic feasibility of the overall process, the substitution of corn with cheaper biomasses together with improved process integrations have been proposed [9,30]. The total cost expenditure to produce bioethanol from starch could be reduced by consolidated bioprocessing (CBP) configuration and by using a single microorganism able to both secrete hydrolytic enzymes and ferment the resulting sugars in a single reactor [31,32]. The advantages include the direct utilization of raw starch without pre-treatment steps, eliminating the cost for energy inputs, exogeneous enzymes, maximizing the ethanol yield and minimizing by-product formation [33].

To date, no natural microorganism is available to perform CBP. Genome engineering, such as heterologous gene expression, is fundamental to create a new microbial biocatalyst to be used at industrial scale for the starch-to-ethanol processing [31]. In *S. cerevisiae*, heterologous gene expression is well established. Several amylase genes have been expressed for starch conversion, mainly in laboratory strains and, lately, also in natural and industrial strains [34–37]. However, the conversion rate of raw feedstocks or high substrate loading was not relevant for industrial scale. Even though good progresses have been done, the major challenge is the co-production of both amylases and glucoamylases at optimal levels to achieve high volumetric activities. The effective conversion of raw starch in a short timeframe could be competitive only if the fermentation abilities of the strain are not affected in terms of ethanol yield and starch utilization [32,35,38,39].

This study looked for novel *S. cerevisiae* strains with superior fermenting abilities to be used as host strains for heterologous expression of novel fungal hydrolytic enzymes with the final aim of developing efficient CBP yeast. A collection of wild-type strains, newly isolated from a winery, has been evaluated for fermentative performances at 30 °C under SSF regime of high substrate loading (20% w/v) of starchy materials. A commercial mix of α -amylase and glucoamylase, STARGENTM 002, was used at optimized doses to perform starch hydrolysis. The *S. cerevisiae* Ethanol RedTM strain, currently applied in first and second generation bioethanol plants, served as benchmark [37].

Broken rice, where starch accounts up to 87.5% of dry matter, has been adopted as a model of several agricultural and industrial wastes mainly composed by starch [9]. It is one of the most abundant waste streams of rice processing with more than 45 million tons globally produced per

year [40]. Such enormous amount of cheap biomass would be directly accessible and/or collectable at rice processing sites [24]. Raw corn starch (Sigma-Aldrich, Milano, Italy) was used as control feedstock.

2. Results and Discussion

2.1. Isolation, Genetic Characterization and Fermentative Abilities of Novel Yeast Strains in Glucose

With the final aim of isolating and selecting strains with high fermenting performances from glucose, the winery background was chosen since it is related to ethanol production and yeast are expected to produce and tolerate high alcohol concentrations. Yeast strains were isolated from grape marcs and incubated on Wallerstein Laboratory (WL) plates at 30 °C. Twenty-one isolates were classified as *S. cerevisiae* and first screened for their ability to consume glucose at 30 °C in must nutritive synthetic (MNS) minimal medium supplemented with 200 g/L glucose, as such concentration is typical of the first generation ethanol plants after saccharification of corn [38].

Due to their relatively different phenotypic backgrounds, seven control strains of *S. cerevisiae* were included in this research as benchmarks (Table 1). Three of these reference strains, namely *S. cerevisiae* Fm17, M2n and MEL2, have been already exploited for ethanol production from different lignocellulosic and starchy substrates [18,32,41,42], whereas three additional strains (*S. cerevisiae* HR4, WL3, YI30), recently characterized for their inhibitors tolerance and fermenting abilities [43], were included as additional controls. Finally, *S. cerevisiae* Ethanol Red™ was considered as industrial reference strain, widely applied in both first and second generation ethanol applications [37].

Table 1. *S. cerevisiae* strains used in this study.

<i>S. cerevisiae</i> Strains	Relevant Phenotype and Origin	Source/Reference
L1–L21	wild-type	This study
Ethanol Red™	industrial strain	Fermentis
Fm17	wild-type strain with high lignocellulosic inhibitors tolerance	[41]
M2n	distillery strain	[32]
MEL2	wild type strain from grape marcs	[42]
HR4	wild-type strain from wine fermentations	[43]
WL3	wild-type strain from wine fermentations	[43]
YI30	wild-type strain from wine fermentations	[43]

In this project, the ability of the yeast to utilize glucose was determined as fermenting vigour and expressed in terms of grams of glucose consumed per L of MNS medium, as described in Materials and Methods. Overall, both newly selected isolates and control strains exhibited high and comparable level of fermenting vigour (Figure 1). The newly isolated strains *S. cerevisiae* L1, L2, L5, L7, L8, L9 and L21, were not included as their fermenting abilities were lower than those of the benchmark strain M2n, displaying the bottom fermenting vigour.

Once incubated in 200 g/L glucose, few isolates quickly consumed all the sugar within 15 days (Figure 1). Among them, *S. cerevisiae* L6, L14, L15, L16 and L20 demonstrated outstanding fermentative vigour. Interestingly, their ability outperformed those reported for *S. cerevisiae* MEL2 and *S. cerevisiae* Ethanol Red™, which showed the most favorable vigour among the reference yeast strains. Moreover, the selected newly isolated strains disclosed fermentative efficiency higher than those recently described from high glucose concentrations by several *S. cerevisiae* yeast [42,44,45]. As such, the fermenting capabilities of the novel yeast strains are promising considering also the medium adopted to screen for fermenting vigour. MNS broth, when compared with the formulation of other commonly used defined media [46,47], has indeed the lowest levels of components, macro and micro-nutrients. Therefore, yeast able to grow rapidly and efficiently ferment under nutrient limitation should be considered very interesting for bioethanol industrial scale applications. To further assess their aptitude to ferment starchy substrates under SSF configurations, representative of starch-to-ethanol processes, the novel collection of yeast has been adopted to produce ethanol from broken rice and raw corn starch.

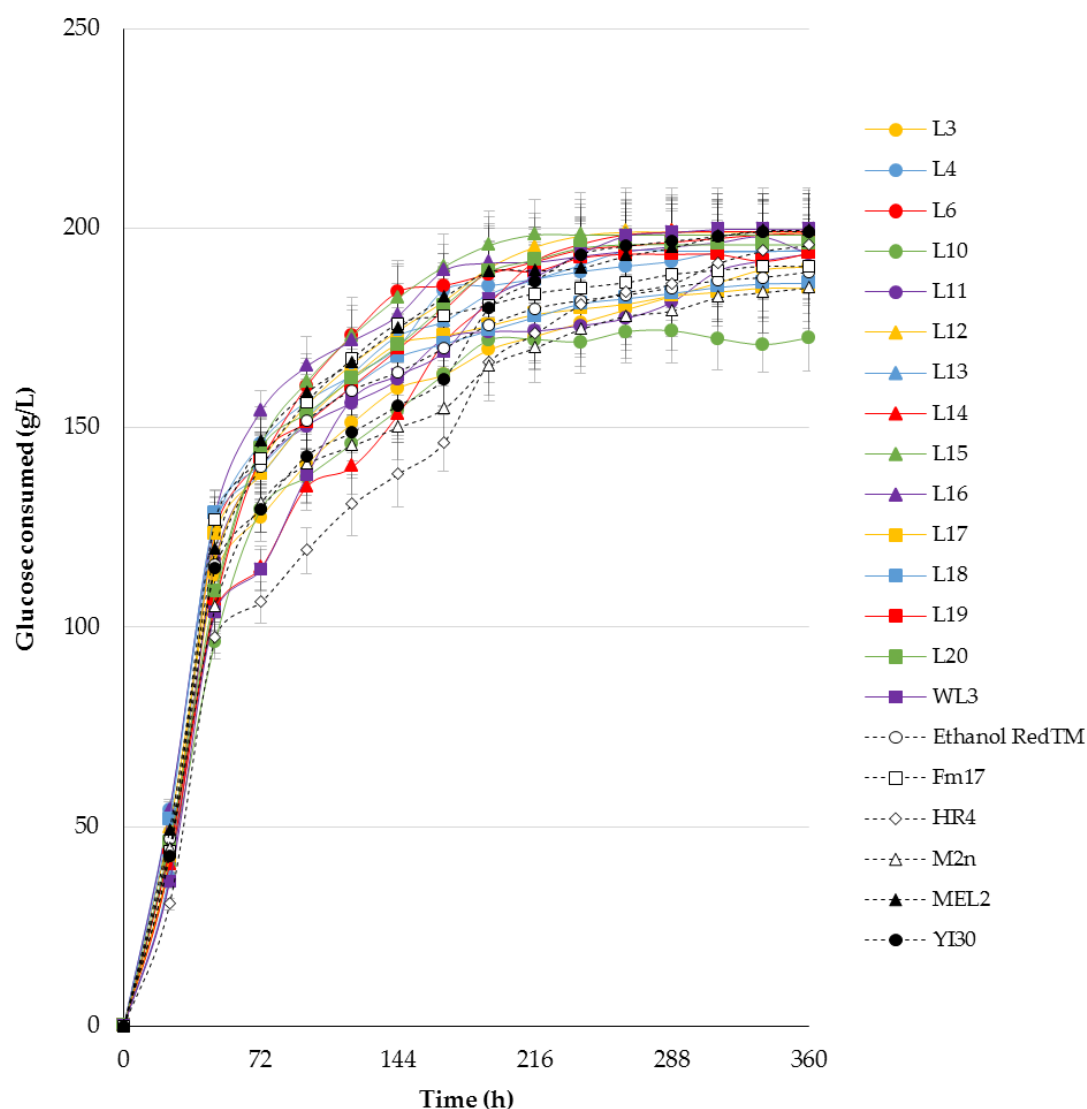


Figure 1. Cumulative sugar utilization (g/L) of *S. cerevisiae* strains in MNS medium with 200 g/L glucose. The experiment was conducted in triplicate (\pm SD).

2.2. Fermentative Abilities under SSF Setting on Starchy Materials

The fermentative vigour of all the strains was then evaluated on broken rice and raw corn starch at high substrate loading (20% w/v) under oxygen-limited conditions at 30 °C. The commercial mixture of amylases STARGENTM 002 was supplied to support starch saccharification. Based on the assumptions that one gram of starch is equivalent to 1.11 g of glucose [48], the final theoretical glucose concentration achievable by complete saccharification of 20% w/v of starchy materials was 194 and 235 g/L of YNB containing 20% w/v of broken rice and corn starch, respectively.

Owing to the great volume of data generated, total cumulative glucose consumption (Figure 2) and fermentation parameters (Table 2) are reported only for the best ten fermenting strains (namely L11, L12, L13, L15, L16, L17, L18, L19 and L20) as well as for the top performing benchmark yeast *S. cerevisiae* WL3 and Ethanol RedTM.

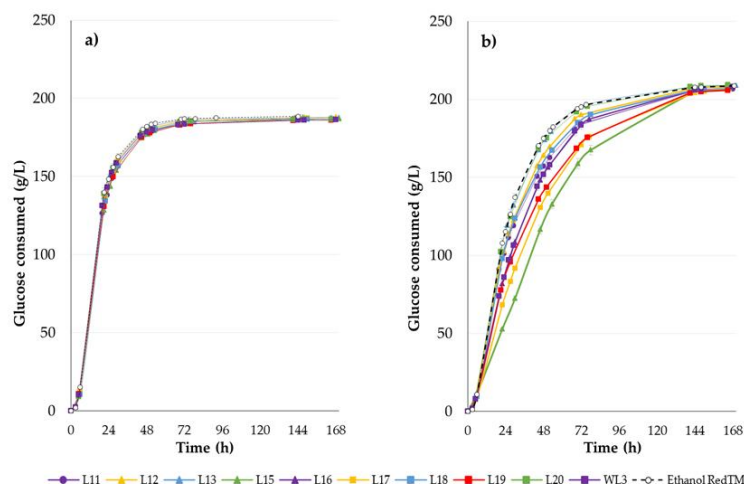


Figure 2. Cumulative sugar utilization (g/L) of *S. cerevisiae* strains at 30 °C in YNB medium with 20% w/v (a) broken rice or (b) raw corn starch in the presence of STARGEN™ 002. The experiment was conducted in triplicate (\pm SD).

In the presence of broken rice, all the selected strains performed comparably and only slight differences in fermenting vigour could be appreciated between the newly isolated and the benchmarks (Figure 1a). The highest glucose consumption on broken rice was approximately 97% of the theoretical content (188 g for L18 and L20 out of 194 g/L). Furthermore, broken rice was confirmed to be a promising material for ethanol production [24] with more than 100 g/L of ethanol produced (Table 2). Nevertheless, this substrate was not suitable for strain selection, since no significant differences, at least in terms of fermenting vigour, were evident among the tested strains. This could be ascribed to the native high amount of simple sugars (mainly glucose, fructose and sucrose) and proteins (8.5% DM) of broken rice (see Materials and Methods), which could have enhanced and supported the fermenting activities.

On the contrary, raw corn starch, with very limited values of protein (0.3% DM, see Table 4) and no free sugars available, demonstrated to be a useful feedstock to screen for the most promising yeast strains. As reported in Figure 1b, indeed, the ten selected novel yeast strains showed comparable but different levels of fermenting vigour. Overall, only about 85% of glucose theoretically obtainable by saccharification of raw corn starch was used (200 g of glucose out of 235 g/L). Noteworthy, a small number of strains, including L13 (up to 208.9 g/L), L20 (up to 206.5 g/L) and WL3 (up to 207.9 g/L), performed very similarly to Ethanol Red™, which clearly reaffirmed its great ability to consume glucose (208.7 g/L) (Figure 2b). The strains demonstrating a glucose consumption significantly lower than Ethanol Red™ were not considered as proficient fermenting yeast.

The ethanol yield, glucose and glycerol content of SSF experiments after 120 h are reported in Table 2. Only minimal amounts of residual glucose were observed in few spent fermentation broths (Table 2), indicating that the majority of the strains were able to completely utilize the sugar. The cluster of selected strains produced ethanol levels significantly greater than Ethanol Red™ from both broken rice and raw corn starch. This means that the industrial yeast *S. cerevisiae* Ethanol Red™, although presenting the fastest glucose consumption rates (Figure 1), was outperformed in terms of ethanol yield by all the selected novel strains as well as by the benchmark *S. cerevisiae* WL3, recently reported for promising fermenting performances [43]. Glycerol was detected as a common secondary fermentation product. According to what is reported for vinification, the concentrations of glycerol were found to be nearly 10 times smaller than the ethanol produced [49]. To increase ethanol production as biofuel, it is fundamental to minimize glycerol formation to better redirect the carbon flux towards ethanol. Interestingly, all newly isolated strains together with the reference *S. cerevisiae* WL3 produced glycerol at comparable levels from both broken rice and raw corn starch confirming their great ability to rapidly convert glucose into ethanol. On the contrary *S. cerevisiae* Ethanol Red™ showed the highest glycerol

production when SSF was conducted on raw starch and high glycerol levels comparatively to ethanol produced also from broken rice (Table 2).

Table 2. Ethanol, glucose and glycerol content of SSF experiment at 30 °C using as substrate broken rice or raw corn starch. The substrate loading for each experiment was 20% (w/v). The experiment was conducted in triplicate (\pm SD). $Y_{E/S}$, % of theoretical maximum ethanol yield per gram of glucose equivalent available.

Strain	Broken Rice				Raw Corn Starch			
	Residual Glucose (g/L)	Glycerol (g/L)	Ethanol Concentration (g/L)	$Y_{E/S}$	Residual Glucose (g/L)	Glycerol (g/L)	Ethanol Concentration (g/L)	$Y_{E/S}$
Ethanol Red™	-	8.83 \pm 0.12	101.05 \pm 0.54	91	0.30 \pm 0.06	10.05 \pm 0.17	109.36 \pm 0.33	86
L11	-	8.75 \pm 0.02	107.70 \pm 0.44	97	1.68 \pm 0.28	9.19 \pm 0.20	116.07 \pm 0.06	91
L12	0.58 \pm 0.14	9.03 \pm 0.03	108.39 \pm 1.22	98	0.82 \pm 0.65	9.21 \pm 0.19	116.22 \pm 1.97	91
L13	0.62 \pm 0.01	9.45 \pm 0.18	107.15 \pm 0.28	97	1.55 \pm 0.76	9.63 \pm 0.04	116.12 \pm 0.96	91
L15	-	8.90 \pm 0.06	107.43 \pm 0.16	97	-	8.24 \pm 0.08	117.17 \pm 0.08	92
L16	-	8.93 \pm 0.04	107.77 \pm 0.21	97	-	9.25 \pm 0.15	117.93 \pm 0.14	92
L17	-	8.36 \pm 0.02	107.16 \pm 0.66	97	-	8.53 \pm 0.01	116.78 \pm 0.42	92
L18	-	7.79 \pm 0.05	106.73 \pm 0.34	96	-	8.45 \pm 0.09	117.35 \pm 1.06	92
L19	-	8.25 \pm 0.08	107.32 \pm 0.25	97	-	8.60 \pm 0.11	116.44 \pm 0.21	91
L20	-	8.17 \pm 0.14	107.19 \pm 0.15	97	-	7.97 \pm 0.09	116.98 \pm 1.73	92
WL3	0.30 \pm 0.01	9.16 \pm 0.12	106.17 \pm 0.36	96	0.29 \pm 0.04	9.60 \pm 0.07	115.05 \pm 0.24	90

Taken together the experiments on fermenting vigour from glucose (Figure 1) and SSF configurations with broken rice and raw starch as substrates (Figure 2 and Table 2) indicated that the newly isolated strains have great potential as ethanol producers, with performances even higher than those exhibited by several benchmark yeast strains. More specifically, *S. cerevisiae* L20 displayed one of the most outperforming phenotypes, especially in the early stage of fermentation, and was then selected for further fermentation experiments at bioreactor scale.

2.3. Scale-up in 1-L Bench Fermenter

S. cerevisiae L20 together with the reference Ethanol Red™ have been investigated for SSF in 1-L bench reactor using 20 % w/v of either broken rice or raw corn starch (Figure 3). When broken rice was used as feedstock, the fermentation trend was similar for both strains (Figure 3). Interestingly, the strains produced comparable ethanol levels (about 86 g/L) after 72 h of fermentation. Nevertheless, the novel strain displayed ethanol performances always better than those of Ethanol Red™, particularly after 24 h of SSF (Table 3), with a maximum productivity of 3.10 g/L/h, which was 1.10-fold than that of the industrial benchmark (2.83 g/L/h). Such ethanol productivity values are of great interest and potential application [39]. Moreover, final ethanol yields were also higher, with the novel strain displaying 86% of the maximum theoretical instead of 83% detected for *S. cerevisiae* Ethanol Red™.

On raw starch, *S. cerevisiae* L20 confirmed to be a promising strain (Figure 3a and Table 3), with almost 101 g/L ethanol produced within 72 h of incubation. On the contrary, as reported in Figure 3b and Table 3, the industrial yeast produced lower alcohol values (up to 94 g/L). Fermenting parameters were again much better for *S. cerevisiae* L20 (Table 3), with a maximum productivity of 3.20 g/L/h, which was 1.33-fold higher than that of the industrial benchmark (2.41 g/L/h). Ethanol yields and carbon conversion values confirmed that the novel strain outperformed the industrial yeast further supporting both the saccharification of starch to glucose and then glucose-to-ethanol fermentation.

Overall, as reported in Table 3, ethanol levels and efficiencies obtained by the yeast strains from both substrates were found to be lower than those detected at smaller scale (Table 2). This finding could be due to an increase of viscosity of the medium which was found to limit the ethanol yield in up-scaling of high gravity SSF experiments on sweet potato [50] or to an increase of stress exposure linked to limited transportation and elimination of CO₂, toxic metabolites and additional heat generated by agitation [51]. This calls for further experimental activities in order to optimize the scaling up of the

process and is in agreement with lower ethanol yields recently obtained up-scaling the simultaneous liquefaction, saccharification and fermentation (SLSF) of broken rice at high gravity [52].

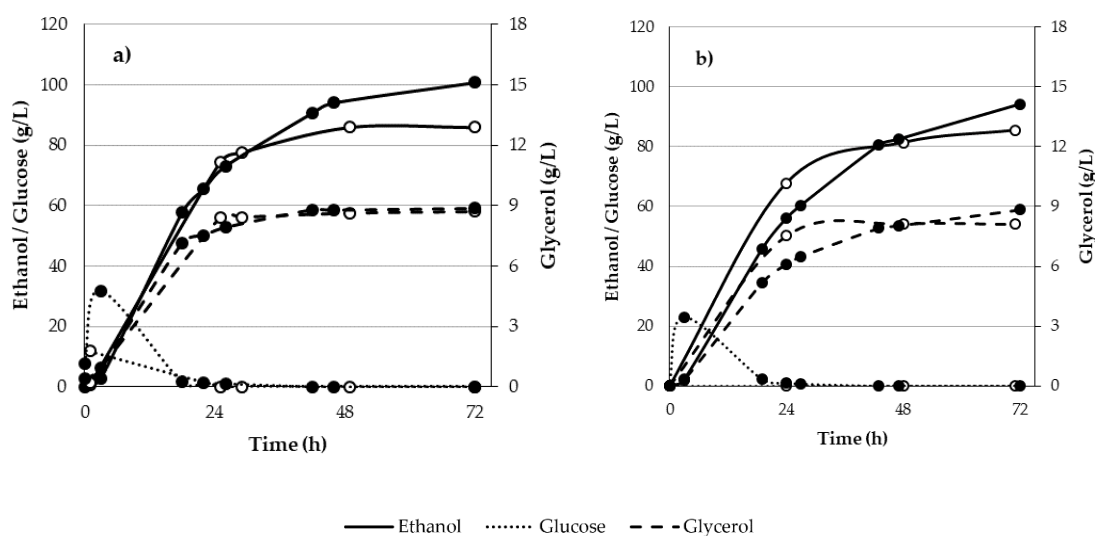


Figure 3. Ethanol, glucose and glycerol production by *S. cerevisiae* wild-type strains (a) L20 and (b) Ethanol Red™ during SSF in 1-L bioreactor with 20% (w/v) of broken rice (○) and raw corn starch (●). The experiment was conducted in duplicate and average values are presented.

Table 3. Conversion of starchy substrates at bioreactor level to ethanol and by-products by *S. cerevisiae* L20 and Ethanol Red™ strains.

Feedstock	<i>S. cerevisiae</i> L20		<i>S. cerevisiae</i> Ethanol Red™	
Broken rice = a glucose equivalent of 198.55 g/L and a total carbon available (mol C) of 6.62				
Product (g/L)	24 h	72 h	24 h	72 h
Glucose	nd	nd	nd	nd
Glycerol	8.40	8.70	7.54	8.12
Ethanol	74.44	87.01	67.86	85.46
CO ₂	71.20	83.23	64.91	81.74
Total carbon	5.13	5.96	4.67	5.84
Carbon conversion (mol C)	77%	90%	71%	88%
Y _{E/S} (% of theoretical)	73%	86%	67%	83%
Q (g/L/h)	3.10	1.21	2.83	1.19
Q _{max} (g/L/h)	3.10 after 24 h		2.83 after 24 h	
Raw corn starch = a glucose equivalent of 238.82 g/L and a total carbon available (mol C) of 7.93				
Product (g/L)	24 h	72 h	24 h	72 h
Glucose	1.04	nd	1.14	nd
Glycerol	7.92	8.86	6.10	8.84
Ethanol	73.10	100.84	56.02	94.20
CO ₂	69.92	96.46	53.58	90.10
Total carbon	5.06	6.87	3.89	6.43
Carbon conversion (mol C)	64%	86%	49%	81%
Y _{E/S} (% of theoretical)	60%	83%	46%	77%
Q (g/L/h)	3.05	1.40	2.33	1.31
Q _{max} (g/L/h)	3.20 after 18 h		2.41 after 18 h	

nd: not detected; Y_{E/S}, theoretical maximum ethanol yield per gram of glucose equivalent available.

3. Materials and Methods

3.1. Feedstocks and Commercial Enzymes

Broken rice was obtained from La Pila (Isola della Scala, Verona, Italy), dried in a forced-air oven at 60 °C for 48 h and milled in a hammer mill to pass throughout a 1.25 mm screen. The raw material was stored at room temperature. Starch from corn (Sigma-Aldrich) was used as benchmark substrate for SSF. No pre-treatments were performed, and raw feedstocks were used as such. The composition in terms of starch and protein, determined according to international standard methods [53], is reported in Table 4. The content of fermentable sugars in broken rice, namely glucose, fructose and sucrose, were assessed at 11.5 g/Kg on a total of sugars of 13 g/Kg.

Table 4. Composition of feedstocks used in this study.

Feedstock	Dry Matter, DM (%)	Protein (% DM)	Starch (% DM)
Broken rice	96.0	8.5	84.0
Raw corn starch	90.3	0.3	95.3

The enzyme mix STARGEN™ 002, kindly supplied by Genencor (DuPont-Danisco group, Itasca, IL, USA), is an optimized blend of *Aspergillus kawachii* α -amylase expressed in *Thricoderma reesei* and glucoamylase from *T. reesei* that works synergistically to hydrolyze granular starch to glucose. The enzymatic activity is 570 Glucoamylase Unit (GAU)/g and specific gravity is 1.14 g/mL. STARGEN™ 002 was used following the supplier's instructions (<http://www.dupont.com/content/dam/dupont/products-and-services/industrial-biotechnology/documents/DuPont-STARGEN002-web-EN.pdf>).

3.2. Yeast Strains, Isolation and Genetic Identification

A collection of twenty-one wild-type *S. cerevisiae* strains was isolated in 2013 from grape marcs of a winery in Melara (Rovigo, Italy) (Table 1). After a storage of 30 days at the winery, fifty grams of marcs were dispersed in 500 mL of sterile physiological water (0.85% NaCl), plated, after appropriate decimal dilutions, on WL medium (Wallerstein Laboratory, Oxoid, Milano, Italy; g/L: yeast extract, 4; casein hydrolysate, 5; D-glucose, 50; KH₂PO₄, 0.55; KCl, 0.425; CaCl₂, 0.125; MgSO₄, 0.125; FeCl₃, 0.0025; MnSO₄, 0.0025; bromocresol green, 0.022) containing 200 μ g/mL chloramphenicol (Sigma-Aldrich, Italy) to contain bacterial growth and incubated at 30 °C for 72 h. After isolation, yeast colonies were purified by growing on Yeast Peptone Dextrose (YPD; g/L: yeast extract, 10; peptone, 20; glucose, 20) at 30 °C for 48 h. Isolates were maintained at –80 °C in YPD containing 20% (v/v) glycerol.

Genetic identification was achieved by D1/D2 region sequence analysis. Amplification of D1/D2 domain was performed using primers NL1 (5'-GCA TAT CAA TAA GCG GAG GAA AAG-3') and NL4 (5'-GGT CCG TGT TTC AAG ACG G-3') according to the protocol described by Kurtzman and Robnett [54]. Amplification products were checked by 1% agarose gel electrophoresis and then subjected to sequencing. Species identification was performed after BlastN alignment (<http://blast.ncbi.nlm.nih.gov/Blast.cgi>) of the obtained sequences with those present in the Gen-Bank public database. A minimum sequence similarity level of 98% was considered for species identification.

3.3. Fermentative Abilities of *S. cerevisiae* Strains in MNS Broth Supplemented with 200 g/L Glucose

S. cerevisiae strains were assessed for their fermentative ability in MNS minimal medium (g/L: (NH₄)₂SO₄, 0.3; (NH₄)₂HPO₄, 0.3; KH₂PO₄, 1; MgSO₄·7H₂O, 0.5; NaCl, 0.1; malic acid, 2; tartaric acid, 3. mg/L: biotin, 0.02; D-pantothenic acid, 0.4; myo-inositol, 2; nicotinic acid, 0.4; thiamine, 0.4; pyridoxine, 0.4; *p*-aminobenzoic acid, 0.2; H₃BO₃, 0.5; CuSO₄·5H₂O, 0.04; KI, 0.1; NaMoO₄·2H₂O, 0.2; ZnSO₄·7H₂O, 0.4; FeCl₃·6H₂O, 0.4; CaCl₂·2H₂O, 100) supplemented with 200 g/L glucose according to the method described by Favaro and colleagues [41]. MNS broth was specifically adopted as

it can be considered quite similar to several poor industrial media [47,55] and can resemble the pre-industrial scale composition of bioethanol broth, where mainly $\text{MgSO}_4 \cdot 7\text{H}_2\text{O}$, $(\text{NH}_4)_2\text{SO}_4$ and little amounts of corn steep liquor are generally added during the fermentation step [56,57]. The commercial strain Ethanol Red™ (Fermentis, Marcq-en-Baroeul, France), currently used for large scale bioethanol fermentation, was included as industrial benchmark together with other yeast strains recently reported for their high promise as bioethanol producers (Table 1).

In short, every glass serum bottle was filled with 100 mL of MNS medium and then sealed using rubber stoppers with a needle for the removal of CO_2 produced during fermentation. Pre-cultures of *S. cerevisiae* strains, grown overnight into YPD broth, were collected, centrifuged and washed twice with sterile physiological water (0.85% NaCl). Yeast cells were then inoculated, with an average cell concentration of 7.5×10^4 cells per mL, into each serum bottle containing 100 mL MNS broth. The incubation was performed in static condition at 30 °C. The pH of medium was set at 3.5 using KOH (5 M). Fermentative vigour was daily monitored by measuring weight loss due to CO_2 production. Results were reported as grams of glucose utilized per L of MNS by using a conversion factor of 2.118 [55]. The experiments were carried out in triplicate.

3.4. Fermentative Abilities of *S. cerevisiae* Strains on Starchy Materials

All strains were screened for fermentative abilities in an SSF regime from broken rice and raw corn starch. Pre-cultures were prepared in YNB broth (with amino acids: Yeast Nitrogen Base 6.7 g/L; Sigma-Aldrich) with 2% w/v of glucose in Erlenmeyer flasks and incubated overnight at 30 °C on a rotatory shaker at 600 rpm. Small-scale SSFs were conducted in 120-mL serum bottles with 20% (w/v) dry substrate and appropriate nitrogen source (YNB with amino acids: 6.7 g/L; Sigma-Aldrich) in a total volume of 100 mL of buffered medium (citrate buffer 0.1 M at pH 4). Yeast cells were inoculated at Optical Density (OD) value of 1 and ampicillin (100 mg/L) and streptomycin (75 mg/L) were added to prevent bacterial contamination. STARGEN™ 002 was then supplemented at ten times the recommended dosage (11.4 g/kg of substrate). Rubber stoppers were used to set up oxygen-limited conditions and a needle was inserted for CO_2 removal. Serum-bottles were incubated at 30 °C on magnetic stirrer with agitation speed at 700 rpm. The experiments were carried out in triplicate.

The fermentative vigour was daily monitored as described above. Results were reported as grams of glucose utilized per liter of medium by a conversion factor of 2.118 [55]. Samples were withdrawn after 5 days, filtered through 0.22- μm and analyzed for their content by high performance liquid chromatography (HPLC) as indicated in 'Analytical methods and calculations'.

3.5. Scale-up of SSF in 1-L Bench Fermenter

The most promising strain, exhibiting an outstanding fermentative performance at small scale SSF, together with the benchmark industrial yeast Ethanol Red™, was up-scaled in a 1-L bioreactor (Applikon Biotechnology, Schiedam, The Netherlands) with a working volume of 900 mL. The BioXpert software version 1.13 (Applikon Biotechnology) was used for data acquisition.

The broth was the same used for small-scale SSF except for pH, which was controlled at 4.0 using automatic titration of 1 M NaOH solution. To maintain oxygen-limited conditions, aeration was not supplied. Yeast cells were inoculated at OD value of 1 and the cultures were stirred at 300 rpm and maintained at 30 °C with a heating blanket. All parameters were controlled by my-Control unit (Applikon Biotechnology). Samples were aseptically collected at regular intervals and kept at -20 °C. Samples were filtered through 0.22- μm and diluted for HPLC analysis performed as described below.

3.6. Analytical Methods and Calculations

Samples from small scale fermentation and bioreactor experiments were analysed for their content in glucose, glycerol and ethanol through liquid chromatography using a Shimadzu Nexera HPLC system, equipped with a RID-10A refractive index detector (Shimadzu, Kyoto, Japan). The chromatographic separations were performed using a Rezex ROA-Organic Acid H+ (8%) column (300 mm \times 7.8 mm,

Phenomenex, Torrance, CA, USA). The column temperature was set at 60 °C and the analysis was performed at a flow rate of 0.6 mL/min using isocratic elution, with 2.5 mM H₂SO₄ as a mobile phase [58].

The ethanol yield, $Y_{E/S}$, (g of ethanol/g of utilized glucose equivalent) was determined considering the amount of glucose equivalent available and compared to the maximum theoretical yield of 0.51 g of ethanol/g of consumed glucose equivalent.

The volumetric productivity (Q) was intended as grams of ethanol per liter of culture per hour (g/L/h) and the maximum volumetric productivity (Q_{max}) was defined as the highest volumetric productivity displayed by the *S. cerevisiae* strains. The theoretical CO₂ yields were determined based on the ethanol produced by each yeast strain, assuming that equimolar ethanol and CO₂ are produced. The percentage of carbon converted to glucose, ethanol, glycerol, and CO₂ was calculated on a mole carbon basis.

Statistical analyses were assessed using the Graphpad Prism 5 package (Graphpad Software, Inc., San Diego, CA, USA). Descriptive statistics mean values and standard deviations were calculated. Data were analysed also by two ways factorial Analysis of Variance (ANOVA) with Duncan test.

4. Conclusions

Developing an amyolytic fermentative organism may overcome important limitations of starch-to-ethanol conversion. The production of alfa-amylases and glucoamylases at high titers still remains a major challenge, despite significant technological advances. By producing efficient amyolytic enzymes, the engineered yeast could reduce bioethanol costs and implement the large-scale biofuel production. Nonetheless, the fermenting yeast must have promising fermenting abilities under SSF configurations.

This paper was successful in selecting and characterizing a cluster of novel yeast strains with fermenting abilities even higher than those of *S. cerevisiae* Ethanol Red™, the most used yeast for first and second generation ethanol. Ethanol yields from glucose under simple fermentation and SSF settings were significantly improved in the case of the newly isolated strains. This finding is of great value considering that, to obtain great additional profits, first generation ethanol plants look for an increase of even 1% in ethanol yield.

Based on the fermentation studies, the collection of novel *S. cerevisiae* strains has great potential for future application in corn-to-ethanol processes. In particular, the selected yeast L20 could be considered as promising for the CBP of different starchy industrial residues and will be engineered for the expression of efficient amyolytic genes.

Author Contributions: N.G. participated in planning of the study, carried out the SSF fermentation experiments, participated in data analysis and interpretation, and drafted the manuscript. L.F. planned the study and the experimental design, carried out the yeast isolation, identification and fermenting vigour characterization, performed data analysis, participated in data interpretation, and revised the manuscript. L.C. participated in the planning of the study and SSF fermentation experiments, composed the graphical abstract, and commented on the manuscript. S.B. participated in fermenting vigour experiments. V.P. participated in SSF fermentation experiments. M.B. participated in data interpretation, and commented on the manuscript. S.C. participated in data interpretation, and commented on the manuscript. All authors read and approved the final manuscript.

Funding: This research was funded by University of Padova [grants GRIC120EG8, 60A08-0924/15, DOR1657411/16; DOR1715524/17, DOR1728499/17, DOR1824847/18; DOR1931153/19].

Acknowledgments: The Authors are grateful to Willem Heber van Zyl (University of Stellenbosch, South Africa) for providing *S. cerevisiae* M2n, HR4, V3, WL3 and YI30.

Conflicts of Interest: The authors declare no conflict of interest.

References

1. Gupta, A.; Verma, J.P. Sustainable bio-ethanol production from agro-residues: A review. *Renew. Sustain. Energy Rev.* **2015**, *41*, 550–567. [[CrossRef](#)]
2. Lin, Y.; Tanaka, S. Ethanol fermentation from biomass resources: Current state and prospects. *Appl. Microbiol. Biotechnol.* **2016**, *69*, 627–642. [[CrossRef](#)]
3. Balat, M.; Balat, H.; Öz, C. Progress in bioethanol processing. *Prog. Energy Combust.* **2008**, *34*, 551–573. [[CrossRef](#)]
4. Mussatto, S.I.; Dragone, G.; Guimarães, P.M.; Silva, J.P.; Carneiro, L.M.; Roberto, I.C.; Vicente, A.; Domingues, L.; Teixeira, J.A. Technological trends, global market, and challenges of bio-ethanol production. *Biotechnol. Adv.* **2010**, *28*, 817–830. [[CrossRef](#)]
5. Ishizaki, H.; Hasumi, K. Ethanol production from biomass. In *Research Approaches to Sustainable Biomass Systems*; Tojo, S., Hirasawa, T., Eds.; Academic Press: Cambridge, MA, USA, 2014; pp. 243–258, ISBN 9780124046092.
6. Aditiya, H.B.; Mahlia, T.M.I.; Chong, W.T.; Nur, H.; Sebayang, A.H. Second generation bioethanol production: A critical review. *Renew. Sustain. Energy Rev.* **2016**, *66*, 631–653. [[CrossRef](#)]
7. Cesaro, A.; Belgiorno, V. Combined biogas and bioethanol production: Opportunities and challenges for industrial application. *Energies* **2015**, *8*, 8121–8144. [[CrossRef](#)]
8. Hossain, N.; Zaini, J.H.; Mahlia, T.M.I. A review of bioethanol production from plant-based waste biomass by yeast fermentation. *Int. J. Technol.* **2017**, *8*, 5. [[CrossRef](#)]
9. Zabed, H.; Sahu, J.N.; Suely, A.; Boyce, A.N.; Faruq, G. Bioethanol production from renewable sources: Current perspectives and technological progress. *Renew. Sustain. Energy Rev.* **2017**, *71*, 475–501. [[CrossRef](#)]
10. Saini, J.K.; Saini, R.; Tewari, L. Lignocellulosic agriculture wastes as biomass feedstocks for second-generation bioethanol production: Concepts and recent developments. *3 Biotech* **2015**, *5*, 337–353. [[CrossRef](#)]
11. Bentivoglio, D.; Finco, A.; Bacchi, M.R.P. Interdependencies between biofuel, fuel and food prices: The case of the brazilian ethanol market. *Energies* **2016**, *9*, 464. [[CrossRef](#)]
12. Balat, M.; Ayar, G. Biomass energy in the world, use of biomass and potential trends. *Energy Sources* **2005**, *27*, 931–940. [[CrossRef](#)]
13. Alvira, P.; Tomàs-Pejò, E.; Ballesteros, M.; Negro, M.J. Pretreatment technologies for an efficient bioethanol production process based on enzymatic hydrolysis: A review. *Bioresour. Technol.* **2010**, *101*, 4851–4861. [[CrossRef](#)]
14. Romanelli, M.G.; Povolo, S.; Favaro, L.; Fontana, F.; Basaglia, M.; Casella, S. Engineering *Delftia acidovorans* DSM39 to produce polyhydroxyalkanoates from slaughterhouse waste. *Int. J. Biol. Macromol.* **2014**, *71*, 21–27. [[CrossRef](#)]
15. Alibardi, L.; Green, K.; Favaro, L.; Vale, P.; Soares, A.; Cartmell, E.; Fernández, Y.B. Performance and stability of sewage sludge digestion under CO₂ enrichment: A pilot study. *Bioresour. Technol.* **2017**, *245*, 581–589. [[CrossRef](#)]
16. Favaro, L.; Todorov, S.D. Bacteriocinogenic LAB strains for fermented meat preservation: Perspectives, challenges, and limitations. *Probiot. Antimicrob. Proteins* **2017**, *9*, 444–458. [[CrossRef](#)]
17. Campanaro, S.; Treu, L.; Kougias, P.G.; Luo, G.; Angelidaki, I. Metagenomic binning reveals the functional roles of core abundant microorganisms in twelve full-scale biogas plants. *Water Res.* **2018**, *140*, 123–134. [[CrossRef](#)]
18. Duan, N.; Ran, X.; Li, R.; Kougias, P.; Zhang, Y.; Lin, C.; Liu, H. Performance evaluation of mesophilic anaerobic digestion of chicken manure with algal digestate. *Energies* **2018**, *11*, 1829. [[CrossRef](#)]
19. Lantz, M.; Prade, T.; Ahlgren, S.; Björnsson, L. Biogas and Ethanol from wheat grain or straw: Is there a trade-off between climate impact, avoidance of iLUC and production cost? *Energies* **2018**, *11*, 2633. [[CrossRef](#)]
20. Favaro, L.; Basaglia, M.; Casella, S. Improving polyhydroxyalkanoate production from inexpensive carbon sources by genetic approaches: A review. *Biofuels Bioprod. Biorefining* **2019**, *13*, 208–227. [[CrossRef](#)]
21. Solomon, B.D.; Barnes, J.R.; Halvorsen, K.E. Grain and cellulosic ethanol: History, economics, and energy policy. *Biomass Bioenergy* **2007**, *31*, 416–425. [[CrossRef](#)]
22. Nitsos, C.; Rova, U.; Christakopoulos, P. Organosolv fractionation of softwood biomass for biofuel and biorefinery applications. *Energies* **2017**, *11*, 50. [[CrossRef](#)]

23. Cripwell, R.; Favaro, L.; Rose, S.H.; Basaglia, M.; Cagnin, L.; Casella, S.; van Zyl, W.H. Utilization of wheat bran as a substrate for bioethanol production using recombinant cellulases and amylolytic yeast. *Appl. Energy* **2015**, *160*, 610–617. [[CrossRef](#)]
24. Favaro, L.; Cagnin, L.; Basaglia, M.; Pizzocchero, V.; van Zyl, W.H.; Casella, S. Production of bioethanol from multiple waste streams of rice milling. *Bioresour. Technol.* **2017**, *244*, 151–159. [[CrossRef](#)]
25. Olguin-Maciel, E.; Larqué-Saavedra, A.; Pérez-Brito, D.; Barahona-Pérez, L.F.; Alzate-Gaviria, L.; Toledano-Thompson, T.; Lappe-Oliveras, P.E.; Huchin-Poot, E.G.; Tapia-Tussell, R. *Brosimum alicastrum* as a novel starch source for bioethanol production. *Energies* **2017**, *10*, 1574. [[CrossRef](#)]
26. Pradyawong, S.; Juneja, A.; Sadiq, M.; Noomhorm, A.; Singh, V. Comparison of cassava starch with corn as a feedstock for bioethanol production. *Energies* **2018**, *11*, 3476. [[CrossRef](#)]
27. Ahorsu, R.; Medina, F.; Constantí, M. Significance and challenges of biomass as a suitable feedstock for bioenergy and biochemical production: A review. *Energies* **2018**, *11*, 3366. [[CrossRef](#)]
28. Nigam, P.; Singh, D. Enzyme and microbial systems involved in starch processing. *Enzyme Microb. Technol.* **1995**, *17*, 770–778. [[CrossRef](#)]
29. Castro, A.M.; Castilho, L.R.; Freire, D.M.G. An overview on advances of amylases production and their use in the production of bioethanol by conventional and non-conventional processes. *Biomass Convers. Biorefinery* **2011**, *1*, 245–255. [[CrossRef](#)]
30. Sánchez, Ó.J.; Cardona, C.A. Trends in biotechnological production of fuel ethanol from different feedstocks. *Bioresour. Technol.* **2008**, *99*, 5270–5295. [[CrossRef](#)]
31. Favaro, L.; Jooste, T.; Basaglia, M.; Rose, S.H.; Saayman, M.; Görgens, J.F.; Casella, S.; van Zyl, W.H. Designing industrial yeasts for the consolidated bioprocessing of starchy biomass to ethanol. *Bioengineered* **2013**, *4*, 97–102. [[CrossRef](#)]
32. Favaro, L.; Viktor, M.J.; Rose, M.H.; Bloom, M.V.; van Zyl, W.H.; Basaglia, M.; Cagnin, L.; Casella, S. Consolidated bioprocessing of starchy substrates into ethanol by industrial *Saccharomyces cerevisiae* strains secreting fungal amylases. *Biotechnol. Bioeng.* **2015**, *112*, 1751–1760. [[CrossRef](#)]
33. Lynd, L.R.; van Zyl, W.H.; McBride, J.E.; Laser, M. Consolidated bioprocessing of cellulosic biomass: An update. *Curr. Opin. Biotechnol.* **2005**, *16*, 577–583. [[CrossRef](#)]
34. Favaro, L.; Jooste, T.; Basaglia, M.; Rose, S.H.; Saayman, M.; Görgens, J.F.; Casella, S.; van Zyl, W.H. Codon-optimized glucoamylase sGAI of *Aspergillus awamori* improves starch utilization in an industrial yeast. *Appl. Microbiol. Biotechnol.* **2012**, *95*, 957–968. [[CrossRef](#)]
35. van Zyl, W.H.; Bloom, M.; Viktor, M.J. Engineering yeasts for raw starch conversion. *Appl. Microbiol. Biotechnol.* **2012**, *95*, 1377–1388. [[CrossRef](#)]
36. Cripwell, R.A.; Rose, S.H.; van Zyl, W.H. Expression and comparison of codon optimised *Aspergillus tubingensis* amylase variants in *Saccharomyces cerevisiae*. *FEMS Yeast Res.* **2017**, *17*. [[CrossRef](#)]
37. Walker, G.M.; Walker, R.S.K. Enhancing yeast alcoholic fermentations. *Adv. Appl. Microbiol.* **2018**, *105*, 87–129. [[CrossRef](#)]
38. Bothast, R.J.; Schlicher, M.A. Biotechnological processes for conversion of corn into ethanol. *Appl. Microbiol. Biotechnol.* **2005**, *67*, 19–25. [[CrossRef](#)]
39. Görgens, J.F.; Bressler, D.C.; van Rensburg, E. Engineering *Saccharomyces cerevisiae* for direct conversion of raw, uncooked or granular starch to ethanol. *Crit. Rev. Biotechnol.* **2014**, *8551*, 1–23. [[CrossRef](#)]
40. Mohd Esa, N.; Ling, T.B. By-products of rice processing: An overview of health benefits and applications. *Rice Res. Open Access* **2016**, *4*, 1–11. [[CrossRef](#)]
41. Favaro, L.; Basaglia, M.; Trento, A.; Van Rensburg, E.; García-Aparicio, M.; van Zyl, W.H.; Casella, S. Exploring grape marc as trove for new thermotolerant and inhibitor-tolerant *Saccharomyces cerevisiae* strains for second-generation bioethanol production. *Biotechnol. Biofuels* **2013**, *6*, 168. [[CrossRef](#)]
42. Favaro, L.; Basaglia, M.; van Zyl, W.H.; Casella, S. Using an efficient fermenting yeast enhances ethanol production from unfiltered wheat bran hydrolysates. *Appl. Energy* **2013**, *102*, 170–178. [[CrossRef](#)]
43. Jansen, T.; Hoff, J.W.; Jolly, N.; van Zyl, W.H. Mating of natural *Saccharomyces cerevisiae* strains for improved glucose fermentation and lignocellulosic inhibitor tolerance. *Folia Microbiol.* **2018**, *63*, 55–68. [[CrossRef](#)]
44. He, L.; Zhao, X.; Bai, F. Engineering industrial *Saccharomyces cerevisiae* strain with the FLO1-derivative gene isolated from the flocculating yeast SPSC01 for constitutive flocculation and fuel ethanol production. *Appl. Energy* **2012**, *100*, 33–40. [[CrossRef](#)]

45. Ortiz-Muñiz, B.; Carvajal-Zarrabal, O.; Torrestiana-Sanchez, B.; Aguilar-Uscanga, M.G. Kinetic study on ethanol production using *Saccharomyces cerevisiae* ITV-01 yeast isolated from sugar cane molasses. *J. Chem. Technol. Biotechnol.* **2010**, *85*, 1361–1367. [[CrossRef](#)]
46. Hahn-Hägerdal, B.; Karhumaa, K.; Larsson, C.U.; Gorwa-Grauslund, M.; Görgens, J.; van Zyl, W.H. Role of cultivation media in the development of yeast strains for large scale industrial use. *Microb. Cell Fact.* **2005**, *4*, 31. [[CrossRef](#)]
47. Dahod, S.K. Raw material selection and medium development for industrial fermentation processes. In *Manual of Industrial Microbiology and Biotechnology*, 2nd ed.; Demain, A.L., Davies, J.E., Eds.; ASM Press: Washington, DC, USA, 1999; pp. 213–220, ISBN 9781555815127.
48. Borglum, G.B. Starch hydrolysis for ethanol production. *Am. Chem. Soc. Div. Fuel Chem.* **1980**, *25*, 264–269.
49. Ribéreau-Gayon, P.; Dubourdieu, D.; Donèche, B.; Lonvaud, A. *Handbook of Enology, Volume 1: The Microbiology of Wine and Vinifications*, 2nd ed.; John Wiley & Sons, Ltd.: Chichester, UK, 2006; ISBN 9780470010365.
50. Zhang, L.; Zhao, H.; Gan, M.; Jin, Y.; Gao, X.; Chen, Q.; Guan, J.; Wang, Z. Application of simultaneous saccharification and fermentation (SSF) from viscosity reducing of raw sweet potato for bioethanol production at laboratory, pilot and industrial scales. *Bioresour. Technol.* **2011**, *102*, 4573–4579. [[CrossRef](#)]
51. Schmidt, F.R. Optimization and scale up of industrial fermentation processes. *Appl. Microbiol. Biotechnol.* **2005**, *68*, 425–435. [[CrossRef](#)]
52. Chu-Ky, S.; Pham, T.H.; Bui, K.L.T.; Nguyen, T.T.; Pham, K.D.; Nguyen, H.D.T.; Luong, H.N.; Tu, V.D.; Nguyen, T.H.; Ho, P.H.; et al. Simultaneous liquefaction, saccharification and fermentation at very high gravity of rice at pilot scale for potable ethanol production and distillers dried grains composition. *Food Bioprod. Process.* **2016**, *98*, 79–85. [[CrossRef](#)]
53. Horwitz, W.; Senzel, A.; Reynolds, H.; Park, D.L. *Official Methods of Analysis of the Association of Official Analytical Chemists*, 12th ed.; Association of Official Analytical Chemists: Washington, DC, USA, 1975.
54. Kurtzman, C.P.; Robnett, C.J. Identification and phylogeny of ascomycetous yeasts from analysis of nuclear large subunit (26S) ribosomal DNA partial sequences. *Int. J. Gen. Mol. Microb.* **1998**, *73*, 331–371. [[CrossRef](#)]
55. Delfini, C. *Scienza e Tecnica di Microbiologia Enologica*; Edizione: Il lievito, Asti, 1995.
56. Zaldivar, J.; Nielsen, J.; Olsson, L. Fuel ethanol production from lignocellulose: A challenge for metabolic engineering and process integration. *Appl. Microbiol. Biotechnol.* **2001**, *56*, 17–34. [[CrossRef](#)]
57. Hamelinck, C.; Van Hooijdonk, G.; Faaij, A. Ethanol from lignocellulosic biomass: Techno-economic performance in short-, middle- and long-term. *Biomass Bioenergy* **2005**, *28*, 384–410. [[CrossRef](#)]
58. Cagnin, L.; Favaro, L.; Gronchi, N.; Rose, S.H.; Basaglia, M.; van Zyl, W.H.; Casella, S. Comparing laboratory and industrial yeast platforms for the direct conversion of cellobiose into ethanol under simulated industrial conditions. *FEMS Yeast Res.* **2019**, foz018. [[CrossRef](#)]



RESEARCH ARTICLE

Comparing laboratory and industrial yeast platforms for the direct conversion of cellobiose into ethanol under simulated industrial conditions

Lorenzo Cagnin^{1,†}, Lorenzo Favaro^{1,*}, Nicoletta Gronchi¹, Shaunita Hellouise Rose², Marina Basaglia¹, Willem Heber van Zyl² and Sergio Casella¹

¹Department of Agronomy Food Natural resources Animals and Environment (DAFNAE), University of Padova, Agripolis, Viale dell'Università 16, 35020 Legnaro (PD), Italy and ²Department of Microbiology, Stellenbosch University, Private Bag X1, Matieland, 7602, Stellenbosch, South Africa

*Corresponding author: Department of Agronomy Food Natural resources Animals and Environment (DAFNAE), Agripolis - University of Padova, Viale dell'Università 16, 35020 Legnaro, PADOVA, ITALY. Tel. +39-049-8272800; Fax: +39 049-8272929; E-mail: lorenzo.favaro@unipd.it

One sentence summary: This study demonstrates the importance of proper platform selection for bioethanol production by comparing the fermentation profiles of a novel industrial yeast expressing fungal β -glucosidase via chromosomal integration and a known laboratory strain expressing that gene via multicopy episomal plasmid, in presence of increasing concentrations of toxic steam-exploded sugarcane bagasse hydrolysate.

Editor: Jens Nielsen

[†]Lorenzo Cagnin, <http://orcid.org/0000-0002-5650-4422>

ABSTRACT

An engineered yeast producing all the cellulases needed for cellulose saccharification could produce ethanol from lignocellulose at a lower cost. This study aimed to express fungal β -glucosidases in *Saccharomyces cerevisiae* to convert cellobiose into ethanol. Furthermore, two engineering platforms (laboratory vs industrial strain) have been considered towards the successful deployment of the engineered yeast under simulated industrial conditions. The industrial *S. cerevisiae* M2n strain was engineered through the δ -integration of the β -glucosidase *Pccbgl1* of *Phanerochaete chrysosporium*. The most efficient recombinant, M2n[pBKD2-*Pccbgl1*]-C1, was compared to the laboratory *S. cerevisiae* Y294[*Pccbgl1*] strain, expressing *Pccbgl1* from episomal plasmids, in terms of cellobiose fermentation in a steam exploded sugarcane bagasse pre-hydrolysate. *Saccharomyces cerevisiae* Y294[*Pccbgl1*] was severely hampered by the pre-hydrolysate. The industrial M2n[pBKD2-*Pccbgl1*]-C1 could tolerate high inhibitors-loading in pre-hydrolysate under aerobic conditions. However, in oxygen limited environment, the engineered industrial strain displayed ethanol yield higher than the laboratory Y294[*Pccbgl1*] only when supplemented with supernatant containing further recombinant β -glucosidase. This study showed that the choice of the host strain is crucial to ensure bioethanol production from lignocellulose. A novel cellobiose-to-ethanol route has been developed and the recombinant industrial yeast could be a promising platform towards the future consolidated bioprocessing of lignocellulose into ethanol.

Keywords: bioethanol; consolidated bioprocessing; sugarcane bagasse; β -glucosidase; industrial yeast; laboratory yeast

Received: 6 October 2018; Accepted: 15 February 2019

© FEMS 2019. All rights reserved. For permissions, please e-mail: journals.permissions@oup.com

INTRODUCTION

Bioethanol is considered the most viable and sustainable biofuel, as it can be produced through biological conversion at large industrial scale, resulting in the formation of less by-products and pollution than thermochemical approaches (Srirangan et al. 2012). Also, bioethanol can share the existing infrastructure used for the distribution of gasoline (Gnansounou and Dauriat 2011). The ideal substrate for bioethanol production would be inexpensive, non-edible biomass such as lignocellulose-rich material, including dedicated energy crops (spruce and birch) and agricultural residues (corn stover and sugarcane bagasse) (Olofsson, Bertilsson and Lidén 2008; Cripwell et al. 2015).

Biological conversion of lignocellulose to ethanol requires expensive pre-treatments in order to overcome the recalcitrance of the lignocellulosic structure and large dosages of costly cellulolytic enzymes to release fermentable sugars (Abbas and Ansumali 2010; Sindhu, Binod and Pandey 2016; Zabed et al. 2016). In addition, pre-treatment of lignocellulosic biomass generally leads to the release of inhibitory by-products (furans, weak acids and phenolic compounds) that hamper the fermentation step, resulting in a negative impact on the economic feasibility of the process (Palmqvist and Hahn-Hägerdal 2000; Jönsson and Martín 2016).

Endoglucanases, cellobiohydrolases and β -glucosidases act synergistically to ensure the hydrolysis of the cellulose. The β -glucosidases play a key role as they cleave cellobiose into glucose, thus, removing the feedback inhibition by the disaccharide on endoglucanases and cellobiohydrolases (Lynd et al. 2002; Taherzadeh and Karimi 2007; Alvira et al. 2010).

Saccharomyces cerevisiae is currently considered one of the most promising platforms for consolidated bioprocessing (CBP) development (Lynd et al. 2005; van Zyl et al. 2007; Olson et al. 2012). The major shortcoming, i.e. its inability to utilize cellulose, could be overcome by heterologous gene expression. Numerous studies showed the successful expression of cellulase encoding genes in *S. cerevisiae* (Van Rooyen et al. 2005; Njokweni, Rose and van Zyl 2012; Liu et al. 2015; Davison, den Haan and van Zyl 2016). In most cases, however, laboratory yeast strains were subjected to genetic modification. Instead, industrial yeast strains commonly display several phenotypic traits that would make them particularly suited to serve as large-scale CBP platforms. Such characteristics include higher ethanol yield, thermostability and an increased tolerance to the inhibitors formed during the substrate pre-treatment (Favaro et al. 2013a; Jansen et al. 2017). The genetic engineering of industrial strains usually relies on chromosomal integration of multiple copies of the gene of interest at repetitive δ -sequences (Favaro et al. 2010; Yamada et al. 2010; Jansen et al. 2017; Song et al. 2017).

In this study, cellulolytic CBP yeast strains were engineered by integration of the *Saccharomycopsis fibuligera* *BGL1* and *Phanerochaete chrysosporium* *Pccbgl1* genes into the δ -sequences. *Saccharomyces cerevisiae* M2n[pBKD2-Pccbgl1]-C1, expressing the β -glucosidase of *P. chrysosporium*, has been selected and the performances of the recombinant yeast were compared to those of a laboratory strain expressing the same gene from an episomal plasmid. As such, this research was specifically intended to compare the phenotypic outputs of two engineered platforms (laboratory vs wild type) for the production of lignocellulosic bioethanol.

To simulate the industrial environment as closely as possible, an hydrolysate from steam pre-treated sugarcane bagasse

was used as substrate and cellobiose concentration was supplemented up to 20 g/L, which is one of the highest levels so far described in lignocellulosic pre-treated substrates (van Maris et al. 2006; Casa-Villegas, Polaina and Martin-Navarro 2018).

MATERIALS AND METHODS

Plasmids, strains, media and growth conditions

Genotypes, phenotypes and sources of bacterial and yeast strains used in this work are summarized in Table 1. Unless otherwise stated, all chemicals were of analytical grade and were purchased from Sigma-Aldrich (Saint Louis, MO, USA). Recombinant plasmids were constructed and amplified in *Escherichia coli* JM109 (Promega, Fitchburg, MI, USA). Bacterial cultures were cultivated at 37°C on a rotary shaker in Luria Bertani medium (LB) or on LB agar (Sambrook and Russell, 2001). Ampicillin was added to a final concentration of 100 μ g/mL for the selection of plasmid-bearing bacteria. Yeast strains were cultivated at 30°C in Yeast extract Peptone Dextrose (YPD) medium (g/L: yeast extract, 10; peptone, 20; and glucose, 20), Synthetic Complete (SC) medium (g/L: Yeast Nitrogen Base with ammonium sulphate (YNB), 6.7; glucose, 10.53; or cellobiose, 10) or 2 \times SC (YNB, 13.4; glucose, 10.53; or cellobiose, 10) unless stated otherwise. SC^{-URA} medium was used in the case of the laboratory strain Y294[Pccbgl1].

Sugarcane bagasse hydrolysate

Sugarcane bagasse, provided by the South African Sugarcane Research Institute (SASRI), was analyzed for the content in lignin, glucan, xylan, arabinan, ash and extractives using the Laboratory Analytical Procedures for biomass analysis provided by the National Renewable Energy Laboratory (NREL) (CO, USA). Accordingly, sugarcane bagasse was composed on a dry weight basis of 19% lignin, 58% glucan, 23% xylan, 3% arabinan, 4% ash and 7% extractives.

Sugarcane bagasse hydrolysate was obtained in a steam explosion plant equipped with a 19 L reactor vessel, a collection tank and a 40 bar electrical boiler. Milled sugarcane bagasse samples were dried in a drying chamber to a final moisture content of 10% (w/w). Aliquots of the resulting material were loaded into the steam pre-treatment reactor and treated at 200°C for 10 min. After the material was exploded, the hydrolysate was removed using a locally-manufactured dead-end press with the remaining solids having a moisture content of 40% (w/w). The hydrolysate was refrigerated at pH 2.5 until use. Sugars and inhibitors concentrations were analyzed by High Performance Liquid Chromatography (HPLC).

To evaluate the fermentation performance of yeast strains on sugarcane hydrolysate, increasing concentrations (5, 10, 20, 30, 40%, v/v) of sugarcane hydrolysate, hereafter, referred to as SH (Sugarcane Hydrolysate), were formulated with redistilled water and named 5% SH, 10% SH, 20% SH, 30% SH and 40% SH, respectively.

DNA manipulation and plasmids construction

Restriction enzyme digestion, electrophoresis, DNA ligation, isolation and transformation were performed using standard methods according to Sambrook and Russell (Sambrook and Russell 2001). DNA fragments were purified from agarose gels

Table 1. Plasmids and strains used in this study.

Plasmid/Strain	Relevant genotype	Reference
pBKD1	<i>bla</i> δ -sites-PGK1 _P -PGK1 _T TEF1 _P ^a -KanMX-TEF1 _T ^a - δ -sites	(Mcbride et al. 2008)
pBKD2	<i>bla</i> δ -sites-ENO1 _P -ENO1 _T TEF1 _P ^a -KanMX-TEF1 _T ^a - δ -sites	(Mcbride et al. 2008)
pBKD1-BGL1	<i>bla</i> δ -sites-PGK1 _P -XYNSEC-BGL1-PGK1 _T TEF1 _P ^a -KanMX-TEF1 _T ^a - δ -sites	(Mcbride et al. 2008)
pBKD1-Pccbgl1b	<i>bla</i> δ -sites-PGK1 _P - XYNSEC- Pccbgl1b -PGK1 _T TEF1 _P ^a -KanMX-TEF1 _T ^a - δ -sites	This work
pBKD1-Pccbgl1	<i>bla</i> δ -sites-PGK1 _P - XYNSEC- Pccbgl1-PGK1 _T TEF1 _P ^a -KanMX-TEF1 _T ^a - δ -sites	This work
pBKD2-BGL1	<i>bla</i> δ -sites-ENO1 _P - XYNSEC-BGL1-ENO1 _T TEF1 _P ^a -KanMX-TEF1 _T ^a - δ -sites	This work
pBKD2-Pccbgl1b	<i>bla</i> δ -sites-ENO1 _P - XYNSEC- Pccbgl1b -ENO1 _T TEF1 _P ^a -KanMX-TEF1 _T ^a - δ -sites	This work
pBKD2-Pccbgl1	<i>bla</i> δ -sites-ENO1 _P - XYNSEC- Pccbgl1-ENO1 _T TEF1 _P ^a -KanMX-TEF1 _T ^a - δ -sites	This work
<i>E. coli</i> JM109	<i>endA1</i> , <i>recA1</i> , <i>gyrA96</i> , <i>thi</i> , <i>hsdR17</i> (<i>r_k</i> ⁻ , <i>m_k</i> ⁺), <i>relA1</i> , <i>supE44</i> , Δ (<i>lac-proAB</i>), [<i>F</i> ⁺ <i>traD36</i> , <i>proAB</i> , <i>laqI</i> ^a Z Δ M15]	Promega (Fitchburg, MI, USA)
<i>S. cerevisiae</i> M2n	Industrial distillery strain	(Favaro et al. 2015)
<i>S. cerevisiae</i> M2n[pBKD2-Pccbgl1]-C1	Pccbgl1 multiple copy δ -integration	This work
<i>S. cerevisiae</i> Y294	<i>a leu2-3112 ura3-52 his3 trp1-289</i>	ATCC 201 160
<i>S. cerevisiae</i> Y294[Pccbgl1]	URA3 ENO1 _P -XYNSEC- Pccbgl1-ENO1 _T	(Njokweni, Rose and van Zyl 2012)

^aTEF1 promoter and terminator from *Ashbya gossypii*

with Wizard® SV Gel and PCR Clean-Up System (Promega, Fitchburg, MI, USA). Restriction enzymes were supplied by New England Biolabs (Ipswich, MA, USA) and Fermentas—Thermo Fisher Scientific (Waltham, MA, USA). T4 DNA ligase and RNase were provided by New England Biolabs (Ipswich, MA, USA) and Sigma-Aldrich (Saint Louis, MO, USA), respectively.

The protein accession numbers of *S. fibuligera* BGL1 and *P. chrysosporium* Pccbgl1b and Pccbgl1 are AAA34314.1, Q25BW4.1 and AAC26489.1, respectively.

The *S. fibuligera* BGL1 and *P. chrysosporium* Pccbgl1b and Pccbgl1 were obtained from the pBKD1-BGL1, pBKD1-Pccbgl1b and pBKD1-Pccbgl1 plasmids using *PacI* and *AscI* restriction enzymes, respectively. The genes were subcloned into the same restriction sites of pBKD2, generating pBKD2-BGL1, pBKD2-Pccbgl1b and pBKD2-Pccbgl1, respectively.

Yeast transformation

The industrial M2n strain was engineered by δ -integration. pBKD1-BGL1 and pBKD2-BGL1 plasmids were digested using *XhoI* and *PvuII*. pBKD1- Pccbgl1b, pBKD1- Pccbgl1, pBKD2- Pccbgl1b and pBKD2-Pccbgl1 were digested with *AccI* and *ApaI*. Transformants were selected on YPD plates supplemented with 1 M sorbitol and with 200 μ g/mL geneticin.

Mitotic stability of the transformants was evaluated according to Favaro et al. 2012. Strains were cultivated in non-selective YPD broth and incubated on a rotating wheel at 30°C. A 0.1% v/v sample was obtained daily and sequentially transferred to 5 mL batch cultures. After 120 generations, appropriate serial dilutions were plated onto YPD agar and esculin plates with or without supplementation with geneticin (200 μ g/mL). Esculin was used as indicator of β -glucosidase activity, as described below. Stable transformants indicated a comparable number of colonies both in the presence and in absence of selective pressure after 48 h incubation at 30°C.

Enzyme activity assays

Antibiotic resistant *S. cerevisiae* strains were transferred onto esculin plates (SC plates supplemented with 1 g/L esculin and 0.5 g/L ferric citrate) and incubated at 30°C for 2 days. The formation of a dark halo of precipitated esculetin around the colony was indicative of β -glucosidase activity (Njokweni, Rose and van Zyl 2012). The enzymatic activity was assessed quantitatively using 4-nitrophenyl β -D-glucopyranoside (pNPG) (Njokweni, Rose and van Zyl 2012). *Saccharomyces cerevisiae* strains were grown in YPD medium for 48 h. Samples of whole cell cultures (10 μ L) were added to a 90 μ L mixture containing 88 μ L 0.05 M citrate buffer pH 5.0 and 2 μ L 0.25 M pNPG in 96-well plates. After 15 min incubation at 60°C, 100 μ L 1 M Na₂CO₃ was added to terminate the enzymatic reaction. The parental *S. cerevisiae* M2n strain and the recombinant *S. cerevisiae* Y294[Pccbgl1] laboratory strain were used as negative and positive control strains, respectively. The absorbance was measured at 400 nm with a Spectrafluor microtiter reader (Tecan, Männedorf, Switzerland).

Enzymatic activities were expressed as nkat/mL, which is defined as the enzyme activity needed to release 1 nmol of 4-Nitrophenol (Sigma-Aldrich, Saint Louis, MO, USA) per second per mL of culture. Enzymatic activities were also reported as nanokatals per gram dry cell weight (nkat/(g DCW)), which is defined as the enzyme activity needed to release 1 nmol of 4-nitrophenol per second per gram dry cell weight. The experiments were carried out in triplicate.

Yeast strains were inoculated into 60 mL YPD medium in 250 mL Erlenmeyer flasks at an initial OD₆₀₀ of 0.2 and incubated at 30°C for 72 h. Samples were taken at 24 h intervals to determine DCW as previously described (Den Haan et al. 2007). The β -glucosidase activity was determined for the (i) the supernatant of the cell culture, (ii) the yeast cells and (iii) the whole cell culture at 50°C using 0.05 M citrate buffer (at pH 4.0, 5.0 and 6.0). Supernatant was obtained by centrifugation of the cell culture (4000 \times g for 2 min). The initial sample volume (1 mL) was restored by adding an appropriate amount of sterile deionized

water to the supernatant and the pelleted cells to compare enzymatic activities displayed in the different systems.

Optimal pH for Pccbgl1 was determined at 60°C in 0.05 M citrate buffer (at pH 4.0, 4.5, 5.0, 5.5 and 6.0) and 0.05 M citrate-phosphate buffer (at pH 2.5, 3.0 and 3.5) using the cell-free supernatant. Effect of temperature on enzymatic activity was determined at 30, 40, 50, 60 and 70°C in 0.05 M citrate buffer at the optimal pH.

The effect of temperature on the enzymatic stability was determined by incubating the supernatant of yeast cultures (grown in YPD at 30°C for 48 h) in water bath at different temperatures (30, 40 and 60°C) for increasing residence time. At specific intervals, ranging from 0 to 24 h and, from 1 to 20 min at 60°C, samples of the supernatant were removed and the residual enzymatic activity determined.

The stability of Pccbgl1 was evaluated in the presence of SH 20%. The supernatant of yeast cultures grown in YPD at 30°C for 48 h was supplemented with 20% SH. In the control condition, the same volume of water was added instead of SH. The solutions were incubated at 30°C. Samples were obtained at specific intervals, ranging from 0 to 144 h, and the residual enzymatic activity determined.

Growth kinetics

Yeast aerobic growth was studied in buffered (citrate buffer 0.05 M pH 5.0) and unbuffered SC medium supplemented with 10 g/L cellobiose or the equivalent molar amount of glucose (10.53 g/L). *Saccharomyces cerevisiae* Y294[Pccbgl1] required supplementation with tryptophan (76 mg/L), histidine (76 mg/L) and leucine (360 mg/L) to ensure auxotrophic growth. Media were sterilized using a 0.22 µm sterile filter. Pre-cultures were cultivated to stationary phase in unbuffered medium containing glucose. Cells were centrifuged at 5400 × g for 3 min, washed twice with a saline solution (0.9% NaCl) and used to inoculate 120 mL medium to an (OD₆₀₀) of 0.2 in triplicate experiments and incubated at 30°C on a rotary shaker for 100 h. Cultures were periodically sampled to measure OD₆₀₀ and to detect cellobiose, glucose and ethanol concentration with HPLC.

Screening for inhibitor tolerance

The *S. cerevisiae* M2n[pBKD2-Pccbgl1]-C1 and Y294[Pccbgl1] strains were assessed for the ability to sustain growth in defined medium in the presence of sugarcane bagasse pre-hydrolysate (SH). Yeast strains were cultivated overnight in unbuffered SC medium containing 10.53 g/L glucose. The cultures were centrifuged at 5400 × g for 3 min, washed twice with a saline solution (0.9% NaCl) and used to inoculate 5 mL of SC medium containing either 10.53 g/L glucose or cellobiose (10 g/L) and glucose (1 g/L) to an initial OD₆₀₀ of 1.0, using 15 mL test tubes. The media were supplemented with different concentrations of SH: 0%, 10%, 20%, 30% and 40% (v/v) and the pH adjusted to pH 5.0 with 5 M NaOH (followed by filter sterilization; 0.22 µm) prior to inoculation. Strains were cultivated for 48 h at 30°C on a rotating mixer. The inhibitor tolerance of the strains was assessed based on the relative growth (OD₆₀₀ value, %), calculated as the ratio between the increment in OD₆₀₀ of cell cultures with or without supplementation with SH.

$$\text{Relative growth} = \frac{OD_{f(n\%SH)} - OD_{i(n\%SH)}}{OD_{f(n\%SH)} - OD_{i(n\%SH)}}$$

where OD_f and OD_i indicate final and initial OD₆₀₀, respectively, and n%SH each concentration of SH tested.

Small-scale fermentation studies

Fermentation performances were assessed in buffered and unbuffered SC medium supplemented with glucose or cellobiose (as described in the Growth kinetics section), containing 0% SH, 5% SH, 10% SH, 20% SH and 30% SH. In the presence of SH, the pH was adjusted to 5.0 with 5 M NaOH. In fermentation experiments involving the exogenous addition of recombinant β-glucosidase produced by M2n[pBKD2-Pccbgl1]-C1, volumes of supernatant of a 24 h aerobic culture of *S. cerevisiae* M2n[pBKD2-Pccbgl1]-C1 were added to the fermentation medium to obtain a starting enzymatic activity of 20 nkat/mL.

Pre-cultures of yeast strains grown to early stationary phase in unbuffered broth containing 10.53 g/L glucose were used as inoculum. Cells were collected, washed as described in Growth kinetics and used to inoculate 100 mL medium to an initial OD₆₀₀ of 1.0 in triplicate experiments using 120 mL glass serum bottles. The small-scale fermentations were carried out under oxygen-limited conditions. The bottles were sealed with rubber stoppers, incubated at 30°C and mixed on a magnetic stirrer. Syringe needles pierced through the bottle stopper served for sampling purposes and carbon dioxide removal. Yeast growth was measured as absorbance at 600 nm. Samples obtained before and during fermentation were analyzed for glucose, cellobiose, ethanol, glycerol, furfural, HMF and acetic acid content using HPLC.

Analytical methods, calculations and statistical analysis

Sugars, glycerol and ethanol were detected in samples, filtered through 0.22-µm, and diluted prior to HPLC analysis (Favaro et al. 2017). In short, liquid chromatography analysis was accomplished using a Shimadzu Nexera HPLC system, with a RID-10A refractive index detector (Shimadzu, Kyoto, Japan) and a Phenomenex Rezex ROA-Organic Acid H⁺ (8%) column (300 mm × 7.8 mm). The column temperature was set at 65°C and the flow rate was 0.6 mL/min using isocratic elution, with 0.01 M H₂SO₄ as a mobile phase.

The ethanol yield, (g of ethanol/g of utilized glucose equivalent) was determined considering the amount of glucose/cellobiose consumed during the fermentation and compared to the maximum theoretical yield of 0.51 g of ethanol/g of consumed glucose equivalent.

Statistical analyses were assessed using the Graphpad Prism 5 package (Graphpad Software, Inc., San Diego, California). Descriptive statistics, mean values and standard deviations were calculated. Data were analyzed also by two ways factorial ANOVA (Analysis Of Variance) with Duncan test.

RESULTS AND DISCUSSION

Integrative plasmid construction and yeast transformation

A first step towards obtaining a cellulolytic CBP yeast will be β-glucosidase expression in the industrial *S. cerevisiae* M2n strain (Favaro et al. 2015). The *S. fibuligera* BGL1 and the *P. chrysosporium* Pccbgl1b and Pccbgl1 previously indicated high levels of activities when expressed in laboratory strains from multicopy plasmids (Van Rooyen et al. 2005; Njokweni, Rose and van Zyl 2012). These

genes were selected for integration into the δ -sequences of the M2n industrial yeast strain and the *Trichoderma reesei* β -xyylanase 2 secretion signal (XYNSEC) was provided for efficient secretion of the β -glucosidase enzymes. *BGL1*, *Pccbgl1b* and *Pccbgl1* were, respectively, cloned into the integrative plasmids pBKD1 (regulatory control of the constitutive *S. cerevisiae* PGK1 promoter) and pBKD2 (regulatory control of the constitutive *S. cerevisiae* ENO1 promoter).

All vectors were linearized prior to electrotransformation of the *S. cerevisiae* M2n parental strain. Recombinant clones were identified by producing black zones surrounding the colonies upon growth on esculin plates and the strains with the largest halos were selected. Their extracellular β -glucosidase activity was subsequently quantified using 4-nitrophenyl- β -D-glucopyranoside (pNPG) as substrate (see Table S1, Supporting Information). β -glucosidase activity of the recombinants ranged from nearly 150 to 3500 nanokatals per gram of dry cell weight (nkat/(g DCW)) and the strain M2n[pBKD2-*Pccbgl1*]-C1, secreting the *P. chrysosporium* *Pccbgl1*, selected for further study based on the activity displayed on esculin plates and its ability to grow on cellobiose as the only carbohydrate source (Fig. 1A and B). On the contrary, the parental yeast demonstrated no β -glucosidase activity or growth on cellobiose. The M2n[pBKD2-*Pccbgl1*]-C1 strain was found to be mitotically stable as the yeast maintained both the geneticin resistance and the hydrolytic activity on esculin plate.

Characterization of the recombinant β -glucosidase

The β -glucosidase activity displayed by M2n[pBKD2-*Pccbgl1*]-C1 was determined in whole cell culture, the supernatant and cell-associated fraction assays. At all pH values tested, the activity in the supernatant represented about 80% of the total activity detected in the cell culture (Table 2), indicating that *Pccbgl1* is mostly secreted extracellularly and the XYNSEC sequence successfully mediated the protein secretion. A portion of the enzyme, however, remains cell-associated. This finding is consistent with previous reports expressing the same *Pccbgl1* gene in laboratory yeast strains (Njokweni, Rose and van Zyl 2012). Once assayed at 50°C, *Pccbgl1* displayed maximum pNPG hydrolysis at pH 5.0 (Fig. 1C). At pH 3.0 and 2.5, the activity was reduced by 92 and 99%, respectively. At the optimal pH of 5.0, the activity peaked at 60°C (Fig. 1D).

The highest enzymatic activity in cell-free supernatant was quantified as 3500 nkat/(g DCW), after incubating a cell culture of M2n[pBKD2-*Pccbgl1*]-C1 at 30°C for 48 h in rich YPD. When cultured in defined Synthetic Complete (SC) broth, the recombinant showed a 1800 nkat/(g DCW) β -glucosidase activity. Unlike rich medium, defined media lack amino acids and other biosynthetic precursors resulting in reduced growth and lower enzymatic activity (Hahn-Hägerdal et al. 2005; Favaro et al. 2013b).

Enzyme thermostability is a desirable attribute in industrial processes, including bioethanol production from lignocellulosic substrates. Therefore, the stability of the *Pccbgl1* enzyme was evaluated at 30°C, working temperature in industrial large-scale fermenters (Siqueira et al. 2008), 40°C, conditions favorable to thermotolerant yeast (Favaro et al. 2013a) and 60°C, optimal temperature for *Pccbgl1* (Fig. 1D). The *Pccbgl1* displayed high stability at 30°C and 40°C for 24 h (Fig. 1E). The enzymatic activity was reduced to 44% within 5 min of incubation at 60°C with no activity detected after 20 min (Fig. 1F). The ability to maintain the hydrolytic efficiency at high temperatures results in reduced need for enzyme replenishment, thus, lowering the cost of the process (Bisaria and Kondo 2013). The higher activity displayed

at 40°C indicates that *Pccbgl1* is well suited for the expression in thermotolerant yeast strains selected for high fermentation yields at elevated temperatures (Favaro et al. 2013a). At 40°C the substrate hydrolysis rate is double that of at 30°C (Fig. 1D), while its activity remains stable at least for up to 24 h after secretion (Fig. 1E).

Aerobic growth on glucose or cellobiose

This research was specifically intended to compare the phenotypic outputs of two engineered platforms (laboratory vs wild type) for the production of ethanol from cellobiose. δ -integration applied to the laboratory yeast Y294 yielded recombinants expressing *Pccbgl1* with limited enzymatic activities (up to 470 ± 19 nkat/g DCW) not comparable to those described for M2n[pBKD2-*Pccbgl1*]-C1 (Table 2). The Y294[*Pccbgl1*] strain expressing the same gene from an episomal plasmid displayed a β -glucosidase activity 3-fold higher (Njokweni, Rose and van Zyl 2012) than that of M2n[pBKD2-*Pccbgl1*]-C1 and was considered the most suitable laboratory benchmark yeast for M2n[pBKD2-*Pccbgl1*]-C1.

The industrial M2n[pBKD2-*Pccbgl1*]-C1 strain and the *S. cerevisiae* Y294[*Pccbgl1*] laboratory strain were then aerobically evaluated for their ability to consume glucose or cellobiose, in both buffered and unbuffered SC (Fig. 2). Parental *S. cerevisiae* M2n was used as reference strain.

In unbuffered broth (black lines), the M2n[pBKD2-*Pccbgl1*]-C1 quickly consumed the glucose, reaching a final optical density at 600 nm (OD₆₀₀) of 6.8 (Fig. 2A). Growth kinetics of the recombinant strain are comparable to those showed by the parental M2n strain (Fig. 2B), indicating that yeast transformation and β -glucosidase production do not cause any major metabolic burden to the recombinant yeast. On cellobiose in unbuffered medium, M2n[pBKD2-*Pccbgl1*]-C1 reached a final OD₆₀₀ of 4.6 after 100 h (Fig. 2D). The recombinant strain consumed only 3.3 g/L of cellobiose. As expected, the parental M2n strain displayed no growth on cellobiose as sole carbohydrate source (Fig. 2E).

Laboratory Y294[*Pccbgl1*] strain reached a final OD₆₀₀ of 5.5 after 48 h when cultured on glucose (Fig. 2C) and a final OD₆₀₀ of 6.2 on cellobiose in unbuffered medium (Fig. 2F). The majority of cellobiose (9.5 g/L out of 10 g/L) was consumed, which is attributed to the high copy-number expression of *Pccbgl1* from multicopy episomal plasmids.

The yeast strains were also evaluated in buffered SC medium (0.05 M citrate buffer, pH5), containing glucose or cellobiose (Fig. 2, gray lines), since a change in pH significantly affects the β -glucosidase activity (Fig. 1C). The M2n[pBKD2-*Pccbgl1*]-C1 and M2n strains exhibited more biomass production on glucose in buffered than in unbuffered medium, showing similar kinetics. The glucose was completely depleted after 8 h. The two strains reached similar optical densities, about 2 times higher than in unbuffered medium (Fig. 2A and b). Increased optical density in buffered medium can be explained by considering the diminished necessity to pump protons out of the cell in order to maintain a stable cytoplasmic pH, which occurs at the expense of ATP (Piper et al. 1998). In fact, an increase in ATP requirement results in a lower biomass yield. In addition, acidification of the cytoplasm causes the inhibition of essential metabolic functions, including glycolysis (Pampulha and Loureiro-Dias 2000).

The M2n[pBKD2-*Pccbgl1*]-C1 strain consumed all the cellobiose available in the buffered system (Fig. 2D). As a consequence, the final OD₆₀₀ of the recombinant strain in buffered broth containing cellobiose was 1.5-fold higher than in glucose (Fig. 2A).

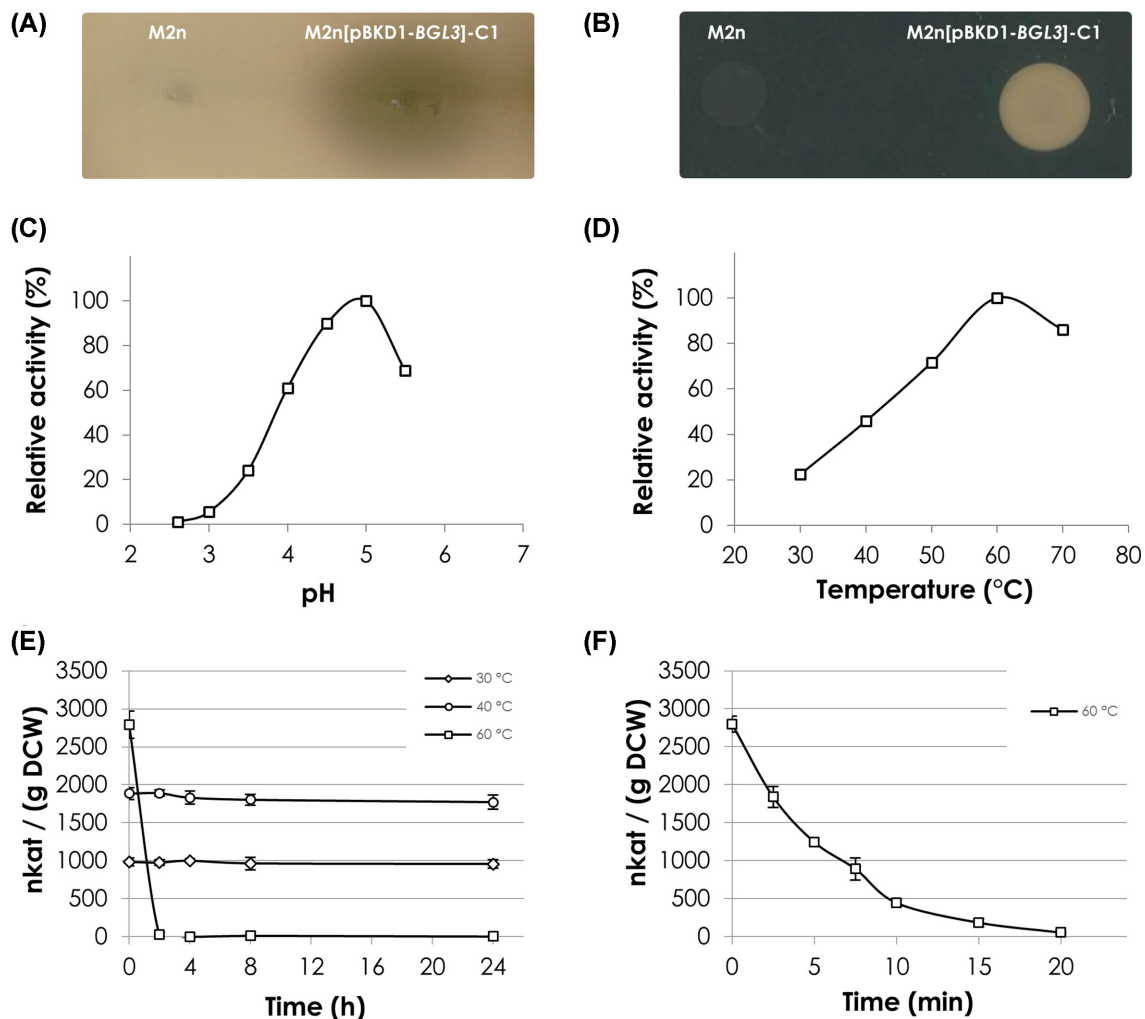


Figure 1. Characterization of the recombinant Pccbgl1 secreted by *S. cerevisiae* M2n[pBKD2-Pccbgl1]-C1. Extracellular β -glucosidase activity resulted in (A) the formation of a dark halo on SC plates containing esculin or (B) growth on cellobiose as sole carbon source. *Saccharomyces cerevisiae* M2n served as negative control. The secreted Pccbgl1 was used to determine the effect of pH (C) and temperature (D) on β -glucosidase activity. The stability of the Pccbgl1 was monitored at different temperatures over 24 h (E, F). Activity is expressed as a percentage of the highest value. Data shown are the mean values of three replicates and standard deviations are included.

Table 2. Enzymatic activity of Pccbgl1 secreted by M2n[pBKD2-Pccbgl1].

	pH		
	4.0	5.0	6.0
Whole cell culture	1268 ± 242	2492 ± 49	1044 ± 143
Supernatant	1054 ± 13	1988 ± 105	795 ± 12
Cell-bound	443 ± 170	649 ± 9	206 ± 23

M2n[pBKD2-Pccbgl1] was cultured for 48 h in YPD medium. The enzymatic activity, expressed in nkat/(g DCW), was measured at 50°C at different pH values. Data shown are the mean values of three replicates and standard deviations are included.

Fermentation is a much less efficient mechanism for energy production than respiration and, as a result, less biomass is produced (Gombert et al. 2001). When using glucose as sole carbon source, M2n[pBKD2-Pccbgl1]-C1 is more prone to convert the sugar into biomass through the least efficient aerobic fermentation (Crabtree effect), mainly in the early growth phases, when glucose concentration is high. Instead, when cellobiose is slowly cleaved into glucose, the sugar may never reach the concentration that triggers aerobic fermentation. In these conditions, the

sugar is then converted into energy via the more efficient respiration route, thus supporting higher biomass yield.

The Y294[Pccbgl1] laboratory strain reached slightly lower optical density value than M2n[pBKD2-Pccbgl1]-C1 and the parental M2n strains. The final OD₆₀₀ was 5.0 when cultured in buffered medium containing glucose (Fig. 2C) and 5.8 on cellobiose (Fig. 2F), similarly to what detected in unbuffered medium (black lines). In cellobiose Y294[Pccbgl1] did not show final OD₆₀₀ significantly higher than in glucose, which can be explained by the quick turn over of cellobiose into glucose due to

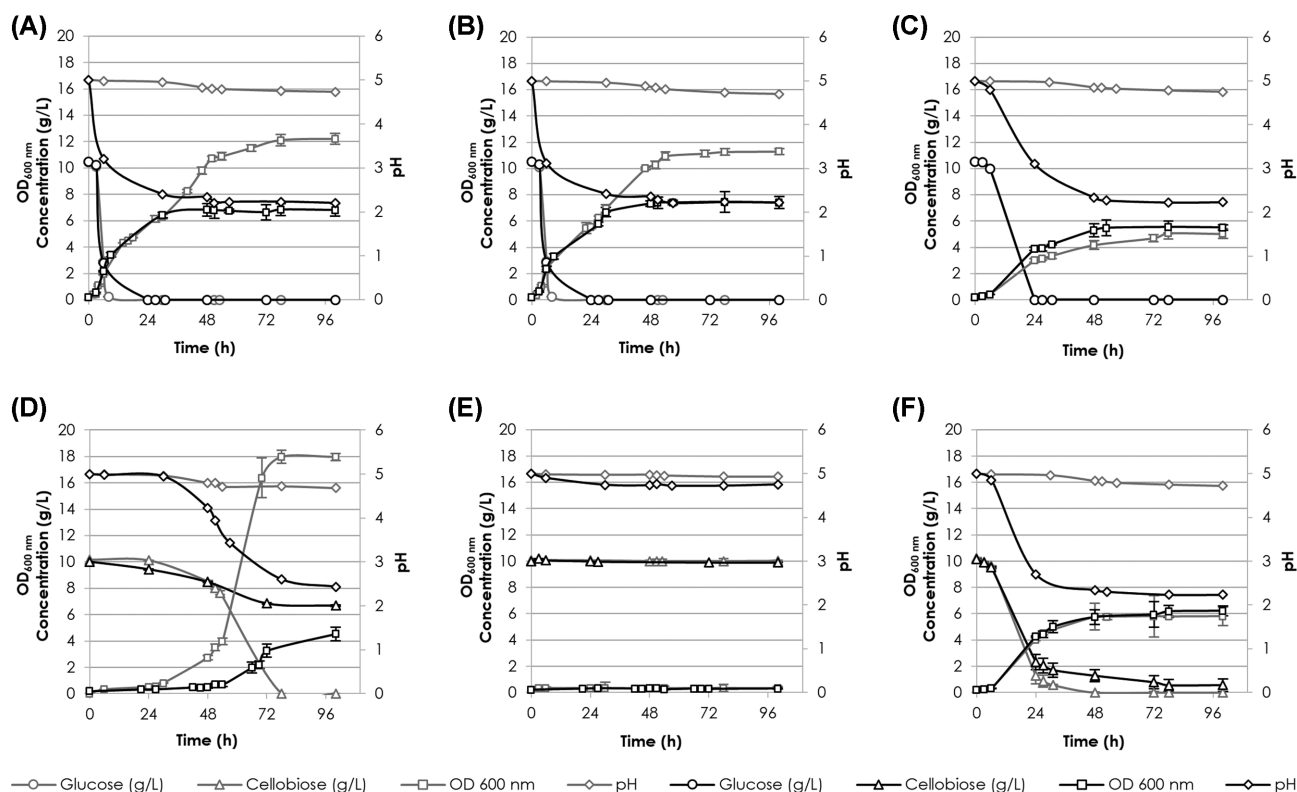


Figure 2. Aerobic growth kinetics from glucose or cellobiose by recombinant yeast strains expressing *Pccbgl1*. The *S. cerevisiae* M2n[pBKD2-*Pccbgl1*]-C1 (A, D), M2n (B, E) and Y294[*Pccbgl1*] (C, F) strains were aerobically cultivated in unbuffered (black lines) and buffered (grey lines) SC broth, respectively, containing glucose (10.53 g/L) (A, B, C) or cellobiose (10 g/L) (D, E, F) as sole carbohydrate source. Data shown are the mean values of three replicates and standard deviations are included.

the increased β -glucosidase production obtained by multicopy gene expression. Glucose concentrations as low as 0.15 g/L were shown to cause this phenomenon in *S. cerevisiae*, being strongly strain-dependent (Verduyn et al. 1984). HPLC analysis indicated ethanol production consequently to the decrease of cellobiose in both buffered and unbuffered medium (data not shown), further supporting this hypothesis.

Fermentation performances on glucose and cellobiose

The *S. cerevisiae* M2n[pBKD2-*Pccbgl1*]-C1, M2n and Y294[*Pccbgl1*] strains were evaluated in small scale fermentations in unbuffered and buffered SC medium containing glucose and cellobiose as sole carbohydrate sources. The recombinant M2n[pBKD2-*Pccbgl1*]-C1 exhibited a fermentation pattern similar to that of the parental strain in unbuffered medium containing glucose (Fig. 3A and B). Both yeast consumed the entire carbohydrate source available, yielding 4.3 g/L of ethanol after 6 h, corresponding to 80% of the theoretical yield. Similarly, final OD₆₀₀ reached about 3.40, confirming no evident metabolic burden on strain M2n[pBKD2-*Pccbgl1*]-C1. The strain M2n[pBKD2-*Pccbgl1*]-C1 could not utilize all cellobiose in unbuffered medium (Fig. 3D). About 1 g/L remained after 144 h of fermentation. The strain produced 3.6 g/L of ethanol, corresponding to 67% of the theoretical yield. As expected, the parental M2n strain was not capable of fermenting cellobiose (Fig. 3E).

Laboratory strain Y294[*Pccbgl1*] showed final ethanol yield from glucose (4.3 g/L, 80% of the theoretical) identical to the other strains in unbuffered medium, yet at a lower fermentation rate, completely consuming glucose only after 24 h (Fig. 3C).

From cellobiose, the Y294[*Pccbgl1*] strain exhibited a similar fermentation profile to M2n[pBKD2-*Pccbgl1*]-C1 (Fig. 3F). However, the laboratory strain consumed all cellobiose available, producing 4.2 g/L of ethanol, which corresponds to 78% of the theoretical yield due to the higher volumetric enzymatic activity. Therefore, the ethanol productivity on cellobiose was similar to that of glucose (Fig. 3C).

The use of buffer did not benefit the M2n and Y294[*Pccbgl1*] strains' fermentations (Fig. 3E and F), but was beneficial to the cellobiose fermentation by M2n[pBKD2-*Pccbgl1*]-C1, which completely consumed all the disaccharide (Fig. 3D). The recombinant strain produced 3.9 g/L of ethanol, corresponding to 73% of the theoretical yield. As a result, cellobiose fermentation in buffered system resulted in a 10% improvement in final ethanol concentration, compared to fermentation in unbuffered broth.

Screening for inhibitor tolerance

The two engineered strains were then evaluated for their ability to withstand increasing concentrations of SH, obtained after steam explosion of sugarcane bagasse. This substrate is one of the most available lignocellulosic feedstocks in the world and, together with steam pre-treatment, which is one of the most commonly used pre-treatments (Duque et al. 2016), would result in representative conditions for world-wide bioethanol production.

After steam pretreatment of sugarcane bagasse at 200°C for 10 min, limited levels of sugars (mainly xylose and cellobiose) and high inhibitor concentrations, including 3.0 g/L furaldehydes, more than 19 g/L weak acids and considerable levels of aldehydes and phenolic acids were detected in the hydrolysate

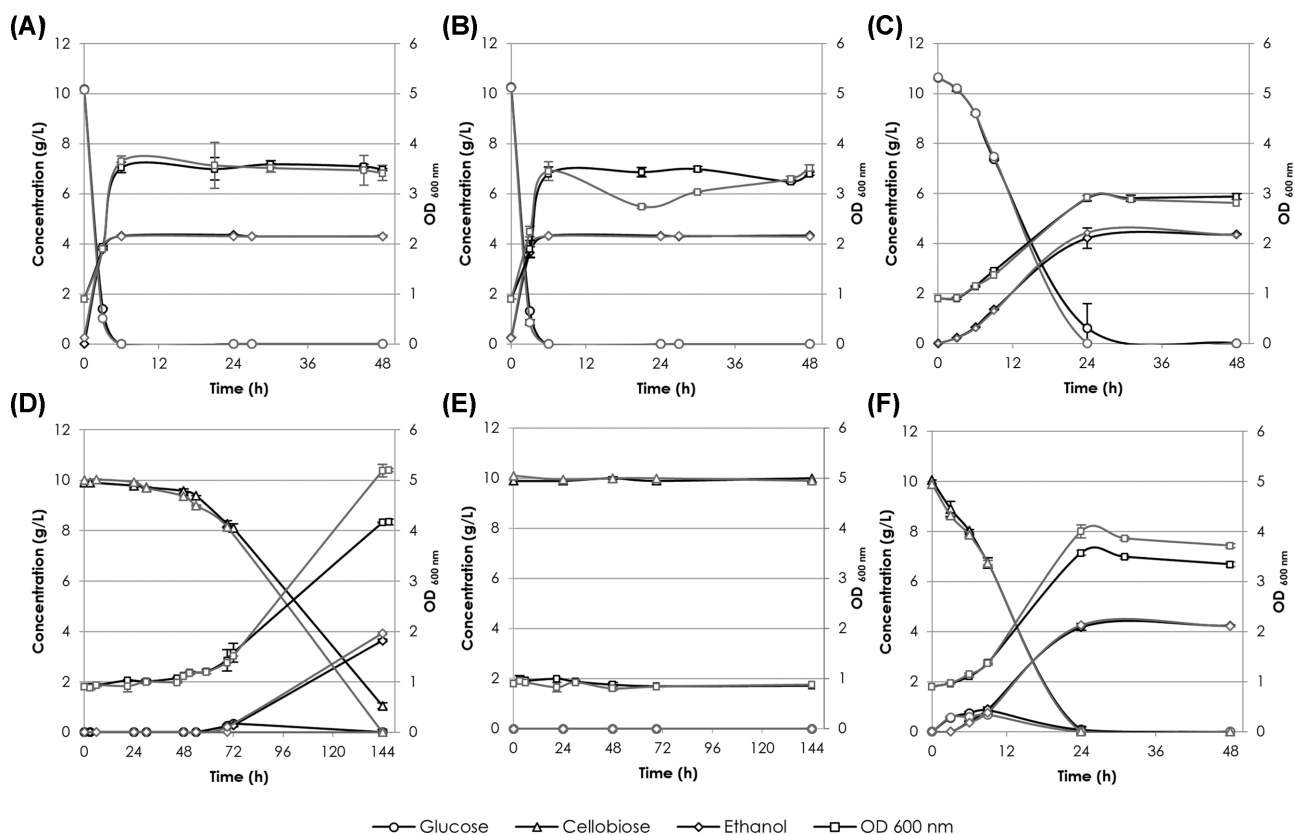


Figure 3. Ethanol production under oxygen limited conditions from glucose or cellobiose by recombinant yeast strains expressing *Pccbgl1*. The *S. cerevisiae* M2n[pBKD2-Pccbgl1]-C1 (A, D), M2n (B, E) and Y294[Pccbgl1] (C, F) strains were cultivated under oxygen-limited conditions in unbuffered (black lines) and buffered (gray lines) SC broth containing glucose (10.53 g/L) (A, B, C) or cellobiose (10 g/L) (D, E, F) as sole carbohydrate source. Data shown are the mean values of three replicates and standard deviations are included.

Table 3. Composition of steam-exploded sugarcane bagasse hydrolysate used in this study.

Component	Concentration
Cellobiose (g/L)	1.9
Glucose (g/L)	0.9
Xylose (g/L)	7.9
Arabinose (g/L)	0.8
Formic acid (g/L)	3.0
Acetic acid (g/L)	16.3
HMF (g/L)	0.7
Furfural (g/L)	2.3
Gallic acid (mg/L)	4.5
Vanillin (mg/L)	260.0
Syringaldehyde (mg/L)	29.5
Ferulic acid (mg/L)	29.4
Vanillic acid (mg/L)	32.0
Syringic acid (mg/L)	46.0
p-Coumaric acid (mg/L)	84.9

SH (Table 3). This composition is comparable to those recently described after sugarcane bagasse steam explosion by other authors (Martín et al. 2002; Favaro et al. 2013a; Verardi et al. 2016). Martín and colleagues, for instance, described the failure of their yeast strain to ferment a steam-exploded sugarcane hydrolysate with 7.4 g/L weak acids and 4.5 g/L furans.

The yeast strains were first evaluated then for their ability to grow aerobically in SC medium containing either glucose (10.53

g/L) or cellobiose (10 g/L) and glucose (1 g/L) in the presence of different concentrations of SH (0%, 10%, 20%, 30% and 40%). OD₆₀₀ was measured after 48 h of incubation. For each strain, the tolerance was evaluated as relative growth (OD₆₀₀ value, %) by comparing the increase in OD₆₀₀ observed for each tested SH concentration and that measured in the control culture, not supplemented with SH.

The M2n[pBKD2-Pccbgl1]-C1 strain exhibited the highest relative growth at each SH concentration (Table 4). In the presence of 30% SH in glucose-supplemented medium, this strain was capable of increasing the initial optical density by 44% compared to the control, and by 28% in 40% SH. On the other hand, the growth of Y294[Pccbgl1] was severely affected when exposed to the lowest concentration of SH. Similar results were observed in the presence of both cellobiose and glucose, with an overall higher growth reduction for both strains (Table 4). The general lack of resistance to lignocellulosic inhibitors by the laboratory strain and increased tolerance by industrial strain is consistent with other studies found in literature (Demeke et al. 2013; Pereira et al. 2014; Favaro et al. 2016; Deparis et al. 2017; Kong et al. 2018).

Fermentation in lignocellulosic pre-hydrolysate

The M2n[pBKD2-Pccbgl1]-C1 and Y294[Pccbgl1] strains were cultivated under oxygen-limited conditions and evaluated in SC containing different concentrations of SH (0%, 5%, 10%, 20% and 30%). In glucose-supplemented medium, *S. cerevisiae* M2n[pBKD2-Pccbgl1]-C1 confirmed its robustness as it was capable of growing significantly also in 30% SH as early as after 6 h

Table 4. Relative aerobic growth in the presence of SH after 48 h of cultivation.

Medium	Strain	Relative growth (%)			
		10% SH	20% SH	30% SH	40% SH
Glucose ^a	M2n[pBKD2-Pccbgl1]-C1	61	56	44	28
	Y294[Pccbgl1]	46	28	8	3
Cellobiose ^b	M2n[pBKD2-Pccbgl1]-C1	79	48	32	0
	Y294[Pccbgl1]	63	21	0	0

^aSC medium supplemented with 10.53 g/L glucose.

^bSC medium supplemented with 10 g/L cellobiose and 1 g/L glucose.

Standard deviation was consistently less than 7%.

from inoculation (Fig. 4A). Moreover, glucose-to-ethanol conversion was quite fast in every fermenting kinetic (Fig. 4C). The laboratory strain, Y294[Pccbgl1], showed little or no growth at 20% SH or higher (Fig. 4B). The glucose consumption took longer and Y294[Pccbgl1] consumed all glucose available only by 24 h, with the exception of 30% SH (Fig. 4D).

Overall, ethanol levels were similar for both strains, with increased production at higher concentration of SH. In the control broth, the M2n[pBKD2-Pccbgl1]-C1 and Y294[Pccbgl1] strains produced about 4.4 g/L ethanol, corresponding to 82% of the theoretical, whereas the highest ethanol concentrations (nearly 6 g/L) were obtained for both strains in the presence of 30% SH, exceeding the maximum theoretical yield (5.4 g/L). This finding can be partly explained by the presence of additional fermentable sugars in SH, including glucose, which amounts for 0.9 g/L (Table 3), and possibly other previously undetected substrates that the yeast may have used as unconventional carbon source(s). Furthermore, yeast metabolism may have rerouted a significant part of the energy available to ethanol production to detoxify inhibitors at the expense of biomass production. This hypothesis seems to be supported by OD₆₀₀ values negatively correlating with SH loads and ethanol production for both strains (Fig. 4). Moreover, HPLC analysis indicates the presence of increasing concentrations of acetic acid in all fermentation media, up to 6 g/L (0.1 M) in 30% SH (data not shown). The occurrence of several weak acids, including acetic acid, in SH is known to promote ethanol production at the expense of biomass (Larsson et al. 1999; Palmqvist and Hahn-Hägerdal 2000; Pampulha and Loureiro-Dias 2000).

In the presence of cellobiose and SH, the M2n[pBKD2-Pccbgl1]-C1 strain was not capable of producing considerable biomass or ethanol (Fig. 5A and C). In 5% SH, the strain reached a final OD₆₀₀ of 1.40 after 96 h. At higher SH concentrations, lower or no biomass increase was detected. Ethanol production was limited, ranging from 0.8 g/L in 30% SH to 1.0 g/L in 5% to 20% SH (Fig. 4C). The available glucose, amounting to 1.0 g/L, was rapidly consumed under all conditions, while up to 1.0 g/L of cellobiose was fermented (Fig. 5C).

The Y294[Pccbgl1] strain reached similar optical densities to those displayed from glucose (Fig. 5B). Cellobiose was completely consumed in less than 24 h in 10% SH. However, at higher SH concentrations, the strain performed worse than in glucose (Fig. 4B). Complete hydrolysis of the substrate in 20% SH required up to 48 h, while only about 40% of the available cellobiose was consumed after 48 h in 30% SH (Fig. 5D). Similarly to that observed on glucose, final ethanol production negatively correlates with the amount of sugarcane pre-hydrolysate in the medium, up to 20% SH. The Y294[Pccbgl1] strain produced almost 6 g/L of ethanol in 20% SH, yet with a lower productivity compared to the other SH concentrations. Instead, the inability to

consume all the substrate in 30% SH was reflected in the final ethanol concentration (Fig. 5D).

Biomass production and fermentative performances from cellobiose were severely impaired, particularly in M2n[pBKD2-Pccbgl1]-C1, by the presence of increasing concentrations of SH under oxygen-limited conditions. A number of chemical species typically contained in lignocellulosic pre-hydrolysates has an inhibitory effect on cellulases, including β -glucosidases (Jönsson, Alriksson and Nilvebrant 2013; Mhlongo et al. 2015). The slow or limited cellobiose hydrolysis could be linked to the inhibition or deactivation of Pccbgl1 mediated by the SH inhibitors. As reported in Materials and Methods section, the long-term exposure of Pccbgl1 to SH has been assessed indicating no enzymatic inhibition or deactivation. The recombinant protein indeed retained its 99% activity after incubation at 30°C for 72 h in the presence of 20%SH. Therefore, the limited ability of *S. cerevisiae* M2n[pBKD2-Pccbgl1]-C1 to ferment cellobiose in the presence of SH should be ascribed to the low level of β -glucosidase production rather than enzyme inhibition. The amount of ATP obtained via the fermentative pathway is significantly lower than in aerobiosis (Lagunas et al. 1986). Therefore, it is expected that higher cellobiose hydrolysis is required under anaerobic conditions than in the presence of oxygen, to cope with high amounts of inhibitors and to increase biomass. The low amount of Pccbgl1 activity (about 8 nkat/mL) available in the medium during the onset of fermentation with M2n[pBKD2-Pccbgl1]-C1 could be responsible for an overall limited enzymatic activity, which impedes further utilization of the available carbon source.

The fermentation conditions were finely tuned in presence of a high concentration of SH (20% v/v) to improve the M2n[pBKD2-Pccbgl1]-C1 fermentation ability. The medium composition was doubled (2 × SC, 10 g/L cellobiose) since the amount of available nitrogen is known to have an effect on yeast cell growth and enzymatic activity (Hahn-Hägerdal et al. 2005). Spent medium containing Pccbgl1 from a 24-h M2n[pBKD2-Pccbgl1]-C1 culture was used to boost the conversion of cellobiose to ethanol. Reference fermentations were carried out using 2 × SC without the addition of Pccbgl1. Under the same experimental conditions, the laboratory strain Y294[Pccbgl1] displayed ethanol levels and profiles not significantly different from those reported in Fig. 5D, using only SC broth (data not shown). This finding could be explained considering that the laboratory strain produces high β -glucosidase activity and the supplementation of 2 × SC and additional β -glucosidase did not significantly yield higher enzymatic activity and thus neither ethanol productivity or ethanol yield in the laboratory yeast.

On the contrary, in the absence of SH, *S. cerevisiae* M2n[pBKD2-Pccbgl1]-C1 obtained increased growth and ethanol productivity in 2 × SC (Fig. 6A) compared to SC medium (Fig.

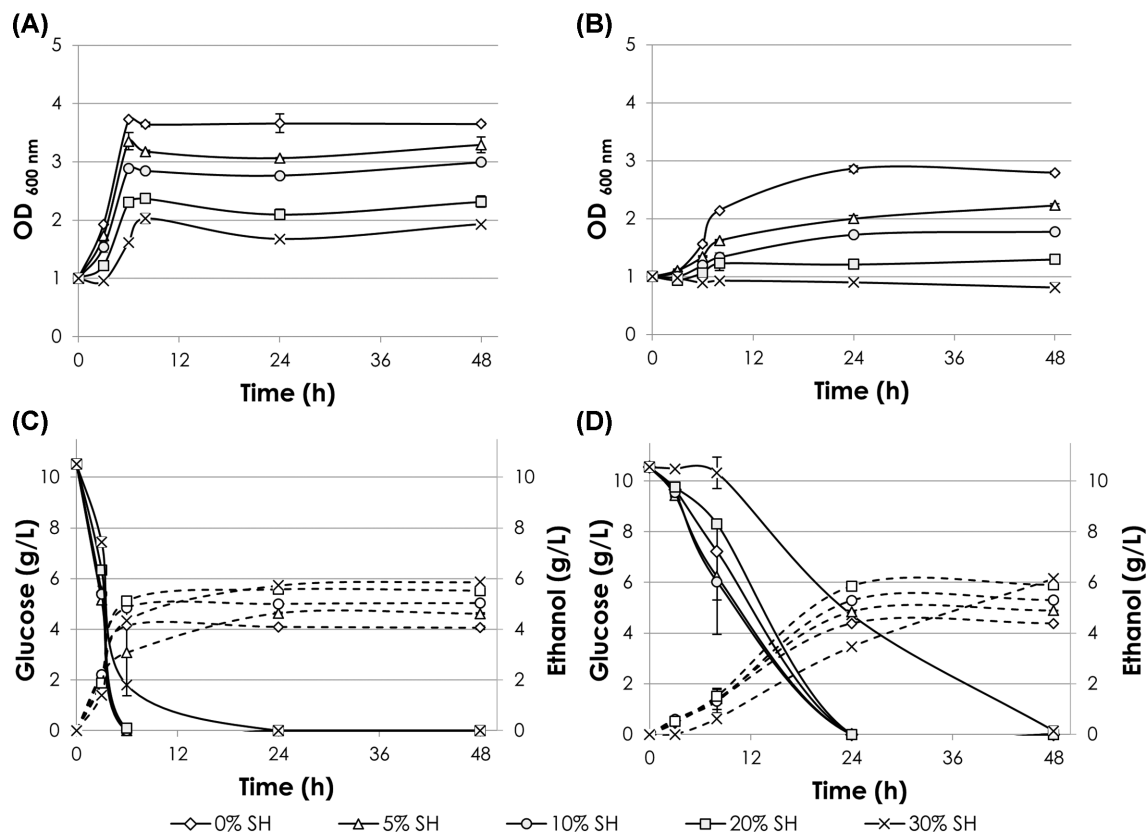


Figure 4. Ethanol production under oxygen limited conditions from glucose by recombinant yeast strains expressing *Pccbgl1* in the presence of steam exploded sugarcane pre-hydrolysate (SH). The *S. cerevisiae* M2n[pBKD2-*Pccbgl1*]-C1 (A, C) and Y294[*Pccbgl1*] (B, D) strains were cultivated under oxygen-limited conditions in SC medium supplemented with glucose (10.53 g/L) in the presence of SH (0%, 5%, 10%, 20% and 30%, v/v). The optical density (A, B), glucose (black lines) and ethanol (dotted lines) concentrations (C, D) were monitored over time. Data points represent the mean values of three replicates and standard deviations are included.

3D). Enzymatic activity rapidly increased with cell growth and allowed the conversion of cellobiose into 4.6 g/L ethanol, corresponding to 78% of the theoretical yield. The addition of the recombinant *Pccbgl1* (20 nkat/mL) strongly reduced the lag-phase observed for M2n[pBKD2-*Pccbgl1*]-C1 with cultivation in SC medium (Fig. 4D and 6B). The yeast was further able to secrete functional β -glucosidase with a final volumetric activity of 40 nkat/mL. Consequently, the quick cell growth was supported by the rapid depletion of cellobiose. A final concentration of 4.2 g/L ethanol was obtained, amounting to 71% of the theoretical value.

Pccbgl1 supplementation at the beginning of the fermentation was also beneficial in the presence of 20% SH (Fig. 6C). *Saccharomyces cerevisiae* M2n[pBKD2-*Pccbgl1*]-C1 was able to grow and deplete all the available cellobiose. The enzymatic activity and cellobiose consumption rate were lower than those reported without SH (Fig. 6B). Nevertheless, 4.3 g/L of ethanol was produced corresponding to 73% of the theoretical value. The above results clearly confirmed that the reduced amount of β -glucosidase produced by the engineered strain was the limiting step in the fermentation of cellobiose in the presence of SH.

CONCLUSIONS

This work assessed for the first time the suitability of two host platforms (wild vs laboratory yeast) in a novel engineered cellobiose-to-ethanol route under simulated industrial environment.

The high enzymatic activity ensured by multicopy plasmids is a key factor to overcome the weakness to high inhibitors

concentrations, typical of laboratory yeast. On the contrary, *S. cerevisiae* M2n[pBKD2-*Pccbgl1*]-C1 confirmed that industrial strain offers higher resistance to the same stressful conditions. This strain could be a suitable candidate for lignocellulosic ethanol production, yet requiring supplementation of additional β -glucosidase to allow high ethanol yield. These findings suggest that the choice of a proper and robust yeast strain to be engineered for cellulase(s) secretion together with the high expression levels of the recombinant genes are crucial tools towards the successful implementation of the engineered phenotypes at industrial level.

SUPPLEMENTARY DATA

Supplementary data are available at [FEMSYR](https://femsyr.oup.com/femsyr/article-abstract/19/2/foz018/53333308) online.

ACKNOWLEDGEMENTS

The authors would like to acknowledge Valentino Pizzocchero (M.Sc., University of Padova) for HPLC analysis and are grateful to Prof. Johann F Görgens (Stellenbosch University), who supplied the steam-pre-treated sugarcane bagasse hydrolysate.

FUNDING

This work was supported by University of Padova [grants GRIC120EG8, DOR1715524/17, DOR1728499/17 and DOR1824847/18], Regione Veneto (PSR 2007–2013, Misura 124) [grant 2307660] and the bilateral joint research projects between

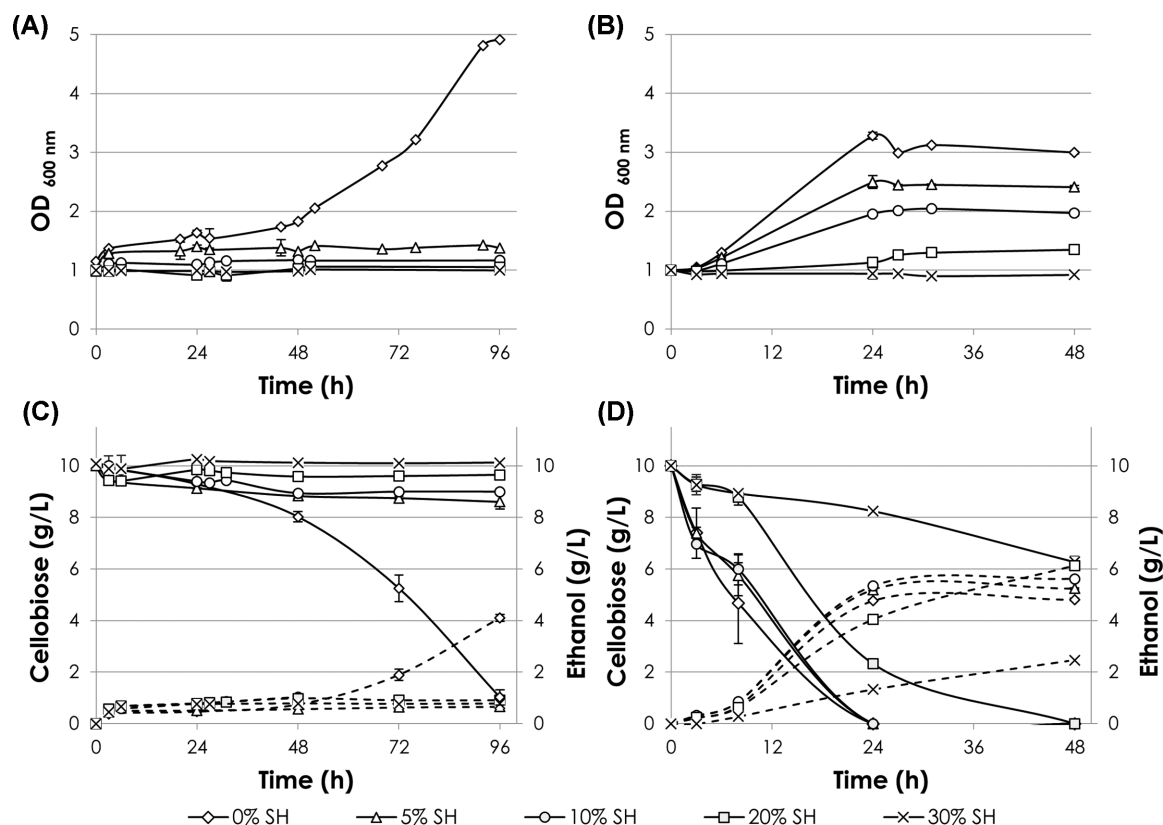


Figure 5. Ethanol production under oxygen limited conditions from cellobiose by recombinant yeast strains expressing *Pccbgl1* in the presence of steam exploded sugarcane pre-hydrolysate (SH). The *S. cerevisiae* M2n[pBKD2-*Pccbgl1*]-C1 (A, C) and Y294[*Pccbgl1*] (B, D) strains were cultivated under oxygen-limited conditions in SC medium supplemented with cellobiose (10 g/L) and glucose (1 g/L) in the presence of SH (0%, 5%, 10%, 20% and 30%, v/v). The optical density (A, B), cellobiose (black lines) and ethanol (dotted lines) concentrations (C, D) were monitored over time. Data shown are the mean values of three replicates and standard deviations are included.

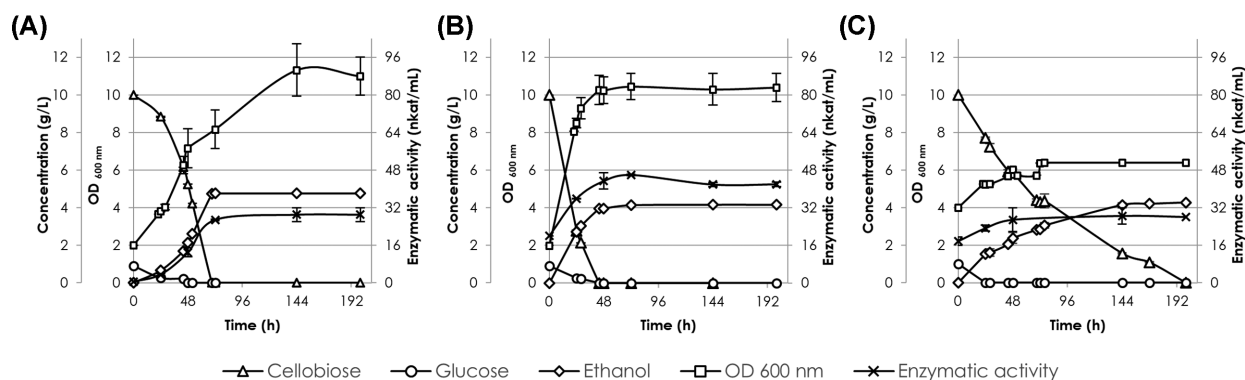


Figure 6. Ethanol production under oxygen limited conditions from cellobiose by *S. cerevisiae* M2n[pBKD2-*Pccbgl1*]-C1 in the presence of 20% steam exploded sugarcane pre-hydrolysate (SH). The strain was cultivated under oxygen-limited conditions in $2 \times$ SC supplemented with cellobiose (10 g/L) and glucose (1 g/L) (A). The effect of *Pccbgl1* addition (spent medium containing *Pccbgl1* from a 24 h M2n[pBKD2-*Pccbgl1*]-C1 culture) were monitored in combination with 0% SH (B) and 20% SH (C). Data shown are the mean values of two replicates and standard deviations are included.

Italy and South Africa [grant ZA11MO2 and ZA18MO04]. LC was recipient of an 'Assegno di ricerca (Tipo A)' (University of Padova, BIRD161039/16).

Conflict of interest. None declared.

REFERENCES

- Abbas A, Ansumali S. Global potential of rice husk as a renewable feedstock for ethanol biofuel production. *Bioenergy Res* 2010;3:328–34.
- Alvira P, Tomas-Pejo E, Ballesteros M et al. Pretreatment technologies for an efficient bioethanol production process based on enzymatic hydrolysis: a review. *Bioresource Technol* 2010;101:4851–61.

- Bisaria VS, Kondo A. *Bioprocessing of Renewable Resources To Commodity Bioproducts*. Hoboken, New Jersey: Wiley, 2013.
- Casa-Villegas M, Polaina J, Martin-Navarro J. Cellobiose fermentation by *Saccharomyces cerevisiae*: comparative analysis of intra versus extracellular sugar hydrolysis. *Process Biochem* 2018;**75**:59–67.
- Cripwell R, Favaro L, Rose SH et al. Utilisation of wheat bran as a substrate for bioethanol production using recombinant cellulases and amylolytic yeast. *Appl Energy* 2015;**160**:610–7.
- Davison SA, den Haan R, van Zyl WH. Heterologous expression of cellulase genes in natural *Saccharomyces cerevisiae* strains. *Appl Microbiol Biotechnol* 2016;**100**:8241–54.
- Demeke MM, Dumortier F, Li Y et al. Combining inhibitor tolerance and D-xylose fermentation in industrial *Saccharomyces cerevisiae* for efficient lignocellulose-based bioethanol production. *Biotechnol Biofuels* 2013;**6**:120.
- Den Haan R, Rose SH, Lynd LR et al. Hydrolysis and fermentation of amorphous cellulose by recombinant *Saccharomyces cerevisiae*. *Metab Eng* 2007;**9**:87–94.
- Deparis Q, Claes A, Foulquié-Moreno MR et al. Engineering tolerance to industrially relevant stress factors in yeast cell factories. *FEMS Yeast Res* 2017;**17**, DOI: 10.1093/femsyr/fox036.
- Duque A, Manzanares P, Ballesteros I et al. Chapter 15 – steam explosion as lignocellulosic biomass pretreatment. In: Muscatto SI (ed). *Biomass Fractionation Technologies for a Lignocellulosic Feedstock Based Biorefinery*. Amsterdam: Elsevier, 2016, 349–68.
- Favaro L, Basaglia M, Trento A et al. Exploring grape marc as trove for new thermotolerant and inhibitor-tolerant *Saccharomyces cerevisiae* strains for second-generation bioethanol production. *Biotechnol Biofuels* 2013a;**6**:168.
- Favaro L, Cagnin L, Basaglia M et al. Production of bioethanol from multiple waste streams of rice milling. *Bioresource Technol* 2017;**244**:151–9.
- Favaro L, Corte L, Roscini L et al. A novel FTIR-based approach to evaluate the interactions between lignocellulosic inhibitory compounds and their effect on yeast metabolism. *RSC Adv* 2016;**6**:47981–9.
- Favaro L, Jooste T, Basaglia M et al. Codon-optimized glucoamylase sGA1 of *Aspergillus awamori* improves starch utilization in an industrial yeast. *Appl Microbiol Biotechnol* 2012;**95**:957–68.
- Favaro L, Jooste T, Basaglia M et al. Designing industrial yeasts for the consolidated bioprocessing of starchy biomass to ethanol. *Bioengineered* 2013b;**4**:97–102.
- Favaro L, Jooste T, Basaglia M et al. Engineering amylolytic yeasts for industrial bioethanol production. *Chem Engineer Trans* 2010;**20**:97–102.
- Favaro L, Viktor MJ, Rose SH et al. Consolidated bioprocessing of starchy substrates into ethanol by industrial *Saccharomyces cerevisiae* strains secreting fungal amylases. *Biotechnol Bioeng* 2015;**112**:1751–60.
- Gnansounou E, Dauriat A. Chapter 6 – techno-economic analysis of lignocellulosic ethanol. In: Pandey A, Larroche C, Ricke SC et al. (eds). *Biofuels*. Amsterdam: Academic Press, 2011, 123–48.
- Gombert AK, Dos Santos MM, Christensen B et al. Network identification and flux quantification in the central metabolism of *Saccharomyces cerevisiae* under different conditions of glucose repression. *J Bacteriol* 2001;**183**:1441–51.
- Hahn-Hägerdal B, Karhumaa K, Larsson CU et al. Role of cultivation media in the development of yeast strains for large scale industrial use. *Microb Cell Fact* 2005;**4**:31.
- Jansen MLA, Bracher JM, Papapetridis I et al. *Saccharomyces cerevisiae* strains for second-generation ethanol production: from academic exploration to industrial implementation. *FEMS Yeast Res* 2017;**17**, DOI: 10.1093/femsyr/fox044.
- Jönsson LJ, Alriksson B, Nilvebrant N-O. Bioconversion of lignocellulose: inhibitors and detoxification. *Biotechnol Biofuels* 2013;**6**:16.
- Jönsson LJ, Martín C. Pretreatment of lignocellulose: formation of inhibitory by-products and strategies for minimizing their effects. *Bioresource Technol* 2016;**199**:103–12.
- Kong II, Turner TL, Kim H et al. Phenotypic evaluation and characterization of 21 industrial *Saccharomyces cerevisiae* yeast strains. *FEMS Yeast Res* 2018;**18**, DOI: 10.1093/femsyr/foy001.
- Lagunas R, De Investigaciones I, Csic B et al. Misconceptions about the energy metabolism of *Saccharomyces cerevisiae*. *Yeast*. 1986;**2**:221–8.
- Larsson S, Palmqvist E, Hahn-Hägerdal B et al. The generation of fermentation inhibitors during dilute acid hydrolysis of softwood. *Enzyme Microb Technol* 1999;**24**:151–9.
- Liu Z, Inokuma K, Ho S-H et al. Combined cell-surface display and secretion-based strategies for production of cellulosic ethanol with *Saccharomyces cerevisiae*. *Biotechnol Biofuels* 2015;**8**:162.
- Lynd LR, Van Zyl WH, McBride JE et al. Consolidated bioprocessing of cellulosic biomass: an update. *Curr Opin Biotechnol* 2005;**16**:577–83.
- Lynd LR, Weimer PJ, Van Zyl WH et al. Microbial cellulose utilization: fundamentals and biotechnology. *Microbiol Mol Biol Rev* 2002;**66**:506–77.
- Martín C, Galbe M, Nilvebrant NO et al. Comparison of the fermentability of enzymatic hydrolyzates of sugarcane bagasse pretreated by steam explosion using different impregnating agents. *Appl Biochem Biotechnol – Part A Enzym Eng Biotechnol* 2002;**98–100**:699–716.
- Mcbride JEE, Deleault KM, Lynd LR et al. Recombinant yeast strains expressing tethered cellulase enzymes. 2008. U.S. Patent Application No. 12/516, 175.
- Mhlongo SI, Haan Den R, Viljoen-bloom M et al. Lignocellulosic hydrolysate inhibitors selectively inhibit / deactivate cellulase performance. *Enzyme Microb Technol* 2015;**81**:16–22.
- Njokweni AP, Rose SH, van Zyl WH. Fungal β -glucosidase expression in *Saccharomyces cerevisiae*. *J Ind Microbiol Biotechnol* 2012;**39**:1445–52.
- Olofsson K, Bertilsson M, Lidén G. A short review on SSF – an interesting process option for ethanol production from lignocellulosic feedstocks. *Biotechnol Biofuels* 2008;**1**:7.
- Olson DG, McBride JE, Joe Shaw A et al. Recent progress in consolidated bioprocessing. *Curr Opin Biotechnol* 2012;**23**:396–405.
- Palmqvist E, Hahn-Hägerdal B. Fermentation of lignocellulosic hydrolysates. II: Inhibitors and mechanisms of inhibition. *Bioresource Technol* 2000;**74**:25–33.
- Pampulha ME, Loureiro-Dias MC. Energetics of the effect of acetic acid on growth of *Saccharomyces cerevisiae*. *FEMS Microbiol Lett* 2000;**184**:69–72.
- Pereira FB, Romani A, Ruiz HA et al. Industrial robust yeast isolates with great potential for fermentation of lignocellulosic biomass. *Bioresource Technol* 2014;**161**:192–9.
- Piper P, Mahé Y, Thompson S et al. The Pdr12 ABC transporter is required for the development of weak organic acid resistance in yeast. *EMBO J* 1998;**17**:4257–65.
- Sambrook J, Russell DW. *Molecular Cloning – Sambrook & Russel – Vol. 1, 2, 3. 3rd edn*. New York: Cold Spring Harb Lab Press, 2001, DOI: 10.1002/humu.1186.abs.
- Sindhu R, Binod P, Pandey A. Biological pretreatment of lignocellulosic biomass – an overview. *Bioresource Technol* 2016;**199**:76–82.

- Siqueira PF, Karp SG, Carvalho JC et al. Production of bioethanol from soybean molasses by *Saccharomyces cerevisiae* at laboratory, pilot and industrial scales. *Bioresource Technol* 2008;**99**:8156–63.
- Song X, Liu Q, Mao J et al. POT1-mediated δ -integration strategy for high-copy, stable expression of heterologous proteins in *Saccharomyces cerevisiae*. *FEMS Yeast Res* 2017;**17**, DOI: 10.1093/femsyr/fox064.
- Srirangan K, Akawi L, Moo-Young M et al. Towards sustainable production of clean energy carriers from biomass resources. *Appl Energy* 2012;**100**:172–86.
- Taherzadeh MJ, Karimi K. Enzyme-based hydrolysis processes for ethanol from lignocellulosic materials: a review, *BioResources*. 2007;**2**:703-38.
- van Maris AJA, Abbott DA, Bellissimi E et al. Alcoholic fermentation of carbon sources in biomass hydrolysates by *Saccharomyces cerevisiae*: current status. *Antonie van Leeuwenhoek, Int J Gen Mol Microbiol* 2006;**90**:391–418.
- Van Rooyen R, Hahn-Hägerdal B, La Grange DC et al. Construction of cellobiose-growing and fermenting *Saccharomyces cerevisiae* strains. *J Biotechnol* 2005;**120**:284–95.
- van Zyl WH, Lynd LR, den Haan R et al. Consolidated bioprocessing for bioethanol production using *Saccharomyces cerevisiae*. *Adv Biochem Eng Biotechnol* 2007;**108**:205–35.
- Verardi A, Blasi A, De Bari I et al. Steam pretreatment of *Saccharum officinarum* L. bagasse by adding of impregnating agents for advanced bioethanol production. *Ecotoxicol Environ Saf* 2016;**134**:293–300.
- Verduyn C, Zomerdijk TPL, Dijken JP et al. Continuous measurement of ethanol production by aerobic yeast suspensions with an enzyme electrode. *Appl Microbiol Biotechnol* 1984;**19**:181–5.
- Yamada R, Tanaka T, Ogino C et al. Gene copy number and ploidy on products formation in yeast. *Appl Microbiol Biotechnol* 2010;**88**:849–57.
- Zabed H, Sahu JN, Boyce AN et al. Fuel ethanol production from lignocellulosic biomass: an overview on feedstocks and technological approaches. *Renew Sustain Energy Rev* 2016;**66**:751–74.